frontiers | Research Topics

Vector-based cancer immunotherapy

Edited by
Björn L. Frendéus, Yaohe Wang, Ine Lentacker
and Monika Semmrich

Published in
Frontiers in Immunology
Frontiers in Oncology

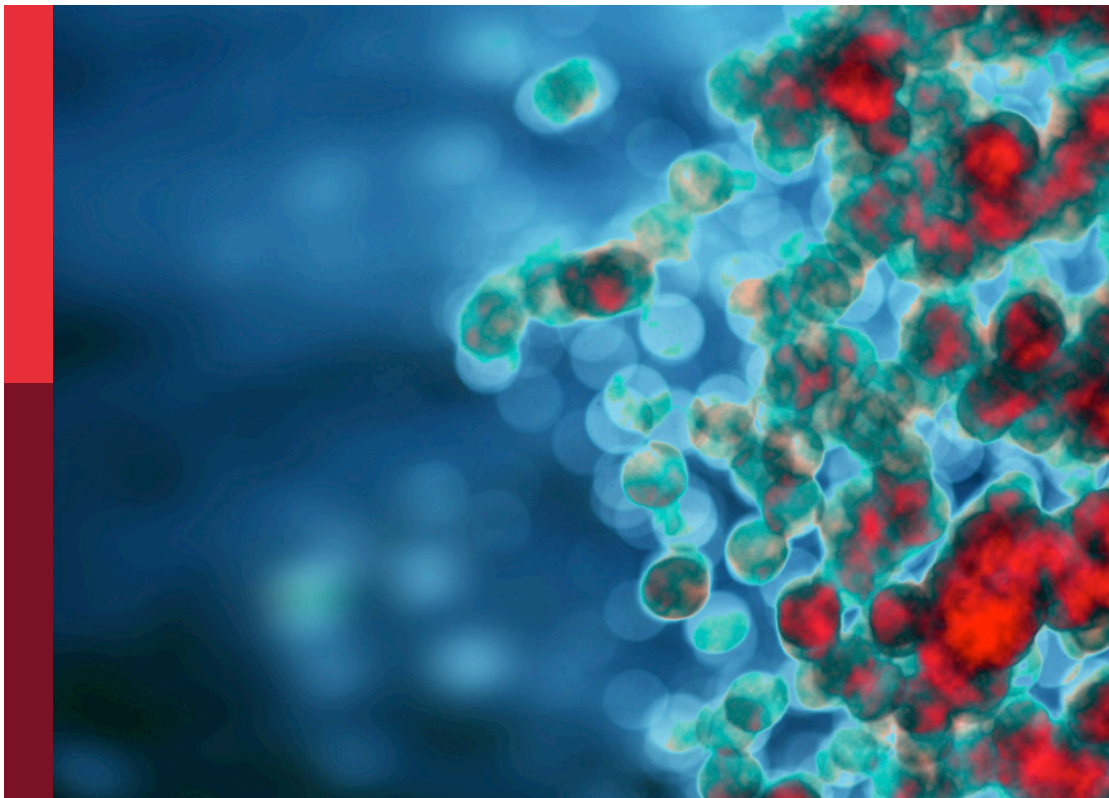

ISSN 1664-8714
ISBN 978-2-8325-5547-7
DOI 10.3389/978-2-8325-5547-7

About Frontiers

Frontiers is more than just an open access publisher of scholarly articles: it is a pioneering approach to the world of academia, radically improving the way scholarly research is managed. The grand vision of Frontiers is a world where all people have an equal opportunity to seek, share and generate knowledge. Frontiers provides immediate and permanent online open access to all its publications, but this alone is not enough to realize our grand goals.

Frontiers journal series

The Frontiers journal series is a multi-tier and interdisciplinary set of open-access, online journals, promising a paradigm shift from the current review, selection and dissemination processes in academic publishing. All Frontiers journals are driven by researchers for researchers; therefore, they constitute a service to the scholarly community. At the same time, the *Frontiers journal series* operates on a revolutionary invention, the tiered publishing system, initially addressing specific communities of scholars, and gradually climbing up to broader public understanding, thus serving the interests of the lay society, too.

Dedication to quality

Each Frontiers article is a landmark of the highest quality, thanks to genuinely collaborative interactions between authors and review editors, who include some of the world's best academicians. Research must be certified by peers before entering a stream of knowledge that may eventually reach the public - and shape society; therefore, Frontiers only applies the most rigorous and unbiased reviews. Frontiers revolutionizes research publishing by freely delivering the most outstanding research, evaluated with no bias from both the academic and social point of view. By applying the most advanced information technologies, Frontiers is catapulting scholarly publishing into a new generation.

What are Frontiers Research Topics?

Frontiers Research Topics are very popular trademarks of the *Frontiers journals series*: they are collections of at least ten articles, all centered on a particular subject. With their unique mix of varied contributions from Original Research to Review Articles, Frontiers Research Topics unify the most influential researchers, the latest key findings and historical advances in a hot research area.

Find out more on how to host your own Frontiers Research Topic or contribute to one as an author by contacting the Frontiers editorial office: frontiersin.org/about/contact

Vector-based cancer immunotherapy

Topic editors

Björn L. Frendéus — BioInvent, Sweden

Yaohe Wang — Queen Mary University of London, United Kingdom

Ine Lentacker — Ghent University, Belgium

Monika Semmrich — BioInvent, Sweden

Citation

Frendéus, B. L., Wang, Y., Lentacker, I., Semmrich, M., eds. (2024). *Vector-based cancer immunotherapy*. Lausanne: Frontiers Media SA.

doi: 10.3389/978-2-8325-5547-7

Table of contents

frontiers | Frontiers in Immunology

TYPE Mini Review
PUBLISHED 30 March 2023
DOI 10.3389/fimmu.2023.1155728

OPEN ACCESS

EDITED BY
Ramesh Akkina,
Colorado State University, United States

REVIEWED BY
Vladimir Alexeevich Gushchin,
Russian Academy of Medical Sciences, Russia

*CORRESPONDENCE
David E. Fisher
DFISHER3@mgh.harvard.edu

SPECIALTY SECTION
This article was submitted to Vaccines and Molecular Therapeutics, a section of the journal Frontiers in Immunology

RECEIVED 31 January 2023
ACCEPTED 22 March 2023
PUBLISHED 30 March 2023

CITATION
Xu Z and Fisher DE (2023) mRNA melanoma vaccine revolution spurred by the COVID-19 pandemic. *Front. Immunol.* 14:1155728. doi: 10.3389/fimmu.2023.1155728

mRNA melanoma vaccine revolution spurred by the COVID-19 pandemic

Ziyang Xu[1] and David E. Fisher[2*]

[1]Department of Medicine, Massachusetts General Hospital, Boston, MA, United States, [2]Department of Dermatology, Massachusetts General Hospital, Boston, MA, United States

The advent of mRNA vaccines represents a significant advance in the field of vaccinology. While several vaccine approaches (mRNA, DNA, recombinant protein, and viral-vectored vaccines) had been investigated at the start of the COVID-19 pandemic, mRNA vaccines quickly gained popularity due to superior immunogenicity at a low dose, strong safety/tolerability profiles, and the possibility of rapid vaccine mass manufacturing and deployment to rural regions. In addition to inducing protective neutralizing antibody responses, mRNA vaccines can also elicit high-magnitude cytotoxic T-cell responses comparable to natural viral infections; thereby, drawing significant interest from cancer immunotherapy experts. This mini-review will highlight key developmental milestones and lessons we have learned from mRNA vaccines during the COVID-19 pandemic, with a specific emphasis on clinical trial data gathered so far for mRNA vaccines against melanoma and other forms of cancer.

KEYWORDS

mRNA vaccination, COVID – 19, melanoma, cancer vaccination, neoantigen

1 Introduction

For the past decade, cancer immunotherapy has been a mainstay treatment for advanced melanoma and non-small-cell lung cancer (NSLC). Reversal of the suppressive tumor microenvironment by checkpoint blockade against PD-1, PD-L1, and CTLA4 could potentiate immunosurveillance which may significantly impact clinical outcomes for patients (1). Efforts to further adjuvant the immune system through cancer vaccines had, unfortunately, yielded largely disappointing results in Phase 3 trials due to limited ability of peptide vaccines to induce CD8+ T-cell responses, induction of T cells with a restricted repertoire insufficient to counter cancer cells with heterogeneous epitope expression profiles, and inadequate induction of additional arms of the immune systems (CD4+ T cells and B cells) for synergistic tumor killing (2, 3). mRNA vaccines represent a promising strategy to tackle these challenges. They have been under development for two decades, but brought to the limelight through the COVID-19 pandemic. Massive deployment of the vaccines to billions of people in over a hundred countries across the world has modernized our infrastructure to ramp up production of such vaccines and has

allowed us to gain a deep appreciation of the immune responses induced by as well as adverse effect profiles associated with mRNA vaccination in a relatively short period of time (4). Researchers and oncologists are excited to learn that mRNA vaccines can not only elicit neutralizing antibodies, commonly regarded as a key correlate of protection against SARS-CoV-2 infection, but also induce CD8+ T cell responses that mediate early protection against the virus and help surveil and eradicate tumor reservoirs in cancer patients (5). Several mRNA vaccine candidates have been advanced into clinical studies and induced positive clinical responses in several early phase clinical trials, particularly against melanoma. This review seeks to highlight lessons we have learned about mRNA vaccines during the COVID-19 pandemic and recent clinical trial data of various mRNA vaccine candidates against melanoma.

2 Overview of historical development of mRNA vaccine

In vitro transcribed (IVT) mRNAs were first used as a vector for gene transfer, whereby Wolff et al. first reported *in vivo* expression of transgenes in mouse muscles inoculated with the mRNA vector (6). Shortly after, scientists observed mRNAs encoding influenza hemagglutinin and cancer embryonic antigen (CEA) were capable of eliciting CD8+ and antigen-specific antibody responses, respectively, and started to appreciate its potential as a vector for vaccination (7, 8). However, development of the mRNA vaccines stalled in the early phase as scientists started to realize challenges associated with this platform. First, mRNA transcripts are inherently temperature-sensitive— upon dilution, they can last 6 to 12 hours at room temperature, and such cold-chain transport of the vaccines for deployment in humans can create logistical nightmares (9). Second, mRNA vaccines could trigger significant local inflammatory responses through activation of the cellular pattern recognition receptor (PRR) which can lead to dose-limiting toxicity (DLT) and significantly reduce *in vivo* transgene expression (10). Over the years, a majority of these challenges have been addressed through advanced purification and liposome formulation techniques to improve *ex vivo* and *in vivo* stability of mRNA transcripts, incorporation of modified nucleoside bases with lower likelihood of triggering PRR, and sequence-level engineering to optimize transcript stability and translation efficiency.

2.1 Optimization of mRNA transcripts

Foreign mRNAs are inherently immunogenic to the innate immune response. TLR7 and TLR8 receptors in the endosomal compartment can recognize single-stranded mRNA transcripts which are rich in unmodified guanosine and uridine-rich motifs. TLR7/8 activation can lead to type I interferon production, mediating premature degradation of the mRNA transcript and local injection reactions clinically (10). Importantly, modified nucleotides such as pseudouridine (Ψ), N6-methyladenine (m6A), 5-methylcytosine(m5C), 2-thiouracil (s2U), and 5-methyluracil (m5U) can help cloak mRNA vaccines from the innate immune system; thereby, improving the translation efficiency of the mRNA vaccines (Figure 1) (11, 12).

In vitro transcribed mRNAs frequently retain triphosphates at the 5'-end which could inadvertently trigger PRR and Type I interferon pathway activation. In eukaryotic cells, m7GpppN cap can be added to nascent mRNA transcripts through concerted actions of RNA triphosphatase, RNA guanylyltransferase, and RNA (guanine-7)-methyltransferase (13). To bypass this complex biochemical process, naturally occurring 7-methylguanosine (m7GDP) could be added directly to the *in vitro* transcription reaction mixture. Further, to avoid incorrect incorporation of m7GDP in the mRNA transcripts, anti-reverse cap analogs (ARCA) could be used alternatively to force RNA polymerase to incorporate ARCA in the forward orientation and produce fully translatable mRNA transcripts with ARCA at the 5'-end (14).

Finally, the 3'-polyA tail of *in vitro* transcribed mRNA could also be optimized. Poly-A tails are frequently added to the 3'-end of mRNA transcripts directly by RNA-polymerase or by Poly-A-polymerase. They impede RNA degradation by RNA exonucleases, significantly increasing *in vitro* and *in vivo* half-life of the transcripts. Stability of the Poly-A tail could be further improved with the use of the hydrolysis-resistant ATP analogue, ATPαS, during *in vitro* transcription. Alternatively, an oligo(dT) domain can be directly incorporated into the template DNA plasmid to precisely control the number of nucleotide bases in the Poly-A tail (15, 16).

2.2 Sequence-level engineering

Optimization of mRNA transcript sequence is also critical to the vector's stability and translational efficiency. Transport RNAs (tRNAs) occur at different frequencies in different target tissues. Therefore, design of the mRNA sequence should carefully consider the mode of vaccine delivery (intradermal, intramuscular versus intravenous) to fully utilize the endogenous tRNA pool (codon usage). In addition, mRNA sequence is frequently optimized for both mouse and humans to enable preclinical evaluation of the vaccine candidates in animal models (17). In addition, increasing mRNA GC content can improve thermal stability and reduce local innate immunogenicity of the transcripts (18). Finally, secondary structures (such as stem loops and hairpins) should be minimized in the mRNA transcripts, as they can slow ribosomal scanning and reduce transgene expression (19).

The 5' and 3' untranslated regions (UTR) not only affect thermal stability of mRNAs but also could regulate translation of the transcripts (20). Incorporation of internal ribosomal entry sites or the Kozak sequence in the 5'-UTR can facilitate ribosomal loading and translation initiation. The 3'-UTR could either incorporate a stabilization motif such as the β-globulin 3'-UTR to prolong transcript half-life or a regulatory motif such as the miRNA-122 binding site to achieve tissue specific expression and minimize systemic toxicity by reducing off-target transgene expression in the liver (21, 22).

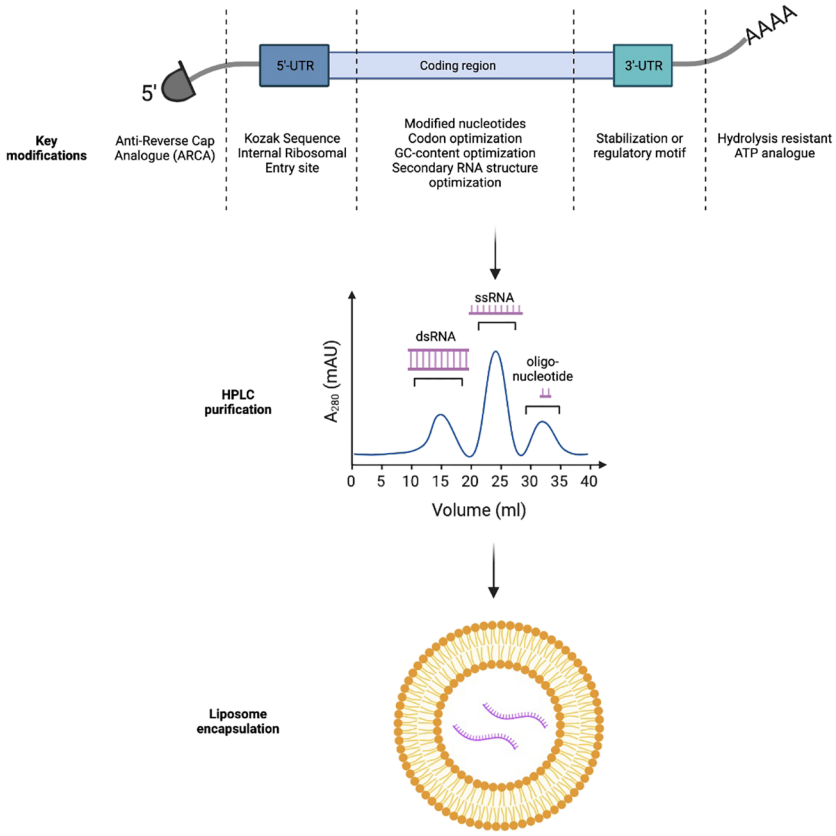

FIGURE 1
Key strategies to improve *in-vivo* expression and immunogenicity profiles of mRNA-based immunotherapeutics.

2.3 Advanced purification and formulation techniques

Double stranded RNA (dsRNA) can be either recognized by TLR3 in the endosome or RIG-I in the cytosol to trigger local type I interferon responses (23). Careful removal of the dsRNA byproducts from *in vitro* generated transcripts through High Performance Liquid Chromatography (HPLC) can thereby reduce local reactivity of mRNA vaccines (24). More recently, Baiersdorfer et al. reported the use of cellulose in ethanol-containing buffer to selectively bind dsRNA byproducts, to rapidly purify *in vitro* generated mRNA transcripts (25).

Formulation of purified mRNA transcripts has a significant influence on the transcript thermal stability (and thereby, shelf-life), transgene uptake by the target tissues, and the vaccine's adverse effect profiles. Non-formulated (naked) mRNAs have previously been studied in several clinical trials. However, they demonstrated limited uptake and immunogenicity due to low thermal stability and poor transit across cellular membrane secondary to the negative charges on the RNA backbone (26). Self-assembled cationic polymers, such as protamine, have also been used to encapsulate negatively charged mRNAs for *in vivo* delivery. Currently, there are several protamine-formulated mRNA vaccines under clinical investigations. CV-9201, for example, is a vaccine encoding five non-small cell lung cancer (NSCLC) tumor-associated antigens (TAAs) used to treat Stage IIIb or IV NSCLC in a Phase 1/2 study. The study demonstrates that CV-9201 was well-tolerated and could induce antigen-specific T cell responses but failed to improve overall survival in vaccine recipients as compared to historical controls (27). Finally, lipid nanoparticles (LNPs) are now considered as the mainstay vector for *in vivo* mRNA delivery and have been used in both the Pfizer/Bio-N-Tech as well as the Moderna COVID-19 vaccines. LNPs utilize a mixture of cholesterol, charged lipids and polyethylene glycol (PEG) derivatives to form micelles that can stabilize negatively charged mRNA transcripts, be preferentially taken up by antigen-presenting cells (APCs) such as dendritic cells and macrophages, and offload cargos in acidic endosomes (28). In addition to being vaccine carriers, LNPs can directly serve as vaccine adjuvants through induction of IL-6 secretion, which is critical for follicular T helper (T_Fh) cell maturation (29). Furthermore, the LNPs can be further functionalized through decoration of monoclonal antibodies on their surfaces to potentiate specific targeting of these LNPs to desired cell types, thereby reducing toxicity associated with systemic administration. For example, CD5-targeted LNPs could selectively deliver mRNA to T cells for *in vivo* engineering of CAR-T cells against fibroblasts to treat heart failure in a murine model (30).

3 Lessons learnt from the SARS-CoV-2 pandemic

An unprecedented opportunity was created for the development of mRNA vaccines during the COVID-19 pandemic. As the original Wuhan strain was extremely contagious and associated with high mortality, academic institutions and pharmaceutical companies rapidly designed, produced and tested vaccine candidates at record speed. For the Pfizer/BioNTech vaccine, animal studies were commenced in Jan 2020 following the release of the SARS-CoV-2 genome. Phase 1/2 study initiated in April whereas Phase 2/3 study commenced in July of 2020, with the vaccine approved by the US FDA under Emergency Use Authorization (EUA) in December 2020. It was rapidly deployed to healthcare workers fighting at the frontlines against COVID-19 (31). Pre-approval clinical studies and post-marketing surveillance data generated for both Pfizer/BioNTech and Moderna vaccines were reported to be positive. For Pfizer/BioNTech vaccines, two doses of vaccine at 30 μg doses three weeks apart conferred 95% protection two months following vaccination and retained a protective efficacy of 83.7% after four months (32). The Moderna vaccine given at 100 μg dose four weeks apart conferred 94.1% protection within 64 days of vaccination and remained 90% protective after six months (33). Adverse events were mostly self-limiting, with fever and fatigue being reported as the most common events for the Pfizer vaccine in 3.8% of trial participants, and 38.1% and 15.8% of trial participants developing moderate and severe side effects after receiving the second dose of the Moderna vaccine, respectively (32, 33). Both vaccines had reduced protection against variants of concern, with the Pfizer vaccine conferring 56% and 74% protection against the omicron variant after the second and third dose respectively, due to significant mutations in the Spike protein promoting viral evasion from neutralizing antibodies generated by mRNA vaccines which were designed for the original Wuhan strain (34). Both vaccines also generated strong T-cell responses. The Moderna vaccine, for example, generated strong Th1-based CD4+ T cell responses in humans (35). While the initial analysis did not detect robust CD8+ T cell responses from the Moderna vaccine by intracellular cytokine staining (36), a subsequent study using MHC-I specific CD8 T cell sorting showed one or two doses of mRNA vaccines induced polyfunctional CD8 T cells with magnitudes comparable to natural viral infection, and with faster kinetics as compared to induction of CD4+ and neutralizing antibody responses (37). The unique ability of mRNA vaccines to induce CD8+ T-cell responses, as compared to other routes of vaccination such as protein subunit vaccines, make them an attractive platform to develop cancer vaccines.

4 mRNA cancer vaccines under clinical development

Currently several mRNA cancer vaccine candidates are under clinical investigation. These vaccines may target tumor associated antigens (TAA or antigens overexpressed in cancerous cells that may also be present in normal tissue), tumor-specific antigens (TSA or antigens that spontaneously arise in tumors and are therefore unique to cancer cells), or seek to prime the endogenous immune system (immunostimulants).

mRNA vaccines against TAA are currently being investigated for treatment of metastatic castration-resistant prostate cancer (NCT04382898, NCT01817738), ovarian cancer (NCT04163094), and NSCLC (NCT05142189, NCT00923312, NCT01915524) with or without CPI (NCT04382898, NCT05142189) and with or without adjuvant/neoadjuvant chemotherapies (NCT04163094, NCT05142189). NSCLC-specific mRNA vaccines CV9201 (NCT00923312) and CV9202 (NCT01915524) were found to be safe, and induced antigen-specific T-cell responses in 63% and 84% subjects respectively. However, CV9201 was not found to improve progression-free survival or overall survival in trial participants (27, 38). As TAAs are highly expressed in most cancer tissues, vaccine cocktails targeting these antigens do not need to be individualized and can be given to patients with a specific oncologic diagnosis without *a priori* knowledge of tumor transcriptomic signatures. However, as TAAs are also expressed in healthy tissues, vaccines have the theoretical risk of inducing autoimmunity (39). Central and peripheral tolerance mechanisms can also limit the magnitude of induced T cell responses (40).

To overcome these hurdles, vaccines could also be designed against TSA. For examples, vaccines could target components of oncogenic viruses (such as HPV E6 and E7 protein), which are only expressed in infected and transformed cells. BNT113 is an HPV E6/7 mRNA vaccine used for treatment of HPV-positive head and neck squamous cell carcinoma currently being studied in Phase 1 (NCT03418480) and Phase 2 (NCT04534205) trials along with PD-1 inhibitor pembrolizumab (41). TSA mRNA vaccines may also target neo-epitopes that spontaneously arise from mutational events within cancer cells. These vaccines may target cancer-driver mutations- the mRNA-5671 vaccine which targets four KRAS mutations in colorectal cancer, pancreatic cancer and NSCLC is currently being studied in a Phase I trial (NCT03948763) in combination with pembrolizumab (42). To increase the breadth of induced T-cell repertoire against tumors, these vaccines may alternatively encode a cocktail of non-driver neo-epitopes that are identified through deep sequencing of tumor exomes or transcriptomes and predicated to have high patient-specific MHC Class I binding affinity through *in silico* binding algorithms. For example, the mRNA-4650 (NCT03480152) was a personalized neo-antigen vaccine encoding up-to 20 neo-epitopes against metastatic gastrointestinal tumors. In a Phase 1 study, the vaccine induced neoantigen-specific CD8+ and CD4+ T-cell responses in three of four subjects but did not induce significant clinical responses. Further analysis showed predominant elicitation of CD4+, as opposed to CD8+, T cell responses by vaccines despite selection of HLA-I restricted epitopes during vaccine design, highlighting challenges with the *in silico* prediction algorithm (43).

mRNA can also be used as a vector for potent *in vivo* expression of biologics such as monoclonal antibodies and cytokines. mRNA encoded cytokines are often injected intratumorally to limit systemic adverse effect. For example, a Phase 1 trial investigates (NCT03739931) intra-tumoral injection of mRNA-2752 encoding three cytokines OX40L/IL23/IL36γ along with anti-PD-L1 antibody durvalumab in patients with solid tumors or lymphoma. Preliminary analyses showed

dose-limiting toxicity (due to cytokine release syndrome) in one of thirty patients receiving 8mg mRNA-2752, increased cytokine IFNγ and TNFα expression in both tumor and plasma, and partial responses in two of the forty-five patients, highlighting some potential (as well as limitations) of this approach (44).

5 Development of mRNA vaccines against melanoma

Melanoma arises from pigment-producing melanocytes and is the most aggressive form of skin cancer. It is the 5th most common form of cancer in the US and is affected by both environmental (exposure to UV radiation) and host (pigmentation characteristics, immunosuppression, hereditary) factors (45). While the early form of melanoma is readily curable through resection, the five-year survival rate for Stage 4 melanoma is only 34% (46), although recent therapeutic progress has begun to improve prognosis. As cutaneous melanoma typically harbors a relatively high mutational burden (and therefore, potentially immunogenic neo-epitopes) and is readily accessible, multiple immunotherapies have been developed in the past decade. CPI has been shown to significantly prolong survival in patients with advanced melanoma and is approved as single agent and in combination approaches by the FDA (47). Several attempts had been made to develop melanoma specific mRNA vaccines to further improve the efficacy of CPI.

Preclinical development of mRNA melanoma vaccines has been extensive. In mice, orthotopic models using B16F10 melanoma cells have been used to test vaccine candidates (48). Kreiter et al. developed an mRNA vaccine, which harbors multiple MHC class I/II-restricted neoepitopes sequenced from B16F10 cells (49). The vaccine induced potent tumor-specific CD4+ and CD8+ T-cell responses in mice and protected 60-80% from lethal tumor challenge. More recently, Chen et al. reported a novel formulation of LNP, called 113-O12B, with improved trafficking to lymph nodes as compared to liver. 113-O12 encapsulated mRNA vaccine encoding Trp2 180-188 epitope conferred complete response in 40% of mice challenged with B16F10 melanoma cells (50).

Currently, there are several LNP-formulated mRNA melanoma vaccines in clinical trial (Table 1). BNT111 is one of the lead candidates by BioNTech targeting melanoma tumor-associated antigens (NY-ESO-1, MAGE-C3, Tyrosinase and TPTE) currently in a Phase 2 trial (NCT04526899). In the prior Phase 1 trial, BNT111 was found to induce both CD4+ and/or CD8+ T cell responses in 39 of 50 patients (78%). In one arm where checkpoint inhibitor-experienced patients received both the vaccine and PD-1 targeting antibody cemiplimab, six of the 17 patients (35%) had partial responses to the regimen and two patients (12%) had stable disease (51). Two personalized mRNA cancer vaccines (Moderna vaccine mRNA-4157 and BioNTech vaccine BNT122) have also been advanced to Phase 2 clinical trials (NCT03815058, NCT03897881). While the data for BNT122 in melanoma is still pending at the time of this writing, the BioNTech vaccine platform attained promising results against pancreatic ductal adenocarcinoma (PDAC) in a Phase 1 trial, inducing neoantigen-specific T cell responses in 8 out of 16 participants (50%) from undetectable levels to a median of 2.9% in peripheral blood. In addition, those patients with *de-novo* immune responses had a significantly longer recurrence-free survival (RFS) (52). For mRNA-4157, the Phase 1 trial (NCT03313778) showed that the vaccine was well-tolerated and induced neoantigen-specific T cell responses. While the data has not been published in a peer-reviewed journal, Moderna and Merck recently announced that their Phase 2 trial (NCT03897881) comparing adjuvant treatment with mRNA-4157 in combination with pembrolizumab, reduced risk of recurrence or death in patients with stage 3 or 4 melanoma following complete resection, by 44% (HR=0.56 [95% CI, 0.31-1.08]) as compared to patients receiving pembrolizumab alone (54). mRNA-4157 has now been advanced to a Phase 3 trial where recruitment of participants will begin in 2023. While these various vaccines encode either TAA or TSA, non-coding RNA may also be used as adjuvant to enhance endogenous anti-tumor responses. CV8102 by CureVac consists of a non-capped, non-coding RNA complexed with a carrier peptide that is directly injected intratumorally to activate cellular TLR7/8 and RIG-1 pathways to enhance native immunity. In a Phase 1 trial (NCT03291002), CV8102 alone or in combination with CPI was observed to induce regression of injected and distant tumors in several subjects with melanoma (55).

6 Conclusion and prospects

Since their invention three decades ago, mRNA vaccines have come a long way with multiple advances. These include modification of nucleotides, capping, sequence engineering, purification and LNP formulation, that collectively help to overcome key barriers (thermal instability and local reactogenicity) and empower the platform to be a promising tool in our fight against cancer. The COVID-19 pandemic significantly expedited RNA vaccine development, producing a deep appreciation for its immune/adverse effect profile and comfort in designing novel vaccines for quick first-in-human studies. mRNA vaccines are unique in their ability to activate multiple arms of the immune system (B cells, CD4+ and CD8+ T cells), and preliminary (not yet published) data with the Moderna melanoma neoantigen vaccine appears promising in the Phase 2 study.

However, key challenges in the field still remain. While CD8+ T cell responses are induced by the mRNA vaccines, the magnitudes of responses in humans appear to be significantly lower than those in animal studies, corresponding to more limited anti-tumor efficacy in the context of advanced disease studies to date. Further attempts to amplify cellular responses through self-amplifying RNAs (57) or antigen design through protein engineering might further improve response rates (58–60). For neoantigen-based vaccines, only a fraction of the predicted epitopes appear effective at inducing CD8+ T-cell responses (61). Ongoing improvements with *in- silico* prediction algorithms or novel *in vitro* HLA-binding assays will likely improve antigen design and best utilize the RNA cassettes. Finally, even the best-designed vaccine might not adequately overcome the suppressive tumor microenvironment at distant metastatic sites. A multimodal approach involving vaccines, CPI and immunostimulants might work synergistically (62), and should be utilized in future trial designs to attain optimal outcomes in patients with advanced melanoma or other types of malignancies, including those with lower intrinsic mutational burdens.

TABLE 1 Summary of the recent clinical trial data with mRNA melanoma vaccines/immunotherapies.

Target/ Administration	Clinical Trial Number	Phase	Adjuvant therapy	Adverse event profile	Efficacy Profile	Reference
BNT111 (NY-ESO-1, MAGE-C3, Tyrosinase and TPTE), given I.V.	NCT02410733	I	With or without Cemiplimab	Flu-like symptom, no dose-limiting toxicity	Expansion and activation of circulating tumor-antigen-specific T cells with memory-function and strong cytotoxic activity	(51)
	NCT04526899	II			Monotherapy: 3/25 partial response, 7/25 stable disease, 1/25 complete metabolic remission; Combined with CPI: 6/17 with partial response	
BNT122 (20 tumor-associated neo-antigens against melanoma), given I.V.	NCT03815058	I	With or without Atezolizumab	1/16 with Grade III fever/ hypertension, no other Grade III or higher AE reported	*De-novo* neoantigen-specific T cell response in half (8/16) of patients, those with T-cell response had significantly longer progression-free survival than those without	(52)
BNT122 (20 tumor-associated neo-antigens against PDAC), given I.V.	NCT04161755	I				
mRNA-4157 (multiple tumor-associated neo-antigens against solid malignancy), given I.M.	NCT03313778	I	With or without pembrolizumab	No Grade III or higher AE reported; no dose-limiting toxicity observed	Neoantigen specific T cell responses have been detected by IFN-γ ELISpot from PBMCs.	(53)
mRNA-4157 (multiple tumor-associated neo-antigens against melanoma), given I.M.	NCT03897881	II	With pembrolizumab	Serious treatment-related adverse events occurred in 14.4% of patients who received the combination arm of mRNA-4157/V940 and KEYTRUDA versus 10% with KEYTRUDA alone	Adjuvant treatment of mRNA-4157 in combination with pembrolizumab reduced the risk of recurrence or death in patients with metastatic melanoma by 44% (HR=0.56 [95% CI, 0.31-1.08]) as compared to patients receiving pembrolizumab alone	(54)
CV8102 (non-coding, non-capped RNA), given intratumorally	NCT03291002	I	With or without anti-PD-1 antibodies	Most frequent AEs were Grade 1/2, including fatigue, fever, chills, and headache	Increased intra-tumoral T cell infiltration in 4/8 patients receiving CV8102 alone, and 10/18 patients receiving CV8102, and anti-PD-1 therapy	(55)
mRNA-2752 (three cytokines OX40L/IL23/ IL36γ), given intratumorally in patients with lymphoma and solid tumors including melanoma	NCT03739931	I	With or without durvalumab	Dose-limiting toxicity (due to cytokine release syndrome) in one of thirty patients receiving 8 mg	Increased IFNγ and TNFα expression in both tumor and plasma; Partial responses in 2/45 patients (DLBCL and squamous-cell bladder carcinoma); 15/45 patients with stable disease	(56)

Author contributions

ZX was involved in conceptualization, writing, and revision of the manuscript. DF was involved in conceptualization, writing, and revision of the manuscript. All authors contributed to the article and approved the submitted version.

Funding

The following funding agencies for support of research in the Fisher Lab: NIH (R01AR072304, R01AR043369; P01CA163222; R01CA222871), US Department of Defense Melanoma Academy Leadership Award, and the Dr. Miriam and Sheldon G. Adelson Medical Research Foundation.

Acknowledgments

The authors gratefully acknowledge Dr. Tamar Babila-Propp for review of the manuscript.

Conflict of interest

DF has a financial interest in Soltego, a company developing salt inducible kinase inhibitors for topical skin-darkening treatments

that might be used for a broad set of human applications. The interests of DF were reviewed and are managed by Massachusetts General Hospital and Partners HealthCare in accordance with their conflict-of-interest policies.

The other author declare that the research was conducted in the absence of any commercial or financial relationships that could be construed as a potential conflict of interest.

Publisher's note

References

1. Thallinger C, Fureder T, Preusser M, Heller G, Mullauer L, Holler C, et al. Review of cancer treatment with immune checkpoint inhibitors : Current concepts, expectations, limitations and pitfalls. *Wien Klin Wochenschr* (2018) 130:85–91. doi: 10.1007/s00508-017-1285-9

2. Schwartzentruber DJ, Lawson DH, Richards JM, Conry RM, Miller DM, Treisman J, et al. gp100 peptide vaccine and interleukin-2 in patients with advanced melanoma. *N Engl J Med* (2011) 364:2119–27. doi: 10.1056/NEJMoa1012863

3. Liu J, Fu M, Wang M, Wan D, Wei Y, Wei X. Cancer vaccines as promising immuno-therapeutics: platforms and current progress. *J Hematol Oncol* (2022) 15:28. doi: 10.1186/s13045-022-01247-x

4. Dagan N, Barda N, Kepten E, Miron O, Perchik S, Katz MA, et al. BNT162b2 mRNA covid-19 vaccine in a nationwide mass vaccination setting. *N Engl J Med* (2021) 384:1412–23. doi: 10.1056/NEJMoa2101765

5. Reinscheid M, Luxenburger H, Karl V, Graeser A, Giese S, Ciminski K, et al. COVID-19 mRNA booster vaccine induces transient CD8+ T effector cell responses while conserving the memory pool for subsequent reactivation. *Nat Commun* (2022) 13:4631. doi: 10.1038/s41467-022-32324-x

6. Wolff JA, Malone RW, Williams P, Chong W, Acsadi G, Jani A, et al. Direct gene transfer into mouse muscle in vivo. *Science* (1990) 247:1465–8. doi: 10.1126/science.1690918

7. Martinon F, Krishnan S, Lenzen G, Magne R, Gomard E, Guillet JG, et al. Induction of virus-specific cytotoxic T lymphocytes *in vivo* by liposome-entrapped mRNA. *Eur J Immunol* (1993) 23:1719–22. doi: 10.1002/eji.1830230749

8. Conry RM, LoBuglio AF, Loechel F, Moore SE, Sumerel LA, Barlow DL, et al. A carcinoembryonic antigen polynucleotide vaccine for human clinical use. *Cancer Gene Ther* (1995) 2:33–8.

9. Uddin MN, Roni MA. Challenges of storage and stability of mRNA-based COVID-19 vaccines. *Vaccines (Basel)* (2021) 9(9):1033. doi: 10.3390/vaccines9091033

10. Heil F, Hemmi H, Hochrein H, Ampenberger F, Kirschning C, Akira S, et al. Species-specific recognition of single-stranded RNA *via* toll-like receptor 7 and 8. *Science* (2004) 303:1526–9. doi: 10.1126/science.1093620

11. Nance KD, Meier JL. Modifications in an emergency: The role of N1-methylpseudouridine in COVID-19 vaccines. *ACS Cent Sci* (2021) 7:748–56. doi: 10.1021/acscentsci.1c00197

12. Morais P, Adachi H, Yu YT. The critical contribution of pseudouridine to mRNA COVID-19 vaccines. *Front Cell Dev Biol* (2021) 9:789427. doi: 10.3389/fcell.2021.789427

13. Wang SP, Deng L, Ho CK, Shuman S. Phylogeny of mRNA capping enzymes. *Proc Natl Acad Sci U.S.A.* (1997) 94:9573–8. doi: 10.1073/pnas.94.18.9573

14. Jemielity J, Fowler T, Zuberek J, Stepinski J, Lewdorowicz M, Niedzwiecka A, et al. Novel "anti-reverse" cap analogs with superior translational properties. *RNA* (2003) 9:1108–22. doi: 10.1261/rna.5430403

15. Strzelecka D, Smietanski M, Sikorski PJ, Warminski M, Kowalska J, Jemielity J. Phosphodiester modifications in mRNA poly(A) tail prevent deadenylation without compromising protein expression. *RNA* (2020) 26:1815–37. doi: 10.1261/rna.077099.120

16. Kim SC, Sekhon SS, Shin WR, Ahn G, Cho BK, Ahn JY, et al. Modifications of mRNA vaccine structural elements for improving mRNA stability and translation efficiency. *Mol Cell Toxicol* (2022) 18:1–8. doi: 10.1007/s13273-021-00171-4

17. Xia X. Detailed dissection and critical evaluation of the Pfizer/BioNTech and moderna mRNA vaccines. *Vaccines (Basel)* (2021) 9(7):734. doi: 10.3390/vaccines9070734

18. Park JW, Lagniton PNP, Liu Y, Xu RH. mRNA vaccines for COVID-19: what, why and how. *Int J Biol Sci* (2021) 17:1446–60. doi: 10.7150/ijbs.59233

19. Wayment-Steele HK, Kim DS, Choe CA, Nicol JJ, Wellington-Oguri R, Watkins AM, et al. Theoretical basis for stabilizing messenger RNA through secondary structure design. *bioRxiv* (2021). doi: 10.1101/2020.08.22.262931

20. Cao J, Novoa EM, Zhang Z, Chen WCW, Liu D, Choi GCG, et al. High-throughput 5' UTR engineering for enhanced protein production in non-viral gene therapies. *Nat Commun* (2021) 12:4138. doi: 10.1038/s41467-021-24436-7

21. Liu T, Liang Y, Huang L. Development and delivery systems of mRNA vaccines. *Front Bioeng Biotechnol* (2021) 9:718753. doi: 10.3389/fbioe.2021.718753

22. Jain R, Frederick JP, Huang EY, Burke KE, Mauger DM, Andrianova EA, et al. MicroRNAs enable mRNA therapeutics to selectively program cancer cells to self-destruct. *Nucleic Acid Ther* (2018) 28:285–96. doi: 10.1089/nat.2018.0734

23. de Bouteiller O, Merck E, Hasan UA, Hubac S, Benguigui B, Trinchieri G, et al. Recognition of double-stranded RNA by human toll-like receptor 3 and downstream receptor signaling requires multimerization and an acidic pH. *J Biol Chem* (2005) 280:38133–45. doi: 10.1074/jbc.M507163200

24. Kariko K, Muramatsu H, Ludwig J, Weissman D. Generating the optimal mRNA for therapy: HPLC purification eliminates immune activation and improves translation of nucleoside-modified, protein-encoding mRNA. *Nucleic Acids Res* (2011) 39:e142. doi: 10.1093/nar/gkr695

25. Baiersdorfer M, Boros G, Muramatsu H, Mahiny A, Vlatkovic I, Sahin U, et al. A facile method for the removal of dsRNA contaminant from *In vitro*-transcribed mRNA. *Mol Ther Nucleic Acids* (2019) 15:26–35. doi: 10.1016/j.omtn.2019.02.018

26. Pardi N, Hogan MJ, Porter FW, Weissman D. mRNA vaccines - a new era in vaccinology. *Nat Rev Drug Discovery* (2018) 17:261–79. doi: 10.1038/nrd.2017.243

27. Sebastian M, Schroder A, Scheel B, Hong HS, Muth A, von Boehmer L, et al. A phase I/IIa study of the mRNA-based cancer immunotherapy CV9201 in patients with stage IIIB/IV non-small cell lung cancer. *Cancer Immunol Immunother* (2019) 68:799–812. doi: 10.1007/s00262-019-02315-x

28. Tenchov R, Bird R, Curtze AE, Zhou Q. Lipid nanoparticles horizontal line from liposomes to mRNA vaccine delivery, a landscape of research diversity and advancement. *ACS Nano* (2021) 15:16982–7015. doi: 10.1021/acsnano.1c04996

29. Alameh MG, Tombacz I, Bettini E, Lederer K, Sittplangkoon C, Wilmore JR, et al. Lipid nanoparticles enhance the efficacy of mRNA and protein subunit vaccines by inducing robust T follicular helper cell and humoral responses. *Immunity* (2021) 54:2877–2892.e7. doi: 10.1016/j.immuni.2021.11.001

30. Rurik JG, Tombacz I, Yadegari A, Mendez Fernandez PO, Shewale SV, Li L, et al. CAR T cells produced *in vivo* to treat cardiac injury. *Science* (2022) 375:91–6. doi: 10.1126/science.abm0594

31. Mulligan MJ, Lyke KE, Kitchin N, Absalon J, Gurtman A, Lockhart S, et al. Phase I/II study of COVID-19 RNA vaccine BNT162b1 in adults. *Nature* (2020) 586:589–93. doi: 10.1038/s41586-020-2639-4

32. Polack FP, Thomas SJ, Kitchin N, Absalon J, Gurtman A, Lockhart S, et al. Safety and efficacy of the BNT162b2 mRNA covid-19 vaccine. *N Engl J Med* (2020) 383:2603–15. doi: 10.1056/NEJMoa2034577

33. Baden LR, El Sahly HM, Essink B, Kotloff K, Frey S, Novak R, et al. Efficacy and safety of the mRNA-1273 SARS-CoV-2 vaccine. *N Engl J Med* (2021) 384:403–16. doi: 10.1056/NEJMoa2035389

34. Risk M, Hayek SS, Schiopu E, Yuan L, Shen C, Shi X, et al. COVID-19 vaccine effectiveness against omicron (B.1.1.529) variant infection and hospitalisation in patients taking immunosuppressive medications: a retrospective cohort study. *Lancet Rheumatol* (2022) 4:e775–84. doi: 10.1016/S2665-9913(22)00216-8

35. Woldemeskel BA, Garliss CC, Blankson JN. SARS-CoV-2 mRNA vaccines induce broad CD4+ T cell responses that recognize SARS-CoV-2 variants and HCoV-NL63. *J Clin Invest* (2021) 131:e149335. doi: 10.1172/JCI149335

36. Hogan MJ, Pardi N. mRNA vaccines in the COVID-19 pandemic and beyond. *Annu Rev Med* (2022) 73:17–39. doi: 10.1146/annurev-med-042420-112725

37. Oberhardt V, Luxenburger H, Kemming J, Schulien I, Ciminski K, Giese S, et al. Rapid and stable mobilization of CD8(+) T cells by SARS-CoV-2 mRNA vaccine. *Nature* (2021) 597:268–73. doi: 10.1038/s41586-021-03841-4

38. Papachristofilou A, Hipp MM, Klinkhardt U, Fruh M, Sebastian M, Weiss C, et al. Phase ib evaluation of a self-adjuvanted protamine formulated mRNA-based active cancer immunotherapy, BI1361849 (CV9202), combined with local radiation treatment in patients with stage IV non-small cell lung cancer. *J Immunother Cancer* (2019) 7:38. doi: 10.1186/s40425-019-0520-5

39. Sultan H, Trillo-Tinoco J, Rodriguez P, Celis E. Effective antitumor peptide vaccines can induce severe autoimmune pathology. *Oncotarget* (2017) 8:70317–31. doi: 10.18632/oncotarget.19688

40. Ugel S, Peranzoni E, Desantis G, Chioda M, Walter S, Weinschenk T, et al. Immune tolerance to tumor antigens occurs in a specialized environment of the spleen. *Cell Rep* (2012) 2:628–39. doi: 10.1016/j.celrep.2012.08.006

41. Klinghammer K, Saba NF, Castelluci E, Colevas AD, Rutkowski T, Greil R, et al. 155P BNT113 + pembrolizumab as first-line treatment in patients with unresectable recurrent/metastatic HNSCC: Preliminary safety data from AHEAD-MERIT. *Immuno-Oncol Technol* (2022) 16:100267. doi: 10.1016/j.iotech.2022.100267

42. Nagasaka M. ES28.04 emerging mechanisms to target KRAS directly. *J Thorac Oncol* (2021) 16:S96–7.

43. Cafri G, Gartner JJ, Zaks T, Hopson K, Levin N, Paria BC, et al. mRNA vaccine-induced neoantigen-specific T cell immunity in patients with gastrointestinal cancer. *J Clin Invest* (2020) 130:5976–88. doi: 10.1172/JCI134915

44. Hewitt SL, Bai A, Bailey D, Ichikawa K, Zielinski J, Karp R, et al. Durable anticancer immunity from intratumoral administration of IL-23, IL-36gamma, and OX40L mRNAs. *Sci Transl Med* (2019) 11(477):eaat9143. doi: 10.1126/scitranslmed.aat9143

45. Watson M, Holman DM, Maguire-Eisen M. Ultraviolet radiation exposure and its impact on skin cancer risk. *Semin Oncol Nurs* (2016) 32:241–54. doi: 10.1016/j.soncn.2016.05.005

46. Hamid O, Robert C, Daud A, Hodi FS, Hwu WJ, Kefford R, et al. Five-year survival outcomes for patients with advanced melanoma treated with pembrolizumab in KEYNOTE-001. *Ann Oncol* (2019) 30:582–8. doi: 10.1093/annonc/mdz011

47. Huang AC, Zappasodi R. A decade of checkpoint blockade immunotherapy in melanoma: understanding the molecular basis for immune sensitivity and resistance. *Nat Immunol* (2022) 23:660–70. doi: 10.1038/s41590-022-01141-1

48. Hill RP, Chambers AF, Ling V, Harris JF. Dynamic heterogeneity: rapid generation of metastatic variants in mouse B16 melanoma cells. *Science* (1984) 224:998–1001. doi: 10.1126/science.6719130

49. Kreiter S, Vormehr M, van de Roemer N, Diken M, Lower M, Diekmann J, et al. Mutant MHC class II epitopes drive therapeutic immune responses to cancer. *Nature* (2015) 520:692–6. doi: 10.1038/nature14426

50. Chen J, Ye Z, Huang C, Qiu M, Song D, Li Y, et al. Lipid nanoparticle-mediated lymph node-targeting delivery of mRNA cancer vaccine elicits robust CD8(+) T cell response. *Proc Natl Acad Sci U.S.A.* (2022) 119:e2207841119. doi: 10.1073/pnas.2207841119

51. Sahin U, Oehm P, Derhovanessian E, Jabulowsky RA, Vormehr M, Gold M, et al. An RNA vaccine drives immunity in checkpoint-inhibitor-treated melanoma. *Nature* (2020) 585:107–12. doi: 10.1038/s41586-020-2537-9

52. Balachandran VP, Rojas LA, Sethna Z, Soares K, Derhovanessian E, Mueller F, et al. Phase I trial of adjuvant autogene cevumeran, an individualized mRNA neoantigen vaccine, for pancreatic ductal adenocarcinoma. *J Clin Oncol* (2022) 40:2516–6. doi: 10.1200/JCO.2022.40.16_suppl.2516

53. Burris HA, Patel MR, Cho DC, Clarke JM, Gutierrez M, Zaks TZ, et al. A phase I multicenter study to assess the safety, tolerability, and immunogenicity of mRNA-4157 alone in patients with resected solid tumors and in combination with pembrolizumab in patients with unresectable solid tumors. *J Clin Oncol* (2019) 37:2523–3. doi: 10.1200/JCO.2019.37.15_suppl.2523

54. Merck. *Moderna and Merck announce mRNA-4157/V940, an investigational personalized mRNA cancer vaccine, in combination with KEYTRUDA® (pembrolizumab), met primary efficacy endpoint in phase 2b KEYNOTE-942 trial* (2022). Available at: https://www.merck.com/news/moderna-and-merck-announce-mrna-4157-v940-an-investigational-personalized-mrna-cancer-vaccine-in-combination-with-keytruda-pembrolizumab-met-primary-efficacy-endpoint-in-phase-2b-keynote-94/.

55. Eigentler T, Bauernfeind FG, Becker JC, Brossart P, Fluck M, Heinzerling L, et al. A phase I dose-escalation and expansion study of intratumoral CV8102 as single-agent or in combination with anti-PD-1 antibodies in patients with advanced solid tumors. *J Clin Oncol* (2020) 38:3096–6. doi: 10.1200/JCO.2020.38.15_suppl.3096

56. Patel MR, Bauer TM, Jimeno A, Wang D, LoRusso P, Do KT, et al. A phase I study of mRNA-2752, a lipid nanoparticle encapsulating mRNAs encoding human OX40L, IL-23, and IL-36γ, for intratumoral (iTu) injection alone and in combination with durvalumab. *J Clin Oncol* (2020) 38:3092–2. doi: 10.1200/JCO.2020.38.15_suppl.3092

57. Blakney AK, Ip S, Geall AJ. An update on self-amplifying mRNA vaccine development. *Vaccines (Basel)* (2021) 9(2):97. doi: 10.3390/vaccines9020097

58. Xu Z, Wise MC, Chokkalingam N, Walker S, Tello-Ruiz E, Elliott STC, et al. *In vivo* assembly of nanoparticles achieved through synergy of structure-based protein engineering and synthetic DNA generates enhanced adaptive immunity. *Adv Sci (Weinh)* (2020) 7:1902802. doi: 10.1002/advs.201902802

59. Irvine DJ, Dane EL. Enhancing cancer immunotherapy with nanomedicine. *Nat Rev Immunol* (2020) 20:321–34. doi: 10.1038/s41577-019-0269-6

60. Xu Z, Chokkalingam N, Tello-Ruiz E, Wise MC, Bah MA, Walker S, et al. A DNA-launched nanoparticle vaccine elicits CD8(+) T-cell immunity to promote *In vivo* tumor control. *Cancer Immunol Res* (2020) 8:1354–64. doi: 10.1158/2326-6066.CIR-20-0061

61. Esprit A, de Mey W, Bahadur Shahi R, Thielemans K, Franceschini L, Breckpot K. Neo-antigen mRNA vaccines. *Vaccines (Basel)* (2020) 8(4):776. doi: 10.3390/vaccines8040776

62. Moynihan KD, Opel CF, Szeto GL, Tzeng A, Zhu EF, Engreitz JM, et al. Eradication of large established tumors in mice by combination immunotherapy that engages innate and adaptive immune responses. *Nat Med* (2016) 22:1402–10. doi: 10.1038/nm.4200

frontiers | Frontiers in Immunology

TYPE Review
PUBLISHED 02 November 2023
DOI 10.3389/fimmu.2023.1285113

OPEN ACCESS

EDITED BY
Björn L. Frendéus,
BioInvent, Sweden

REVIEWED BY
Marc Garcia-Moure,
University of Texas MD Anderson Cancer Center, United States
Rui Guo,
Jilin University, China
Gao Zhang,
The University of Hong Kong, Hong Kong SAR, China

*CORRESPONDENCE
Yaohui Chen
mcb.chenyaohui@gmail.com

†These authors have contributed equally to this work and share first authorship

RECEIVED 29 August 2023
ACCEPTED 18 October 2023
PUBLISHED 02 November 2023

CITATION
Hu M, Liao X, Tao Y and Chen Y (2023) Advances in oncolytic herpes simplex virus and adenovirus therapy for recurrent glioma.
Front. Immunol. 14:1285113.
doi: 10.3389/fimmu.2023.1285113

Advances in oncolytic herpes simplex virus and adenovirus therapy for recurrent glioma

Mingming Hu[1,2†], XuLiang Liao[1,2†], Yi Tao[1,2†] and Yaohui Chen[1,3*]

[1]Institute of Thoracic Oncology, West China Hospital, Sichuan University, Chengdu, China, [2]Frontiers Science Center for Disease-Related Molecular Network, West China Hospital, Sichuan University, Chengdu, China, [3]Department of Thoracic Surgery, West China Hospital, Sichuan University, Chengdu, China

Recurrent glioma treatment is challenging due to molecular heterogeneity and treatment resistance commonly observed in these tumors. Researchers are actively pursuing new therapeutic strategies. Oncolytic viruses have emerged as a promising option. Oncolytic viruses selectively replicate within tumor cells, destroying them and stimulating the immune system for an enhanced anticancer response. Among Oncolytic viruses investigated for recurrent gliomas, oncolytic herpes simplex virus and oncolytic adenovirus show notable potential. Genetic modifications play a crucial role in optimizing their therapeutic efficacy. Different generations of replicative conditioned oncolytic human adenovirus and oncolytic HSV have been developed, incorporating specific modifications to enhance tumor selectivity, replication efficiency, and immune activation. This review article summarizes these genetic modifications, offering insights into the underlying mechanisms of Oncolytic viruses' therapy. It also aims to identify strategies for further enhancing the therapeutic benefits of Oncolytic viruses. However, it is important to acknowledge that additional research and clinical trials are necessary to establish the safety, efficacy, and optimal utilization of Oncolytic viruses in treating recurrent glioblastoma.

KEYWORDS

oncolytic viruses, cancer therapy, recurrent gliomas, oncolytic herpes simplex virus, adenovirus therapy

1 Introduction

Gliomas, specifically glioblastomas (GBM), represent a majority of central nervous system malignancies and are the most common primary brain tumors. Gliomas originate from glial or progenitor cells and are classified into four grades by the World Health Organization (WHO). Glioblastoma (GBM), the most aggressive primary brain tumor in adults, accounts for 16% of all central nervous system tumors (1). It is classified as a grade 4 glioma according to the WHO grading system (2). The standard treatment for GBM includes surgical therapy, radiation therapy, and temozolomide (TMZ) therapy (3). Combining TMZ with radiation therapy can raise the 2-year survival rate to 26.5%,

compared to a lower rate of 10.4% with radiation therapy alone (4). However, despite the use of surgical intervention, postoperative radiotherapy, and chemotherapy, GBM remains highly invasive, leading to metastasis, recurrence, and mortality (5). The median survival time for GBM patients is approximately 15 months (1), with minimal likelihood of resurgery for relapsed cases (6–9). Recurrent glioblastoma (rGBM) presents a significant challenge in neurooncology, characterized by increased tumor cell density, neovascularization, blood-brain barrier disruption, permeability, tortuous neovascularization, uneven thickness, and slow blood flow. The pathophysiological mechanism underlying pseudoprogression remains unclear; however, it is believed to involve vascular endothelial, blood-brain barrier, and oligodendrocyte damage, leading to local inflammation, increased blood-brain barrier permeability, and vasogenic edema, resulting in abnormal lesion enhancement on imaging. Surgical resection is often impractical for recurrent tumors, which demonstrate reduced therapy responsiveness and invasion into functional brain areas (4–10). Consequently, median overall survival (mOS) after relapse is approximately 6 months, with no established standard treatment for rGBM, leading to patient mortality within 12-15 months of initial diagnosis (10, 11). RGBM often exhibits resistance to temozolomide (TMZ, a DNA alkylating agent), the standard GBM chemotherapy agent (4). Despite advancements in genetic studies of GBM, no molecular targeting agent has been identified to prolong OS in patients with rGBM.

Tumor immunotherapy is a promising approach to activating specific immune responses against cancer cells within the body, offering the advantages of targeted, efficient treatment with reduced harm to healthy tissues. Unlike conventional methods like surgery, targeting, radiotherapy, and chemotherapy, immunotherapy does not directly eliminate cancer cells. Instead, it mobilizes immune cells capable of recognizing tumors, enhances the body's immune system's ability to combat cancer, and relies on these cells to indirectly control and eliminate cancer cells. This strategy has minimal side effects, ensuring safety and efficacy (12). Immunotherapy, including immune checkpoint inhibitors, has shown efficacy in clinical trials for various tumor types (13). However, its effectiveness in patients with recurrent glioma is limited due to factors such as the tumor heterogeneity of GBM, the presence of the blood-brain barrier, and the immunosuppressive nature of the tumor microenvironment (TME)[(14). Glioma, a tumor with heterogeneous characteristics including proliferative potential, invasiveness, histological grade, and clinical behavior, presents a significant challenge for immunotherapy (15). Studies have highlighted the obstacles caused by glioma cells' immune evasion mechanisms, such as antigen loss or downregulation, which hinder vaccine therapy and CAR-T cell therapy (16). Moreover, the glioma tumor microenvironment contains more immunosuppressive cells than immune effector cells, contributing to the establishment of an immunosuppressive state that promotes glioma growth, invasion, and metastasis (17). Conversely, oncolytic virus (OVs) therapy exhibits promise in early clinical trials for GBM. OVs can selectively infect and destroy tumor cells while modulating the immune system to enhance the anti-tumor response (18).

OVs represent a form of immunotherapy that selectively infect and destroy cancer cells, leading to the release of infectious virus particles that contribute to the destruction of residual tumors. These viruses can impede cancer cell replication or be genetically modified to specifically target and eliminate them. Moreover, OVs have the ability to activate the suppressed immune system, resulting in an adaptive anti-tumor immune response while suppressing tumor growth (19). Both preclinical and clinical trials have evaluated OVs derived from herpes simplex virus-1 (HSV-1), adenovirus (Ad), Newcastle disease virus (NDV), and reovirus (RV) for the treatment of rGBM, demonstrating promising therapeutic effects. However, further clinical trials are necessary to validate these findings.

This review aims to provide an overview of the oncolytic mechanisms of different OVs, including oHSV, CRAd, and others (Figure 1). Additionally, we discuss the survival benefits and safety profiles based on major preclinical and clinical trials of oncolytic viruses in glioma, specifically rGBM (Table 1). Currently, PVS-RIPO and DNX-2401 have received fast track designation from the US Food and Drug Administration (FDA), while G47Δ has been approved by the Japanese Ministry of Health, Labor and Welfare for the treatment of malignant glioma. Furthermore, numerous other OVs have demonstrated significant anti-tumor potential in both preclinical and clinical trials. Our goal is to provide a reference for researchers involved in the development of novel OVs, facilitate improved clinical trials for OVs, and offer valuable recommendations for the application of OVs in glioma treatment.

2 Oncolytic herpes simplex virus (oHSV)

HSV-1, an enveloped double-stranded DNA virus belonging to the Herpesviridae family, primarily infects and replicates in nervous tissue. Its antitumor activity was first observed in the 1950s when cancer patients with concurrent viral infections experienced tumor reduction (20). As a result, researchers explored different newly discovered viruses as potential cancer treatments. However, these therapies often caused significant toxicity to healthy tissues alongside tumor reduction, leading to a decline in the pursuit of viral-based cancer treatments (21). In 1989, Robert Martuza reported the inactivation of HSV-1 virus using the thymidine kinase gene. Subsequent treatment of glioma-bearing mice with this modified virus demonstrated no encephalitis. This discovery marked a turning point, making OVs a viable therapeutic option for GBM (22). To enhance safety and specificity, successive generations of OVs have been developed through genetic modification of the original HSV-1 wild type virus (Figure 2).

2.1 The first-generation oHSV lacking self-replication ability

2.1.1 dlsptk HSV

The first modified version of herpes simplex virus (HSV), called dlsptk HSV, was developed in 1989 by Coen (23) and Martuza published the use of HSV dlsptk in 1991 (22). This engineered virus lacks the thymidine kinase protein (TK), which is necessary for viral replication in non-dividing cells. Studies by T. Valyi-Nagy showed

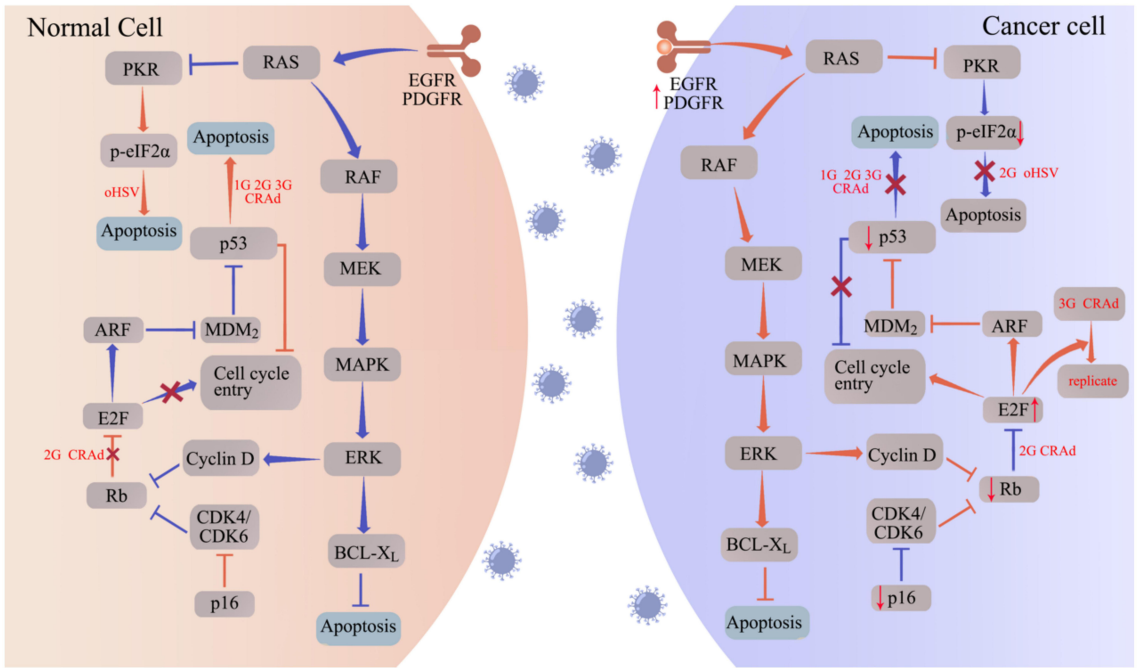

FIGURE 1
oHSV and CRAd replicate specifically in tumor cells by targeting tumor-associated pathways. Aberrantly expressed proteins in tumor cells promote the replication and oncolytic activity of oHSV and CRAd. In normal cells (left panel), the cell cycle is regulated by proteins such as protein kinase R (PKR), p16, retinoblastoma (Rb), and the tumor suppressor p53. Upon infection with oHSV and CRAd, these cell cycle regulators facilitate apoptosis, hindering viral replication. Conversely, cancer cells often exhibit disruptions in these cell cycle regulators, such as p53 and Rb mutations, to support uncontrolled proliferation. Consequently, when infected with oHSV and CRAd, cancer cells fail to initiate the apoptotic program, allowing for viral replication within the tumor cells. The abbreviations used in the figure are as follows: 1G/2G/3G oHSV refers to first generation, second generation, and third-generation oHSV respectively; 1G/2G/3G CRAd stands for first generation, second generation, and third-generation CRAD; CDK represents cyclin-dependent kinase; EGFR denotes epidermal growth factor receptor; ERK signifies extracellular signal-regulated kinase; MAPK refers to mitogen-activated protein kinase; MEK stands for MAPK/ERK kinase; PDGFR represents platelet-derived growth factor receptor.

that dlsptk HSV significantly extended the survival of mice with subcutaneous and orthotopic tumor models (24). However, it's important to note that this modified virus still poses a risk of infection in immunocompromised patients. To ensure patient safety, alternative modifications of HSV-1 have been explored for tumor therapy.

2.1.2 hrR3

The hrR3 mutant of HSV-1 was created by deleting ICP6 (UL39), the gene responsible for encoding the large subunit of viral ribonucleotide reductase. This enzyme plays a vital role in converting ribonucleotides to deoxyribonucleotides (dNMP) needed for viral genome synthesis. As a result, the absence of ICP6 in HSV-1 limits the availability of dNMP, thereby restricting the replication of hrR3 mutants to actively proliferating cells (25). Studies have shown that the mutant has considerable anti-cancer prospects. In previous studies, hrR3 showed a strong killing effect on human glioblastoma cell line cells, and in animal experiments, treatment with 5×10^6 hrR3 plaque forming units showed a significant inhibitory effect on tumor growth (26). Experiments in which mutant herpes simplex virus 1 (hrR3) was injected into gliomas implanted in the brain of rats showed the lack of efficacy of hrR3 in the eradication of cancer due to interference of the immune system (27). As oHSV is further modified, safer and more effective oHSVs are made.

2.2 The second generation oHSV designed to target tumor cells with PKR-eIF2α mutations

The presence of the γ34.5 protein is crucial for assessing the neuropathogenicity of HSV. In normal cells, HSV infection triggers the phosphorylation of eIF2α by the cell's protein kinase R (PKR), which prevents viral protein synthesis. However, the γ34.5 complex of HSV counteracts this process by dephosphorylating eIF2α, allowing wild-type HSV to replicate effectively in these cells. On the other hand, if γ34.5 is deleted from HSV, the modified virus loses its ability to replicate in normal cells. Interestingly, in cancer cells with a defective antiviral PKR-eIF2α pathway, deleting γ34.5 enables selective replication of HSV in these cells (28, 29). ICP6 is a large subunit of ribonucleotide reductase (RR) that is critical for viral replication and growth in nondividing cells. By deleting γ34.5 and inactivating ICP6, a safer second-generation oHSV was generated. Proliferation of the second-generation oHSV was restricted to tumor cells with PKR-eIF2α mutations.

2.2.1 G207

G207 was generated by inserting the Escherichia coli lacZ gene into the coding sequence of viral ICP6 (UL39) and deleting two copies of the γ34.5 (RL1) locus in the viral genome (30). The ICP6 gene encodes the vital RR subunit essential for viral replication in

TABLE 1 OVs clinical trials.

Trial Number	Phase	Virus	Other Treatments	Target	Status	Start Date	Country	Report	numbers
	I	G207		Brain malignant glial tumor	completed	Feb, 1998 - May 1999			21
NCT00157703	Ib	G207		recurrent/progressive malignant glioma.	completed	Jan, 2002 - Aug, 2003	USA	Mol Ther.2014 May	6
NCT02457845	I	G207	radiation (5 Gy)	Recurrent Supratentorial Brain Tumors in Children	Active, not recruiting	May 2016-	USA		13
NCT02031965	I	HSV1716	dexamethasone; therapeutic conventional surgery	Refractory or Recurrent HGG	Terminated	Dec 2013-May 2016	USA		2
NCT03152318	I	rQNestin34.5v.2	Cyclophosphamide(CPA)	recurrent malignant glioma	Recruiting	July 18, 2017-	USA		62
UMIN-CTR: UMIN000002661	I/II	G47Δ		recurrent or progressive glioblastoma	completed	Nov, 2009- Nov, 2014	Japan	2022 Jul 21.	13
UMIN-CTR: UMIN000015995	II	G47Δ		Residual or recurrent glioblastoma	Active, not recruiting	Dec, 2014-	Japan		
	I	ONYX-015		malignant glioma	completed	Jan, 2000 - May 2002	USA	2004年11月	24
	II	ONYX-015	5-FU; cisplatin	recurrent head and neck cancer	completed		USA	2000年8月	37
NCT00805376	I	DNX-2401		Recurrent Malignant GBM	completed	Feb, 2009-Feb, 2015	USA	2018.5	37
NCT03178032	I/II	DNX-2401		Diffuse pontine GBM (DIPG)	completed	May, 2017-Jan, 2021	Spain		12
NCT01956734	Ib	DNX-2401	TMZ	Glioblastoma at First Recurrent	completed	Sep, 2013-Mar, 2017	Spain		31
NCT02197169	Ib	DNX-2401	IFN-γ	GBM and gliosarcoma (GS)	completed	July, 2014-July 2018	USA		37
NCT03714334	I	DNX-2440		Patients with first or second recurrence of GBM	Terminated (Break of stock)	Oct, 2018–	Spain		16
NCT02798406	II	DNX-2401	pembrolizumab	GBM and GS	completed	Jun 14, 2016- Jul 15, 2021	USA and Canada	2023 Jun	49
NCT02444546	I	Pelareore	GM-CSF	Pediatric Patients with Relapsed or Refractory Brain Tumors	Completed	Jun 21, 2015-Nov, 2022	USA		6
NCT01491893	I	Pelareore		Recurrent WHO Grade IV Malignant Glioma	Completed	Apr, 2012-Oct, 2021	USA	2018.7	61
NCT03043391	I	PVSRIPO		recurrent WHO grade III or IV malignant glioma in pediatric patients	Active, not recruiting	Dec, 2017-	USA		12

(Continued)

10.3389/fimmu.2023.1285113

10.3389/fimmu.2023.1285113

TABLE 1 Continued

Trial Number	Phase	Virus	Other Treatments	Target	Status	Start Date	Country	Report	numbers
NCT02986178	II	PVSRIPO		recurrent WHO grade IV malignant glioma in adults	Active, not recruiting	June 1, 2017-	USA		122
NCT01470794	I	Toca 511	Toca FC	rHGG	Completed	February 2012-April 12, 2016	USA	2018 Sep	58
NCT01156584	I	Toca 511	Toca FC	rHGG	Completed	July 2010-August 18, 2016	USA		54
NCT01985256	I	Toca 511	Toca FC	recurrent or progressive Grade III or Grade IV GBM	Completed	February 2014-March 3, 2016	USA		17

non-dividing cells. Removing these genes restricts HSV-1 G207 proliferation to tumor cells (30). In preclinical animal models, the efficacy of G207 has been extensively demonstrated. Administration of 10^9 plaque forming units (pfu) of G207 in BALB/c mice and Aotus nancymai owl monkeys' brains showed no adverse effects (31). Remarkably, whereas 10^3 pfu of wild-type HSV-1 proves lethal for Aotus nancymai owl monkeys, G207 has exhibited safety. Magnetic resonance imaging and histopathological evaluation of these primates revealed no central nervous system abnormalities, cell structure alterations, or presence of HSV immune response cells. These findings preliminarily verify the safety of G207 (32).

Markert et al. conducted a phase I clinical trial with 21 adults having advanced brain gliomas, demonstrating the safety of G207 without significant adverse effects. Tumor growth was suppressed in eight patients after one month of vaccination, and two patients achieved disease-free survival exceeding five years (33). These findings provide a strong basis for further clinical trials to explore the therapeutic potential of G207 in adults with recurrent brain gliomas. In another phase I trial implemented by James M. Markert et al., G207 combined with radiation therapy was investigated in nine patients with progressive, relapsed glioblastoma (34). The trial confirmed the safety of single-dose oncolytic HSV therapy augmented with radiation for treating malignant glioma patients. Despite observing reductions in tumor size and improved survival time, the absence of a control group necessitates additional clinical trials (NCT00157703) to establish the clinical therapeutic effect of G207.

G207 has demonstrated efficacy in treating adult patients with rGBM in multiple clinical trials. However, current research is mainly focused on assessing its effectiveness in pediatric patients with rGBM. Gregory K. Friedman conducted a phase I clinical trial (NCT02457845) to evaluate the safety, efficacy, and immune response of G207 in children with recurrent or progressive cerebellar brain tumors. The study aimed to enroll 15 participants and provide preliminary insights into using G207 to treat pediatric brain gliomas. The results showed that Intratumoral G207, alone or combined with radiation, had an acceptable adverse-event profile and exhibited evidence of responses in patients with recurrent or progressive high-grade glioma in pediatric cases. Additionally, G207 treatment converted immunologically "cold" tumors to "hot". However, the loss of γ34.5 in G207 improved safety but impaired viral replication in glioblastoma stem cells (GSC) (35).

2.2.2 HSV-1716

HSV-1716 is an example of an HSV variant that has undergone a 759-bp deletion in both copies of the ICP 34.5 gene, resulting in reduced neurotoxicity compared to the wild-type virus (36, 37). Additionally, the deletion of γ34.5 significantly limits the replication potential of HSV-1716 specifically in tumor cells.

HSV-1716 is worth noting that the antitumor effect of HSV-1716 is not solely attributed to its oncolytic activity but also to its direct anti-angiogenic properties. Through *in vitro* and *in vivo* experiments, Fabian Benencia et al. have confirmed the direct anti-angiogenic effects of the oHSV: HSV-1716 (38). One study demonstrates that HSV-1716 can specifically inhibit pediatric high-grade glioma (pHGG) and diffuse intrinsic pontine glioma

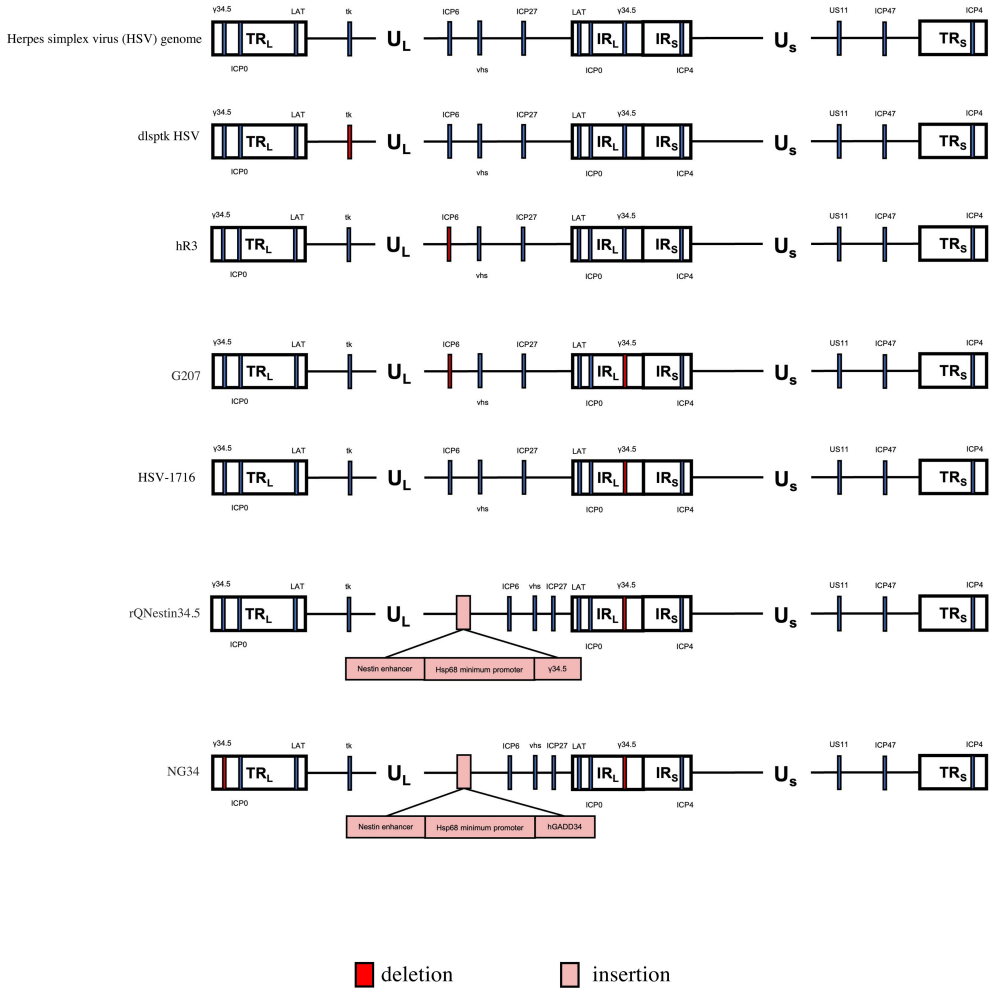

FIGURE 2
Genetic diagram of each generation of oncolytic HSV-1. The HSV-1 genome consists of long and short unique regions (UL and US) each bounded by terminal (T) and internal (I) repeat regions (R_L, and R_S). TK, thymidine kinase protein (TK). US11, unique short 11 gene. hGM-CSF, human granulocyte-macrophage colony stimulating factor gene. hGADD34, human homologue GADD34 replaces ICP34.5 for PP1 binding and eIF2a dephosphorylation. Nestin enhancer ,a glioma-specific enhancer.

(DIPG) migration and invasion, highlighting a novel mechanism of action for an OV against a principal hallmark of cancer. HSV1716 was also evaluated in this study, as it has previously been applied in early-phase trials for high-grade gliomas (39). Nine patients with high-grade glioma who had relapsed after curative treatment were treated with HSV-1716 injection to evaluate the safety of 1716 in patients with recurrent malignant glioma. The safety of HSV-1716 in the treatment of gliomas was demonstrated without toxic effects at intratumoral doses up to 10^5 p.f.u (40).. Another study involved 12 patients with rGBM who received tumor injections of 10^5 HSV1716 p.f.u. Viral replication and an immune response to HSV1716 were detected after vaccination, proving that HSV1716 replicates in rGBM and does not trigger a toxic reaction in the patient (41). S Harrowet al. enrolled 12 patients with advanced gliomas for intratumoral injection of HSV1716 to observe the treatment of HSV1716. The results showed a promising improvement in the survival of GBM patients after HSV1716 inoculation compared to the expected median survival of GBM patients (42). An additional clinical trial of HSV-1716 for glioma included two patients with recurrent pediatric glioma who underwent surgical resection. However, the results of this trial (NCT02031965) have not yet been reported.

2.2.3 rQNestin34.5 and NG34

Deletion of two copies of γ34.5 in HSV restricts its replication in tumor cells, albeit with a significant reduction in overall replicative capacity. To address this issue, Hiromasa Kambara et al. developed rQNestin34.5, a novel selective mutant of HSV-1 (43). This mutant reintroduces a single copy of γ1 34.5 into the viral genome under the control of the nestin gene enhancer (a glioma-specific enhancer) and the hsp68 promoter.*In vitro* and *in vivo* experiments demonstrated robust replication and oncolytic activity of rQNestin34.5 specifically in glioma cells (44). Safety evaluations conducted in immunized and immunodeficient mice further supported its safety profile (43). Notably, the Dana-Farber Cancer Institute is currently sponsoring a Phase I clinical trial (NCT03152318) investigating the therapeutic potential of rQnestine 34.5V. 2, a transgenic HSV-1 virus, in recurrent glioblastoma alongside cyclophosphamide-based immunoregulation.

In the absence of active nestin enhancer, transcriptional leakage and minimal functionality from the hsp68 promoter in normal CNS neuronal cells may generate a small amount of ICP34.5, potentially leading to neurotoxicity induced by rQNestin34.5 (44, 45). NG34, an enhanced version of rQNestin34.5, employs GADD34 as a substitute for ICP34.5 to bind PP1 and dephosphorylate eIF2α (46). This replacement eliminates the beclin-1 binding motif responsible for neurotoxicity and autophagy inhibition in ICP34.5 (47). In human *in situ* GBM mice, NG34 demonstrates comparable efficacy to QNestin34.5 while exhibiting reduced neurotoxicity.

Tumor cells commonly express PD-1 to suppress immune cell destruction (48, 49). Intra-tumor administration of an oHSV carrying a scFv (single chain fragment variable) antibody against PD-1 can enhance the anti-tumor immune response without compromising the virus's oncolytic efficacy. NG34scFvPD-1, obtained by modifying NG34 with CMV-controlled scFvPD-1 cDNA, has shown expression of a single-chain antibody against mouse PD-1 in animal experiments. NG34scFvPD-1 exhibits comparable oncolytic properties to NG34 *in vitro* and improved survival rates in immunoactive mice. Furthermore, immunocompetent mice develop anti-tumor immune memory, protecting against tumor metastasis (50).

2.2.4 G47Δ

The G47Δ vector, a modified version of HSV-1 based on the G207 vector, was constructed by further deleting the α47 gene. Because the expression of the α47 gene inhibits the antigen presenting (TAP) associated transporter, this deletion leads to increased MHC class I expression in infected cells, resulting in enhanced activation against tumor T cells. Additionally, G47Δ incorporates the late US11 gene under the control of the early α47 promoter, effectively suppressing the growth properties of the γ34.5 deficient mutant (51). It is noteworthy that G47Δ has obtained approval in Japan for glioblastoma treatment.

The University of Tokyo conducted a clinical study (UMIN-CTR: UMIN000002661) on G47Δ in patients with recurrent brain gliomas for the first time, specifically glioblastoma (52). This open-label, single-armed phase I-II trial aimed to assess the safety of intracranial administration of G47Δ. Subsequently, IMSUT Hospital initiated a Phase II clinical trial (UMIN-CTR: UMIN000015995) to evaluate the effectiveness and safety of G47Δ in patients with residual or recurrent glioblastoma who had previously received radiation therapy and TMZ chemotherapy. The trial involved intratumoral and repeated administration of G47Δ in 19 adult patients with rGBM. After excluding those with IDH1 mutations, among the remaining 13 patients, the one-year survival rate after G47Δ initiation was 84.2%, with a median OS of 20.2 months and a median PFS of 4.7 months. In comparison, treatment with chemotherapeutic agents resulted in a median OS of 5.0 months and a median PFS of 1.8 months. G47Δ demonstrated superior survival benefits and a favorable safety profile for treating rGBM (53). These pivotal trial findings led to the conditional and time-limited approval of G47Δ for GBM by the Ministry of Health, Labour and Welfare (MHLW) on June 11, 2021, positioning G47Δ as a potential breakthrough in glioblastoma treatment, offering improved survival outcomes and the possibility of a cure for a subset of patients. It may become the first new drug since TMZ and the first new treatment since TTF.

G47Δ is currently undergoing preclinical and clinical studies for stomach cancer, prostate cancer, and other types of cancer, where it has demonstrated superior anti-tumor efficacy compared to G207 and excellent safety characteristics. At lower multiple infection rates, G47Δ exhibits enhanced killing effects in human prostate cancer cell lines LNCaP and DU145, resulting in a 22-fold increase in viral production. Treatment with G47Δ in a mouse model of prostate cancer reduces tumor growth in established s.c. TRAMP and HONDA tumors, as well as inhibiting the recurrence of HONDA tumors previously regressed by androgen ablation therapy (54).

Furthermore, G47Δ shows promising therapeutic potential for human gastric cancer. *In vitro* experiments confirm favorable cytopathic effects and replication of G47Δ in nine tested human gastric cancer cell lines. *In vivo* intratumoral inoculation of G47Δ (at 2×10^5 or 1×10^6 pfu) significantly suppresses subcutaneous tumor growth in MKN45, MKN74, and 44As3 models (55).

In summary, these findings indicate that G47Δ may possess potent inhibitory effects on various tumor types beyond brain gliomas.

3 Adenovirus -based oncolytic viruses

Oncolytic adenovirus (also known as conditionally replicating adenovirus or CRAd) is a natural selection or genetically engineered adenovirus. Utilizing the distinguishing characteristics of tumor cells and normal cells in terms of structure and metabolic pathways, oncolytic adenovirus selectively proliferates and replicates within tumor cells, resulting in their lysis. Specifically, wild-type adenovirus has been enhanced to replicate within tumor cells and effectively lyse the target cells while minimizing its toxicity toward normal cells. At present, the third-generation of adenovirus modification for glioma treatment has been achieved. Genetically engineered or screened conditionally replicating viruses utilize aberrant molecular/genetic pathways within tumors, ensuring non-toxicity in normal cells. They are designed to replicate efficiently solely within cancer cells, leading to the lysis and destruction of the infected cancer cells (56).

Adenovirus is a nonenveloped virus with icosahedral capsid containing a 36kD double-stranded linear genome. The genome of the virus can be categorized into two distinct regions: the early gene region (E1-E4) and the late gene region. The former primarily governs viral replication and transcriptional regulation, while the latter plays a pivotal role in the synthesis of structural proteins (57). Within the early gene region, viral regulatory proteins are encoded, which play a crucial role in controlling the expression of late genes. Notably, the initial expression of E2 products, including those stemming from the E1 gene, is essential for adenovirus genome replication, virus packaging, and protein translation processes (58). Due to this significance, current genetic modification strategies for adenovirus primarily concentrate on targeting the E1 region (Figure 3).

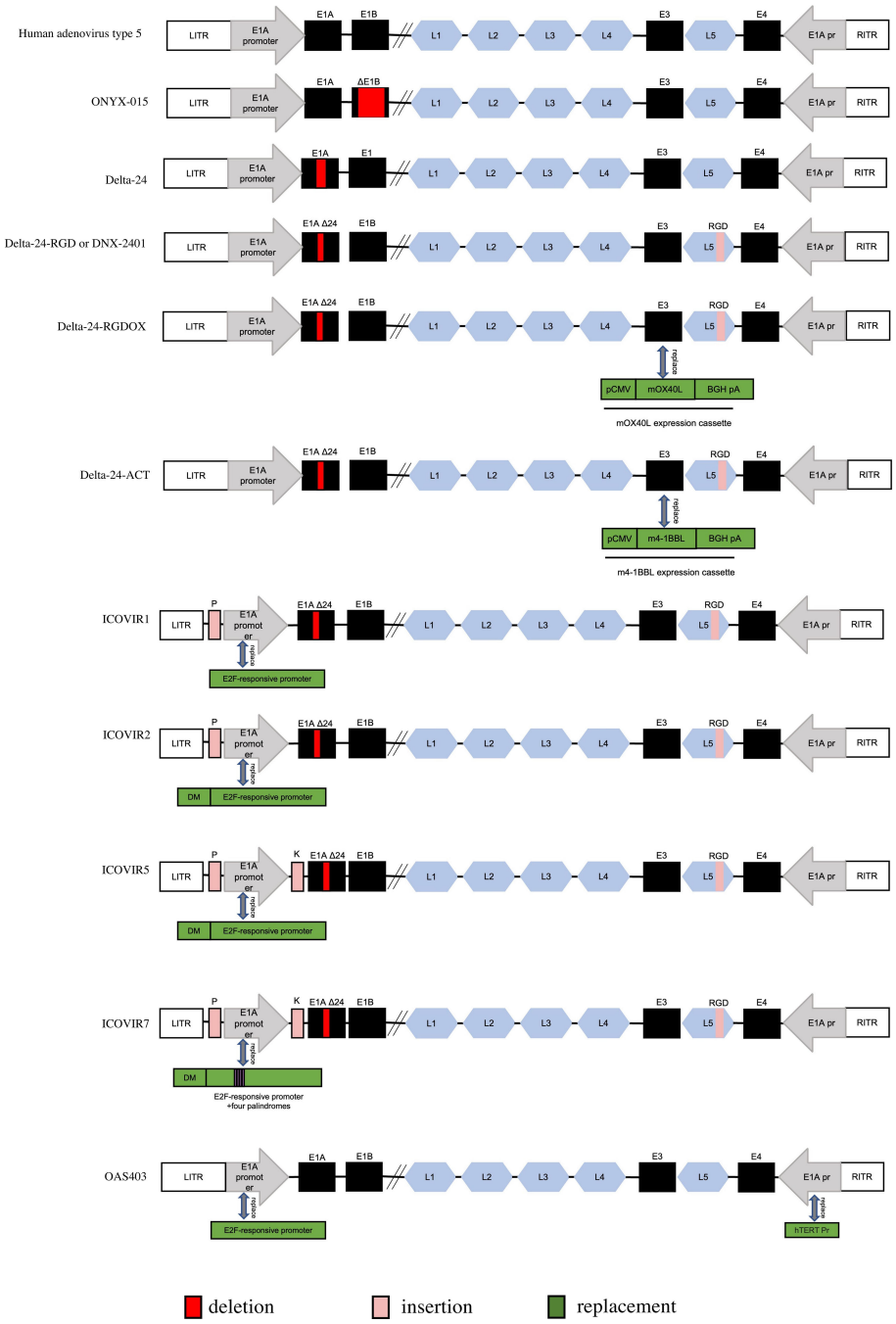

FIGURE 3
Genetic diagram of each generation of Oncolytic adenovirus. ITR, inverted terminal repeat. E1AΔ24: a deletion of 24 base pairs within the E1A region. DM, insulator DM-1. E2Fp, E2F-responsive promoter. K, a Kozak sequence. P, E2F-responsive palindromes (8 E2F-binding sites). RGD, an RGD integrin-binding motif in the HI loop of the fiber. pCMV, the cytomegalovirus promoter. mOX40L, mouse OX40L cDNA. BGH PA, bovine growth hormone poly-adenylation signal. The mOX40L expression cassette replaces the E3 region in Delta-24-RGDOX. hTERT Pr, human telomerase reverse transcriptase promoter.

3.1 The first-generation CRAds specifically targeting p53 mutated cancer cells

The wild-type p53 protein acts as a tumor suppressor, preventing abnormal cell proliferation and eliminating cells with abnormalities. Mutated p53, on the other hand, loses its regulatory function in controlling the normal cell cycle (59, 60). GBM is an aggressive brain cancer with a poor prognosis, and the frequency of p53 mutations varies between primary and secondary GBM. Approximately 30% of primary cases and 65% of secondary cases exhibit p53 mutations (61). In wild-type adenovirus infection, p53-mediated apoptosis is activated during the S phase. However, adenovirus E1B protein inactivates p53, inhibiting p53-mediated apoptosis and promoting viral replication (62). To address this, the

first conditional adenovirus was developed by introducing E1B deficiency, exemplified by ONYX-015.

3.1.1 ONYX-015

ONYX-015 is a genetically modified CRAd derived from a human type 2/5 chimeric adenovirus with an E1B deletion. This modification allows ONYX-015 to selectively replicate in cancer cells lacking functional p53 while sparing normal cells with intact p53 (63–65). Initial reports indicated that ONYX-015 selectively killed p53-deficient tumor cells (62) [66]. The NABTT CNS Consortium conducted a Phase I trial to evaluate the efficacy and safety of ONYX-015 in recurrent brain gliomas. Twenty-four adult patients with recurrent gliomas received multiple injections of ONYX-015 at the margins of resected recurrent gliomas. The median time to progression after treatment was 46 days, and the median survival time was 6.2 months. No serious adverse events occurred in any of the 24 patients, validating the therapeutic safety of ONYX-015. The NABTT CNS Consortium conducted a Phase I trial to evaluate the efficacy and safety of ONYX-015 in recurrent brain gliomas. Twenty-four adult patients with recurrent gliomas received multiple injections of ONYX-015 at the margins of resected recurrent gliomas. The median time to progression after treatment was 46 days, and the median survival time was 6.2 months. No serious adverse events occurred in any of the 24 patients, validating the therapeutic safety of ONYX-015 (67). However, ONYX-015 did not exhibit significant antitumor effects on recurrent gliomas, suggesting that p53 may not play a key role in the tumor selectivity of ONYX-015. A Phase II clinical trial combining intratumor ONYX-015 therapy with standard intravenous cisplatin and 5-fluorouracil (5-FU) chemotherapy in patients with recurrent squamous cell carcinoma of the head and neck yielded promising results, with tumors not progressing at 6 months in the combination group (68).

Recent studies have shown that ONYX-015 replication is not strictly restricted to p53-mutated tumor cells and can replicate and eliminate cells even when the p53 pathway is intact (64, 65) [69–72]. The tumor selectivity of ONYX-015 relies not only on the p53 protein but also on the RNA export function of E1B-55K provided by tumor cells. Additionally, ONYX-015 exhibits limited replication and toxicity in tumor cells without p53 mutations (68). Despite these findings, ONYX-015 currently does not have any registered clinical trials in the United States following the withdrawal of a Phase I trial by the Dana-Farber Cancer Institute in 2013.

3.2 The second-generation CRAd specifically targeting cancer cells with mutations in the Rb pathway

ONYX-015's limited progress in clinical trials is attributed to its untargeted viral replication and inability to infect CAR (Coxsackie adenovirus receptor)-deficient tumor cells. However, the presence of multiple adenovirus genes targeting cell cycle regulators provides an opportunity to develop oncolytic adenoviruses that can target alternative pathways. Since abnormalities in the p16/Rb/E2F pathway are present in most gliomas, viral therapies targeting the Rb pathway were developed as the second-generation of CRAd (73).

3.2.1 DNX-2401

A typical example of a second-generation CRAd targeting the Rb pathway is the Delta-24 adenovirus derived from human adenovirus type 5. Delta-24 carries a 24-base pair deletion in the Rb-binding domain of the E1A gene, resulting in a mutant E1A (mE1A) protein. Normally, the E1A protein binds to the Rb protein, releasing E2F and allowing cell progression into the S phase. In Delta-24, however, mE1A fails to effectively bind the Rb protein, leading to limited E2F release. As a result, Delta-24 cannot replicate in normal cells since mE1A is unable to bind the Rb protein and release E2F (74). Notably, Stolarek, R et al. demonstrated that Delta-24 exhibits replicative capability and cytotoxicity against medulloblastoma cells (75).

Delta-24 has demonstrated the ability to sensitize glioma cells to the camptothecin analogue irinotecan (CPT-11), both *in vitro* and *in vivo*. This effect is achieved through the upregulation of topoisomerase I expression and the induction of cancer cell accumulation in the S phase. The sequential administration of Delta-24 and CPT-11 has shown a significant extension in the survival time of animals with glioma. Therefore, the combination of adenovirus therapy and chemotherapy enhances its anticancer effect (76).

To enter host cells, Delta-24 first binds to the coxsackievirus and adenovirus receptor (CAR) on the cell surface. However, certain cancers, including glioblastoma, exhibit low levels of CAR, which greatly limits the infectivity of Delta-24. The internalization of adenovirus into host cells is facilitated by secondary interactions between the RGD motif on the Penton-based protein ring and integrins ($\alpha v\beta 5$ and $\alpha v\beta 3$) (77). In order to address this limitation, the gene encoding the arginine-glycine aspartic acid (RGD) peptide was introduced into the viral fiber knob receptor of Delta-24, resulting in the second-generation Delta-24-RGD or DNX-2401. Integrins are commonly overexpressed on cancer cells (78). Consequently, the infection rate of Delta-24-RGD in glioblastoma was significantly increased (79, 80).

Lang et al. conducted a Phase I dose escalation trial of DNX-2401 in 37 patients with rGBM. Group A (n=25) received eight dose levels of DNX-2401 via a single intratumoral injection to assess safety and reactivity, while Group B underwent intratumoral injection using a permanently implanted catheter, followed by en bloc resection after 14 days to obtain post-treatment specimens. The results revealed that 20% of patients in Group A experienced survival beyond three years, with at least three patients exhibiting over 95% reduction in enhanced tumor survival, resulting in more than three years of PFS. Evaluation of post-treatment specimens demonstrated virus replication and spread within the tumor in Group B, indicating direct virus-induced oncolysis. These clinical trial findings suggest that DNX-2401 can achieve prolonged survival through its direct oncolytic effect and induction of immune-mediated anti-glioma response (NCT00805376) (81). These observations agreed with preclinical studies showing that

Delta-24-RGD infection induces autophagy and immunogenic cell death in glioblastoma (82, 83).

In a pre-clinical study by Martinez-Velez N, the anti-glioma effects of Delta-24-RGD were assessed in pediatric pHGG and DIPGs models. The experimental data indicated significant antitumor effects of Delta-24-RGD in both cell lines and mouse models of pHGG and DIPG. Additionally, Delta-24-RGD administration triggered an anti-tumor immune response alongside its oncolytic effects. These promising preclinical findings lay the foundation for a Phase I/II clinical trial investigating DNX-2401 (NCT03178032) (84).

3.2.2 DNX-2401 and chemotherapy

In 2017, a Phase I trial (NCT01956734) evaluated the combination of DNX-2401 and TMZ for treating rGBM. Likewise, Clinica Universidad de Navarra conducted a Phase 1b, randomized, multicenter, open-label study (TARGET-I, NCT02197169) from 2014 to 2018, investigating conditional replicative adenovirus (DNX-2401) and interferon gamma (IFN-γ) for recurrent glioblastoma. However, no published results are available from these trials, necessitating additional clinical trials to demonstrate DNX-2401's efficacy in treating rGBM.

In a completed Phase II trial (NCT02798406), the efficacy and safety of DNX-2401 in combination with Pembrolizumab for treating rGBM were investigated. The study included 49 glioma patients who received intratumoral treatment with various doses of DNX-2401 viral particles (vp) ($5*10^8$ vp, $5*10^9$ vp, and $5*10^8$ vp DNX-2401) alongside Pembrolizumab. The median OS was 12.5 months (10.7 to 13.5 months). Additionally, 56.2% (95%CI 41.1-70.5%) of patients achieved clinical benefit, defined as disease stabilization or improvement. Importantly, no toxic effects were observed with DNX-2401, even at a maximum dose of $5*10^{10}$ vp. These findings demonstrate the safety and significant survival benefits of combining DNX-2401 and Pembrolizumab for selected patients with recurrent brain gliomas (85). Clinical trials have shown a survival benefit when using DNX-2401 in combination with chemotherapy. However, it is worth noting that these trials lacked a negative control group that used chemotherapy alone. Additional clinical trials are required to confirm whether the combination of DNX-2401 and chemotherapy can indeed extend patient survival.

3.2.3 DNX-2401 and radiotherapy

Radiotherapy (RT) is commonly used in managing gliomas, but its effectiveness is limited to temporary clinical improvements. Thus, researchers evaluated the feasibility, safety, and efficacy of combining Delta-24-RGD with RT for pHGGs and DIPGs. This combination significantly improved survival rates and increased immune cell infiltration at the tumor site in treated mice (86). These promising findings suggest the potential of Delta-24-RGD and RT combination therapy for clinical use in pHGGs and DIPGs.

3.2.4 Delta-24-ACT

Delta-24-ACT, a modified oncolytic adenovirus, incorporates the 4-1BB ligand (4-1BBL) to enhance its therapeutic capabilities. Infected glioma cells express elevated levels of 4-1BB ligand, which binds to TNFRSF9 (CD137; 4-1BB), a co-stimulatory receptor. This interaction activates T cells and immune cells, augmenting the oncolytic effect of the adenovirus. The antitumor effects and induction of T cell activation by Delta-24-ACT have been validated in glioma cell lines. In CT-2A tumor-bearing glioma mouse models, both Delta-24-RGD and Delta-24-ACT improved median survival, with Delta-24-ACT exhibiting slightly superior efficacy over Delta-24-RGD treatment (87). Preclinical models have demonstrated the potent antitumor effects of 4-1BB agonists. However, in clinical trials, their use in cancer treatment has been hindered by notable hepatotoxicity (88, 89). To overcome this challenge, one potential approach is specifically targeting Delta-24-ACT to tumor cells. This allows bypassing the systemic administration of 4-1BB agonists and improving safety. By delivering Delta-24-ACT directly into the tumor, it can disrupt microenvironment tolerance observed in DIPG, triggering proinflammatory changes that activate T cells and generate immune memory (90). The safety and preclinical efficacy of Delta-24-ACT have been well-established. Yet, further clinical trials are necessary to evaluate its oncolytic effect and induction of anti-tumor immune response, as it represents a potential novel oncolytic virus.

3.2.5 Delta-24-RGDOX (DNX-2440)

Delta-24-RGDOX (DNX-2440), an improved version of Delta-24-RGD, stimulates immunostimulating OX40 ligand (OX40L) expression on infected tumor cells, activating T cells recognizing tumor cell antigens. In immunologically competent mouse glioma models, Delta-24-RGDOX induces more effective *in situ* autologous cancer vaccination than Delta-24-RGD, resulting in a lasting tumor-specific therapeutic effect (91). Currently, an ongoing Phase I clinical trial (NCT03714334) at Clinica Universidad de Navarra investigates stereotactic injection therapy using OVs DNX-2440 for patients experiencing their first or second recurrence of GBM.

3.3 The third-generation CRAds utilizing the human E2F-1 promoter

Transcription factors of the E2F family play an important role in entry into the S phase of the cell cycle (92, 93). E2F function is inhibited upon binding to the retinoblastoma tumor suppressor protein (pRb). Binding of E2F factors to nonphosphorylated pRb prevents E2F-mediated transactivation, but this complex also actively represses transcription when bound to the promoter. It is thought that all RB pathways in tumors have changes that inhibit the binding of pRb to E2F, which leads to an increase in free E2F (94, 95). the third-generation CRAds were obtained by replacing The E1A promoter of the second-generation CRAds with the human E2F-1 promoter. E2F-1 promoter can selectively replicate. The third-generation CRAds in tumor cells and reduce hepatotoxicity.

3.3.1 ICOVIR-1、ICOVIR-2、ICOVIR-5

To enhance adenovirus selectivity for glioma cancer cells, Majem et al. replaced the native E1A promoter in Delta-24-RGD with the human E2F-1 promoter, resulting in ICOVIR-1 (96). They further introduced the DM-1 element upstream of the E2F-1 promoter to create ICOVIR-2, which acted as an enhancer blocking insulator to reduce activity against normal cells. Cell experiments demonstrated that both ICOVIR-1 and ICOVIR-2 effectively prevented E1A expression in normal human cells, leading to reduced viral replication (97).

Based on ICOVIR-2, ICOVIR-5 was optimized by inserting the CCACC sequence (Kozak sequence) before the first codon of the E1a gene. This alteration aimed to enhance transcription of the heteroe2F-1 promoter (98). In 2013, Garcia et al. conducted a Phase I clinical trial with injectable ICOVIR-5 in 14 melanoma patients. While ICOVIR-5 could reach melanoma metastases after single intravenous administration, tumor regression was not observed in the evaluated patients. These findings support ICOVIR-5's potential for treating disseminated cancer. Currently, no clinical trials are investigating ICOVIR-5 for glioma treatment (99). Nevertheless, as a safer and more potent conditional adenovirus, ICOVIR-5 holds significant promise for clinical applications in glioma treatment.

3.3.2 OAS403

The oncolytic adenovirus OAS403 utilizes a human adenovirus type 5 vector with the incorporation of the E2F-1 promoter. This promoter regulates the early region E1A in OAS403, while a human telomerase reverse transcriptase promoter controls the E4 region, which encodes toxic viral proteins responsible for cell damage (100). The inclusion of the human telomerase reverse transcriptase promoter in the E4 region allows selective expression of these toxic proteins specifically in cancer cells (101, 102). In a mouse tumor model, a single intravenous injection of OAS403 at a dosage of 3×10^{12} vp/kg showed significant antitumor efficacy. Particularly, in a preestablished LNCaP prostate tumor model, systemic administration of OAS403 resulted in complete tumor regression in over 80% of cases at tolerable doses. Moreover, an increase in site-specific viral replication within the tumor was observed, with no discernible growth in the liver. Additionally, combining OAS403 treatment with Adriamycin significantly enhanced its efficacy (103). OAS403 shows promise for treating various human cancers, including recurrent glioma. An alternative variant, ICOVIR-7, incorporates an additional E2F response site palindrome within the insulated E2F-1 promoter to exert greater control over E1A-δ24 and enhance E2F-dependent E1A gene expression (104).

4 Other oncolytic viruses

In addition to oHSV and CRAd, various other OVs such as reovirus, poliovirus, and retrovirus have been modified and explored for their potential in treating brain glioma. Notably, Pelareore (reovirus), PVSRIPO (poliovirus), and Toca 511 (retrovirus) have made significant clinical advancements.

4.1 Pelareore

Reovirus is a non-encapsulated icosahedral double-stranded RNA virus that selectively targets cells with activated Ras signaling pathways. It has therapeutic potential for various solid and hematological tumors, including pancreatic, colorectal, thyroid, and lung cancers, as well as acute myeloid leukemia (105–107). REOLYSIN® (Pelareore), derived from reovirus strain type 3 Dearing virus, is an FDA-designated fast track treatment for metastatic breast cancer and metastatic pancreatic ductal adenocarcinoma. Safety of reovirus has been demonstrated in two Phase I trials involving adult brain tumor patients, without reaching the MTD (108, 109). Studies on mice have shown the efficacy of the GM-CSF (sargramostim)/intravenous REOLYSIN® regimen for brain glioma (110). A Phase I trial on six pediatric patients with recurrent or refractory advanced brain tumors has explored the combination of GM-CSF and Pelareore, but the MTD remains undetermined (NCT02444546). Regrettably, despite the induction of an immune response in patients using the combination of GM-CSF and pelareoreep, no complete or partial tumor response was observed. Instead, all patients experienced disease progression within 60 days (111). The limited clinical efficacy of pelareore in glioma may be attributed to factors like the blood-brain barrier and immune clearance. To optimize the antitumor effect of pelareore, future clinical trials could explore the use of multiple para-tumor injections in combination with GM-CSF. This approach shows potential for enhancing the therapeutic outcomes of pelareore and requires further investigation.

4.2 Recombinant nonpathogenic polio-rhinovirus chimera (PVSRIPO)

PVSRIPO, also known as lerapolturev, is a modified version of poliovirus type 1 (Mahoney), where the internal ribosome entry site is replaced with the human rhinovirus type 2 I.E. element. While maintaining its affinity for the CD155 receptor, PVSRIPO exhibits reduced virulence compared to the wild-type poliovirus (112, 113). The FDA recognized its potential and granted PVSRIPO breakthrough therapy designation in 2016. The efficacy of PVSRIPO has been confirmed in a Phase I clinical trial involving 61 adult patients with recurrent WHO grade IV malignant glioma. In this trial, intratuminal infusion of PVSRIPO established a safe dose (3.3×10^{9} TCID50) for direct delivery to intracranial tumors. The results showed significantly higher OS rates at 24 and 36 months in the PVSRIPO immunotherapy group compared to historical controls (21% vs 14% at 24 months; 21% vs 4% at 36 months) (NCT01491893) (114). The median survival in children with recurrent glioma is typically less than 6 months. However, a Phase I clinical trial administered polio-rhinovirus chimera lerapolturev to patients, resulting in one patient (1/8) surviving beyond 22 months. This finding suggests the potential of PVSRIPO (poliovirus) to prolong the lifespan of rGBM. Nonetheless, further validation through extensive studies is necessary to affirm these trial results conclusively (115). Building on this progress, Duke

University is currently conducting a Phase II clinical study involving 122 adult patients with glioblastoma. The study aims to investigate the safety, efficacy (antitumor response, and survival) of PVSRIPO (NCT02986178). Moreover, preclinical studies have shown that combining PVSRIPO with immune checkpoint inhibitors can effectively target tumors. Consequently, a Phase II trial combining PVSRIPO and the immune checkpoint inhibitor Pembrolizumab is underway, involving 30 patients with recurrent glioblastoma (NCT04479241).

4.3 Toca 511

Toca 511 is a modified non-soluble mouse leukemia virus vector that incorporates the cytosine deaminase (CD) enzyme gene, allowing for selective infection of tumor cells (116–119). Selective infection of tumor cells by Toca 511 results in the expression of the CD enzyme, which facilitates the conversion of the prodrug 5-fluorocytosine (Toca FC) into 5-FU within these cells, enabling targeted chemotherapy (120, 121). Toca 511 causes direct cytotoxicity and proinflammatory state of cancer cells via 5-FU. In a Phase I clinical study (NCT01470794), 43 patients with recurrent glioblastoma were treated with Toca 511, leading to a median survival of 13.6 months, compared to 7.1 months for untreated patients (122). Two additional Phase I studies (NCT01156584 and NCT01985256) demonstrated that intratumoral and intravenous administrations of Toca 511 as standalone treatments for rHGG is safe and tolerable.

However, a Phase III clinical trial (NCT02414165) involving 403 patients with recurrent glioblastoma and anaplastic astrocytoma treated with Toca 511/FC did not demonstrate a significant advantage over the standard of care (SOC) group. The Toca 511/FC group showed a median survival of 11.1 months, while the SOC group exhibited a median survival of 12.22 months (122). Further clinical trials are needed to provide robust evidence regarding the efficacy of Toca 511/FC in the treatment of recurrent glioma.

4.4 Zika virus

Zika virus (ZIKV) belongs to the Flaviviridae family and is an RNA virus. Its viral genome encodes a single polyprotein through a sole open reading frame, subsequently cleaved by cellular and viral proteases into ten proteins (123). Since 2015, ZIKV infection in pregnant women has emerged as a global public health emergency due to its association with microcephaly and other congenital diseases (124). Recent studies have identified ZIKV's specific targeting of GSCs and its oncolytic activity (125). Moreover, ZIKV has been found to participate in viral endocytosis mediated by SOX2 and integrin avb5, which play roles in immune response suppression, GBM progression, and GSC maintenance (126–128). Notably, integrin avb5, typically expressed at low levels in normal tissues, exhibits heightened expression in tumors (128). Consequently, ZIKV has garnered attention as a potential oncolytic virus for treating GBM.

A safer live-attenuated Zika virus vaccine, ZIKV-LAV, was developed to enhance sensitivity to the host's innate immune response. This vaccine is characterized by a 10-nucleotide deletion in the 3' untranslated region (3'UTR) of the viral genome (129). Administration of ZIKV-LAV via brain injection in mice showed no detectable behavioral abnormalities, neurovirulence, or organ damage, confirming its high safety profile. Furthermore, ZIKV-LAV-treated mice exhibited significantly longer median survival times compared to the mock group (130, 131).

Contrarily, glioma slice cultures exhibit resistance to Zika virus infection unlike NPC, which is attributed to interferon-beta secretion by myeloid cells in the glioblastoma tumor microenvironment (132, 133). The combination of CDK4/6 inhibitors with ZIKV-LAV enhances the selective replication of the vaccine, resulting in significant inhibition of tumor growth and prolonged survival in glioma mice. Although ZIKV-LAV is currently in the preclinical stage, the combination of ZIKV-LAV with immunosuppressants shows promise as a novel immunotherapy for glioma.

5 Discussion

5.1 Current status

In the past 20 years, oncolytic viruses have achieved exciting results in the treatment of glioma. OVs have displayed promising results in the treatment of glioma over the past two decades, thanks to the development and application of genetic engineering technologies. These advancements have rendered OVs more specific, effective, and safe. Numerous oncolytic virus studies are currently undergoing phase I, II, and III clinical trials. While the first-generation of OVs, including dlsptk HSV and ONYX-015, demonstrated promise in preclinical trials, they were ultimately eliminated due to safety concerns and non-significant oncolytic effects during clinical trials. Subsequent modifications gave rise to second/third-generation oHSV and CRad, which exhibit great potential in treating glioma. Notably, DNX 2401 combined with PD-1 significantly prolonged the survival time of patients with glioma, and G47Δ has received approval for glioma treatment in Japan. Furthermore, ICOVIR-7 has shown promise in preclinical trials by displaying lower toxicity and increased antitumor efficacy compared to ICOVIR-5 in a subcutaneous xenograft mouse model (134). A comprehensive summary of ongoing and completed human trials investigating OVs in glioma can be found in Table 1. Despite the favorable progress achieved in most current OVs clinical trials, several limitations persist. These trials often impose strict inclusion criteria driven primarily by safety concerns, resulting in a limited patient population and random trial outcomes. Moreover, the evaluation of OVs efficacy and potential long-term consequences in GBM remains inadequate. The reliance on historical survival as a control further emphasizes the necessity for prospective randomized trials to effectively assess the effectiveness of OVs.

5.2 Future directions

To ensure the consistency between preclinical and clinical test results, conducting animal experiments is crucial for evaluating the safety and effectiveness of OVs-related products prior to clinical trials. However, it should be noted that the antitumor effect of OVs is partially mediated by inducing an immune response against the virus. Therefore, using immunodeficient mice in the PDX model to evaluate the oncolytic effects of OVs on brain gliomas disregards the impact of the immune response. Utilizing an induced glioma model can provide a more comprehensive assessment of OV's therapeutic efficacy.

Despite promising results in preclinical and clinical trials, OVs have not yet demonstrated improved patient outcomes compared to standard care modalities like surgery, radiotherapy, and chemotherapy. This lack of improvement can be attributed to factors such as tumor heterogeneity, immune evasion, therapy resistance, limitations of the blood-brain barrier (BBB), and TME. To enhance therapeutic efficacy, it is recommended to classify OVs based on specific brain glioma types and target the p53 and Rb pathways according to their respective mutation types.

Numerous studies have investigated different routes of administration for OVs in glioma treatment, including intravenous injection, arterial injection, inhalation, intratumoral injection, and convection-enhanced delivery (CED). Intratumoral injection and CED are preferred due to their ability to provide local drug delivery to tumor lesions without opening the blood-brain barrier, although surgery is required (135). Alternatively, direct systemic administration can utilize adjunctive measures to actively open the blood-brain barrier, avoiding surgery (136). Developing new delivery routes that penetrate the blood-brain barrier and target tumors precisely is critical. Nanoparticles or cell-based carriers present non-invasive alternatives for patients who cannot undergo neurosurgical procedures. Improved imaging models are clinically needed to assess patient responses to OVs treatment and guide subsequent therapy. Additionally, determining the maximum safe dose of each OV is essential to maximize killing effect while ensuring patient safety.

The immune response, responsible for clearing OVs and hindering their replication, is a major reason for the effectiveness of oncolytic virotherapy. Combining OVs with immunosuppressants, such as anti-PD1 antibodies, has shown promise in clinical trials (137). Achieving a balance between immune response and clearance through the use of immunosuppressants and multi-dose OVs delivery requires further investigation. Combining oncolytic virotherapy with T cell therapy can help proliferate T cells in the local tumor microenvironment for optimal efficacy. Further understanding of immune mechanisms can aid in the development of improved OVs and expand their potential.

5.3 Conclusions and perspective

Recurrent gliomas, grade 4 tumors with a poor prognosis, do not see significant improvement in survival rates despite standard treatments like surgery, radiation therapy, and TMZ chemotherapy (138). New treatment methods are therefore necessary to improve patient outcomes.

One such promising approach is oncolytic virus therapy. This viral genome-based treatment selectively replicates in tumor cells while targeting them specifically, making it a hopeful treatment option for patients with recurrent tumors. Advancements in oncolytic virus genome modification have led to improvements in safety and anticancer efficacy. First-generation OVs include dlsptk HSV and ONYX-015, while second-and third-generation OVs consist mainly of oHSV and CRAd, respectively. Although recurrent glioma has a high mortality rate and poor prognosis, oncolytic virus therapy shows promise in improving patient outcomes due to its favorable safety profile. By directly targeting glioma cells and inducing cell death through selective replication and immune stimulation via acting as antigens, oncolytic viruses hold potential as a treatment option. However, safety and efficacy concerns remain, emphasizing the importance of developing safer and more effective oncolytic virus vectors. Additionally, optimizing virus delivery routes, enhancing specificity to tumor cells, limiting antiviral responses, enhancing anti-tumor immunity, reprogramming and reshaping the tumor immune microenvironment, and identifying drugs with similar anticancer effects are viable ways to improve oncolytic virus therapy.

Author contributions

MH: Data curation, Formal Analysis, Methodology, Writing – original draft, Writing – review & editing. XL: Methodology, Writing – review & editing. YT: Data curation, Formal Analysis, Writing – original draft. YC: Funding acquisition, Supervision, Writing – review & editing.

Funding

The author(s) declare financial support was received for the research, authorship, and/or publication of this article. This work was supported by the 1.3.5 project for disciplines of excellence, West China Hospital, Sichuan University (Y.C., ZYJC21015).

Conflict of interest

The authors declare that the research was conducted in the absence of any commercial or financial relationships that could be construed as a potential conflict of interest.

Publisher's note

References

1. Thakkar JP, Dolecek TA, Horbinski C, Ostrom QT, Lightner DD, Barnholtz-Sloan JS, et al. Epidemiologic and molecular prognostic review of glioblastoma. *Cancer Epidemiol Biomarkers Prev* (2014) 23(10):1985–96. doi: 10.1158/1055-9965.EPI-14-0275

2. Louis DN, Perry A, Wesseling P, Brat DJ, Cree IA, Figarella-Branger D, et al. The 2021 WHO classification of tumors of the central nervous system: a summary. *Neuro Oncol* (2021) 23(8):1231–51. doi: 10.1093/neuonc/noab106

3. Linz U. Commentary on Effects of radiotherapy with concomitant and adjuvant temozolomide versus radiotherapy alone on survival in glioblastoma in a randomised phase III study: 5-year analysis of the EORTC-NCIC trial (Lancet Oncol. 2009;10:459-466). *Cancer* (2010) 116(8):1844–6. doi: 10.1002/cncr.24950

4. Stupp R, Mason WP, van den Bent MJ, Weller M, Fisher B, Taphoorn MJ, et al. Radiotherapy plus concomitant and adjuvant temozolomide for glioblastoma. *N Engl J Med* (2005) 352(10):987–96. doi: 10.1056/NEJMoa043330

5. Wilson TA, Karajannis MA, Harter DH. Glioblastoma multiforme: State of the art and future therapeutics. *Surg Neurol Int* (2014) 5:64. doi: 10.4103/2152-7806.132138

6. Kumar AA, Abraham Koshy A. Regression of recurrent high-grade glioma with temozolomide, dexamethasone, and levetiracetam: case report and review of the literature. *World Neurosurg* (2017) 108:990.e911–990.e916. doi: 10.1016/j.wneu.2017.08.136

7. McNeill KA. Epidemiology of brain tumors. *Neurol Clin* (2016) 34(4):981–98. doi: 10.1016/j.ncl.2016.06.014

8. Weller M, van den Bent M, Tonn JC, Stupp R, Preusser M, Cohen-Jonathan-Moyal E, et al. European Association for Neuro-Oncology (EANO) guideline on the diagnosis and treatment of adult astrocytic and oligodendroglial gliomas. *Lancet Oncol* (2017) 18(6):e315–29. doi: 10.1016/S1470-2045(17)30194-8

9. Laub CK, Stefanik J, Doherty L. Approved treatments for patients with recurrent high-grade gliomas. *Semin Oncol Nurs* (2018) 34(5):486–93. doi: 10.1016/j.soncn.2018.10.005

10. Weller M, Cloughesy T, Perry JR, Wick W. Standards of care for treatment of recurrent glioblastoma–are we there yet? *Neuro Oncol* (2013) 15(1):4–27. doi: 10.1093/neuonc/nos273

11. Campos B, Olsen LR, Urup T, Poulsen HS. A comprehensive profile of recurrent glioblastoma. *Oncogene* (2016) 35(45):5819–25. doi: 10.1038/onc.2016.85

12. Xu S, Tang L, Li X, Fan F, Liu Z. Immunotherapy for glioma: Current management and future application. *Cancer Lett* (2020) 476:1–12. doi: 10.1016/j.canlet.2020.02.002

13. Gong J, Chehrazi-Raffle A, Reddi S, Salgia R. Development of PD-1 and PD-L1 inhibitors as a form of cancer immunotherapy: a comprehensive review of registration trials and future considerations. *J Immunother Cancer* (2018) 6(1):8. doi: 10.1186/s40425-018-0316-z

14. Jackson CM, Choi J, Lim M. Mechanisms of immunotherapy resistance: lessons from glioblastoma. *Nat Immunol* (2019) 20(9):1100–9. doi: 10.1038/s41590-019-0433-y

15. Vartanian A, Singh SK, Agnihotri S, Jalali S, Burrell K, Aldape KD, et al. GBM's multifaceted landscape: highlighting regional and microenvironmental heterogeneity. *Neuro Oncol* (2014) 16(9):1167–75. doi: 10.1093/neuonc/nou035

16. Sterner RC, Sterner RM. CAR-T cell therapy: current limitations and potential strategies. *Blood Cancer J* (2021) 11(4):69. doi: 10.1038/s41408-021-00459-7

17. Mirzaei R, Sarkar S, Yong VWT. Cell exhaustion in glioblastoma: intricacies of immune checkpoints. *Trends Immunol* (2017) 38(2):104–15. doi: 10.1016/j.it.2016.11.005

18. Achard C, Surendran A, Wedge ME, Ungerechts G, Bell J, Ilkow CS. Lighting a fire in the tumor microenvironment using oncolytic immunotherapy. *EBioMedicine* (2018) 31:17–24. doi: 10.1016/j.ebiom.2018.04.020

19. Li J, Meng Q, Zhou X, Zhao H, Wang K, Niu H, et al. Gospel of Malignant Glioma: Oncolytic virus therapy. *Gene* (2022) 818:146217. doi: 10.1016/j.gene.2022.146217

20. Kelly E, Russell SJ. History of oncolytic viruses: genesis to genetic engineering. *Mol Ther* (2007) 15(4):651–9. doi: 10.1038/sj.mt.6300108

21. Huebner RJ, Rowe WP, Schatten WE, Smith RR, Thomas LB. Studies on the use of viruses in the treatment of carcinoma of the cervix. *Cancer* (1956) 9(6):1211–8. doi: 10.1002/1097-0142(195611/12)9:6<1211::aid-cncr2820090624>3.0.co;2-7

22. Martuza RL, Malick A, Markert JM, Ruffner KL, Coen DM. Experimental therapy of human glioma by means of a genetically engineered virus mutant. *Science* (1991) 252(5007):854–6. doi: 10.1126/science.1851332

23. Coen DM, Kosz-Vnenchak M, Jacobson JG, Leib DA, Bogard CL, Schaffer PA, et al. Thymidine kinase-negative herpes simplex virus mutants establish latency in mouse trigeminal ganglia but do not reactivate. *Proc Natl Acad Sci U.S.A.* (1989) 86(12):4736–40. doi: 10.1073/pnas.86.12.4736

24. Valyi-Nagy T, Gesser RM, Raengsakulrach B, Deshmane SL, Randazzo BP, Dillner AJ, et al. A thymidine kinase-negative HSV-1 strain establishes a persistent infection in SCID mice that features uncontrolled peripheral replication but only marginal nervous system involvement. *Virology* (1994) 199(2):484–90. doi: 10.1006/viro.1994.1150

25. Goldstein DJ, Weller SK. Herpes simplex virus type 1-induced ribonucleotide reductase activity is dispensable for virus growth and DNA synthesis: isolation and characterization of an ICP6 lacZ insertion mutant. *J Virol* (1988) 62(1):196–205. doi: 10.1128/JVI.62.1.196-205.1988

26. Mineta T, Rabkin SD, Martuza RL. Treatment of Malignant gliomas using ganciclovir-hypersensitive, ribonucleotide reductase-deficient herpes simplex viral mutant. *Cancer Res* (1994) 54(15):3963–6.

27. Friedman A, Tian JP, Fulci G, Chiocca EA, Wang J. Glioma virotherapy: effects of innate immune suppression and increased viral replication capacity. *Cancer Res* (2006) 66(4):2314–9. doi: 10.1158/0008-5472.CAN-05-2661

28. He B, Gross M, Roizman B. The gamma(1)34.5 protein of herpes simplex virus 1 complexes with protein phosphatase 1alpha to dephosphorylate the alpha subunit of the eukaryotic translation initiation factor 2 and preclude the shutoff of protein synthesis by double-stranded RNA-activated protein kinase. *Proc Natl Acad Sci U.S.A.* (1997) 94(3):843–8. doi: 10.1073/pnas.94.3.843

29. Cassady KA, Gross M, Roizman B. The second-site mutation in the herpes simplex virus recombinants lacking the gamma134.5 genes precludes shutoff of protein synthesis by blocking the phosphorylation of eIF-2alpha. *J Virol* (1998) 72(9):7005–11. doi: 10.1128/JVI.72.9.7005-7011.1998

30. Mineta T, Rabkin SD, Yazaki T, Hunter WD, Martuza RL. Attenuated multi-mutated herpes simplex virus-1 for the treatment of Malignant gliomas. *Nat Med* (1995) 1(9):938–43. doi: 10.1038/nm0995-938

31. Sundaresan P, Hunter WD, Martuza RL, Rabkin SD. Attenuated, replication-competent herpes simplex virus type 1 mutant G207: safety evaluation in mice. *J Virol* (2000) 74(8):3832–41. doi: 10.1128/jvi.74.8.3832-3841.2000

32. Hunter WD, Martuza RL, Feigenbaum F, Todo T, Mineta T, Yazaki T, et al. Attenuated, replication-competent herpes simplex virus type 1 mutant G207: safety evaluation of intracerebral injection in nonhuman primates. *J Virol* (1999) 73(8):6319–26. doi: 10.1128/JVI.73.8.6319-6326.1999

33. Markert JM, Medlock MD, Rabkin SD, Gillespie GY, Todo T, Hunter WD, et al. Conditionally replicating herpes simplex virus mutant, G207 for the treatment of Malignant glioma: results of a phase I trial. *Gene Ther* (2000) 7(10):867–74. doi: 10.1038/sj.gt.3301205

34. Markert JM, Liechty PG, Wang W, Gaston S, Braz E, Karrasch M, et al. Phase Ib trial of mutant herpes simplex virus G207 inoculated pre-and post-tumor resection for recurrent GBM. *Mol Ther* (2009) 17(1):199–207. doi: 10.1038/mt.2008.228

35. Friedman GK, Johnston JM, Bag AK, Bernstock JD, Li R, Aban I, et al. Oncolytic HSV-1 G207 immunovirotherapy for pediatric high-grade gliomas. *N Engl J Med* (2021) 384(17):1613–22. doi: 10.1056/NEJMoa2024947

36. MacLean AR, ul-Fareed M, Robertson L, Harland J, Brown SM. Herpes simplex virus type 1 deletion variants 1714 and 1716 pinpoint neurovirulence-related sequences in Glasgow strain 17+ between immediate early gene 1 and the 'a' sequence. *J Gen Virol* (1991) 72(Pt 3):631–9. doi: 10.1099/0022-1317-72-3-631

37. Chou J, Kern ER, Whitley RJ, Roizman B. Mapping of herpes simplex virus-1 neurovirulence to gamma 134.5, a gene nonessential for growth in culture. *Science* (1990) 250(4985):1262–6. doi: 10.1126/science.2173860

38. Benencia F, Courreges MC, Conejo-Garcia JR, Mohamed-Hadley A, Zhang L, Buckanovich RJ, et al. HSV oncolytic therapy upregulates interferon-inducible chemokines and recruits immune effector cells in ovarian cancer. *Mol Ther* (2005) 12(5):789–802. doi: 10.1016/j.ymthe.2005.03.026

39. Wollmann G, Ozduman K, van den Pol AN. Oncolytic virus therapy for glioblastoma multiforme: concepts and candidates. *Cancer J* (2012) 18(1):69–81. doi: 10.1097/PPO.0b013e31824671c9

40. Rampling R, Cruickshank G, Papanastassiou V, Nicoll J, Hadley D, Brennan D, et al. Toxicity evaluation of replication-competent herpes simplex virus (ICP 34.5 null mutant 1716) in patients with recurrent Malignant glioma. *Gene Ther* (2000) 7(10):859–66. doi: 10.1038/sj.gt.3301184

41. Papanastassiou V, Rampling R, Fraser M, Petty R, Hadley D, Nicoll J, et al. The potential for efficacy of the modified (ICP 34.5(-)) herpes simplex virus HSV1716 following intratumoural injection into human Malignant glioma: a proof of principle study. *Gene Ther* (2002) 9(6):398–406. doi: 10.1038/sj.gt.3301664

42. Harrow S, Papanastassiou V, Harland J, Mabbs R, Petty R, Fraser M, et al. HSV1716 injection into the brain adjacent to tumour following surgical resection of high-grade glioma: safety data and long-term survival. *Gene Ther* (2004) 11(22):1648–58. doi: 10.1038/sj.gt.3302289

43. Chiocca EA, Nakashima H, Kasai K, Fernandez SA, Oglesbee M. Preclinical toxicology of rQNestin34.5v.2: an oncolytic herpes virus with transcriptional regulation of the ICP34.5 neurovirulence gene. *Mol Ther Methods Clin Dev* (2020) 17:871–93. doi: 10.1016/j.omtm.2020.03.028

44. Kambara H, Okano H, Chiocca EA, Saeki Y. An oncolytic HSV-1 mutant expressing ICP34.5 under control of a nestin promoter increases survival of animals even when symptomatic from a brain tumor. *Cancer Res* (2005) 65(7):2832–9. doi: 10.1158/0008-5472.CAN-04-3227

45. Kaufmann JK, Chiocca EA. Glioma virus therapies between bench and bedside. *Neuro Oncol* (2014) 16(3):334–51. doi: 10.1093/neuonc/not310

46. Kanai R, Zaupa C, Sgubin D, Antoszczyk SJ, Martuza RL, Wakimoto H, et al. Effect of gamma34.5 deletions on oncolytic herpes simplex virus activity in brain tumors. *J Virol* (2012) 86(8):4420–31. doi: 10.1128/JVI.00017-12

47. He B, Chou J, Brandimarti R, Mohr I, Gluzman Y, Roizman B. Suppression of the phenotype of gamma(1)34.5- herpes simplex virus 1: failure of activated RNA-dependent protein kinase to shut off protein synthesis is associated with a deletion in the domain of the alpha47 gene. *J Virol* (1997) 71(8):6049–54. doi: 10.1128/JVI.71.8.6049-6054.1997

48. Reardon DA, Freeman G, Wu C, Chiocca EA, Wucherpfennig KW, Wen PY, et al. Immunotherapy advances for glioblastoma. *Neuro Oncol* (2014) 16(11):1441–58. doi: 10.1093/neuonc/nou212

49. Cully M. Combinations with checkpoint inhibitors at wavefront of cancer immunotherapy. *Nat Rev Drug Discovery* (2015) 14(6):374–5. doi: 10.1038/nrd4648

50. Passaro C, Alayo Q, De Laura I, McNulty J, Grauwet K, Ito H, et al. Arming an oncolytic herpes simplex virus type 1 with a single-chain fragment variable antibody against PD-1 for experimental glioblastoma therapy. *Clin Cancer Res* (2019) 25(1):290–9. doi: 10.1158/1078-0432.CCR-18-2311

51. Todo T, Martuza RL, Rabkin SD, Johnson PA. Oncolytic herpes simplex virus vector with enhanced MHC class I presentation and tumor cell killing. *Proc Natl Acad Sci U.S.A.* (2001) 98(11):6396–401. doi: 10.1073/pnas.101136398

52. Todo T, Ino Y, Ohtsu H, Shibahara J, Tanaka M. A phase I/II study of triple-mutated oncolytic herpes virus G47Δ in patients with progressive glioblastoma. *Nat Commun* (2022) 13(1):4119. doi: 10.1038/s41467-022-31262-y

53. Todo T, Ito H, Ino Y, Ohtsu H, Ota Y, Shibahara J, et al. Intratumoral oncolytic herpes virus G47Δ for residual or recurrent glioblastoma: a phase 2 trial. *Nat Med* (2022) 28(8):1630–9. doi: 10.1038/s41591-022-01897-x

54. Fukuhara H, Martuza RL, Rabkin SD, Ito Y, Todo T. Oncolytic herpes simplex virus vector g47delta in combination with androgen ablation for the treatment of human prostate adenocarcinoma. *Clin Cancer Res* (2005) 11(21):7886–90. doi: 10.1158/1078-0432.CCR-05-1090

55. Sugawara K, Iwai M, Yajima S, Tanaka M, Yanagihara K, Seto Y, et al. Efficacy of a third-generation oncolytic herpes virus G47Delta in advanced stage models of human gastric cancer. *Mol Ther Oncolytics* (2020) 17:205–15. doi: 10.1016/j.omto.2020.03.022

56. Sze DY, Reid TR, Rose SC. Oncolytic virotherapy. *J Vasc Interv Radiol* (2013) 24 (8):1115–22. doi: 10.1016/j.jvir.2013.05.040

57. Matthews DA, Russell WC. Adenovirus core protein V is delivered by the invading virus to the nucleus of the infected cell and later in infection is associated with nucleoli. *J Gen Virol* (1998) 79(Pt 7):1671–5. doi: 10.1099/0022-1317-79-7-1671

58. Vayda ME, Rogers AE, Flint SJ. The structure of nucleoprotein cores released from adenovirions. *Nucleic Acids Res* (1983) 11(2):441–60. doi: 10.1093/nar/11.2.441

59. Levine AJ. p53, the cellular gatekeeper for growth and division. *Cell* (1997) 88 (3):323–31. doi: 10.1016/s0092-8674(00)81871-1

60. Hernandez Borrero LJ, El-Deiry WS. Tumor suppressor p53: Biology, signaling pathways, and therapeutic targeting. *Biochim Biophys Acta Rev Cancer* (2021) 1876 (1):188556. doi: 10.1016/j.bbcan.2021.188556

61. Zhang Y, Dube C, Gibert MJr., Cruickshanks N, Wang B, Coughlan M, et al. The p53 pathway in glioblastoma. *Cancers (Basel)* (2018) 10(9):297. doi: 10.3390/cancers10090297

62. Bischoff JR, Kirn DH, Williams A, Heise C, Horn S, Muna M, et al. An adenovirus mutant that replicates selectively in p53-deficient human tumor cells. *Science* (1996) 274(5286):373–6. doi: 10.1126/science.274.5286.373

63. Edwards SJ, Dix BR, Myers CJ, Dobson-Le D, Huschtscha L, Hibma M, et al. Evidence that replication of the antitumor adenovirus ONYX-015 is not controlled by the p53 and p14(ARF) tumor suppressor genes. *J Virol* (2002) 76(24):12483–90. doi: 10.1128/jvi.76.24.12483-12490.2002

64. Rothmann T, Hengstermann A, Whitaker NJ, Scheffner M, zur Hausen H. Replication of ONYX-015, a potential anticancer adenovirus, is independent of p53 status in tumor cells. *J Virol* (1998) 72(12):9470–8. doi: 10.1128/JVI.72.12.9470-9478.1998

65. Geoerger B, Grill J, Opolon P, Morizet J, Aubert G, Terrier-Lacombe MJ, et al. Oncolytic activity of the E1B-55 kDa-deleted adenovirus ONYX-015 is independent of cellular p53 status in human Malignant glioma xenografts. *Cancer Res* (2002) 62(3):764–72.

66. Heise C, Sampson-Johannes A, Williams A, McCormick F, Von Hoff DD, Kirn DH. ONYX-015, an E1B gene-attenuated adenovirus, causes tumor-specific cytolysis and antitumoral efficacy that can be augmented by standard chemotherapeutic agents. *Nat Med* (1997) 3(6):639–45. doi: 10.1038/nm0697-639

67. Chiocca EA, Abbed KM, Tatter S, Louis DN, Hochberg FH, Barker F, et al. A phase I open-label, dose-escalation, multi-institutional trial of injection with an E1B-Attenuated adenovirus, ONYX-015, into the peritumoral region of recurrent Malignant gliomas, in the adjuvant setting. *Mol Ther* (2004) 10(5):958–66. doi: 10.1016/j.ymthe.2004.07.021

68. Khuri FR, Nemunaitis J, Ganly I, Arseneau J, Tannock IF, Romel L, et al. a controlled trial of intratumoral ONYX-015, a selectively-replicating adenovirus, in combination with cisplatin and 5-fluorouracil in patients with recurrent head and neck cancer. *Nat Med* (2000) 6(8):879–85. doi: 10.1038/78638

69. Dix BR, O'Carroll SJ, Myers CJ, Edwards SJ, Braithwaite AW. Efficient induction of cell death by adenoviruses requires binding of E1B55k and p53. *Cancer Res* (2000) 60 (10):2666–72.

70. Goodrum FD, Ornelles DA. p53 status does not determine outcome of E1B 55-kilodalton mutant adenovirus lytic infection. *J Virol* (1998) 72(12):9479–90. doi: 10.1128/JVI.72.12.9479-9490.1998

71. Hall AR, Dix BR, O'Carroll SJ, Braithwaite AW. p53-dependent cell death/apoptosis is required for a productive adenovirus infection. *Nat Med* (1998) 4(9):1068–72. doi: 10.1038/2057

72. Turnell AS, Grand RJ, Gallimore PH. The replicative capacities of large E1B-null group A and group C adenoviruses are independent of host cell p53 status. *J Virol* (1999) 73(3):2074–83. doi: 10.1128/JVI.73.3.2074-2083.1999

73. Fueyo J, Gomez-Manzano C, Alemany R, Lee PS, McDonnell TJ, Mitlianga P, et al. A mutant oncolytic adenovirus targeting the Rb pathway produces anti-glioma effect. *vivo. Oncogene* (2000) 19(1):2–12. doi: 10.1038/sj.onc.1203251

74. Ene CI, Fueyo J, Lang FF. Delta-24 adenoviral therapy for glioblastoma: evolution from the bench to bedside and future considerations. *Neurosurg Focus* (2021) 50(2):E6. doi: 10.3171/2020.11.FOCUS20853

75. Stolarek R, Gomez-Manzano C, Jiang H, Suttle G, Lemoine MG, Fueyo J. Robust infectivity and replication of Delta-24 adenovirus induce cell death in human medulloblastoma. *Cancer Gene Ther* (2004) 11(11):713–20. doi: 10.1038/sj.cgt.7700731

76. Gomez-Manzano C, Alonso MM, Yung WK, McCormick F, Curiel DT, Lang FF, et al. Delta-24 increases the expression and activity of topoisomerase I and enhances the antiglioma effect of irinotecan. *Clin Cancer Res* (2006) 12(2):556–62. doi: 10.1158/1078-0432.CCR-05-1892

77. Fueyo J, Alemany R, Gomez-Manzano C, Fuller GN, Khan A, Conrad CA, et al. Preclinical characterization of the antiglioma activity of a tropism-enhanced adenovirus targeted to the retinoblastoma pathway. *J Natl Cancer Inst* (2003) 95 (9):652–60. doi: 10.1093/jnci/95.9.652

78. Wickham TJ, Mathias P, Cheresh DA, Nemerow GR. Integrins alpha v beta 3 and alpha v beta 5 promote adenovirus internalization but not virus attachment. *Cell* (1993) 73(2):309–19. doi: 10.1016/0092-8674(93)90231-e

79. Jiang H, Gomez-Manzano C, Aoki H, Alonso MM, Kondo S, McCormick F, et al. Examination of the therapeutic potential of Delta-24-RGD in brain tumor stem cells: role of autophagic cell death. *J Natl Cancer Inst* (2007) 99(18):1410–4. doi: 10.1093/jnci/djm102

80. Stepanenko AA, Sosnovtseva AO, Valikhov MP, Chernysheva AA, Cherepanov SA, Yusubalieva GM, et al. Superior infectivity of the fiber chimeric oncolytic adenoviruses Ad5/35 and Ad5/3 over Ad5-delta-24-RGD in primary glioma cultures. *Mol Ther Oncolytics* (2022) 24:230–48. doi: 10.1016/j.omto.2021.12.013

81. Lang FF, Conrad C, Gomez-Manzano C, Yung WKA, Sawaya R, Weinberg JS, et al. Phase I study of DNX-2401 (Delta-24-RGD) oncolytic adenovirus: replication and immunotherapeutic effects in recurrent Malignant glioma. *J Clin Oncol* (2018) 36 (14):1419–27. doi: 10.1200/JCO.2017.75.8219

82. Jiang H, Fueyo J. Healing after death: antitumor immunity induced by oncolytic adenoviral therapy. *Oncoimmunology* (2014) 3(7):e947872. doi: 10.4161/21624011.2014.947872

83. Jiang H, Gomez-Manzano C, Rivera-Molina Y, Lang FF, Conrad CA, Fueyo J. Oncolytic adenovirus research evolution: from cell-cycle checkpoints to immune checkpoints. *Curr Opin Virol* (2015) 13:33–9. doi: 10.1016/j.coviro.2015.03.009

84. Martinez-Velez N, Garcia-Moure M, Marigil M, Gonzalez-Huarriz M, Puigdelloses M, Gallego Perez-Larraya J, et al. The oncolytic virus Delta-24-RGD elicits an antitumor effect in pediatric glioma and DIPG mouse models. *Nat Commun* (2019) 10(1):2235. doi: 10.1038/s41467-019-10043-0

85. Nassiri F, Patil V, Yefet LS, Singh O, Liu J, Dang RMA, et al. Oncolytic DNX-2401 virotherapy plus pembrolizumab in recurrent glioblastoma: a phase 1/2 trial. *Nat Med* (2023) 29(6):1370–8. doi: 10.1038/s41591-023-02347-y

86. Kiyokawa J, Wakimoto H. Preclinical and clinical development of oncolytic adenovirus for the treatment of Malignant glioma. *Oncolytic Virother* (2019) 8:27–37. doi: 10.2147/OV.S196403

87. Puigdelloses M, Garcia-Moure M, Labiano S, Laspidea V, Gonzalez-Huarriz M, Zalacain M, et al. CD137 and PD-L1 targeting with immunovirotherapy induces a potent and durable antitumor immune response in glioblastoma models. *J Immunother Cancer* (2021) 9(7):e002644. doi: 10.1136/jitc-2021-002644

88. Chester C, Sanmamed MF, Wang J, Melero I. Immunotherapy targeting 4-1BB: mechanistic rationale, clinical results, and future strategies. *Blood* (2018) 131(1):49–57. doi: 10.1182/blood-2017-06-741041

89. Yonezawa A, Dutt S, Chester C, Kim J, Kohrt HE. Boosting cancer immunotherapy with anti-CD137 antibody therapy. *Clin Cancer Res* (2015) 21 (14):3113–20. doi: 10.1158/1078-0432.CCR-15-0263

90. Laspidea V, Puigdelloses M, Labiano S, Marrodan L, Garcia-Moure M, Zalacain M, et al. Exploiting 4-1BB immune checkpoint to enhance the efficacy of oncolytic virotherapy for diffuse intrinsic pontine gliomas. *JCI Insight* (2022) 7(7):e154812. doi: 10.1172/jci.insight.154812

91. Jiang H, Rivera-Molina Y, Gomez-Manzano C, Clise-Dwyer K, Bover L, Vence LM, et al. Oncolytic adenovirus and tumor-targeting immune modulatory therapy improve autologous cancer vaccination. *Cancer Res* (2017) 77(14):3894–907. doi: 10.1158/0008-5472.CAN-17-0468

92. Helin K. Regulation of cell proliferation by the E2F transcription factors. *Curr Opin Genet Dev* (1998) 8(1):28–35. doi: 10.1016/s0959-437x(98)80058-0

93. Johnson DG, Schneider-Broussard R. Role of E2F in cell cycle control and cancer. *Front Biosci* (1998) 3:d447–448. doi: 10.2741/a291

94. Dyson N. The regulation of E2F by pRB-family proteins. *Genes Dev* (1998) 12 (15):2245–62. doi: 10.1101/gad.12.15.2245

95. Nevins JR. The Rb/E2F pathway and cancer. *Hum Mol Genet* (2001) 10(7):699–703. doi: 10.1093/hmg/10.7.699

96. Suzuki K, Fueyo J, Krasnykh V, Reynolds PN, Curiel DT, Alemany R. A conditionally replicative adenovirus with enhanced infectivity shows improved oncolytic potency. *Clin Cancer Res* (2001) 7(1):120–6.

97. Majem M, Cascallo M, Bayo-Puxan N, Mesia R, Germa JR, Alemany R. Control of E1A under an E2F-1 promoter insulated with the myotonic dystrophy locus insulator reduces the toxicity of oncolytic adenovirus Ad-Delta24RGD. *Cancer Gene Ther* (2006) 13(7):696–705. doi: 10.1038/sj.cgt.7700940

98. Alonso MM, Cascallo M, Gomez-Manzano C, Jiang H, Bekele BN, Perez-Gimenez A, et al. ICOVIR-5 shows E2F1 addiction and potent antiglioma effect. *vivo. Cancer Res* (2007) 67(17):8255–63. doi: 10.1158/0008-5472.CAN-06-4675

99. Garcia M, Moreno R, Gil-Martin M, Cascallo M, de Olza MO, Cuadra C, et al. A phase 1 trial of oncolytic adenovirus ICOVIR-5 administered intravenously to cutaneous and uveal melanoma patients. *Hum Gene Ther* (2019) 30(3):352–64. doi: 10.1089/hum.2018.107

100. Tauber B, Dobner T. Adenovirus early E4 genes in viral oncogenesis. *Oncogene* (2001) 20(54):7847–54. doi: 10.1038/sj.onc.1204914

101. Gorziglia MI, Lapcevich C, Roy S, Kang Q, Kadan M, Wu V, et al. Generation of an adenovirus vector lacking E1, e2a, E3, and all of E4 except open reading frame 3. *J Virol* (1999) 73(7):6048–55. doi: 10.1128/JVI.73.7.6048-6055.1999

102. Halbert DN, Cutt JR, Shenk T. Adenovirus early region 4 encodes functions required for efficient DNA replication, late gene expression, and host cell shutoff. *J Virol* (1985) 56(1):250–7. doi: 10.1128/JVI.56.1.250-257.1985

103. Ryan PC, Jakubczak JL, Stewart DA, Hawkins LK, Cheng C, Clarke LM, et al. Antitumor efficacy and tumor-selective replication with a single intravenous injection of OAS403, an oncolytic adenovirus dependent on two prevalent alterations in human cancer. *Cancer Gene Ther* (2004) 11(8):555–69. doi: 10.1038/sj.cgt.7700735

104. Cascallo M, Alonso MM, Rojas JJ, Perez-Gimenez A, Fueyo J, Alemany R. Systemic toxicity-efficacy profile of ICOVIR-5, a potent and selective oncolytic adenovirus based on the pRB pathway. *Mol Ther* (2007) 15(9):1607–15. doi: 10.1038/sj.mt.6300239

105. White CL, Twigger KR, Vidal L, De Bono JS, Coffey M, Heinemann L, et al. Characterization of the adaptive and innate immune response to intravenous oncolytic reovirus (Dearing type 3) during a phase I clinical trial. *Gene Ther* (2008) 15(12):911–20. doi: 10.1038/gt.2008.21

106. Coffey MC, Strong JE, Forsyth PA, Lee PW. Reovirus therapy of tumors with activated Ras pathway. *Science* (1998) 282(5392):1332–4. doi: 10.1126/science.282.5392.1332

107. Prestwich RJ, Ilett EJ, Errington F, Diaz RM, Steele LP, Kottke T, et al. Immune-mediated antitumor activity of reovirus is required for therapy and is independent of direct viral oncolysis and replication. *Clin Cancer Res* (2009) 15(13):4374–81. doi: 10.1158/1078-0432.CCR-09-0334

108. Forsyth P, Roldan G, George D, Wallace C, Palmer CA, Morris D, et al. A phase I trial of intratumoral administration of reovirus in patients with histologically confirmed recurrent Malignant gliomas. *Mol Ther* (2008) 16(3):627–32. doi: 10.1038/sj.mt.6300403

109. Kicielinski KP, Chiocca EA, Yu JS, Gill GM, Coffey M, Markert JM. Phase 1 clinical trial of intratumoral reovirus infusion for the treatment of recurrent Malignant gliomas in adults. *Mol Ther* (2014) 22(5):1056–62. doi: 10.1038/mt.2014.21

110. Ilett E, Kottke T, Donnelly O, Thompson J, Willmon C, Diaz R, et al. Cytokine conditioning enhances systemic delivery and therapy of an oncolytic virus. *Mol Ther* (2014) 22(10):1851–63. doi: 10.1038/mt.2014.118

111. Schuelke MR, Gundelach JH, Coffey M, West E, Scott K, Johnson DR, et al. Phase I trial of sargramostim/pelareorep therapy in pediatric patients with recurrent or refractory high-grade brain tumors. *Neurooncol Adv* (2022) 4(1):vdac085. doi: 10.1093/noajnl/vdac085

112. Gromeier M, Alexander L, Wimmer E. Internal ribosomal entry site substitution eliminates neurovirulence in intergeneric poliovirus recombinants. *Proc Natl Acad Sci U.S.A.* (1996) 93(6):2370–5. doi: 10.1073/pnas.93.6.2370

113. Merrill MK, Bernhardt G, Sampson JH, Wikstrand CJ, Bigner DD, Gromeier M. Poliovirus receptor CD155-targeted oncolysis of glioma. *Neuro Oncol* (2004) 6 (3):208–17. doi: 10.1215/S1152851703000577

114. Desjardins A, Gromeier M, Herndon JE 2nd, Beaubier N, Bolognesi DP, Friedman AH, et al. Recurrent glioblastoma treated with recombinant poliovirus. *N Engl J Med* (2018) 379(2):150–61. doi: 10.1056/NEJMoa1716435

115. Thompson EM, Landi D, Brown MC, Friedman HS, McLendon R, Herndon JE 2nd, et al. Recombinant polio-rhinovirus immunotherapy for recurrent paediatric high-grade glioma: a phase 1b trial. *Lancet Child Adolesc Health* (2023) 7(7):471–8. doi: 10.1016/S2352-4642(23)00031-7

116. Perez OD, Logg CR, Hiraoka K, Diago O, Burnett R, Inagaki A, et al. Design and selection of Toca 511 for clinical use: modified retroviral replicating vector with improved stability and gene expression. *Mol Ther* (2012) 20(9):1689–98. doi: 10.1038/mt.2012.83

117. Huang TT, Parab S, Burnett R, Diago O, Ostertag D, Hofman FM, et al. Intravenous administration of retroviral replicating vector, Toca 511, demonstrates therapeutic efficacy in orthotopic immune-competent mouse glioma model. *Hum Gene Ther* (2015) 26(2):82–93. doi: 10.1089/hum.2014.100

118. Ostertag D, Amundson KK, Lopez Espinoza F, Martin B, Buckley T, Galvao da Silva AP, et al. Brain tumor eradication and prolonged survival from intratumoral conversion of 5-fluorocytosine to 5-fluorouracil using a nonlytic retroviral replicating vector. *Neuro Oncol* (2012) 14(2):145–59. doi: 10.1093/neuonc/nor199

119. Tai CK, Wang WJ, Chen TC, Kasahara N. Single-shot, multicycle suicide gene therapy by replication-competent retrovirus vectors achieves long-term survival benefit in experimental glioma. *Mol Ther* (2005) 12(5):842–51. doi: 10.1016/j.ymthe.2005.03.017

120. Twitty CG, Diago OR, Hogan DJ, Burrascano C, Ibanez CE, Jolly DJ, et al. Retroviral replicating vectors deliver cytosine deaminase leading to targeted 5-fluorouracil-mediated cytotoxicity in multiple human cancer types. *Hum Gene Ther Methods* (2016) 27(1):17–31. doi: 10.1089/hgtb.2015.106

121. Logg CR, Robbins JM, Jolly DJ, Gruber HE, Kasahara N. Retroviral replicating vectors in cancer. *Methods Enzymol* (2012) 507:199–228. doi: 10.1016/B978-0-12-386509-0.00011-9

122. Cloughesy TF, Landolfi J, Hogan DJ, Bloomfield S, Carter B, Chen CC, et al. Phase 1 trial of vocimagene amiretrorepvec and 5-fluorocytosine for recurrent high-grade glioma. *Sci Transl Med* (2016) 8(341):341ra75. doi: 10.1126/scitranslmed.aad9784

123. Sirohi D, Chen Z, Sun L, Klose T, Pierson TC, Rossmann MG, et al. The 3.8 A resolution cryo-EM structure of Zika virus. *Science* (2016) 352(6284):467–70. doi: 10.1126/science.aaf5316

124. Heymann DL, Hodgson A, Sall AA, Freedman DO, Staples JE, Althabe F, et al. Zika virus and microcephaly: why is this situation a PHEIC? *Lancet* (2016) 387 (10020):719–21. doi: 10.1016/S0140-6736(16)00320-2

125. Zhu Z, Gorman MJ, McKenzie LD, Chai JN, Hubert CG, Prager BC, et al. Zika virus has oncolytic activity against glioblastoma stem cells. *J Exp Med* (2017) 214 (10):2843–57. doi: 10.1084/jem.20171093

126. Suva ML, Rheinbay E, Gillespie SM, Patel AP, Wakimoto H, Rabkin SD, et al. Reconstructing and reprogramming the tumor-propagating potential of glioblastoma stem-like cells. *Cell* (2014) 157(3):580–94. doi: 10.1016/j.cell.2014.02.030

127. Gangemi RM, Griffero F, Marubbi D, Perera M, Capra MC, Malatesta P, et al. SOX2 silencing in glioblastoma tumor-initiating cells causes stop of proliferation and loss of tumorigenicity. *Stem Cells* (2009) 27(1):40–8. doi: 10.1634/stemcells.2008-0493

128. Zhu Z, Mesci P, Bernatchez JA, Gimple RC, Wang X, Schafer ST, et al. Zika Virus Targets Glioblastoma Stem Cells through a SOX2-Integrin alpha(v)beta(5) Axis. *Cell Stem Cell* (2020) 26(2):187–204.e110. doi: 10.1016/j.stem.2019.11.016

129. Shan C, Muruato AE, Nunes BTD, Luo H, Xie X, Medeiros DBA, et al. A live-attenuated Zika virus vaccine candidate induces sterilizing immunity in mouse models. *Nat Med* (2017) 23(6):763–7. doi: 10.1038/nm.4322

130. Chen Q, Wu J, Ye Q, Ma F, Zhu Q, Wu Y, et al. Treatment of human glioblastoma with a live attenuated zika virus vaccine candidate. *mBio* (2018) 9(5): e01683-18. doi: 10.1128/mBio.01683-18

131. Nair S, Mazzoccoli L, Jash A, Govero J, Bais SS, Hu T, et al. Zika virus oncolytic activity requires CD8+ T cells and is boosted by immune checkpoint blockade. *JCI Insight* (2021) 6(1). doi: 10.1172/jci.insight.144619

132. Bulstrode H, Girdler GC, Gracia T, Aivazidis A, Moutsopoulos I, Young AMH, et al. Myeloid cell interferon secretion restricts Zika flavivirus infection of developing and Malignant human neural progenitor cells. *Neuron* (2022) 110(23):3936–3951.e3910. doi: 10.1016/j.neuron.2022.09.002

133. Alvarado AG, Kornblum HI. Interfer(on)ing with zika virus. *Neuron* (2022) 110 (23):3853–4. doi: 10.1016/j.neuron.2022.10.027

134. Rojas JJ, Cascallo M, Guedan S, Gros A, Martinez-Quintanilla J, Hemminki A, et al. A modified E2F-1 promoter improves the efficacy to toxicity ratio of oncolytic adenoviruses. *Gene Ther* (2009) 16(12):1441–51. doi: 10.1038/gt.2009.103

135. D'Amico RS, Aghi MK, Vogelbaum MA, Bruce JN. Convection-enhanced drug delivery for glioblastoma: a review. *J Neurooncol* (2021) 151(3):415–27. doi: 10.1007/s11060-020-03408-9

136. Li J, Zhao J, Tan T, Liu M, Zeng Z, Zeng Y, et al. Nanoparticle drug delivery system for glioma and its efficacy improvement strategies: A comprehensive review. *Int J Nanomedicine* (2020) 15:2563–82. doi: 10.2147/IJN.S243223

137. Kardani K, Sanchez Gil J, Rabkin SD. Oncolytic herpes simplex viruses for the treatment of glioma and targeting glioblastoma stem-like cells. *Front Cell Infect Microbiol* (2023) 13:1206111. doi: 10.3389/fcimb.2023.1206111

138. Nguyen HM, Guz-Montgomery K, Lowe DB, Saha D. Pathogenetic features and current management of glioblastoma. *Cancers (Basel)* (2021) 13(4):856. doi: 10.3390/cancers13040856

10.3389/fimmu.2023.1285113

Glossary

GBM	Glioblastomas
WHO	The World Health Organization
TMZ	Temozolomide
rGBM	Recurrent glioblastoma
mOS	Median overall survival
OV	Oncolytic virus
HSV-1	Herpes simplex virus-1
Ad	Adenovirus
NDV	Newcastle disease virus
RV	Reovirus
oHSV	Oncolytic herpes simplex virus
TK	Thymidine kinase protein
dNMP	Deoxyribonucleotides
PKR	Protein kinase R
RR	Ribonucleotide reductase
pfu	Plaque forming units
GSC	Glioblastoma stem cells
pHGG	Pediatric high-grade glioma
DIPG	Diffuse intrinsic pontine glioma
scFv	Single chain fragment variable
TAP	The antigen presenting
MHLW	Ministry of Health, Labour and Welfare
CRAds	Cancer-Selective Replicating Adenoviruses
5-FU	5-fluorouracil
CAR	Coxsackie adenovirus receptor
mE1A	Mutant E1A
CPT-11	Camptothecin analogue irinotecan
RGD	Arginine-glycine aspartic acid
pHGG	Pediatric high-grade gliomas
DIPGs	Diffuse intrinsic pontine gliomas
vp	Viral particles
RT	Radiotherapy
4-1BBL	4-1BB ligand
DNX-2440	Delta-24-RGDOX
OX40L	OX40 ligand
pRb	The retinoblastoma tumor suppressor protein
PVSRIPO	Recombinant nonpathogenic polio-rhinovirus chimera
CD	Cytosine deaminase
Toca FC	Prodrug 5-fluorocytosine
SOC	Standard of care
ZIKV	Zika virus
GSCs	Glioblastoma multiforme stem cells
3'UTR	3' untranslated region
BBB	Blood-brain barrier
TME	Tumor microenvironment
CED	Convection-enhanced delivery

frontiers | Frontiers in Immunology

TYPE Correction
PUBLISHED 19 December 2023
DOI 10.3389/fimmu.2023.1352909

OPEN ACCESS

APPROVED BY
Frontiers Editorial Office,
Frontiers Media SA, Switzerland

*CORRESPONDENCE
Yaohui Chen
mcb.chenyaohui@gmail.com

†These authors have contributed equally to this work and share first authorship

RECEIVED 09 December 2023
ACCEPTED 12 December 2023
PUBLISHED 19 December 2023

CITATION
Hu M, Liao X, Tao Y and Chen Y (2023) Corrigendum: Advances in oncolytic herpes simplex virus and adenovirus therapy for recurrent glioma.
Front. Immunol. 14:1352909.
doi: 10.3389/fimmu.2023.1352909

Corrigendum: Advances in oncolytic herpes simplex virus and adenovirus therapy for recurrent glioma

Mingming Hu[1,2†], XuLiang Liao[1,2†], Yi Tao[1,2†] and Yaohui Chen[1,3*]

[1]Institute of Thoracic Oncology, West China Hospital, Sichuan University, Chengdu, China, [2]Frontiers Science Center for Disease-Related Molecular Network, West China Hospital, Sichuan University, Chengdu, China, [3]Department of Thoracic Surgery, West China Hospital, Sichuan University, Chengdu, China

KEYWORDS

oncolytic viruses, cancer therapy, recurrent gliomas, oncolytic herpes simplex virus, adenovirus therapy

A Corrigendum on

Advances in oncolytic herpes simplex virus and adenovirus therapy for recurrent glioma

By Hu M, Liao X, Tao Y and Chen Y (2023) *Front. Immunol.* 14:1285113. doi: 10.3389/fimmu.2023.1285113

In the published article, there was an error in the **Funding** statement. We overlooked the fund that supported this article.

The correct Funding statement appears below:

"This work was supported by the 1.3.5 project for disciplines of excellence, West China Hospital, Sichuan University (Y.C., ZYJC21015)."

The authors apologize for this error and state that this does not change the scientific conclusions of the article in any way. The original article has been updated.

Publisher's note

All claims expressed in this article are solely those of the authors and do not necessarily represent those of their affiliated organizations, or those of the publisher, the editors and the reviewers. Any product that may be evaluated in this article, or claim that may be made by its manufacturer, is not guaranteed or endorsed by the publisher.

frontiers | Frontiers in Oncology

TYPE Original Research
PUBLISHED 20 November 2023
DOI 10.3389/fonc.2023.1259314

OPEN ACCESS

EDITED BY
Yaohe Wang,
Queen Mary University of London,
United Kingdom

REVIEWED BY
Nayara Tessarollo,
ICESP, Brazil
Tahir Bashir Dar,
Cedars Sinai Medical Center, United States

*CORRESPONDENCE
Lukasz Kuryk
lkuryk@pzh.gov.pl
Mariangela Garofalo
mariangela.garofalo@unipd.it

RECEIVED 15 July 2023
ACCEPTED 13 October 2023
PUBLISHED 20 November 2023

CITATION
Garofalo M, Wieczorek M, Anders I, Staniszewska M, Lazniewski M, Prygiel M, Zasada AA, Szczepińska T, Plewczynski D, Salmaso S, Caliceti P, Cerullo V, Alemany R, Rinner B, Pancer K and Kuryk L (2023) Novel combinatorial therapy of oncolytic adenovirus AdV5/3-D24-ICOSL-CD40L with anti PD-1 exhibits enhanced anti-cancer efficacy through promotion of intratumoral T-cell infiltration and modulation of tumour microenvironment in mesothelioma mouse model. *Front. Oncol.* 13:1259314. doi: 10.3389/fonc.2023.1259314

Novel combinatorial therapy of oncolytic adenovirus AdV5/3-D24-ICOSL-CD40L with anti PD-1 exhibits enhanced anti-cancer efficacy through promotion of intratumoral T-cell infiltration and modulation of tumour microenvironment in mesothelioma mouse model

Mariangela Garofalo[1]*, Magdalena Wieczorek[2], Ines Anders[3], Monika Staniszewska[4], Michal Lazniewski[4,5], Marta Prygiel[6], Aleksandra Anna Zasada[6], Teresa Szczepińska[4], Dariusz Plewczynski[7,8], Stefano Salmaso[1], Paolo Caliceti[1], Vincenzo Cerullo[9,10,11,12,13], Ramon Alemany[14], Beate Rinner[3], Katarzyna Pancer[2] and Lukasz Kuryk[2,4,15]*

[1]Department of Pharmaceutical and Pharmacological Sciences, University of Padova, Padova, Italy, [2]Department of Virology, National Institute of Public Health, National Institute of Hygiene (NIH) - National Research Institute, Warsaw, Poland, [3]Division of Biomedical Research, Medical University of Graz, Graz, Austria, [4]Centre for Advanced Materials and Technologies, Warsaw University of Technology, Warsaw, Poland, [5]Department of Bacteriology and Biocontamination Control, National Institute of Public Health, National Institute of Hygiene (NIH) - National Research Institute, Warsaw, Poland, [6]Departament of Sera and Vaccines Evaluation, National Institute of Public Health, National Institute of Hygiene (NIH) - National Research Institute, Warsaw, Poland, [7]Laboratory of Bioinformatics and Computational Genomics, Faculty of Mathematics and Information Science, Warsaw University of Technology, Warsaw, Poland, [8]Laboratory of Functional and Structural Genomics, Centre of New Technologies, University of Warsaw, Warsaw, Poland, [9]Drug Research Program (DRP), ImmunoViroTherapy Lab (IVT), Division of Pharmaceutical Biosciences, Faculty of Pharmacy, University of Helsinki, Helsinki, Finland, [10]Helsinki Institute of Life Science (HiLIFE), University of Helsinki, Helsinki, Finland, [11]Translational Immunology Program (TRIMM), Faculty of Medicine Helsinki University, University of Helsinki, Helsinki, Finland, [12]Digital Precision Cancer Medicine Flagship (iCAN), University of Helsinki, Helsinki, Finland, [13]Department of Molecular Medicine and Medical Biotechnology and CEINGE, Naples University Federico II, Naples, Italy, [14]Oncobell Program of Bellvitge Biomedical Research Institute (IDIBELL), ProCure Program of Catalan Institute of Oncology (ICO), Avinguda de la Granvia de l'Hospitalet, L'Hospitalet de Llobrega, Barcelona, Spain, [15]Clinical Science, Valo Therapeutics, Helsinki, Finland

Introduction: Malignant mesothelioma is a rare and aggressive form of cancer. Despite improvements in cancer treatment, there are still no curative treatment modalities for advanced stage of the malignancy. The aim of this study was to evaluate the anti-tumor efficacy of a novel combinatorial therapy combining AdV5/3-D24-ICOSL-CD40L, an oncolytic vector, with an anti-PD-1 monoclonal antibody.

Methods: The efficacy of the vector was confirmed *in vitro* in three mesothelioma cell lines – H226, Mero-82, and MSTO-211H, and subsequently the antineoplastic properties in combination with anti-PD-1 was evaluated in xenograft H226 mesothelioma BALB/c and humanized NSG mouse models.

Results and discussion: Anticancer efficacy was attributed to reduced tumour volume and increased infiltration of tumour infiltrating lymphocytes, including activated cytotoxic T-cells (GrB+CD8+). Additionally, a correlation between tumour volume and activated CD8+ tumour infiltrating lymphocytes was observed. These findings were confirmed by transcriptomic analysis carried out on resected human tumour tissue, which also revealed upregulation of CD83 and CRTAM, as well as several chemokines (CXCL3, CXCL9, CXCL11) in the tumour microenvironment. Furthermore, according to observations, the combinatorial therapy had the strongest effect on reducing mesothelin and MUC16 levels. Gene set enrichment analysis suggested that the combinatorial therapy induced changes to the expression of genes belonging to the "adaptive immune response" gene ontology category. Combinatorial therapy with oncolytic adenovirus with checkpoint inhibitors may improve anticancer efficacy and survival by targeted cancer cell destruction and triggering of immunogenic cell death. Obtained results support further assessment of the AdV5/3-D24-ICOSL-CD40L in combination with checkpoint inhibitors as a novel therapeutic perspective for mesothelioma treatment.

KEYWORDS

immune checkpoint inhibitors, immunotherapy, oncolytic adenovirus, mesothelioma, anti PD-1, TILs, CD40L, ICOSL

Introduction

Malignant mesothelioma (MM) is an aggressive and very rare type of cancer that develops within the layer of mesothelial cells. The worldwide incidence of this malignancy has risen over the last decade, and an increase in the number of cases in the future is anticipated. Unfortunately, MM is almost universally lethal, and the median survival time from diagnosis is up to 12 months. Although new treatment options are currently available, they are not curative, and new drugs are highly needed to provide hope for mesothelioma patients (1–3).

The immune system plays a pervasive role in the prevention and treatment of cancer. Malignant tumors, on the other hand, can evolve a variety of immune suppression strategies (4). Several immunomodulating drugs have been explored as anti-cancer treatments and launched into clinical settings in recent years. Among them immune checkpoint inhibitors (CPIs), acting against PD-1 (programmed cell death protein 1), PD-L1 (programmed death ligand 1), and CTLA-4 (cytotoxic T-lymphocyte-associated protein 4), have exhibited antitumor activity in a variety of tumor types, including metastatic melanoma, lung cancer, and breast malignancies (5). These CPIs have demonstrated significant therapeutic efficacy in metastatic carcinomas by reverting effector T-cell depletion and malfunction, improving anti-tumoral characteristics, and therefore enhancing T-cell activation (6). However, results of clinical trials show only limited overall survival of patients treated with anti-PD-1. Nevertheless, clinical trials PROMISE-Meso (NCT02991482) and CONFIRM (NCT03063450) suggest that PD-1 inhibitors, like pembrolizumab and nivolumab, have modest but clinically relevant activity in relapsed MM (7).

A promising anti-cancer strategy in solid cancer therapy is virotherapy. Oncolytic viruses (OVs) can infect and reproduce specifically within tumor cells, inevitably culminating to tumor cell lysis (8–13). OVs can elicit powerful, systemic, and persistent anti-tumor immunity in addition to direct and localized anti-tumor action (14–19). Many molecules are released by dying tumor cells, triggering antitumor immunity, and generating therapeutic responses even at distant tumor locations (20–23). Nevertheless, despite extensive research, oncolytic viruses have shown limited efficacy against solid tumors as monotherapy. Therefore, the refinement of novel and more efficacious oncolytic vectors is needed.

Immunotherapy functions well for metastatic carcinomas and can complement standard chemotherapeutics and radiotherapy (24). It has been shown that combining OVs with CPIs can elicit a synergistic antitumor efficacy that may contribute to improved therapeutic outcomes (14, 20, 25, 26). Thus, the present study was designed to evaluate the anti-tumor effectiveness of the

Abbreviations: APC, antigen presenting cells; ATP, adenosine triphosphate; CD40L, CD40 ligand (CD154); CPI, checkpoint inhibitors; CR2, conserved region 2; CRT, calreticulin; CTLA-4, lymphocyte-associated protein 4; DC, dendritic cells; FBS, fetal bovine serum; GO, Gene Ontology; GrB+CD8+, activated cytotoxic T cells; HMGB1, high mobility group box 1; i.t., intratumoral; i.v., intravenous; ICD, immunogenic cell death; ICOSL, inducible co-stimulator ligand; MM, malignant mesothelioma; MTS, CellTiter 96 AQueous One Solution Cell Proliferation Assay; OVs, oncolytic viruses; PD-1, programmed cell death protein 1; PD-L1, programmed death ligand 1; s.c., subcutaneous; TILs, tumor-infiltrating lymphocytes; TME, tumor microenvironment; VP, viral particles.

combinatorial therapy encasing oncolytic vector AdV5/3-D24-ICOSL-CD40L, expressing two powerful co-stimulatory molecules: inducible co-stimulator ligand (ICOSL) and CD40 ligand (CD40Land CD154) (25), with an anti-PD-1 monoclonal antibody, in both immunodeficient and humanized xenografted mesothelioma H266 mouse models. Importantly, it was previously shown that intratumoral (i.t.) therapy with oncolytic adenovirus armed with ICOSL can activate innate immunity and upregulates the expression of T-cell co-stimulatory receptors (23). In addition, it has been reported elsewhere that an OV coding for CD40L induced tumor regression *in vivo* by demonstrating apoptotic impacts, leading to an increased calreticulin (CRT) exposure and HMGB1 (high mobility group box 1) and ATP (adenosine triphosphate) output (27).

Moreover, we studied possible correlation between the level of tumor-infiltrating lymphocytes (TILs) and anti-cancer effect (tumor volume control). Importantly, transcriptomic analyses have been carried out to better understand clinical responses to therapy and seek for prognostic markers. Our study demonstrated that AdV5/3-D24-ICOSL-CD40L co-administered with human anti-PD-1 offers anti-cancer benefits in tested advanced mesothelioma mouse models. Profiling of the tumor microenvironment (TME) revealed sustained AdV5/3-D24-ICOSL-CD40L-induced immune cell infiltration correlating with tumor growth inhibition. Together, these results support further assessment of the virus in combination with anti-PD-1 for the management and treatment of malignant mesothelioma patients.

Materials and methods

Cell lines, viruses, anti-PD-1 antibodies

MSTO-211H (ACC 390, DSMZ, Germany) and NCI-H226 (H226, CRL-5826, ATCC, Manassas, VA) human malignant biphasic mesothelioma cells were grown in RPMI 1640 supplemented with 10% heat inactivated fetal bovine serum (FBS) (Gibco Laboratories), 2 mM L-glutamine (Gibco Laboratories), and 1% penicillin and streptomycin (Gibco Laboratories). Mero-82 (09100105-1VL) was a human epithelioid mesothelioma cell line procured from Sigma Aldrich and grown in Hams F10 with 15% heat-inactivated FBS (Gibco Laboratories), 2 mM L-glutamine (Gibco Laboratories), and 1% penicillin and streptomycin (Gibco Laboratories). Cell Bank Australia provided the mouse mesothelioma cell line AB12. The murine cell line was grown in RPMI 1640 medium containing 1% penicillin/streptomycin (Gibco Laboratories), 2 mM L-glutamine (Gibco Laboratories), and 10% FBS (Gibco Laboratories). The AdV5/3-D24-ICOSL-CD40L (consisting of a 24-bp deletion in E1A Conserved Region 2 (CR2), a CMV-ICOSL-CD40L expression cassette inserted in the E3 region, and Ad5/3 hybrid fiber), and AdV5/3-D24 (consisting of a 24-bp deletion in E1A Conserved Region 2 (CR2), and Ad5/3 hybrid fiber) adenovirus vectors utilized in this study are chimeric type 5/3 adenoviruses created and amplified using viral production procedures (25). Anti-mouse CD279 (PD1) antibody was purified and resuspended as per the manufacturer's instructions (BioLegend). Anti-PD-1 antibodies (pembrolizumab) were purchased from Merck.

CAR, CD46, DSG2, and PD-L1 expression in cancer cell lines

H226, MSTO-211H, and Mero-82 were stained with mouse monoclonal anti-CAR antibody (Santa Cruz Biotech, Dallas, TX, USA) followed by 1:2,000 Alexa-Fluor 488 secondary antibody (Abcam, Cambridge, UK) or mouse monoclonal anti-DSG2 antibody (Abcam, Cambridge, UK) and then with 1:2,000 Alexa-Fluor 488 secondary antibody (Abcam, Cambridge, UK). Rabbit anti-PD-L1 antibodies (Alexa Fluor 488, Abcam, ab209959) were used to measure PD-L1 expression (at least 1×10^4 cells/events were examined by flow cytometry, BD FACSCantoTM II (Franklin Lakes, NJ, USA)). Flow cytometry analysis was performed on FlowJo v10 software.

Cell viability: MTS cytotoxicity assay

H226, MSTO-211H, and Mero-82 mesothelioma cell lines were seeded at a density of 1×10^4 cells/well in a 96-well plate and kept under standard growth conditions (RPMI 1640/Hams F10, supplemented with 5% FBS, 1% L-glutamine, and 1% penicillin/streptomycin). After overnight incubation, cells were treated as follows: (i) culture media, (ii) AdV5/3-D24-ICOSL-CD40L (0.1, 1, 10, and 100 viral particles (VP)/cell), and (iii) AdV5/3-D24 (0.1, 1, 10, 100 VP/cell), with or without anti-PD-1 (100 μg/mL). The viability of the cells was assessed 96 h after treatment employing the CellTiter 96 AQueous One Solution Cell Proliferation Assay (MTS) as directed by the manufacturer (Promega, Madison, WI, USA). A 96-well plate spectrophotometer (Victor NivoTM, PerkinElmer) was used to detect the absorbance at 490 nm. The experiment was run in triplicate.

Immunogenic cell death

CRT exposure. At 5×10^5 cells per well, cell lines were seeded in triplicate into six-well plates. According to the treatment combinations listed above, cells were infected with 100 VP/cell of the tested oncolytic adenovirus and/or anti-PD-1 drugs (50 μg/mL). After 48 h, cells were collected and stained with 1:1,000 diluted rabbit polyclonal anti-calreticulin antibody (Abcam, Cambridge, UK) for 40 min at 4°C, followed by flow cytometry (Franklin Lakes, NJ, USA) (14).

HMGB-1 release. Cell lines were seeded in triplicate into 96-well plates at a density of 1×10^4 cells/well and infected with 100 VP/cell of evaluated oncolytic adenovirus and/or anti-PD-1 drugs as per the treatment combinations shown above. Supernatants were collected after a time span of 72 h, and HMGB-1 was quantified using an ELISA kit according to the manufacturer's instructions (MBL International, Woburn, MA) (14).

ATP release. Cell lines were seeded in triplicates onto 96-well plates at a density of 1×10^4 cells/well and treated as described before.

Following 72 h, supernatants were recovered, and luminometric analysis was performed using the ATP Determination Kit (Promega, Madison, WI) according to the manufacturer's procedure (Varioscan Flash, Thermo Fisher Scientific, Waltham, MA) (14).

In vivo studies

Animal procedures were approved by the Austrian Federal Ministry of Science and Research, the Italian Ministry of Health, and the Warsaw University of Life Sciences' II Local Ethical Committee for Animal Experiments. Mesothelioma xenografts were established by injecting 6×10^6 H226 cells subcutaneously (s.c.) into one or both sides of BALB/c nude mice (n=5 mice per group, 5 tumors per group) or human CD34+ hematopoietic stem-cell-engrafted NSG variant mice (hu-CD34+, Jax Laboratories) (n=4 mice per group, 8 tumors per group). During the acclimation and treatment phase, all animals were monitored for clinical symptoms, morbidity, and death daily. Clinical signs in animal health scoring have been monitored (Supplementary Table S1). Selected organs such as the spleen, liver, heart, kidneys, lungs, brain, and tumors underwent basic necropsy assessment. Prior to the start of treatment, tumors of sizes ~5 × 5 mm in diameter were randomized. Mice were given treatments according to the ones enlisted in Supplementary Table S2, S3 (immunodeficient mesothelioma H226 mouse model, humanized mesothelioma H226 mouse model). At least twice a week, the size of the tumor was measured using a caliper in two dimensions. At each timepoint, the longest and shortest diameters of the tumor were measured, and the tumor volume was computed using the formula 0.52 length × $(\text{width})^2$. To monitor the tumor development of H226 cells in BALBc nude mice and NSG variant mice (hu-CD34+), micro-ultrasound measurement (Vevo3100, Fujifilm VisualSonics) was performed at least twice a week. For ultrasound examinations, the animals were anesthetized using 2% isoflurane and 2.5 L/min O_2 and then placed on a heated platform. The region of interest was depilated, and the tumor investigated and measured in coronal and transverse planes using transducers of 52–70 MHz. After ultrasound investigation, the animals were cleaned from gel residues, transferred back to their home cage, and monitored until fully awake.

Immune cell infiltrates—*ex vivo* analyses

The percentage number of human immune cell populations were monitored by flow cytometry: human CD45+ lymphocytes (BD, cat. number: 564105), T cells hCD3+ (BD, cat. number: 555339), CD4+ T cells (hCD3+ hCD4+, BD, cat. number: 557852), CD8+ T cells (hCD3+ hCD8+, BD, cat. number: 560179), activated CD8+ (hCD3+ hGrB+ hCD8+, BD, cat. number: 560212), and FoxP3 (hCD3+ hCD4+ hFoXP3+, BD, cat. number: 560046). Tumors were harvested and subsequently dissociated with cell strainer (day 35—end of study). Immune cells were isolated by following the protocol described earlier (28). After dissociation, cells were washed using BD Perm/Wash™ buffer (cat. no. 554723) and stained with antibodies for 30 min at 4°C in the dark and then suspended in stain buffer FBS (BD, cat no. 554656). Samples were acquired using BD Lyric FACS Flow. The populations were gated with forward and side scattering (FSC-A/SSC-A dot plot) in leukocytic regions. Flow cytometry analysis was performed on FlowJo v10 software.

Quantitative real-time PCR

The quantification of adenoviral DNA copies has been performed according to the protocol described earlier (1). Samples were analyzed using LighCycler qPCR machine (LighCycler 480, Roche, Basel, Switzerland).

Gene expression analyses

Whole transcriptome analysis, using total RNA sequencing (Illumina NextSeq, sequenced in paired-end mode) of available tumors (end of study) from humanized H226 mice was performed. Eight publicly available RNA-seq data for H226 cell line (GSM4117346) (29) were used to enrich the control group that originally comprised of two samples. In brief, reads were first trimmed of nucleotides from both ends if their quality in Phred scale was below 30; afterwards, only reads longer than 40 bp were kept. Reads were subsequently aligned to the human genome (hg38) using the align function from the Rsubread package (ver. 2.10.1). Only reads with the flags 99, 147, 83, or 163 were kept for further analysis. Reads were assigned to genes, as defined by the GENCODE annotation (ver. 39), using the feature counts function. A total of 18,254 genes for which at least seven samples had at least four reads assigned were kept. As data come from two experiments, batch effects were removed with the ComBat function from the SVA package (ver. 3.44) using non-parametric adjustments. Differential expression between groups (control, 10 samples; AdV5/3-D24-ICOSL-CD40L, six samples; pembrolizumab, three samples; AdV5/3-D24-ICOSL-CD40L + pembrolizumab, two samples) was performed using limma (ver. 3.52). Gene ontology (GO) enrichment was analyzed with topGO (ver. 2.48) with the Fisher's exact test and weight01 algorithm. Relative levels of different immune cells were calculated from RNA-seq data using the quanTIseq and MCP-counter methods (30) using the immunedeconv package (ver 2.0.4) (31).

Statistical analysis

In vitro and *in vivo* variables were analyzed using GraphPad Prism software (version 9). A repeated measures with ANOVA and Mann–Whitney t-test were used in the statistical analysis. The Pearson correlation coefficient was utilized to look for possible correlations

between tumor volume and the percentage of CD4+, CD8+, GrB+CD8+, and FoxP3 cells in tumor-infiltrating lymphocytes.

Results

Evaluation of cell viability by MTS cytotoxicity assay

The *in vitro* cytotoxicity efficacy of AdV5/3-D24-ICOSL-CD40L was tested in H226, Mero-82, and MSTO-211H cell lines to check whether the presence of the double transgenes into the viral backbone could affect the *in vitro* oncolytic activity. Oncolytic potency of tested oncolytic adenoviruses was confirmed. Treatment with oncolytic adenovirus AdV5/3-D24-ICOSL-CD40L showed enhanced *in vitro* efficacy compared to AdV5/3-D24 in all tested mesothelioma cell lines. Although not statistically significant (Figure 1A), the results suggest that the incorporation of co-stimulator transgenes (ICOSL and CD40L) did not impair oncolytic properties of the vector. Interestingly, the combinatory therapy of both tested oncolytic adenoviruses with anti-PD-1 showed enhanced killing efficacy *in vitro* on three tested cell lines (Figure 1B) presumably due to drugs toxicity.

Immunogenic cell death assessment

Markers for immunogenic cell death (ICD), such as the exposure of calreticulin to cell surface and the extracellular release of ATP and HMGB1 (32), were measured from mesothelioma cell cultures after exposure to the virus, anti-PD-1, or combination of both. The infected cell lines with tested oncolytic adenoviruses resulted in ICD *in vitro* (expression of calreticulin, release of ATP, and HM-GB1). Immunogenic cell death was observed when treated with the virus and combinatory therapy (Supplementary Figure S1). H226 cell line was the most susceptible for cell death when treated with the virus and with the combinatory therapy.

CAR, CD46, DSG2, and PD-L1 expression in mesothelioma cell lines

All mesothelioma cells lines (MSTO-211H, H226, and Mero-82) expressed high level of CD46 (93%, 99%, and 99%, respectively) and DSG2 (99%, 99%, and 98%, respectively) on their surfaces. Finally, MSTO-211H (88%), H226 (48%), and Mero-82 (94%) expressed CAR. All mesothelioma cell lines express PD-L1 on cell surface (>98%) (Supplementary Figure S2).

In vivo efficacy study in immunodeficient xenograft mesothelioma H226 mouse model

Next, we carried out experiment in immunodeficient xenograft mesothelioma H226 mouse model, where we aimed at assessing oncolytic properties of the virus. Due to known limitations of the model, such as lack of a thymus, impaired immune system, immunological properties of the vector, anti-PD-1 were not able to be properly assessed. Anti-cancer efficacy was observed in mice treated with oncolytic adenovirus Ad5/3-D24-ICOSL-CD40L (vs. mock, $p \leq 0.05$), AdV5/3-D24, combination therapy (AdV5/3-D24 with anti-PD-1 vs. mock, $p \leq 0.05$), and when mice received Ad5/3-D24-ICOSL-CD40L + anti-PD-1. No statistically significant difference in anti-cancer efficacy has been observed between tested oncolytic adenoviruses (Ad5/3-D24-ICOSL-CD40L vs. AdV5/3-D24) (Figures 2A, B). As expected, no treatment efficacy was observed in mice treated with anti-PD-1 alone (Figures 2A, B). At the end of the study, the average volume size of a tumor for mice treated with the AdV5/3-D24, Ad5/3-D24-ICOSL-CD40L, and in their combinatory therapy was, respectively, 56, 55, and 56, 50 mm^3 compared to 99 mm^3 (anti-PD-1) and 95 mm^3 (control). The treatment was well tolerated (Figure 2C). All mice survived till the end of study (day 32). Adenoviral DNA copy number assessed by qPCR revealed presence of adenoviral DNA in tumor cells (Supplementary Figure S3).

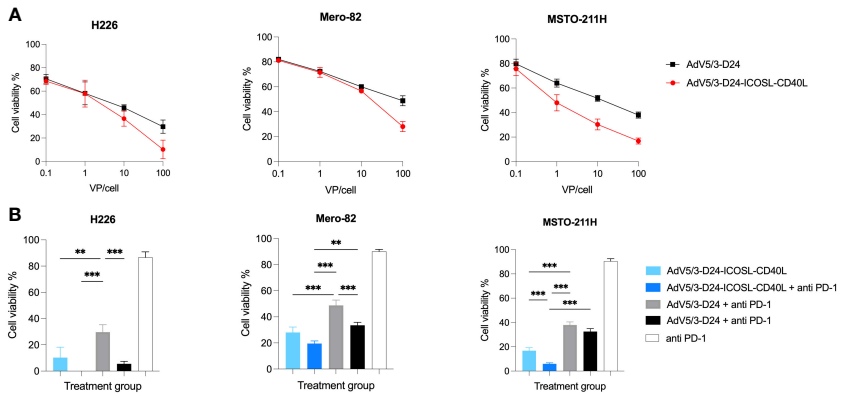

FIGURE 1
In vitro cytotoxicity assay (MTS assay). **(A)** AdV5/3-D24-ICOSL-CD40L and AdV5/3-D24 at concentrations of 0.1, 1, and 10, and 100VP/cell were used to assess cell viability 96-h after infection. **(B)** Combinatory treatment with AdV5/3-D24-ICOSL-CD40L and AdV5/3-D24 at concentrations 100VP/cell with or without anti-PD-1 (100 μg/mL) were used to assess cell viability 96 h after infection. Statistical analyses were carried out with Mann–Whitney t-test. Error bars, mean ± SEM; **p ≤ 0.01, ***p<0.001.

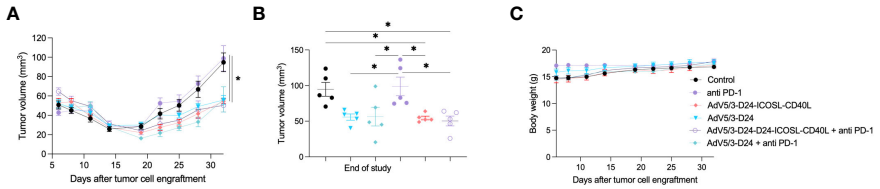

FIGURE 2
Antitumor efficacy of AdV5/3-D24, AdV5/3-D24-ICOSL-CD40L, and anti-PD-1 and the combinatory therapy in mesothelioma H226 xenograft immunodeficient BALB/c nude model (5×10^6 cells/flank, n=5 per group). **(A)** Prior to the start of treatment, tumors of sizes ~5 × 5 mm in diameter were randomized. Once tumors have been formed, the treatment has been initiated. Mice received 1×10^8 VP viruses i.t., 200 µg anti-PD-1 i.v. on days 0, 3, 6, 9, 12, and 15. The control group received PBS administered in a same scheme as treated groups. Tumor volume (mm^3) was measured through the study. At the conclusion of the study, mice were sacrificed, and tumors were extracted. **(B)** Tumor volume (mm^3) measured at the end of the study (day 32). **(C)** Body weight was measured throughout the study. Statistical analyses were carried out with ANOVA test. Error bars, mean ± SEM; *p ≤ 0.05.

In vivo efficacy and immunomodulatory properties of tested agents in humanized xenograft mesothelioma H226 mouse model

To study oncolytic properties of the vector and immunostimulatory functions of the tested agents, humanized xenograft mesothelioma H226 mouse model was exploited. Improved anti-cancer efficacy was observed in combination therapy with AdV5/3-D24-ICOSL-CD40L plus anti-PD-1 versus mock ($p \leq 0.01$) and in mice treated with AdV5/3-D24-ICOSL-CD40L (vs. mock, $p \leq 0.05$) (Figure 3A). After 35 days of treatment, the average volume size of a tumor in combination regime group was 93 mm^3 compared to 216 mm^3 (anti-PD-1), 164 mm^3 (virus alone), 241 mm^3 (control) (Figure 3B). Survival of 100% was reported for mice treated with the virus alone and combinatory therapy (Figure 3C). The treatment was well tolerated (Figure 3D), no pathological changes in necropsy assessment were found (Figures 3E, F). *Ex vivo* analyses revealed local production of ICOSL and CD40L transgenes encoded by the AdV5/3-D24-ICOSL-CD40L (Figure 4) and presence of adenoviral DNA copies in the tumors (Supplementary Figure S3). Enhanced infiltration of activated cytotoxic (GrB+ CD8+ T cells) tumor-infiltrating T cells has been reported in mice treated with the combination regimen (Figure 5, $p \leq 0.01$, combination therapy vs. control). Statistically significant correlation between tumor volume and GrB+CD8+ TILs was seen (Figure 6, p=0,022).

Gene expression analyses

To better characterize the effect of the individual (anti-PD-1, AdV5/3-D24-ICOSL-CD40L) and combinatorial (AdV5/3-D24-ICOSL-CD40L + anti-PD-1) therapies, we performed gene expression analysis by RNA-seq on extracted human H226 mesothelioma xenografts explanted from the humanized mice. To increase statistical power of this analysis, we also included, as control, eight samples from publicly available RNA-seq data for the H226 cell line from the RNA Atlas (GSM4117346). The DGE analysis revealed 3,190, 1,158, and 825 differentially expressed genes compared to control (fold change in log2 scale at least 1, average expression at least −2, and adjusted p-value < 0.05) for AdV5/3-D24-ICOSL-CD40L, anti-PD-1, and AdV5/3-D24-ICOSL-CD40L+ anti-PD-1 therapies, respectively. A set of common 258 genes with expression altered in all therapies with respect to control was observed. A total of 241 genes were overexpressed, and 17 were underexpressed (Supplementary Figure S4). Of the 825 genes, 334 were unique to the combinatorial regimen. This group comprised of several genes associated with activated immune cells like CD83 (log fold change 1.38; adjusted p-value, 0.01, Figure 7A), CRTAM (2.22; 0.01, Figure 7B), CD8B (1,9; 0.03, Figure 7C), or CXCL9 (l2.08, 0.07, Figure 7D). Moreover, several more genes associated with T-cell activation were upregulated in samples treated with either AdV5/3-D24-ICSOL-CD40L or AdV5/3-D24-ICSOL-CD40L + anti-PD-1. These include chemokines CXCL3, CXCL10, CXCL11, and TAP1 (Figures 7E–H). For CXCL11, the observed expression increased by 2.71 and 1.14 for combinatorial and AdV5/3-D24-ICSOL-CD40L therapies, respectively. In samples treated exclusively with CPI, the expression of this protein was increased by 0.23. A similar pattern was observed for all the other above-mentioned genes. MUC16 (also known as CA125) was found among underexpressed genes that were mostly affected by the combinatorial therapy (fold change decreased by 2.33, adjusted p-value < 0.01). We have also observed decreased expression of MSLN in response to all types of treatments; however, the combinatorial therapy had the strongest effect on mesothelin levels (fold change decreased by 1.35; adjusted p-value, 0.01) (Figure 8). Levels of this proteins were not significantly altered in two remaining treatment strategies.

Gene Ontology analysis confirms the abovementioned conclusions, as the genes belonging to the “adaptive immune response” GO category are overrepresented among genes with altered expression in the combinatorial regimen compared to control (p-value 5e−5, Supplementary Figure S5). Other enriched GO category includes “cell surface receptor signalling pathway,” “response to wounding,” and “response to estrogen.” Finally, we decided to check a putative composition of TME observed with our bulk RNA-seq data. Several studies point out that the tumor material analyzed with RNA-sequencing is often contaminated with non-tumor cells, for example tumor-infiltrating immune cells (30), like cytotoxic CD8+ T cells. These cells are able to recognize and eradicate tumor cells and are associated with a good clinical prognosis in different cancer types and have an

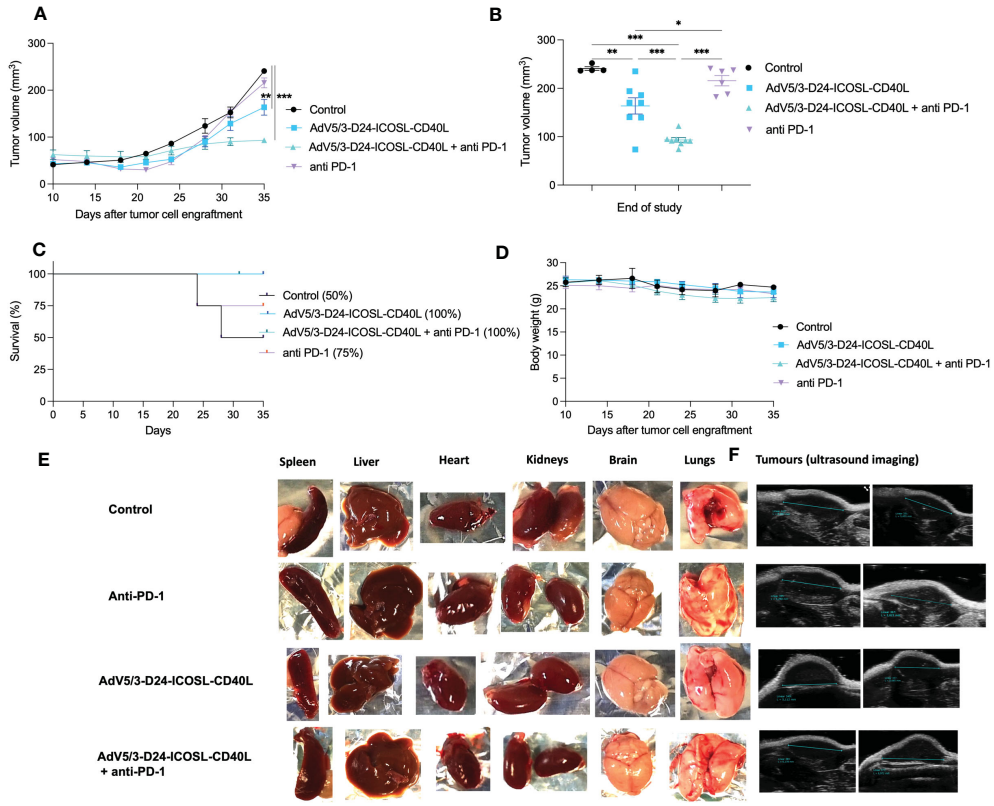

FIGURE 3
Antitumor efficacy of AdV5/3-D24-ICOSL-CD40L anti-PD-1 and the combinatory therapy in humanized mesothelioma H226 NSG nude model ($5x10^6$ cells/flank, n=4 mice per group (8 tumors per group). **(A)** Prior to the start of treatment, tumors of sizes ~5 × 5 mm in diameter were randomized. Once tumors have been formed, the treatment has been initiated. Mice received $2x10^9$ VP viruses i.t., 200 µg anti-PD-1 i.v. on days 0, 3, 6, 9, 12, and 15. The control group received PBS administered in a same scheme as treated groups. Tumor volume (mm^3) was measured through the study. At the conclusion of the study, mice were sacrificed, and tumors were extracted to determine tumor volume. **(B)** Tumor volume (mm^3) measured at the end of the study (day 35). **(C)** Survival profile was calculated by Kaplan–Meier test. **(D)** Body weight was measured throughout the study. **(E)** Morphological examination of organs collected from mice in control and treated with the virus plus anti-PD-1 group. **(F)** Representative ultrasound images for each group. Statistical analyses were carried out with ANOVA test. Error bars, mean ± SEM; *p ≤ 0.05, **p ≤ 0.01, ***p<0.001.

instrumental role in an anti-PD-1 immunotherapy. To determine the putative levels of different immune cells in our data, we used two methods—MCP counter (33) and quanTIseq (30). Both methods decompose bulk RNA-seq expression matrix using expression profile of genes characteristic only to specific cell types. For MCP counter, each cell type is assigned with a score, which correlates with putative number of each cell line. For the quanTIseq for each sample, a fraction of each of predefined cell types is provided. We found out that only the combinatorial therapy resulted in the increased levels of CD8+ T cells in TME (Figure 8). The

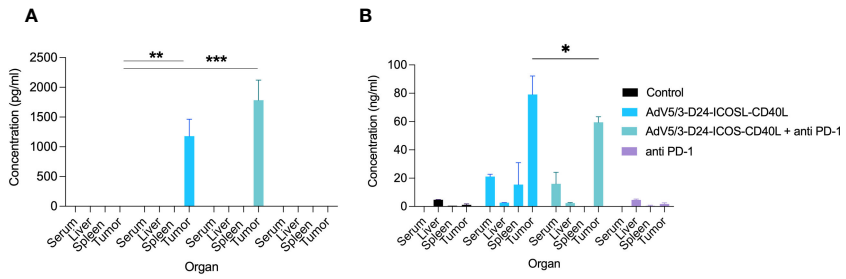

FIGURE 4
Evaluation of ICOSL and CD40L expression in various mouse organs after the treatment with oncolytic adenoviruses, anti-PD-1, and their combinations in humanized mesothelioma H226 model. **(A)** ICOSL concentration was measured from mouse organs (liver, tumor, and spleen) and blood collected at sacrifice after the treatment with ELISA kit (RayBiotech, ELH-B7H2-1) according to manufacturer's instructions. **(B)** CD40L was detected from mouse organs (liver, tumor, and spleen) and blood collected at sacrifice after the treatment with ELISA kit (RayBiotech, ELH-CD40L-1) as per the instructions laid down by the manufacturer. Statistical analyses were carried out with ANOVA test. Error bars, mean ± SM; *p ≤ 0.05, **p ≤ 0.01, ***p<0.001.

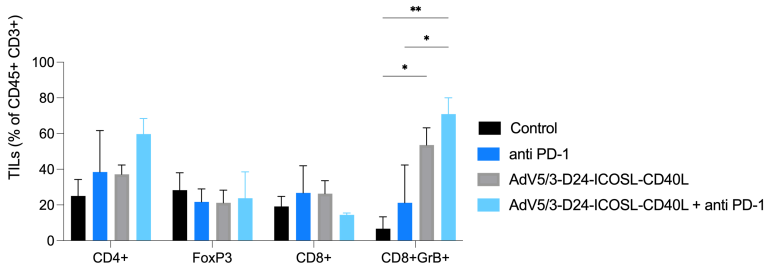

FIGURE 5
Levels of tumor infiltrating lymphocytes CD4+, CD8+, FoxP3, and GrB+CD8+ expression in collected tumors (end of study). Samples were acquired using BD Lyric FACS Flow. Statistical analyses were carried out with ANOVA test. Error bars, mean ± SEM; *p ≤ 0.05, **p ≤ 0.01.

application of AdV5/3-D24-ICOSL-CD40L or pembrolizumab alone did not yield increased levels of this subpopulation of T cells. Gene expression was confirmed by qPCR analyses.

Discussion

Despite huge efforts to improve the understanding and treatment of malignant mesothelioma, clinical practice has not changed dramatically in recent decades. To accelerate the development of novel treatment options, rational and well-designed investigations should be performed, and personalized approaches should be investigated (3, 34). In conjunction with CPIs and chemotherapy, OVs have shown to have a synergistic anti-cancer impact (1, 14, 25). While OVs exhibit clinical potential and a safety attribute in existing immunogenic tumors, clinical response rates are mild (35). As a result, the efficiency of oncolytic vectors must be improved in an attempt to implement them as a universal cancer treatment option.

In such a context, we designed the AdV5/3-D24-ICOSL-CD40L (25) oncolytic vector and tested its anti-cancer effectiveness along with an anti-PD-1 antibody in both immunodeficient and humanized xenografted mesothelioma H226 mouse model. The oncolytic adenovirus AdV5/3-D24-ICOSL-CD40L showed comparable anti-cancer efficacy to the treatment with AdV5/3-D24 in tested mesothelioma cell lines *in vitro*. The observed results are in corroboration with the ones reported elsewhere (14, 25, 36). Results suggest that incorporation of ICOSL and CD40L expression cassette into the genome of AdV5/3-D24-ICOSL-CD40L did not impair oncolytic properties of the vector when compared to AdV5/3-D24.

When contrasted to the other treatment groups, cell line treated with AdV5/3-D24-ICOSL-CD40L in conjunction with anti-PD-1

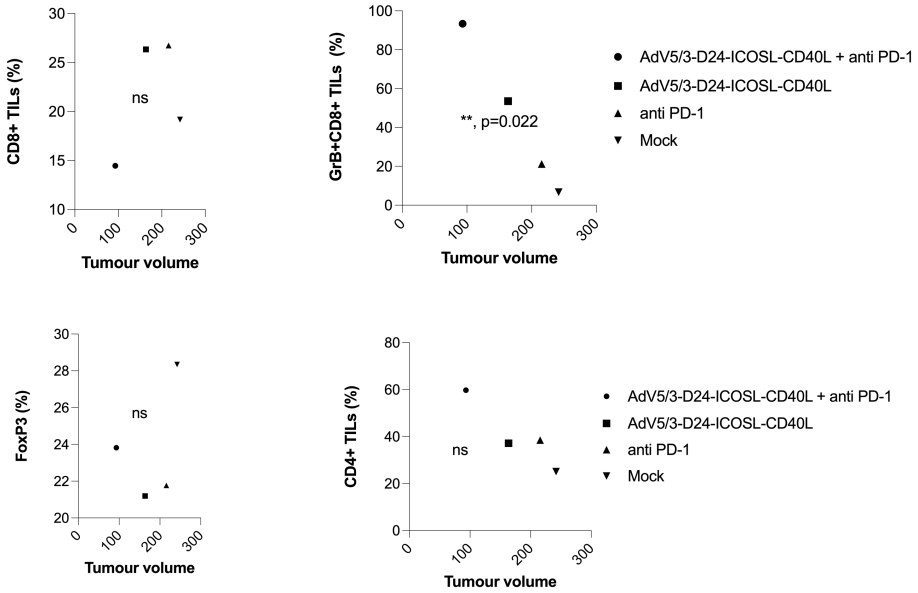

FIGURE 6
Immunomodulatory properties of tested agents in humanized xenograft mesothelioma H226 NSG nude model. At the end of the study, mice were euthanized and tumors collected for immunological analyses from four groups: (i) control, (ii) AdV5/3-D24-ICOSL-CD40L, (iii) anti-PD-1, and (iv) the combinatory therapy (end of study). Tumor-infiltrating lymphocytes CD4+, CD8+, FoxP3, and CD8+GrB+ mean expression has been assessed in collected tumors. Samples were acquired using BD Lyric FACS Flow. Statistical analyses were carried out with ANOVA test; ns, not significant. Error bars, mean ± SEM.

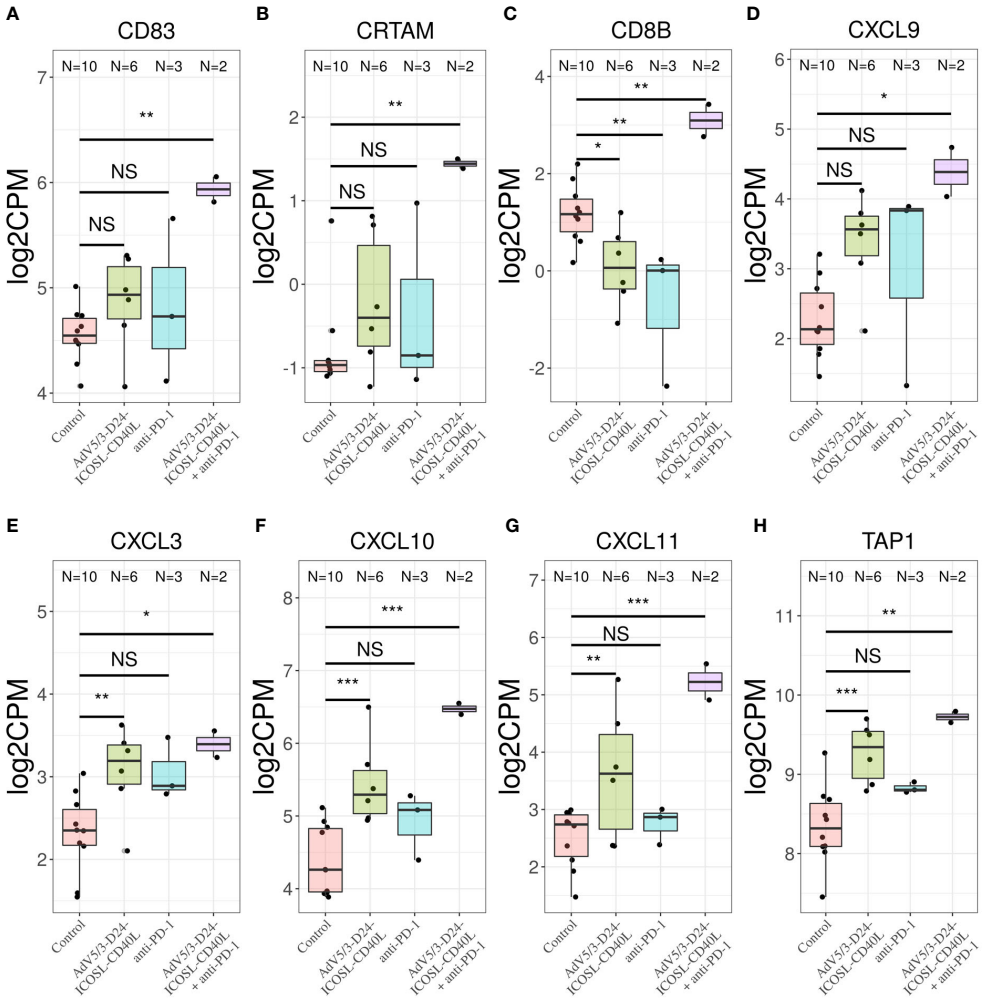

FIGURE 7
Transcriptomic analysis revealed upregulation of **(A)** CD83, **(B)** CRTAM, **(C)** CD8B, and **(D)** CXCL9 only in samples treated with combinatorial therapy. Transcriptomic analysis revealed upregulation of chemokines **(E)** CXCL3, **(F)** CXCL10, **(G)** CXCL11, and **(H)** TAP1 in samples treated with only AdV5/3-D24-ICOSL-CD40L, only anti-PD-1, or both AdV5/3-D24-ICOSL-CD40L + anti-PD-1 regimen, *p ≤ 0.1, **p ≤ 0.05, ***p<0.01; ns, not significant.

demonstrated significantly higher levels of calreticulin exposure and ATP. All these are known hallmarks of activated immunogenic cell death pathway (37). CD91, P2RX7, and TLR4 on dendritic cells are the receptors specific for CRT, ATP, and HMGB1, respectively. The ATP-P2RX7 signaling pathway attracts DCs to the target tumor tissue, the CRT-CD91 pathway enhances DC engulfment of cancer antigens, and the HMGB1-TLR4 route enables the optimum display of cancer antigens (38). Consequently, DC antigen uptake and presentation are thereby improved, resulting in a more adaptable antitumor immune response (39). These findings could indicate that the combinatorial therapy conferred a more cytotoxic immunological effect than the other groups.

Based on the promising *in vitro* results showcased by the combinatorial therapy involving AdV5/3-D24-ICOSL-CD40L, AdV5/3-D24 and their combinations with anti-PD-1, *in vivo* experiments were conducted. The animal model was built on H226 cells, where the virus showed the most effective oncolytic properties *in vitro*. The anti-tumor efficacy of oncolytic adenoviruses (AdV5/3-D24-ICOSL-CD40L or AdV5/3-D24) in mesothelioma H226 xenograft BALB/c nude immunodeficient model illustrated superior reduction in tumor volume when compared to control. Anti-cancer effectiveness was noted in mice treated with oncolytic adenovirus and combination therapy, although no effect of anti-PD-1 was observed. Nevertheless, it is important to underline that the model based on nude BALB/c mice is immunodeficient, and the observed anti-tumor effects have not included any contribution from the hosts' adaptive immune responses. The treatment regimens were well tolerated, and necropsy evaluation revealed no pathological alterations.

Tested oncolytic adenovirus AdV5/3-D24-ICOSL-CD40L is a human-specific vector, replicating selectively in human cancer cells. Anti-PD-1 inhibitor (pembrolizumab) is also a human-specific drug. Therefore, considering the features of the proposed biological agents a proper animal model is a crucial prerequisite for further investigation. To this point, humanized mouse model was utilized to test anti-cancer properties, allowing to investigate both oncolytic properties of the vector and immune responses in human immune system. In fact, improved anti-cancer efficacy was

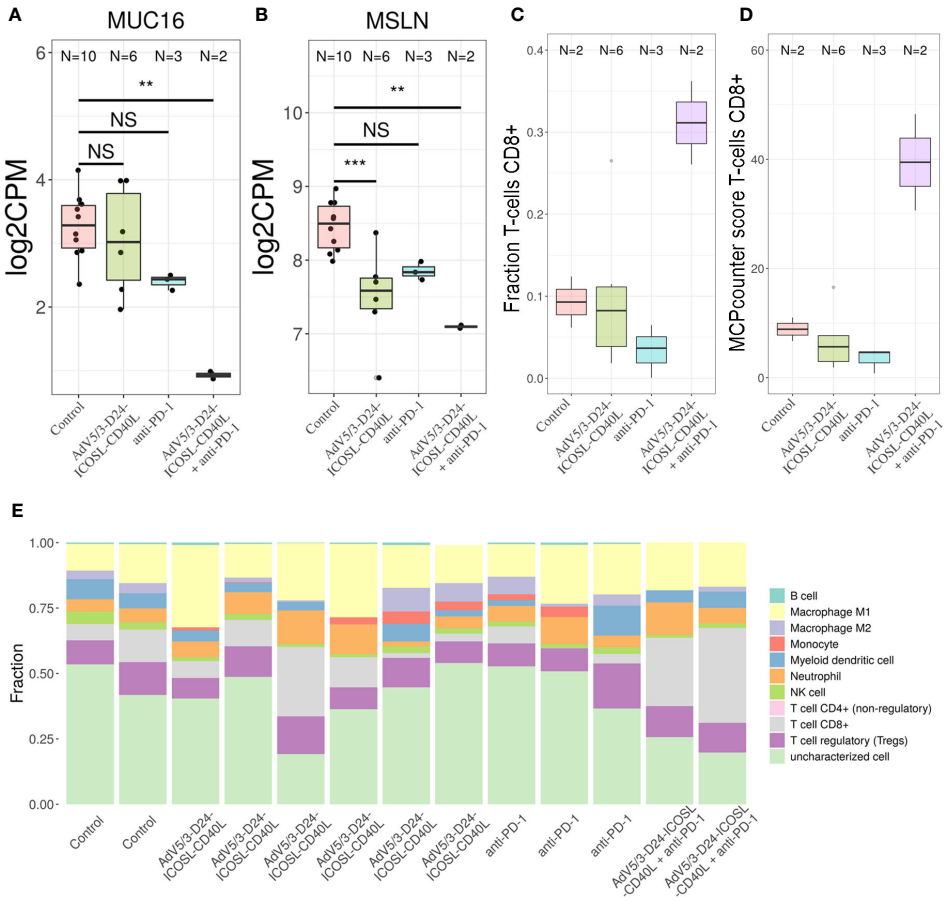

FIGURE 8
Transcriptomic analyses. To determine the putative levels of different immune cells in our data, we used two methods—MCP counter33 and quanTIseq. Both methods decompose bulk RNA-seq expression matrix using expression profile of genes characteristic only to specific cell types. For MCP counter, each cell type is assigned with a score, which correlates with putative number of each cell line. For quanTIseq for each sample, a fraction of each of predefined cell types is provided. We found out that only the combinatorial therapy resulted in the increased levels of CD8+ T cells in TME. Transcriptomic analyses revealed that **(A)** MUC16 and **(B)** MSLN were found among genes that expression was substantially decreased by the combinatorial therapy; **p ≤ 0.05, ***p<0.01. Putative levels of CD8+ T cells in TME analyzed with- quanTIseq **(C)** and MCP counter **(D)** using bulk RNA-seq data. The combinatorial therapy resulted in the highest levels of CD8+ T cells. **(E)** The application of AdV5/3-D24-ICOSL-CD40L or pembrolizumab alone did not yield increased levels of this subpopulation of T cells. Composition of TME predicted with quanTIseq using bulk RNA-seq data. ns, not significant.

observed in humanized xenograft H226 mesothelioma NSG mouse model [improved anti-cancer efficacy was observed in combination therapy with AdV5/3-D24-ICOSL-CD40L plus anti-PD-1 versus mock ($p \leq 0.01$) and in mice treated with AdV5/3-D24-ICOSL-CD40L (vs. mock, $p \leq 0.05$)] implying the suitable entry of adenovirus in the tumor cells, which can further lead to better anti-cancer effectiveness of the proposed therapy. The said fact was evidenced by the expression of CAR, DSG-2, and CD46 receptors and PD-L1 in human mesothelioma cell lines.

Our results corroborate with the outcome of a study utilizing the Ad5/3-D24-GM-CSF virus with pembrolizumab in the humanized A2058 melanoma huNOG mouse model (14, 21). In that study, the authors observed a drop in tumor volume as compared to pembrolizumab monotherapy (14, 21). In fact, therapy with another oncolytic virus T-VEC with pembrolizumab was also well tolerated, with no associated toxicities, and a spike in intra-tumoral CD8+ T cells, raised PD-L1 expression, and IFN-gene expression was observed, according to the clinical study reports (Phase Ib) (40). These findings suggest that through altering the TME, oncolytic vectors could improve pembrolizumab efficacy. These superior efficacy results lend up a scope in extending overall survival in patients with melanoma. In line with these findings, Cook et al. (41) showed that Coxsackievirus A21 (CAVATAK) synergized in anti-cancer efficacy when administered with immune CPIs. A trial assessing CAVATAK with ipilimumab resulted in 50% objective responses in melanoma patients (18, 41). Encouraging data have been also reported in a treatment with VALO-D102, an oncolytic vector, encoding for OX40L and CD40L, used in PeptiCRAd cancer vaccine system. The local administration of PeptiCRAd strongly elevated tumor-specific T-cell responses, inhibited tumor growth, and in combination with anti-PD-1, significantly improved anti-cancer effect (18, 23). Similar data have been also reported by Hemminki lab where i.t. administration of oncolytic adenovirus expressing TNFa and IL-2 improved systemic response to anti-PD-1 therapy, by re-shaping the TME of both injected and non-

injected tumors (22), further supporting the rationale for combination of anti-PD-1 with oncolytic vectors virus for the treatment of human cancer.

Adenoviral DNA copy number as assessed by qPCR revealed viral DNA presence in tumor cells. This is not a surprise, as adenoviral vectors target tumors by multiplying in and destroying cancer cells resulting in tumor death. The afflicted tumor cell experiences lysis when the replication cycle is completed, releasing offspring virions that are competent enough for infecting neighboring tumor cells and successive rounds of vector replication and cell lysis thereby kill the tumor (42). Exogenous proteins expressed by certain genes that affect anti-cancer action or their expression can be manipulated to prevent virus multiplication in cancer cells (43). To this point, *ex vivo* analysis indicated local synthesis of ICOSL and CD40L transgenes encoded by the AdV5/3-D24-ICOSL-CD40L. In solid tumors, ICOSL expression promotes the stimulation of CD8+ cytotoxic T cells, resulting in anti-tumor immune function. In turn, CD40L triggers maturation of antigen presenting cells (APCs). Surprisingly, ICOSL transfected tumor cells indicated that the ligand promotes tumor regression by activating CD8+ cytotoxic T-mediated mechanisms (44). We can speculate that the presence of both co-stimulatory molecules, mamely, CD40L and ICOSL, encoded by the vector contributed to enhanced infiltration of GrB+ CD8+ T cells in the tumors.

This could be the cause for the combo therapy's better *in vivo* efficacy when compared to other treatment regimens. Importantly, antineoplastic efficacy was connected to reduced tumor volume and enhanced infiltration of TILs, including activated cytotoxic T cells (GrB+ CD8+). Moreover, we have observed a negative correlation between tumor volume and GrB+CD8+ TILs, confirming the importance of anti-cancer immune responses in cancer growth control. Indeed, current findings indicate that the presence of CD8+ T cells is predictive of anti-PD-1 therapeutic responses in malignancies such as non-small-cell lung carcinoma and melanoma (43). Therefore, enhancing the infiltration of activated cytotoxic (GrB+CD8+ T cells) tumor-infiltrating T cells by the combinatorial therapy, we can induce anti-cancer effect.

Transcriptomic analysis revealed upregulation of various genes, such as, CD83, CRTAM, CXCL11, and TAP1 only in samples treated with combinatorial therapy. In fact, CD83 is found on a variety of activated immune cells, although it is stably expressed by mature dendritic cells (DC). CD83 also regulates maturation, activation, and homeostasis. Interaction between T cells and APCs is required for optimal TCR activation and development (45) of anti-cancer immune responses. It has been demonstrated that one of gene upregulated during T-cell activation is CRTAM, on both human CD4+ and CD8+ T cells (45). This observation is consistent with previous reports that human CRTAM transcripts are transiently detected in activated CD8+ T cells and NK and NKT cells (45). Levels of CXCL11 correlates with antitumor immunity and an improved prognosis in colon cancer (46). Kristner et al. also showed that the expression of CXCL11 allowed the most stringent prediction of overall survival and disease-free survival in colon colorectal cancer (47), suggesting anti-cancer role of CXCL11. TAP1 is an ABC transporter that forms a TAP complex together with TAP2, levels of which remain relatively stable between analyzed conditions. The transporter TAP allows peptides to enter the ER that can subsequently bind to MHC I molecules for presentation to CD8+ T cells (48). Gene set enrichment analysis indicates that genes with altered expression in combinatorial therapy belong to the "cell surface receptor signaling pathway" and "adaptive immune response" GO category. Decomposition of bulk RNA-seq data also indicate that the increased levels of CD8+ T cells are only observed in TME after the combinatorial therapy. All this supports a notion of enhanced T-cell activation in TME following introduction of CPI together with the modified adenovirus.

Transcriptomic analysis indicates that the combinatorial therapy has the strongest effect on lowering mesothelin and MUC16 levels (confirmed by gene expression analyses). To date, mesothelin is the only tumor biomarker to receive US FDA approval for clinical use in mesothelioma. Mesothelin is usually expressed on the surface of mesothelial cells, and in the cancerous phase, it can be present in the blood (49). Importantly, increased survival rate of patients with ovarian cancer was observed for the group with lowered levels of this protein (50). Our data suggest that lowered mesothelin expression level correlates with anti-cancer efficacy observed in animal studies, thus strengthening the rationale for combinatory treatment using oncolytic adenovirus AdV5/3-D24-ICOSL-CD40L with anti-PD-1 in mesothelioma therapy.

Conclusions

Our *in vivo* studies confer the fact that oncolytic viruses expressing powerful immune modulators could be used to boost the systemic potency of immune CPIs. Therefore, our preclinical observations endorse the concept that by specifically targeting cancer cells and inducing immunogenic cell death, the proposed combinatorial therapy could enhance the anti-cancer performance and the overall survival. Nevertheless, further studies need to be conducted to confirm reported findings.

Data availability statement

The transcriptomic data has been deposited at National Library of Medicine (Accession: PRJNA1010481).

Ethics statement

Ethical approval was not required for the studies on humans in accordance with the local legislation and institutional requirements because only commercially available established cell lines were used. The animal study was approved by Animal procedures were approved by the Austrian Federal Ministry of Science and Research, the Italian Ministry of Health, and the Warsaw University of Life Sciences' II Local Ethical Committee for Animal Experiments. The study was conducted in accordance with the local legislation and institutional requirements.

Author contributions

MG: Data curation, Investigation, Methodology, Resources, Writing – original draft, Writing – review & editing. MW: Resources, Writing – original draft, Writing – review & editing. IA: Data curation, Investigation, Resources, Writing – review & editing. MS: Investigation, Resources, Writing – review & editing, Writing – original draft. ML: Resources, Writing – review & editing, Formal Analysis, Methodology, Software, Writing – original draft. MP: Resources, Writing – review & editing. AZ: Resources, Writing – review & editing. TS: Resources, Writing – review & editing, Data curation, Formal Analysis, Software. DP: Formal Analysis, Resources, Software, Writing – review & editing. SS: Resources, Writing – review & editing. PC: Resources, Writing – review & editing. VC: Resources, Writing – review & editing. RA: Resources, Writing – review & editing. BR: Resources, Writing – review & editing, Data curation. KP: Resources, Writing – review & editing, Writing – original draft. LK: Conceptualization, Data curation, Formal Analysis, Funding acquisition, Investigation, Methodology, Project administration, Resources, Software, Supervision, Visualization, Writing – original draft, Writing – review & editing.

Funding

The author(s) declare financial support was received for the research, authorship, and/or publication of this article. LK was supported by the National Science Centre, Poland, SONATA (2022/47/D/NZ7/03212), SONATINA (2019/32/C/NZ7/00156), and the National Institute of Public Health NIH – National Research Institute, Poland (BW-3/2023, 1BWBW/2022). M.G. acknowledges STARS Starting Grant (STARS StG) (Grant Number: GARO_STARS_MUR22_01) funded by the University of Padua. This publication is based on work in COST Action CA 17140 "Cancer Nanomedicine from the Bench to the Bedside" supported by COST (European Cooperation in Science and Technology) (LK, MG). MS was supported by the Centre for Advanced Materials and Technologies, WUT, Poland and grant POB BioTechMed-1 No. 504/04496/1020/45.010406 and BIOTECHMED-LAB-1 (Excellence Initiative Research University). ML was partially supported by IDUB against COVID-19 project granted by Warsaw University of Technology under the Excellence Initiative Program: Research University (IDUB). DP research was funded by Warsaw University of Technology under the Excellence Initiative Program: Research University (IDUB) and co-supported by Polish National Science Centre (2019/35/O/ST6/02484 and 2020/37/B/NZ2/03757). Computations were performed using the Artificial Intelligence HPC platform financed by the Polish Ministry of Science and Higher Education (Decision No. 7054/IA/SP/2020 of 2020-08-28). TS research was co-funded by (POB Biotechnology and Biomedical Engineering) of Warsaw University of Technology within the Excellence Initiative Program: Research University (IDUB).

Conflict of interest

Author LK was employed by the company Valo Therapeutics and author VC is the co-founder and a shareholder of Valo Therapeutics.

The remaining authors declare that the research was conducted in the absence of any commercial or financial relationships that could be construed as a potential conflict of interest.

Publisher's note

Supplementary material

The Supplementary Material for this article can be found online at: https://www.frontiersin.org/articles/10.3389/fonc.2023.1259314/full#supplementary-material

References

1. Kuryk L, Haavisto E, Garofalo M, Capasso C, Hirvinen M, Pesonen S, et al. Synergistic anti-tumor efficacy of immunogenic adenovirus ONCOS-102 (Ad5/3-D24-GM-CSF) and standard of care chemotherapy in preclinical mesothelioma model. *Int J Cancer* (2016) 139(8):1883–93. doi: 10.1002/ijc.30228

2. Kuryk L, Moller AW, Garofalo M, Cerullo V, Pesonen S, Alemany R, et al. Antitumor-specific T-cell responses induced by oncolytic adenovirus ONCOS-102 (AdV5/3-D24-GM-CSF) in peritoneal mesothelioma mouse model. *J Med Virol* (2018) 90(10):1669–73. doi: 10.1002/jmv.25229

3. Kuryk L, Rodella G, Staniszewska M, Pancer KW, Wieczorek M, Salmaso S, et al. Novel insights into mesothelioma therapy: emerging avenues and future prospects. *Front Oncol* (2022) 12:916839. doi: 10.3389/fonc.2022.916839

4. Chen DS, Mellman I. Oncology meets immunology: the cancer-immunity cycle. *Immunity* (2013) 39(1):1–10. doi: 10.1016/j.immuni.2013.07.012

5. Martini V, D'Avanzo F, Maggiora PM, Varughese FM, Sica A, Gennari A. Oncolytic virotherapy: new weapon for breast cancer treatment. *Ecancermedicalscience* (2020) 14:1149. doi: 10.3332/ecancer.2020.1149

6. Imbert C, Montfort A, Fraisse M, Marcheteau E, Gilhodes J, Martin E, et al. Resistance of melanoma to immune checkpoint inhibitors is overcome by targeting the sphingosine kinase-1. *Nat Commun* (2020) 11(1):437. doi: 10.1038/s41467-019-14218-7

7. Davis A, Ke H, Kao S, Pavlakis N. An update on emerging therapeutic options for Malignant pleural mesothelioma. *Lung Cancer (Auckl)* (2022) 13:1–12. doi: 10.2147/LCTT.S288535

8. Kuryk L, Vassilev L, Ranki T, Hemminki A, Karioja-Kallio A, Levalampi O, et al. Toxicological and bio-distribution profile of a GM-CSF-expressing, double-targeted, chimeric oncolytic adenovirus ONCOS-102 - Support for clinical studies on advanced cancer treatment. *PloS One* (2017) 12(8):e0182715. doi: 10.1371/journal.pone.0182715

9. Capasso C, Magarkar A, Cervera-Carrascon V, Fusciello M, Feola S, Muller M, et al. A novel in silico framework to improve MHC-I epitopes and break the tolerance to melanoma. *Oncoimmunology* (2017) 6(9):e1319028. doi: 10.1080/2162402X.2017.1319028

10. Hirvinen M, Capasso C, Guse K, Garofalo M, Vitale A, Ahonen M, et al. Expression of DAI by an oncolytic vaccinia virus boosts the immunogenicity of the virus and enhances antitumor immunity. *Mol Ther Oncolytics* (2016) 3:16002. doi: 10.1038/mto.2016.2

11. Capasso C, Hirvinen M, Garofalo M, Romaniuk D, Kuryk L, Sarvela T, et al. Oncolytic adenoviruses coated with MHC-I tumor epitopes increase the antitumor immunity and efficacy against melanoma. *Oncoimmunology* (2016) 5(4):e1105429. doi: 10.1080/2162402X.2015.1105429

12. Kuryk L, Moller AW, Vuolanto A, Pesonen S, Garofalo M, Cerullo V, et al. Optimization of early steps in oncolytic adenovirus ONCOS-401 production in T-175 and HYPERFlasks. *Int J Mol Sci* (2019) 20(3). doi: 10.3390/ijms20030621

13. Kuryk L, Møller A-SW. Next generation of oncolytic viruses with the double transgenes PADI1 and TIMP-2 exhibit anti-tumor activity against melanoma in nude mouse and humanized NOG mouse models. *Mol Ther - Oncolytics* (2023) 28, 158–70. doi: 10.1016/j.omto.2023.01.002

14. Kuryk L, Moller AW, Jaderberg M. Combination of immunogenic oncolytic adenovirus ONCOS-102 with anti-PD-1 pembrolizumab exhibits synergistic antitumor effect in humanized A2058 melanoma huNOG mouse model. *Oncoimmunology* (2019) 8(2):e1532763. doi: 10.1080/2162402X.2018.1532763

15. Kuryk L, Moller AW. Chimeric oncolytic Ad5/3 virus replicates and lyses ovarian cancer cells through desmoglein-2 cell entry receptor. *J Med Virol* (2020) 92 (8):1309–15. doi: 10.1002/jmv.25677

16. Ranki T, Pesonen S, Hemminki A, Partanen K, Kairemo K, Alanko T, et al. Phase I study with ONCOS-102 for the treatment of solid tumors - an evaluation of clinical response and exploratory analyses of immune markers. *J Immunother Cancer* (2016) 4:17. doi: 10.1186/s40425-016-0121-5

17. Kuryk L, Moller AW, Jaderberg M. Quantification and functional evaluation of CD40L production from the adenovirus vector ONCOS-401. *Cancer Gene Ther* (2019) 26(1-2):26–31. doi: 10.1038/s41417-018-0038-x

18. Garofalo M, Pancer KW, Wieczorek M, Staniszewska M, Salmaso S, Caliceti P, et al. From immunosuppression to immunomodulation - turning cold tumours into hot. *J Cancer* (2022) 13(9):2884–92. doi: 10.7150/jca.71992

19. Hendrickx R, Stichling N, Koelen J, Kuryk L, Lipiec A, Greber UF. Innate immunity to adenovirus. *Hum Gene Ther* (2014) 25(4):265–84. doi: 10.1089/hum.2014.001

20. Dharmadhikari N, Mehnert JM, Kaufman HL. Oncolytic virus immunotherapy for melanoma. *Curr Treat options Oncol* (2015) 16(3):326. doi: 10.1007/s11864-014-0326-0

21. Kuryk L, Moller AW, Jaderberg M. Abscopal effect when combining oncolytic adenovirus and checkpoint inhibitor in a humanized NOG mouse model of melanoma. *J Med Virol* (2019) 91(9):1702–6. doi: 10.1002/jmv.25501

22. Quixabeira DCA, Cervera-Carrascon V, Santos JM, Clubb JHA, Kudling TV, Basnet S, et al. Local therapy with an engineered oncolytic adenovirus enables antitumor response in non-injected melanoma tumors in mice treated with aPD-1. *Oncoimmunology* (2022) 11(1):2028960. doi: 10.1080/2162402X.2022.2028960

23. Ylosmaki E, Ylosmaki L, Fusciello M, Martins B, Ahokas P, Cojoc H, et al. Characterization of a novel OX40 ligand and CD40 ligand-expressing oncolytic adenovirus used in the PeptiCRAd cancer vaccine platform. *Mol Ther Oncolytics* (2021) 20:459–69. doi: 10.1016/j.omto.2021.02.006

24. Aliru ML, Schoenhals JE, Venkatesulu BP, Anderson CC, Barsoumian HB, Younes AI, et al. Radiation therapy and immunotherapy: what is the optimal timing or sequencing? *Immunotherapy* (2018) 10(4):299–316. doi: 10.2217/imt-2017-0082

25. Garofalo M, Bertinato L, Staniszewska M, Wieczorek M, Salmaso S, Schrom S, et al. Combination therapy of novel oncolytic adenovirus with anti-PD1 resulted in enhanced anti-cancer effect in syngeneic immunocompetent melanoma mouse model. *Pharmaceutics* (2021) 13(4). doi: 10.3390/pharmaceutics13040547

26. Shoushtari A, Olszanski AJ, Nyakas M, Hornyak TJ, Wolchok JD, Levitsky V, et al. Pilot study of ONCOS-102 and pembrolizumab: remodeling of the tumor micro-environment and clinical outcomes in anti-PD1-resistant advanced melanoma. *Clin Cancer Res* (2022). doi: 10.1158/1078-0432.c.6532907

27. Pesonen S, Diaconu I, Kangasniemi L, Ranki T, Kanerva A, Pesonen SK, et al. Oncolytic immunotherapy of advanced solid tumors with a CD40L-expressing replicating adenovirus: assessment of safety and immunologic responses in patients. *Cancer Res* (2012) 72(7):1621–31. doi: 10.1158/0008-5472.CAN-11-3001

28. Kuryk L, Moller AS, Jaderberg M. Combinatory therapy of the oncolytic adenovirus ONCOS-102 and checkpoint inhibitor resulted in abscopal anti-tumor effect in a humanized NOG mouse model of melanoma. *Hum Gene Ther* (2019) 30(11):A53–A.

29. Lorenzi L, Chiu HS, Avila Cobos F, Gross S, Volders PJ, Cannoodt R, et al. The RNA Atlas expands the catalog of human non-coding RNAs. *Nat Biotechnol* (2021) 39 (11):1453–65. doi: 10.1038/s41587-021-00936-1

30. Finotello F, Mayer C, Plattner C, Laschober G, Rieder D, Hackl H, et al. Molecular and pharmacological modulators of the tumor immune contexture revealed by deconvolution of RNA-seq data. *Genome Med* (2019) 11(1):34. doi: 10.1186/s13073-019-0638-6

31. Sturm G, Finotello F, List M. Immunedeconv: an R package for unified access to computational methods for estimating immune cell fractions from bulk RNA-sequencing data. *Methods Mol Biol* (2020) 2120:223–32. doi: 10.1007/978-1-0716-0327-7_16

32. Kepp O, Senovilla L, Kroemer G. Immunogenic cell death inducers as anticancer agents. *Oncotarget* (2014) 5(14):5190–1. doi: 10.18632/oncotarget.2266

33. Petitprez F, Vano YA, Becht E, Giraldo NA, de Reynies A, Sautes-Fridman C, et al. Transcriptomic analysis of the tumor microenvironment to guide prognosis and immunotherapies. *Cancer Immunol Immunother* (2018) 67(6):981–8. doi: 10.1007/s00262-017-2058-z

34. Gray SG. Emerging avenues in immunotherapy for the management of Malignant pleural mesothelioma. *BMC Pulm Med* (2021) 21(1):148. doi: 10.1186/s12890-021-01513-7

35. Ranki T, Joensuu T, Jager E, Karbach J, Wahle C, Kairemo K, et al. Local treatment of a pleural mesothelioma tumor with ONCOS-102 induces a systemic antitumor CD8(+) T-cell response, prominent infiltration of CD8(+) lymphocytes and Th1 type polarization. *Oncoimmunology* (2014) 3(10):e958937. doi: 10.4161/21624011.2014.958937

36. Capasso C, Tahtinen S, Frascaro F, Carpi S, Fusciello M, Cardella D, et al. Boosting the efficacy of PD-L1 blockade with oncolytic vaccine for improved antitumor responses in melanoma. *Cancer Immunol Res* (2016) 4(11). doi: 10.1158/2326-6066.IMM2016-A034

37. Galluzzi L, Humeau J, Buque A, Zitvogel L, Kroemer G. Immunostimulation with chemotherapy in the era of immune checkpoint inhibitors. *Nat Rev Clin Oncol* (2020) 17(12):725–41. doi: 10.1038/s41571-020-0413-z

38. Kroemer G, Galluzzi L, Kepp O, Zitvogel L. Immunogenic cell death in cancer therapy. *Annu Rev Immunol* (2013) 31:51–72. doi: 10.1146/annurev-immunol-032712-100008

39. Spel L, Boelens JJ, Nierkens S, Boes M. Antitumor immune responses mediated by dendritic cells: How signals derived from dying cancer cells drive antigen cross-presentation. *Oncoimmunology* (2013) 2(11):e26403. doi: 10.4161/onci.26403

40. Ribas A, Dummer R, Puzanov I, VanderWalde A, Andtbacka RHI, Michielin O, et al. Oncolytic virotherapy promotes intratumoral T cell infiltration and improves anti-PD-1 immunotherapy. *Cell* (2017) 170(6):1109–19.e10. doi: 10.1016/j.cell.2017.08.027

41. Cook M, Chauhan A. Clinical application of oncolytic viruses: A systematic review. *Int J Mol Sci* (2020) 21(20). doi: 10.3390/ijms21207505

42. Wu H, Mei YF. An oncolytic adenovirus 11p vector expressing adenovirus death protein in the E1 region showed significant apoptosis and tumour-killing ability in metastatic prostate cells. *Oncotarget* (2019) 10(20):1957–74. doi: 10.18632/oncotarget.26754

43. Thommen DS, Koelzer VH, Herzig P, Roller A, Trefny M, Dimeloe S, et al. A transcriptionally and functionally distinct PD-1(+) CD8(+) T cell pool with predictive potential in non-small-cell lung cancer treated with PD-1 blockade. *Nat Med* (2018) 24 (7):994–1004. doi: 10.1038/s41591-018-0057-z

44. Wang B, Jiang H, Zhou T, Ma N, Liu W, Wang Y, et al. Expression of ICOSL is associated with decreased survival in invasive breast cancer. *PeerJ* (2019) 7:e6903. doi: 10.7717/peerj.6903

45. Yeh JH, Sidhu SS, Chan AC. Regulation of a late phase of T cell polarity and effector functions by Crtam. *Cell* (2008) 132(5):846–59. doi: 10.1016/j.cell.2008.01.013

46. Cao Y, Jiao N, Sun T, Ma Y, Zhang X, Chen H, et al. CXCL11 correlates with antitumor immunity and an improved prognosis in colon cancer. *Front Cell Dev Biol* (2021) 9:646252. doi: 10.3389/fcell.2021.646252

47. Kistner L, Doll D, Holtorf A, Nitsche U, Janssen KP. Interferon-inducible CXC-chemokines are crucial immune modulators and survival predictors in colorectal cancer. *Oncotarget* (2017) 8(52):89998–90012. doi: 10.18632/oncotarget.21286

48. Rock KL, Reits E, Neefjes J. Present yourself! By MHC class I and MHC class II molecules. *Trends Immunol* (2016) 37(11):724–37. doi: 10.1016/j.it.2016.08.010

49. Creaney J, Robinson BWS. Malignant mesothelioma biomarkers: from discovery to use in clinical practice for diagnosis, monitoring, screening, and treatment. *Chest* (2017) 152(1):143–9. doi: 10.1016/j.chest.2016.12.004

50. CA-125 antigen levels can predict survival in patients with advanced ovarian cancer. *Nat Clin Pract Oncol* (2007) 4(1):6–. doi: 10.1038/ncponc0676

frontiers | Frontiers in Immunology

TYPE Review
PUBLISHED 01 December 2023
DOI 10.3389/fimmu.2023.1297493

OPEN ACCESS

EDITED BY
Monika Semmrich,
BioInvent, Sweden

REVIEWED BY
Serge M. Candéias,
Commissariat à l'Energie Atomique et aux Energies Alternatives (CEA), France
Ghanbar Mahmoodi Chalbatani,
Mayo Clinic Arizona, United States

*CORRESPONDENCE
Yue Zhang
zhangyuejlcc@163.com
Xunzhe Yin
xzyin@ciac.ac.cn

RECEIVED 20 September 2023
ACCEPTED 16 November 2023
PUBLISHED 01 December 2023

CITATION
Wang B, Zhang Y and Yin X (2023) Advances in tumor immunomodulation based on nanodrug delivery systems. *Front. Immunol.* 14:1297493. doi: 10.3389/fimmu.2023.1297493

Advances in tumor immunomodulation based on nanodrug delivery systems

Bo Wang[1], Yue Zhang[1*] and Xunzhe Yin[2*]

[1]Department of Integrated Chinese and Western Medicine, Jilin Cancer Hospital, Changchun, China, [2]State Key Laboratory of Electroanalytical Chemistry, Changchun Institute of Applied Chemistry, Chinese Academy of Sciences, Changchun, China

Immunotherapy is a therapeutic approach that employs immunological principles and techniques to enhance and amplify the body's immune response, thereby eradicating tumor cells. Immunotherapy has demonstrated effective antitumor effects on a variety of malignant tumors. However, when applied to humans, many immunotherapy drugs fail to target lesions with precision, leading to an array of adverse immune-related reactions that profoundly limit the clinical application of immunotherapy. Nanodrug delivery systems enable the precise delivery of immunotherapeutic drugs to targeted tissues or specific immune cells, enhancing the immune antitumor effect while reducing the number of adverse reactions. A nanodrug delivery system provides a feasible strategy for activating the antitumor immune response by the following mechanisms: 1) increased targeting and uptake of vaccines by DCs, which enhances the efficacy of the immune response; 2) increased tumor cell immunogenicity; 3) regulation of TAMs and other cells by, for example, regulating the polarization of TAMs and interfering with TAN formation, and ECM remodeling by CAFs; and 4) interference with tumor immune escape signaling pathways, namely, the PD-1/PD-L1, FGL1/LAG-3 and IDO signaling pathways. This paper reviews the progress of nanodrug delivery system research with respect to tumor immunotherapy based on tumor immunomodulation over the last few years, discussing the promising future of these delivery systems under this domain.

KEYWORDS

nanodrug delivery systems, tumor immunotherapy, tumor immunomodulation, tumor microenvironment, immune antitumor effect

1 Introduction

Cancer is a grave health concern that poses a significant threat to human life. Currently, the diagnosis and treatment of cancer are arduous challenges (1). According to the latest epidemiological data, in 2020, the number of new cancer cases worldwide approximated to 19.3 million, with an associated death toll of 10 million. According to estimations, the global cancer burden is projected to rise to 28.4 million cases by 2040, representing a 47%

increase compared to the burden in 2020 (2). At present, the principal approaches to cancer therapy encompass surgical intervention, radiotherapy, chemotherapy, targeted therapy, and immunotherapy. As a new tumor treatment method, immunotherapy is based on immunological principles leveraged to activate and promote the enhancement of the body's immune system, thus facilitating an immune response to effectively eradicate tumor cells (3). Compared with conventional treatment, such as chemotherapy, immunotherapy shows a superior curative effect, a prolonged duration of action, and a lower incidence of adverse effects. Immunotherapy has revolutionized the treatment of multiple cancers (4), and it is the focus of recent cancer treatment research (5).

The effectiveness of clinical immunotherapy is hindered by the intricate mechanisms of tumor immune escape, resulting in a low positive response rate (6). Immunotherapy shows a profound therapeutic effect on only a portion of patients (7). Moreover, the distribution of immunotherapy drugs always encompasses various tissues and organs of the body, suggesting a lack of precise tumor targeting that may result in immune-related adverse reactions throughout the body (8, 9). Finding effective immunotherapy regulation methods, increasing the positive effect of immunotherapy, and reducing the incidence of immune-related adverse reactions are hot spots in current immunotherapy research (10).

Nanodrug delivery systems refer to nanocarriers that carry therapeutic drugs for *in vivo* delivery, and they have the advantages of preventing burst release and off-target effects of drugs, exhibiting desirable pharmacokinetic characteristics and flexibly controlling drug release (11). Combining cancer therapeutic drugs with nanocarriers can enable drugs to reach a target site or specific immune cells more accurately, leading to more effective immune responses, higher drug efficacy, and reduced incidence rates of adverse reactions (12). In recent years, many studies on the immunotherapeutic regulation of nanodrug delivery systems have been reported, and great therapeutic effects have been achieved (13). However, due to obstacles involving relevant basic research, production conditions, cost control and clinical trials, the pharmacokinetic study of some nanodrug delivery systems is insufficient, resulting in the current low conversion rate. We believe that the problems of achieving the long-term stability, effectiveness and safety of nanodrug delivery systems themselves, as well as the types of nanodrug delivery systems materials, challenges of industrialization, and cost of preparation methods should be solved one by one. Only in this way can we help break through this bottleneck. This paper reviews the successful application of nanodrug delivery systems within the realm of cancer research immunotherapy regulation over the past several years, the related treatment strategies, and the main challenges to this field and potential development directions.

2 Tumor immunotherapy

Tumor immunotherapy seeks to achieve the objective of stimulating or mobilizing the body's immune system to generate an immune response that is capable of eradicating tumor cells (14). According to a mechanism classification system, tumor immunotherapy regimens can be categorized as "passive immunotherapy" and "active immunotherapy". Passive immunotherapy refers to treatment that directly kills tumors mediated by anti-immune checkpoint-blocking antibodies and cytokines or immune cells expressing immune checkpoints. Passive immunotherapy mainly includes cytokine therapy, immune checkpoint inhibitors and adoptive cell therapy (15). Active immunotherapy refers to therapy that specifically activates the human autoimmune system and induces an active antitumor immune response. Tumor vaccines are the main types of therapies representing active immunotherapy (16).

In tumor immunotherapy, T-cell-mediated immune response activation follows several key steps. Tumor cells release antigens that are taken up by antigen-presenting cells (APCs). APCs reach local lymph nodes through the lymphatic system and then present antigens to naive T cells through the major histocompatibility complex I (MHC I) pathway, thereby triggering the initiation and activation of effector T cells. Effector T cells reach a local tumor site through the blood flow and recognize and kill tumor cells (17, 18). Dead tumor cells release tumor-specific antigens, and APCs capture and take up these antigens, which also activate effector T cells, completing the cancer-immunity cycle (Figure 1). The active participation of CD4+ T cells is also needed for immune response activation. CD4+ T cells are important in the human immune system. They can bind to the non-polypeptide region of MHC II molecules and participate in the signal transduction of antigen recognition by T cell antigen receptors. In tumor immune responses, CD4+ T cells can activate CD8+ T cells through a variety of mechanisms, so that CD8+ T cells can differentiate into cytotoxic T lymphocytes while maintaining and strengthening the antitumor response. On the other hand, even in the absence of CD8+ T cells, CD4+ T cells can also kill tumor cells directly by mechanisms involving IFN-γ (19).

However, due to factors such as defective tumor antigen release, impaired T-cell priming in local lymph nodes, and tumor immunosuppressive signals (such as the downregulation of MHC expression by tumor cells) that enable tumor cells to escape immune surveillance, the cancer-immunity cycle may be impaired, causing tumor progression (20). Therefore, because of dysfunction in the cancer-immunity cycle, formulating personalized immunotherapy leads to better therapeutic effects for patients (21).

3 Overview of nanodrug delivery systems for cancer treatment

In recent years, with the wide application of nanotechnology in medicine, nanodrug delivery systems have been rapidly developed (22). Consequently, these systems can be classified as either naturally occurring natural carriers and synthetic carriers, based on their respective origins. These systems can be categorized into three subtypes: organic nanocarriers, inorganic nanocarriers and composite nanocarriers based on their composition (23). Organic

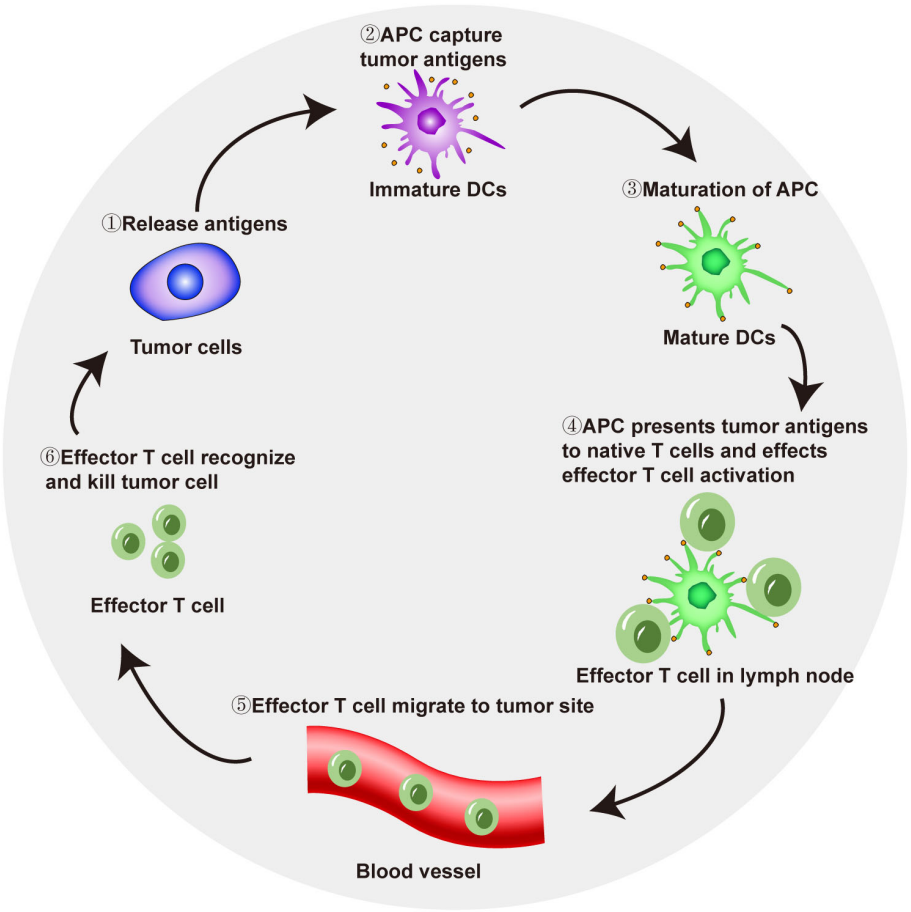

FIGURE 1
Mechanism of T cell-mediated antitumor immune response activation.

nanocarriers consist of organic materials and include lipid-based carriers, viral capsids, polysaccharides and protein particles, while inorganic nanocarriers include metal nanoparticles such as gold or silver nanoparticles, ceramic nanoparticles, quantum dots, and carbon nanoparticles (24). As novel nanocarriers continue to emerge, the clinical and translational applications of nanomedicine will be expanded (25). To date, nanodrug delivery systems have shown many advantages. First, a nanodrug delivery system can reduce the number or degree of adverse reactions induced by chemotherapy drugs. Chemotherapy drugs usually have disadvantages such as low water solubility, instability under physiological conditions and can induce drug resistance and high toxicity. When chemotherapeutic drugs are integrated into nanodrug delivery systems by covalent bonding, physical packing, electrostatic forces or coordination complexation, the limitations of these chemotherapeutic drugs can be reduced (26, 27). The commonly used nanocarriers mainly include proteins, nucleic acids, small-molecule chemotherapeutics, and imaging agents (28–30). Second, the size effect of the nanodrug delivery system also affects the pharmacokinetics, cellular uptake rate, and the penetration and accumulation of drugs in tumor tissues (31, 32). Third, a nanodrug delivery system can also simultaneously deliver tracer drugs, enabling the integration of tumor disease diagnosis and treatment (33). Finally, a nanodrug delivery system may carry multiple therapeutic drugs, thereby achieving the superposition effects of the therapeutic drugs (34).

Nanodrug delivery systems are usually divided into active and passive targeting effects, both of which have their own advantages and disadvantages (35–37). The active targeting effect refers to a combination of nanoparticles with overexpressed tumor cell receptors to achieve the targeting effect. The commonly used targeting receptors include mainly folate, transferrin and epidermal growth factor receptor (38). The passive targeting effect refers to the accumulation of nanoparticles that move through the circulatory systems of the human body and then accumulate in tumors, thereby playing a therapeutic role. Therefore, the passive targeting effect is particularly dependent on the physiological characteristics of the tumor microenvironment (39). A research showed that nanoparticles with diameters in the range of 40-400 nm stayed in the circulatory system for a long time, enabling their high accumulation in tumors, and reduced renal clearance (40). Moreover, the passive targeting effect may result in a random targeting effect, which may lead to insufficient diffusion of drugs in tumors.

After a nanodrug delivery system enters the human body, it needs to overcome many obstacles to achieve a therapeutic effect on

tumor cells (41, 42). First, nanoparticles present in the blood circulatory system interact in a remarkable fashion with the plasma proteins, eventually being sequestered by the reticuloendothelial system (RES). Therefore, circulating nanoparticles must first escape the RES before they can accumulate in tumor tissues. When a nanodrug reaches a tumor tissue, although the tumor blood vessels allow the nanodrug to accumulate, parietal cells may limit nanodrug passage through openings in the capillary wall, thereby decreasing the rate of convective transport of the nanodrug. Moreover, the dense extracellular matrix (ECM) can inhibit the passive diffusion of nanodrugs due to high osmotic pressure. All these factors present obstacles to the transportation of nanodrugs through tumor blood vessels (Figure 2). The transportation of nanodrug delivery systems is a thorny problem. It remains difficult to correctly specify nanodrug delivery systems, and further follow-up research is still needed to accurately adjust the size, shape and hydrophilicity/hydrophobicity of the nanodrug delivery systems to solve the transportation problem.

4 Tumor immunotherapy regulation via a nanodrug delivery system

4.1 Nanodrug delivery systems increase tumor cell vaccine uptake rates and efficiency

Tumor vaccines can specifically activate the human autoimmune system and contribute to the regulation of the antitumor immune response (43). Tumor vaccines are mainly divided into cell vector vaccines, protein vaccines, peptide vaccines and nucleic acid vaccines (44). Nanodrug delivery systems encapsulate tumor antigens and adjuvants into the same carrier (called nano vaccines, particle vaccines, or nanoparticle vaccines) and deliver them into the same APC, preventing immune tolerance caused by the absence of an adjuvant (45). In addition, a nanodrug delivery system also significantly increases the uptake efficiency of tumor antigens by APCs, thereby increasing the antitumor immune response effect. To achieve a stronger immune response effect, nanoparticle vaccines need to meet several conditions, including effective antigen-loading capacity, efficient lymphatic drainage efficiency, and enhanced APC uptake capacity (46).

Dendritic cells (DCs) are important target cells of nanoparticle vaccines. They are important APCs that can take up, process and present antigens, produce cytokines and chemokines, and initiate T-cell-mediated immune responses (47). Specific ligands modified on the surface of nanoparticle vaccines target receptors on the surface of DCs, which increases the uptake efficiency of the DCs through specific endocytic pathways (48). J Chen developed mannose-modified PLL-RT (Man-PLL-RT)-mediated nanovaccines with DC-targeting ability. Man-PLL-RT with antigens (ovalbumin, OVA) and adjuvants (unmethylated cytosine-phosphate-guanine, CpG) coencapsulated by electrostatic interaction that facilitated antigen endocytosis, maturation and cross presentation by DCs (49).

Conventional tumor vaccines activate specific T cells through the action of DCs to induce immune responses indirectly. The efficacy of a tumor vaccine usually contingents upon the suboptimal activation of T cells. S Go developed a nanovaccine that enhanced the T-cell response through its interactions with DCs and T cells to treat cancer. This nanovaccine consisted of a cancer cell membrane nanoparticle (CCM-MPLA) decorated with monophosphoryl lipid A (MPLA). Researchers conjugated anti-CD28 antibodies (aCD28) to the CCM-MPLA particles to produce CCM-MPLA-aCD28 nanoparticles, which induced direct interactions between nanovaccines and tumor-specific T cells. Regardless of the presence or absence of DCs, this nanovaccine activated tumor-specific CD8 T cells, exhibiting more effective induction of tumor-

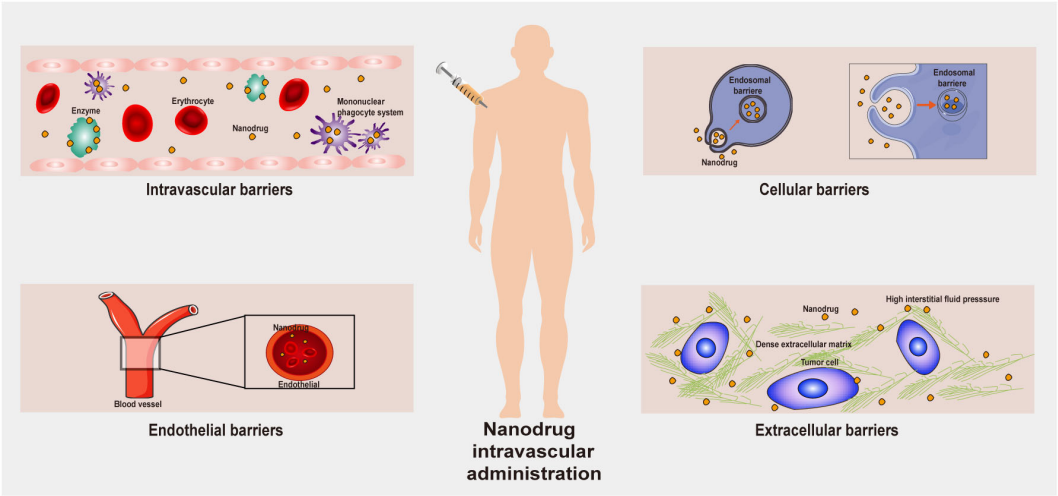

FIGURE 2
Biological barriers that a nanodrug may encounter in the human body.

specific CD8 T-cell responses and exhibiting high antitumor efficacy in tumor-bearing mice (50).

Activation of the stimulator of interference genes (STING) pathway enhanced the antigen-presenting efficiency of DCs, thereby promoting the antitumor immune response of T cells (51, 52). X Jiang developed a PC7A nanovaccine that activated STING. This vaccine induced antigen-specific T cells to undergo robust tumor infiltration, generate a strong antitumor T-cell response, and induce antitumor immune responses and showed higher efficacy when intratumorally administered compared to when it was subcutaneously injected (53).

In addition to utilizing receptor-mediated endocytosis to increase the uptake efficiency of nanovaccines by DCs, strategies based on macropinocytosis were used to increase the internalization efficiency of DCs (54). Macropinocytosis is a transient, actin-driven endocytic process based on membrane folding to create a vacuole that engulfs exogenous fluids and particles on a large scale into cells (55). In contrast to other cells, DCs show efficient uptake of exogenous antigens through macropinocytosis, which can potentially compensate for the insufficient of expression of specific receptors on DCs and thus increase their antigen uptake efficiency. C Yang developed a nanoparticulate vaccine based on a reactive oxygen species (ROS)-responsive nanoparticle core and macropinocytosis-inducing peptide-fused cancer membrane shell. The vaccine was taken up by DCs at a significantly higher rate via CXC-chemokine receptor type 4 (CXCR4)-mediated macropinocytosis and jointly promoted DCs maturation and the T-cell immune response by activating the STING pathway (56).

Spherical nucleic acids (SNAs) are capable of rapid uptake by antigen-presenting cells through receptor-mediated endocytosis. For innate immune responses, the unique adjuvant nucleic acid three-dimensional structure of the SNA shell can provide improved recognition of Toll-like receptors. Nanovaccines have been used in clinical practice for the treatment of prostate cancer, but the efficacy is high, and further research is imminent (57). SNA vaccines developed by researchers can improve the production and secretion of cytokines and can increase polyfunctional cytotoxic T cells and effector memory. In this nanovaccine, human prostate-specific membrane antigen or T-cell receptor γ alternate reading frame protein was integrated into the optimized structure, resulting in a high immune activation rate and a high cytolytic capacity of humanized mouse and human peripheral blood mononuclear cells (hPBMCs) (58). Some researchers have developed immunostimulatory SNA (IS-SNA) nanostructures composed of CpG oligonucleotides as an adjuvant and prostate cancer peptide antigen. This nanovaccine increases the codelivery of CpG and antigen to DCs, thereby improving the cross-priming of antitumor CD8 T cells and generating more effective antitumor immune responses (59).

4.2 Nanodrug delivery systems enhance tumor cell immunogenicity

Low immunogenicity and an immunosuppressive tumor microenvironment are major impediments to efficacious tumor immunotherapy (60). At present, some immunogenic cell death (ICD) inducers, have been confirmed to promote tumor immunotherapy by triggering ICD (61). When tumor cells undergo ICD, they release a variety of tumor-associated antigens and damage-associated molecular patterns (DAMPs) (62–64), such as high mobility group protein 1 (HMGB1), calreticulin (CRT), adenosine-triphosphate (ATP) and heat shock protein (HSP90α) (Figure 3). DAMP promotes the activation of APCs, induces the activation of antigen-specific T cells, promotes the intratumoral infiltration of immune cells, and thus enhances the immune response in tumors (65, 66). Compared with other therapies, DAMPs released by ICD inducers can mobilize immune stimulation, promote the maturation of DCs, and activate T cells, thus achieving a positive tumor chemoimmunotherapy effect (67). According to their ability to activate cell death or release DAMPs, ICD inducers can be divided into two different categories: type I and type II (68). Type I ICD inducers do not induce tumor cell death by increasing endoplasmic reticulum stress, but the effects of lateral endoplasmic reticulum stress produce immunogenicity; type II ICD inducers selectively target the endoplasmic reticulum and release danger and apoptosis signaling molecules because of ROS-dependent endoplasmic reticulum stress. Most chemotherapeutic drugs are type I ICD inducers, while radiotherapy and photodynamic therapy are type II ICD inducers. Due to strong adverse reactions and low tumor-targeting efficiency, ICD inducers use has been limited. A combination of a nanodrug delivery system and ICD inducers makes possible the clinical use of ICD inducers during tumor immunotherapy (69). S Liu developed a doxorubicin (DOX) and 4-(hydroxymethyl) phenylboronic acid pinacol ester (PBAP) prodrug polymer and encapsulated it with chlorin e6 (Ce6) in nanoparticles to obtain hyaluronidase (HAase) and HO dual-sensitive responsive nanoparticles (Ce6/HDP NPs). The NPs displayed efficient intratumoral accumulation and cellular internalization properties due to the active targeting of hyaluronic acid (HA). The strong ICD stimuli, which were induced by ROS production and GSH depletion, led to amplified immunogenicity to activate tumor immunotherapy. The DNA damage caused by the dual effects of chemotherapy and ROS production directly caused tumor cell apoptosis (70).

Radiotherapy, photodynamic therapy and sonodynamic therapy induce the ICD effect of tumor cells through the effects of ROS-induced endoplasmic reticulum stress (71). However, the hypoxic environment of tumors profoundly affects ROS production, which indirectly leads to an insufficient immune response to ICD. Alleviating hypoxia is a key problem that urgently needs to be solved to enable the use of nanodrug delivery systems (72). To solve this problem, M Wang created an albumin-based nanoplatform codelivering IR780, a NLG919 dimer and the hypoxia-activated prodrug tirapazamine (TPZ) as a dual enhancer of synergistic cancer therapy. TPZ-mediated chemotherapy by increasing the photodynamic therapy-induced tumor ICD rate, which induced a stronger antitumor immune response, including an increase in the number of tumor-specific cytotoxic T lymphocytes (73).

In addition to a ROS-based strategy, an endoplasmic reticulum targeting strategy can enhance the ICD effects (74, 75). H Luo found that inhibiting the endoplasmic reticulum-associated protein

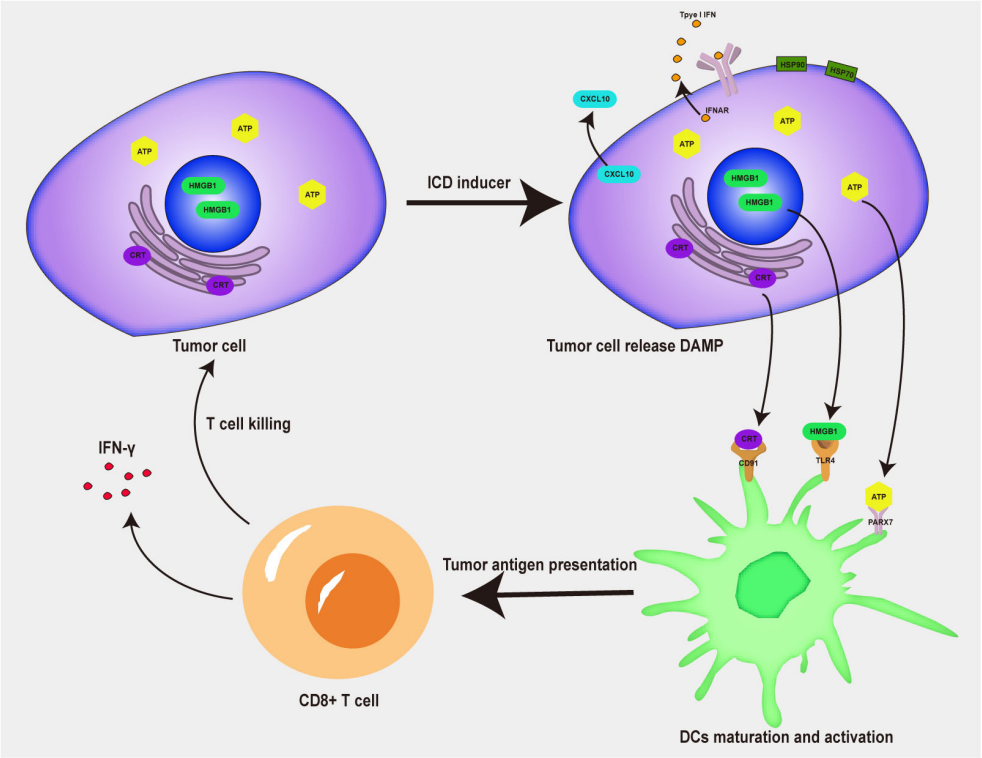

FIGURE 3
Process of ICD inducers inducing immune response.

degradation pathway stimulated the ICD-induced lysate emission from dying esophageal cancer cells in a dose-dependent manner. Dual therapy with an endoplasmic reticulum-associated protein degradation inhibitor combined with medium-dose radiotherapy triggered an antitumor immune response by increasing the maturation and phagocytosis rates of DCs (76).

4.3 Nanodrug delivery systems regulate the tumor microenvironment

The tumor microenvironment (TME) plays a crucial role in the interaction between tumors and immunotherapy (77). As shown in Figure 4, the TME is the surrounding microenvironment in which tumor cells exist and is composed of neutrophils, DCs, T cells, fibroblasts, macrophages, microvessels, various signaling molecules and molecular cytokines (78). Tumor cells can release various cell signaling molecules, which in turn affect their immune microenvironment, induce immune tolerance, and inhibit antitumor immune responses (79). In addition, regulatory T (Treg) cells, tumor-associated macrophages, tumor-associated fibroblasts, and myeloid-derived suppressor cells in the TME can increase immunosuppressive effect and tumor cell evasion rate, further increasing the complexity of the TME (80). Therefore, a nanodrug delivery system can be designed to target immunosuppressive cells or pathways to reduce the immunosuppressive effect of the TME, which is anticipated to increase the efficacy of tumor immunotherapy (81).

4.3.1 Regulation of tumor-associated macrophages

Tumor-associated macrophages (TAMs) are essential interstitial cells in the TME and are composed of two types of cells that either inhibit or promote tumor cell proliferation (82, 83). M1 macrophages have antitumor effects and secrete classical inflammatory cytokines to kill tumors by promoting tumor cell necrosis and immune cell infiltration into the TME (84). M2 macrophages mainly play a role in promoting tumor growth, invasion and metastasis by degrading the tumor ECM, destroying the basement membrane, promoting angiogenesis and recruiting immunosuppressive cells (85). The application of a nanodrug delivery system to regulate TAM activity can enhance the antitumor immune response (86). Commonly used therapeutic strategies include blocking macrophage recruitment, interfering with TAM survival programs, and remodeling M2-type TAMs into the M1 type TAMs (87). S Ha fabricated PLGA nanoparticles encapsulating baicalin and the melanoma antigen Hgp peptide fragment consisting of amino acids 25-33 by using the ultrasonic double-emulsion technique. The nanoparticles were loaded with CpG fragments, and M2pep and α-pep peptides were conjugated onto their surfaces to yield novel nanocomplexes. The nanocomplexes were effectively internalized by M2-phenotype TAMs *in vitro* and *in vivo*. The acidic lysosomal environment was observed to trigger the disintegration of the polydopamine on the nanoparticle surface, leading to the release of the payloads. The release of CpG from the tumor microenvironment is a critical factor in the transformation of M2-phenotype TAMs into M1-phenotype

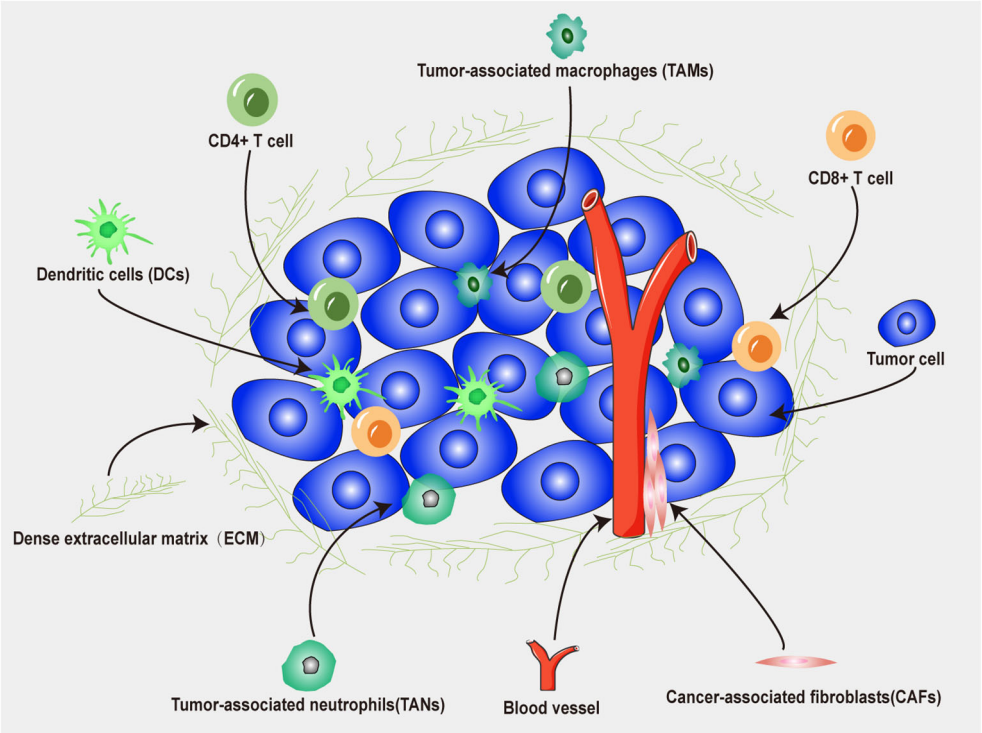

FIGURE 4
Main components of tumor microenvironment.

TAMs, leading to increased secretion of inflammatory cytokines. The decreased secretion of cytokines by TAMs subsequently suppresses tumor angiogenesis, enabling the tumor microenvironment to undergo significant changes (88).

Tumor cells secrete a variety of stimulatory factors, such as macrophage colony-stimulating factor, which can bind to the tyrosine kinase CSF receptor 1 on macrophages, leading to their conversion into the M2-phenotype macrophages. Therefore, blocking the CSF-1R signaling pathway can remodel the M2-phenotype to M1-phenotype macrophages (89). Y-W Chang generated a bifunctional protein by fusing interleukin-10 to ana anti-colony-stimulating factor-1 receptor-blocking antibody. The fusion protein demonstrated significant antitumor activity in multiple cancer models, especially models of head and neck cancer. This bifunctional protein not only led to the anticipated reduction in the number of TAMs but also triggered the proliferation, activation, and metabolic reprogramming of CD8 T cells (90).

4.3.2 Interference with tumor-associated neutrophils

Neutrophils are important components of the immune system and essential immune cells that fight against microbial infection. Neutrophils account for a large proportion of immune cells infiltrating tumor tissues, which are called tumor-associated neutrophils (TANs) (91). TANs exert dual effects on tumors; namely, they show antitumor (the N1 subpopulation) and tumor-promoting activity (the N2 subpopulation). N1 subpopulation TANs induce antitumor activity through antibody-dependent cytotoxicity and other mechanisms, while N2 subpopulation TANs promote tumor growth by enhancing tumor cell metastasis, promoting angiogenesis and inhibiting the action of adaptive immune cells (92, 93).

The use of nanodrug delivery carriers to interfere with neutrophil development and function, destroy their immunosuppressive function and restore their anticancer properties has gradually become a promising therapeutic strategy. Using a nanodrug delivery system to interfere with the development and function of TANs, particularly their immunosuppressive function, and thus restore their anticancer effects is a promising therapeutic strategy (94, 95). Y Wang developed a nanovaccine constructed with SiPCCl-hybridized mesoporous silica with Fe(III)-captopril complexes and coated with the exfoliated membrane of mature DCs via H22-specific neoantigen stimulation. The nanovaccines actively target H22 tumors and induce ICD. Moreover, acid-triggered captopril release into the tumor microenvironment polarized protumoral N2 phenotype neutrophils into antitumor N1 phenotype neutrophils to increase the immune effects (96).

Enhancing the sensitivity of TANs and achieving more precise drug delivery contribute to more profound immune effects. H Dong proposed a novel concept that utilizes a nanoimmunotraining strategy to rapidly activate neutrophil tumor tropism and consequently enhance the targeting capacity of antitumor drugs. An evaluation of this strategy demonstrated significantly increased tumor-targeted accumulation of neutrophils harvested from

nanoimmunotrained mice after either intraperitoneal or intravenous injection of a vaccine-like nano-CpG adjuvant, which led to the precise delivery of nanodrugs (97).

4.3.3 Targeting tumor-associated fibroblasts

Cancer-associated fibroblasts (CAFs) in the tumor microenvironment can promote tumors by interacting with cancer cells (98). Moreover, CAFs can form a solid physical barrier by secreting ECM and other components, hindering the penetration and diffusion of nanodrugs in tumor tissues and reducing the infiltration rate of tumor-infiltrating lymphocytes (99). In addition, CAFs can induce an microenvironment immune tolerance by secreting cytokines (100).

Regulating the formation of CAFs, eliminating CAFs, remodeling CAFs and other strategies can increase the efficiency of nanodrug delivery and relieve TME immunosuppression to enhance antitumor immunotherapy (101, 102). Y Chen developed a nanoparticle that significantly inhibited tumor growth and metastasis by remodeling CAFs in the TME. Y Chen found that salvianolic acid B-loaded PEGylated liposomes (PEG-SAB-Lip) interfere with the activation of CAFs by inhibiting the secretion of TGF-β1. After inhibiting the activation of CAFs, the collagen deposition rate in tumors was reduced, and the penetration rate of nanoparticles in tumors was increased. These outcomes led to the high expression of cytokines and chemokines (CXCL9 and CXCL10) in T helper 1 (Th1) cells and the recruitment of CD4, CD8 T cells, and M1 macrophages to the tumor area (103).

5 Interference with the tumor immune escape signaling pathway

There are many immunosuppressive signaling pathways in TAMs. Malignant cells themselves, or lymphocytes that infiltrate tumors, can abnormally express a variety of immune checkpoint molecules, including PD-1/PD-L1, LAG-3, TIM3, and TIGIT, which inhibit the activation of antigen-specific T cells and facilitate tumor cell immune escape (104, 105). Immune regulatory molecules released by tumor cells, such as TGF-β and indoleamine 2,3-dioxygenase (IDO), can prevent effector T-cell function and even lead to T-cell exhaustion in tumors (106). Exhausted T cells become dysfunctional, are unable to produce cytotoxic effects, and lose the ability to produce antitumor cytokines such as IL-2 and TNF-α, which leads to a reduction in tumor immunotherapy efficiency (107, 108). Therefore, blocking the tumor cell immune escape signaling pathway with a nanodrug delivery system may activate or increase the antitumor immune response.

The upregulation of immune checkpoint molecules in TAM is a significant mechanism contributing to tumor immune evasion, and blocking this signaling pathway can enhance the endogenous antitumor immune effect of the body. Many studies have shown that using immune checkpoint inhibitors to block the PD-1/PD-L1 signaling pathway reversed the immunosuppression of the TME, restored T-cell antitumor activity, and enhanced tumor immunotherapy (109, 110). S Liu prepared atovaquone-loaded human serum albumin (HSA) nanoparticles stabilized via intramolecular disulfide bonds, calling them HSA-ATO NPs. These nanoparticles show excellent bioavailability, tumor targeting ability, and high biosafety. HSA-ATO NPs can promote intratumoral CD8 T-cell recruitment by alleviating hypoxia in the TME, thereby enhancing the efficacy of anti-PD-1 immunotherapy (111).

However, blocking only a single immune escape signaling pathway is not enough to induce a strong antitumor immune effect. FGL1/LAG-3 is a newly discovered immune escape signaling pathway. Similar to the PD-1/PD-L1 signaling pathway, it exerts a variety of biological regulatory effects on T cells (112). Dual blockade of the FGL1/LAG-3 and PD-1/PD-L1 signaling pathways greatly improved the T-cell killing ability of tumor cells. W-J Wan designed a new type of ROS-sensitive nanoparticle and loaded it with FGL1 short interfering RNA (siRNA; siFGL1) and PD-L1 siRNA (siPD-L1), which they formed from a stimulus-responsive polymer with poly-l-lysine-thioketal and modified cis-aconitate to facilitate nanoparticle endosomal escape. Furthermore, the administration of the tumor-penetrating peptide iRGD and ROS-responsive nanoparticles concurrently enhanced the delivery efficiency of siFGL1 and siPD-L1, leading to a significant reduction in the protein levels of FGL1 and PD-L1 in tumor cells (113).

IDO is a ferrous heme-containing oxidoreductase that can degrade tryptophan to yield kynurenine, which can directly inhibit the function of cytotoxic T lymphocytes increase Treg activity to play an immunosuppressive role (114). The tryptophan metabolism signaling pathway activated by IDO is important in promoting tumor cell immune escape. Inhibition of IDO prevented the inhibition of T-cell proliferation in the TME and activated or enhanced autoimmune function (115). C Yang developed a polycaprolactone-based nanoparticle to encapsulate the tryptanthrin derivative CY-1-4. These nanoparticles both induced ICD and inhibited IDO effects while regulating the formation of lymphocyte subsets in the spleen and tumor (116).

6 Conclusions and prospects

Immunotherapy has been a revolutionary treatment for cancer patients. However, due to the complex tumor cell immune escape mechanism, many problems to be solved to increase the efficacy of tumor immunotherapy; these problems include profound differences among individual patients, low rates of positive effects and adverse reactions. Nanodrug delivery systems can improve the pharmacokinetic characteristics of drugs, increase their bioavailability, and reduce their adverse reactions, suggesting their use in a novel approach to cancer immunotherapy. According to the mechanism underlying an activated antitumor immune response, a nanodrug delivery system provides a feasible strategy if it has the following effects: 1) increases the targeting and uptake of vaccines by DCs, thereby enhancing the efficacy of the immune response; 2) increases tumor cell immunogenicity; 3) regulates TAMs and other cells by, for example, regulating the polarization of TAMs and

interfering with TAN formation and ECM remodeling by CAFs; and 4) interferes with tumor immune escape signaling pathways, namely, the PD-1/PD-L1, FGL1/LAG-3 and IDO signaling pathways. Although some achievements have been made in research on nanodrug delivery systems, their practical application still faces some urgent problems. 1) First, the main problems come from the lack of long-term stability, effectiveness and safety of nanodrug delivery systems. Other problems involve the types of delivery systems materials available, the industrialization of preparation methods, packaging and cost issues. The solutions to all of these problems will necessitate comprehensive and in-depth research in the corresponding disciplines or even between multiple disciplines. 2) Secondly, nanodrug delivery systems and their degradation products may not be pharmacologically inert substances, so there are inevitably some potential safety hazards. Current efforts to limit the toxicity of nanodrug delivery systems involve material modification, composition optimization and the development of new materials. 3) Thirdly, the pharmacokinetic behavior of nanodrug delivery systems does not fully satisfy clinical requirements, which also limits the clinical translation of nanodrug delivery systems. Therefore, the key to the application and development of nanodrug delivery systems is to design efficient, safe and intelligent nanodrug delivery systems and study their pharmacokinetics *in vivo* in detail. 4) Finally, tumor tissue has a highly heterogeneous microenvironment, and differences occur among different patients or tumors of the same patient at different times. Widespread tumor heterogeneity presents great difficulties for immunotherapy with nanodrug delivery systems. With the extensive study of genomics and tumor pathological mechanism, researchers should further study and screen for tumor-related markers and should develop more personalized nanodrug delivery systems from the molecular level to achieve better therapeutic effects. With the development of nanotechnology, nanomaterials will also be constantly updated and iterated. We believe that with the ongoing deepening of research and development of science and technology, the advantages of nanodrug delivery systems will be used more extensively in the clinical treatment of malignant tumor diseases and will become a powerful tool for humans to overcome cancer.

Author contributions

BW: Conceptualization, Writing – original draft. YZ: Conceptualization, Investigation, Supervision, Writing – review & editing. XY: Conceptualization, Investigation, Supervision, Writing – original draft, Writing – review & editing.

Funding

The author(s) declare that no financial support was received for the research, authorship, and/or publication of this article.

Conflict of interest

The authors declare that the research was conducted in the absence of any commercial or financial relationships that could be construed as a potential conflict of interest.

Publisher's note

All claims expressed in this article are solely those of the authors and do not necessarily represent those of their affiliated organizations, or those of the publisher, the editors and the reviewers. Any product that may be evaluated in this article, or claim that may be made by its manufacturer, is not guaranteed or endorsed by the publisher.

References

1. Siegel RL, Miller KD, Wagle NS, Jemal A. Cancer statistics, 2023. *CA Cancer J Clin* (2023) 73(1):17–48. doi: 10.3322/caac.21763

2. Sung H, Ferlay J, Siegel RL, Laversanne M, Soerjomataram I, Jemal A, et al. Global cancer statistics 2020: GLOBOCAN estimates of incidence and mortality worldwide for 36 cancers in 185 countries. *CA Cancer J Clin* (2021) 71(3):209–49. doi: 10.3322/caac.21660

3. Dagher OK, Schwab RD, Brookens SK, Posey AD. Advances in cancer immunotherapies. *Cell* (2023) 186(8):1814–1814.e1. doi: 10.1016/j.cell.2023.02.039

4. Bagchi S, Yuan R, Engleman EG. Immune checkpoint inhibitors for the treatment of cancer: clinical impact and mechanisms of response and resistance. *Annu Rev Pathol-mech* (2021) 16:223–49. doi: 10.1146/annurev-pathol-042020-042741

5. Vivekanandhan S, Bahr D, Kothari A, Ashary MA, Baksh M, Gabriel E. Immunotherapies in rare cancers. *Mol Cancer* (2023) 22(1):23. doi: 10.1186/s12943-023-01720-2

6. Martínez-Jiménez F, Priestley P, Shale C, Baber J, Rozemuller E, Cuppen E. Genetic immune escape landscape in primary and metastatic cancer. *Nat Genet* (2023) 55(5):820–31. doi: 10.1038/s41588-023-01367-1

7. Taefehshokr S, Parhizkar A, Hayati S, Mousapour M, Mahmoudpour A, Eleid L, et al. Cancer immunotherapy: Challenges and limitations. *Pathol Res Pract* (2022) 229:153723. doi: 10.1016/j.prp.2021.153723

8. Wang SJ, Dougan SK, Dougan M. Immune mechanisms of toxicity from checkpoint inhibitors. *Trends Cancer* (2023) 9(7):543–53. doi: 10.1016/j.trecan.2023.04.002

9. Kennedy LB, Salama A. A review of cancer immunotherapy toxicity. *CA Cancer J Clin* (2020) 70(2):86–104. doi: 10.3322/caac.21596

10. Wahida A, Buschhorn L, Fröhling S, Jost PJ, Schneeweiss A, Lichter P, et al. The coming decade in precision oncology: six riddles. *Nat Rev Cancer* (2023) 23(1):43–54. doi: 10.1038/s41568-022-00529-3

11. Cheng Z, Li M, Dey R, Chen Y. Nanomaterials for cancer therapy: current progress and perspectives. *J Hematol Oncol* (2021) 14(1):85. doi: 10.1186/s13045-021-01096-0

12. Li Q, Shi Z, Zhang F, Zeng W, Zhu D, Mei L. Symphony of nanomaterials and immunotherapy based on the cancer-immunity cycle. *Acta Pharm Sin B* (2022) 12(1):107–34. doi: 10.1016/j.apsb.2021.05.031

13. Yang B, Gao J, Pei Q, Xu H, Yu H. Engineering prodrug nanomedicine for cancer immunotherapy. *Adv Sci (Weinh)* (2020) 7(23):2002365. doi: 10.1002/advs.202002365

14. Hiam-Galvez KJ, Allen BM, Spitzer MH. Systemic immunity in cancer. *Nat Rev Cancer* (2021) 21(6):345–59. doi: 10.1038/s41568-021-00347-z

15. Schlake T, Thess A, Thran M, Jordan I. mRNA as novel technology for passive immunotherapy. *Cell Mol Life Sci* (2019) 76(2):301–28. doi: 10.1007/s00018-018-2935-4

16. Saxena M, van der Burg SH, Melief C, Bhardwaj N. Therapeutic cancer vaccines. *Nat Rev Cancer* (2021) 21(6):360–78. doi: 10.1038/s41568-021-00346-0

17. Ager A. Cancer immunotherapy: T cells and neutrophils working together to attack cancers. *Cell* (2023) 186(7):1304–6. doi: 10.1016/j.cell.2023.03.005

18. Chen C, Liu X, Chang CY, Wang HY, Wang RF. The interplay between T cells and cancer: the basis of immunotherapy. *Genes (Basel)* (2023) 14(5):1008. doi: 10.3390/genes14051008

19. Basu A, Ramamoorthi G, Albert G, Gallen C, Beyer A, Snyder C, et al. Differentiation and regulation of T_H cells: A balancing act for cancer immunotherapy. *Front Immunol* (2021) 12:669474. doi: 10.3389/fimmu.2021.669474

20. Lei X, Lei Y, Li JK, Du WX, Li RG, Yang J, et al. Immune cells within the tumor microenvironment: Biological functions and roles in cancer immunotherapy. *Cancer Lett* (2020) 470:126–33. doi: 10.1016/j.canlet.2019.11.009

21. Majzner RG, Mackall CL. Tumor antigen escape from CAR T-cell therapy. *Cancer Discovery* (2018) 8(10):1219–26. doi: 10.1158/2159-8290.CD-18-0442

22. Nasir A, Khan A, Li J, Naeem M, Khalil A, Khan K, et al. Nanotechnology, A tool for diagnostics and treatment of cancer. *Curr Top Med Chem* (2021) 21(15):1360–76. doi: 10.2174/1568026621666210701144124

23. Harshita, Wu HF, Kailasa SK. Recent advances in nanomaterials-based optical sensors for detection of various biomarkers (inorganic species, organic and biomolecules). *Luminescence* (2023) 38(7):954–98. doi: 10.1002/bio.4353

24. Tan YY, Yap PK, Xin Lim GL, Mehta M, Chan Y, Ng SW, et al. Perspectives and advancements in the design of nanomaterials for targeted cancer theranostics. *Chem Biol Interact* (2020) 329:109221. doi: 10.1016/j.cbi.2020.109221

25. Yu M, Yang W, Yue W, Chen Y. Targeted cancer immunotherapy: nanoformulation engineering and clinical translation. *Adv Sci (Weinh)* (2022) 9(35): e2204335. doi: 10.1002/advs.202204335

26. Huang P, Wang X, Liang X, Yang J, Zhang C, Kong D, et al. Nano-, micro-, and macroscale drug delivery systems for cancer immunotherapy. *Acta Biomater* (2019) 85:1–26. doi: 10.1016/j.actbio.2018.12.028

27. Wei G, Wang Y, Yang G, Wang Y, Ju R. Recent progress in nanomedicine for enhanced cancer chemotherapy. *Theranostics* (2021) 11(13):6370–92. doi: 10.7150/thno.57828

28. Torres-Vanegas JD, Cruz JC, Reyes LH. Delivery systems for nucleic acids and proteins: barriers, cell capture pathways and nanocarriers. *Pharmaceutics* (2021) 13 (3):428. doi: 10.3390/pharmaceutics13030428

29. Wang QY, Xu YS, Zhang NX, Dong ZP, Zhao BN, Liu LC, et al. Phenylboronic ester-modified anionic micelles for ROS-stimuli response in HeLa cell. *Drug Delivery* (2020) 27(1):681–90. doi: 10.1080/10717544.2020.1748761

30. Ehlerding EB, Grodzinski P, Cai W, Liu CH. Big potential from small agents: nanoparticles for imaging-based companion diagnostics. *ACS Nano* (2018) 12(3):2106–21. doi: 10.1021/acsnano.7b07252

31. Ravindran S, Suthar JK, Rokade R, Deshpande P, Singh P, Pratinidhi A, et al. Pharmacokinetics, metabolism, distribution and permeability of nanomedicine. *Curr Drug Metab* (2018) 19(4):327–34. doi: 10.2174/1389200219666180305154119

32. Li X, Montague EC, Pollinzi A, Lofts A, Hoare T. Design of smart size-, surface-, and shape-switching nanoparticles to improve therapeutic efficacy. *Small* (2022) 18(6): e2104632. doi: 10.1002/smll.202104632

33. Jin W, Dong C, Yang D, Zhang R, Jiang T, Wu D. Nano-carriers of combination tumor physical stimuli-responsive therapies. *Curr Drug Delivery* (2020) 17(7):577–87. doi: 10.2174/1567201817666200525004225

34. Xiang J, Liu K, Xu H, Zhao Z, Piao Y, Shao S, et al. Dual synergistic tumor-specific polymeric nanoparticles for efficient chemo-immunotherapy. *Adv Sci (Weinh)* (2023) 10(29):e2301216. doi: 10.1002/advs.202301216

35. Xu M, Han X, Xiong H, Gao Y, Xu B, Zhu G, et al. Cancer nanomedicine: emerging strategies and therapeutic potentials. *Molecules* (2023) 28(13):5145. doi: 10.3390/molecules28135145

36. Li R, Zheng K, Yuan C, Chen Z, Huang M. Be active or not: the relative contribution of active and passive tumor targeting of nanomaterials. *Nanotheranostics* (2017) 1(4):346–57. doi: 10.7150/ntno.19380

37. Attia MF, Anton N, Wallyn J, Omran Z, Vandamme TF. An overview of active and passive targeting strategies to improve the nanocarriers efficiency to tumour sites. *J Pharm Pharmacol* (2019) 71(8):1185–98. doi: 10.1111/jphp.13098

38. Srinivasarao M, Low PS. Ligand-targeted drug delivery. *Chem Rev* (2017) 117 (19):12133–64. doi: 10.1021/acs.chemrev.7b00013

39. Clemons TD, Singh R, Sorolla A, Chaudhari N, Hubbard A, Iyer KS. Distinction between active and passive targeting of nanoparticles dictate their overall therapeutic efficacy. *Langmuir* (2018) 34(50):15343–9. doi: 10.1021/acs.langmuir.8b02946

40. Shi Y, van der Meel R, Chen X, Lammers T. The EPR effect and beyond: Strategies to improve tumor targeting and cancer nanomedicine treatment efficacy. *Theranostics* (2020) 10(17):7921–4. doi: 10.7150/thno.49577

41. de Lázaro I, Mooney DJ. Obstacles and opportunities in a forward vision for cancer nanomedicine. *Nat Mater* (2021) 20(11):1469–79. doi: 10.1038/s41563-021-01047-7

42. Sindhwani S, Syed AM, Ngai J, Kingston BR, Maiorino L, Rothschild J, et al. The entry of nanoparticles into solid tumours. *Nat Mater* (2020) 19(5):566–75. doi: 10.1038/s41563-019-0566-2

43. Morse MA, Gwin WR, Mitchell DA. Vaccine therapies for cancer: then and now. *Target Oncol* (2021) 16(2):121–52. doi: 10.1007/s11523-020-00788-w

44. DeMaria PJ, Bilusic M. Cancer vaccines. *Hematol Oncol Clin North Am* (2019) 33(2):199–214. doi: 10.1016/j.hoc.2018.12.001

45. Bowen WS, Svrivastava AK, Batra L, Barsoumian H, Shirwan H. Current challenges for cancer vaccine adjuvant development. *Expert Rev Vaccines* (2018) 17 (3):207–15. doi: 10.1080/14760584.2018.1434000

46. Schunke J, Mailänder V, Landfester K, Fichter M. Delivery of immunostimulatory cargos in nanocarriers enhances anti-tumoral nanovaccine efficacy. *Int J Mol Sci* (2023) 24(15):12174. doi: 10.3390/ijms241512174

47. Wooster AL, Girgis LH, Brazeale H, Anderson TS, Wood LM, Lowe DB. Dendritic cell vaccine therapy for colorectal cancer. *Pharmacol Res* (2021) 164:105374. doi: 10.1016/j.phrs.2020.105374

48. Fucikova J, Hensler M, Kasikova L, Lanickova T, Pasulka J, Rakova J, et al. An autologous dendritic cell vaccine promotes anticancer immunity in patients with ovarian cancer with low mutational burden and cold tumors. *Clin Cancer Res* (2022) 28(14):3053–65. doi: 10.1158/1078-0432.CCR-21-4413

49. Chen J, Fang H, Hu Y, Wu J, Zhang S, Feng Y, et al. Combining mannose receptor mediated nanovaccines and gene regulated PD-L1 blockade for boosting cancer immunotherapy. *Bioact Mater* (2022) 7:167–80. doi: 10.1016/j.bioactmat.2021.05.036

50. Go S, Jung M, Lee S, Moon S, Hong J, Kim C, et al. A personalized cancer nanovaccine that enhances T-cell responses and efficacy through dual interactions with dendritic cells and T cells. *Adv Mater* (2023) 29:e2303979. doi: 10.1002/adma.202303979

51. Zhang Y, Shen T, Zhou S, Wang W, Lin S, Zhu G. pH-responsive STING-activating DNA nanovaccines for cancer immunotherapy. *Adv Ther (Weinh)* (2020) 3 (9):2000083. doi: 10.1002/adtp.202000083

52. Zhou L, Hou B, Wang D, Sun F, Song R, Shao Q, et al. Engineering polymeric prodrug nanoplatform for vaccination immunotherapy of cancer. *Nano Lett* (2020) 20 (6):4393–402. doi: 10.1021/acs.nanolett.0c01140

53. Jiang X, Wang J, Zheng X, Liu Z, Zhang X, Li Y, et al. Intratumoral administration of STING-activating nanovaccine enhances T cell immunotherapy. *J Immunother Cancer* (2022) 10(5):e003960. doi: 10.1136/jitc-2021-003960

54. Qiu Z, Liu W, Zhu Q, Ke K, Zhu Q, Jin W, et al. The role and therapeutic potential of macropinocytosis in cancer. *Front Pharmacol* (2022) 13:919819. doi: 10.3389/fphar.2022.919819

55. Mylvaganam S, Freeman SA, Grinstein S. The cytoskeleton in phagocytosis and macropinocytosis. *Curr Biol* (2021) 31(10):R619–32. doi: 10.1016/j.cub.2021.01.036

56. Yang C, Zhang F, Chen F, Chang Z, Zhao Y, Shao D, et al. Biomimetic nanovaccines potentiating dendritic cell internalization *via* CXCR4-mediated macropinocytosis. *Adv Healthc Mater* (2023) 12(5):e2202064. doi: 10.1002/adhm.202202064

57. Liu S, Yu CY, Wei H. Spherical nucleic acids-based nanoplatforms for tumor precision medicine and immunotherapy. *Mater Today Bio* (2023) 22:100750. doi: 10.1016/j.mtbio.2023.100750

58. Teplensky MH, Dittmar JW, Qin L, Wang S, Evangelopoulos M, Zhang B, et al. Spherical nucleic acid vaccine structure markedly influences adaptive immune responses of clinically utilized prostate cancer targets. *Adv Healthc Mater* (2021) 10 (22):e2101262. doi: 10.1002/adhm.202101262

59. Qin L, Wang S, Dominguez D, Long A, Chen S, Fan J, et al. Development of spherical nucleic acids for prostate cancer immunotherapy. *Front Immunol* (2020) 11:1333. doi: 10.3389/fimmu.2020.01333

60. Riley RS, June CH, Langer R, Mitchell MJ. Delivery technologies for cancer immunotherapy. *Nat Rev Drug Discovery* (2019) 18(3):175–96. doi: 10.1038/s41573-018-0006-z

61. Ghiringhelli F, Rébé C. Using immunogenic cell death to improve anticancer efficacy of immune checkpoint inhibitors: from basic science to clinical application. *Immunol Rev* (2023) 18. doi: 10.1111/imr.13263

62. Dolton G, Rius C, Wall A, Szomolay B, Bianchi V, Galloway S, et al. Targeting of multiple tumor-associated antigens by individual T cell receptors during successful cancer immunotherapy. *Cell* (2023) 186(16):3333–3349.e27. doi: 10.1016/j.cell.2023.06.020

63. Roh JS, Sohn DH. Damage-associated molecular patterns in inflammatory diseases. *Immune Netw* (2018) 18(4):e27. doi: 10.4110/in.2018.18.e27

64. Ahmed A, Tait S. Targeting immunogenic cell death in cancer. *Mol Oncol* (2020) 14(12):2994–3006. doi: 10.1002/1878-0261.12851

65. Lee SM, Kim P, You J, Kim EH. Role of damage-associated molecular pattern/cell death pathways in vaccine-induced immunity. *Viruses* (2021) 13(12):2340. doi: 10.3390/v13122340

66. Fucikova J, Kepp O, Kasikova L, Petroni G, Yamazaki T, Liu P, et al. Detection of immunogenic cell death and its relevance for cancer therapy. *Cell Death Dis* (2020) 11 (11):1013. doi: 10.1038/s41419-020-03221-2

67. Zhao Z, Wang X, Wang J, Li Y, Lin W, Lu K, et al. A nanobody-bioorthogonal catalyst conjugate triggers spatially confined prodrug activation for combinational chemo-immunotherapy. *J Med Chem* (2023) 66(17):11951–64. doi: 10.1021/acs.jmedchem.3c00557

68. Huang J, Duan F, Xie C, Xu J, Zhang Y, Wang Y, et al. Microbes mediated immunogenic cell death in cancer immunotherapy. *Immunol Rev* (2023) 8. doi: 10.1111/imr.13261

69. Duan X, Chan C, Lin W. Nanoparticle-mediated immunogenic cell death enables and potentiates cancer immunotherapy. *Angew Chem Int Ed Engl* (2019) 58 (3):670–80. doi: 10.1002/anie.201804882

70. Liu S, Kong X, Fang Y, He Z, Wu H, Ji J, et al. A dual-sensitive nanoparticle-mediated deepening synergistic therapy strategy involving DNA damage and ICD stimuli to treat triple-negative breast cancer. *Biomater Sci* (2023) 11(18):6325–41. doi: 10.1039/d3bm00781b

71. Zhou J, Wang G, Chen Y, Wang H, Hua Y, Cai Z. Immunogenic cell death in cancer therapy: Present and emerging inducers. *J Cell Mol Med* (2019) 23(8):4854–65. doi: 10.1111/jcmm.14356

72. Yang B, Chen Y, Shi J. Reactive oxygen species (ROS)-based nanomedicine. *Chem Rev* (2019) 119(8):4881–985. doi: 10.1021/acs.chemrev.8b00626

73. Wang M, He M, Zhang M, Xue S, Xu T, Zhao Y, et al. Controllable hypoxia-activated chemotherapy as a dual enhancer for synergistic cancer photodynamic immunotherapy. *Biomaterials* (2023) 301:122257. doi: 10.1016/j.biomaterials.2023.122257

74. Shi Y, Wang S, Wu J, Jin X, You J. Pharmaceutical strategies for endoplasmic reticulum-targeting and their prospects of application. *J Control Release* (2021) 329:337–52. doi: 10.1016/j.jconrel.2020.11.054

75. Wu H, Chen W, Chen Z, Li X, Wang M. Novel tumor therapy strategies targeting endoplasmic reticulum-mitochondria signal pathways. *Ageing Res Rev* (2023) 88:101951. doi: 10.1016/j.arr.2023.101951

76. Luo H, Sun Y, Wang L, Liu H, Zhao R, Song M, et al. Targeting endoplasmic reticulum associated degradation pathway combined with radiotherapy enhances the immunogenicity of esophageal cancer cells. *Cancer Biol Ther* (2023) 24(1):2166763. doi: 10.1080/15384047.2023.2166763

77. Traba J, Sack MN, Waldmann TA, Anton OM. Immunometabolism at the nexus of cancer therapeutic efficacy and resistance. *Front Immunol* (2021) 12:657293. doi: 10.3389/fimmu.2021.657293

78. de Visser KE, Joyce JA. The evolving tumor microenvironment: From cancer initiation to metastatic outgrowth. *Cancer Cell* (2023) 41(3):374–403. doi: 10.1016/j.ccell.2023.02.016

79. Sexauer D, Gray E, Zaenker P. Tumour- associated autoantibodies as prognostic cancer biomarkers- a review. *Autoimmun Rev* (2022) 21(4):103041. doi: 10.1016/j.autrev.2022.103041

80. Zhang Y, Zhang Z. The history and advances in cancer immunotherapy: understanding the characteristics of tumor-infiltrating immune cells and their therapeutic implications. *Cell Mol Immunol* (2020) 17(8):807–21. doi: 10.1038/s41423-020-0488-6

81. Cheng Y, Song S, Wu P, Lyu B, Qin M, Sun Y, et al. Tumor associated macrophages and TAMs-based anti-tumor nanomedicines. *Adv Healthc Mater* (2021) 10(18):e2100590. doi: 10.1002/adhm.202100590

82. Chen S, Saeed A, Liu Q, Jiang Q, Xu H, Xiao GG, et al. Macrophages in immunoregulation and therapeutics. *Signal Transduct Target Ther* (2023) 8(1):207. doi: 10.1038/s41392-023-01452-1

83. Mishra AK, Malonia SK. Advancing cellular immunotherapy with macrophages. *Life Sci* (2023) 328:121857. doi: 10.1016/j.lfs.2023.121857

84. Yunna C, Mengru H, Lei W, Weidong C. Macrophage M1/M2 polarization. *Eur J Pharmacol* (2020) 877:173090. doi: 10.1016/j.ejphar.2020.173090

85. Kadomoto S, Izumi K, Mizokami A. Macrophage polarity and disease control. *Int J Mol Sci* (2021) 23(1):144. doi: 10.3390/ijms23010144

86. Kumari N, Choi SH. Tumor-associated macrophages in cancer: recent advancements in cancer nanoimmunotherapies. *J Exp Clin Cancer Res* (2022) 41 (1):68. doi: 10.1186/s13046-022-02272-x

87. Zhao C, Pang X, Yang Z, Wang S, Deng H, Chen X. Nanomaterials targeting tumor associated macrophages for cancer immunotherapy. *J Control Release* (2022) 341:272–84. doi: 10.1016/j.jconrel.2021.11.028

88. Han S, Wang W, Wang S, Yang T, Zhang G, Wang D, et al. Tumor microenvironment remodeling and tumor therapy based on M2-like tumor associated macrophage-targeting nano-complexes. *Theranostics* (2021) 11(6):2892–916. doi: 10.7150/thno.50928

89. Muñoz-Garcia J, Cochonneau D, Télétchéa S, Moranton E, Lanoe D, Brion R, et al. The twin cytokines interleukin-34 and CSF-1: masterful conductors of macrophage homeostasis. *Theranostics* (2021) 11(4):1568–93. doi: 10.7150/thno.50683

90. Chang YW, Hsiao HW, Chen JP, Tzeng SF, Tsai CH, Wu CY, et al. A CSF-1R-blocking antibody/IL-10 fusion protein increases anti-tumor immunity by effectuating tumor-resident CD8 T cells. *Cell Rep Med* (2023) 4(8):101154. doi: 10.1016/j.xcrm.2023.101154

91. Que H, Fu Q, Lan T, Tian X, Wei X. Tumor-associated neutrophils and neutrophil-targeted cancer therapies. *Biochim Biophys Acta Rev Cancer* (2022) 1877 (5):188762. doi: 10.1016/j.bbcan.2022.188762

92. Masucci MT, Minopoli M, Carriero MV. Tumor associated neutrophils. Their role in tumorigenesis, metastasis, prognosis and therapy. *Front Oncol* (2019) 9:1146. doi: 10.3389/fonc.2019.01146

93. Arvanitakis K, Mitroulis I, Germanidis G. Tumor-associated neutrophils in hepatocellular carcinoma pathogenesis, prognosis, and therapy. *Cancers (Basel)* (2021) 13(12):2899. doi: 10.3390/cancers13122899

94. Chellappan DK, Yee LW, Xuan KY, Kunalan K, Rou LC, Jean LS, et al. Targeting neutrophils using novel drug delivery systems in chronic respiratory diseases. *Drug Dev Res* (2020) 81(4):419–36. doi: 10.1002/ddr.21648

95. Chu D, Dong X, Shi X, Zhang C, Wang Z. Neutrophil-based drug delivery systems. *Adv Mater* (2018) 30(22):e1706245. doi: 10.1002/adma.201706245

96. Wang Y, Zhao Q, Zhao B, Zheng Y, Zhuang Q, Liao N, et al. Remodeling tumor-associated neutrophils to enhance dendritic cell-based HCC neoantigen nano-vaccine efficiency. *Adv Sci (Weinh)* (2022) 9(11):e2105631. doi: 10.1002/advs.202105631

97. Dong H, Li Y, Liu Y, Wen Y, Zou Z, Yang T, et al. A nano-immunotraining strategy to enhance the tumor targeting of neutrophils via *in vivo* pathogen-mimicking stimulation. *Biomater Sci* (2019) 7(12):5238–46. doi: 10.1039/c9bm01278h

98. Zhang M, Fang Y, Fu X, Liu J, Liu Y, Zhu Z, et al. Cancer-associated fibroblasts nurture LGR5 marked liver tumor-initiating cells and promote their tumor formation, growth, and metastasis. *Cancer Med* (2023) 12(17):18032–49. doi: 10.1002/cam4.6408

99. Ai W, Liu T, Lv C, Feng X, Wang Q. Modulation of cancer-associated fibroblasts by nanodelivery system to enhance efficacy of tumor therapy. *Nanomed (Lond)* (2023) 18(15):1025–39. doi: 10.2217/nnm-2023-0088

100. Biffi G, Tuveson DA. Diversity and biology of cancer-associated fibroblasts. *Physiol Rev* (2021) 101(1):147–76. doi: 10.1152/physrev.00048.2019

101. Chen Y, McAndrews KM, Kalluri R. Clinical and therapeutic relevance of cancer-associated fibroblasts. *Nat Rev Clin Oncol* (2021) 18(12):792–804. doi: 10.1038/s41571-021-00546-5

102. Chen X, Song E. Turning foes to friends: targeting cancer-associated fibroblasts. *Nat Rev Drug Discovery* (2019) 18(2):99–115. doi: 10.1038/s41573-018-0004-1

103. Chen Y, Hu M, Wang S, Wang Q, Lu H, Wang F, et al. Nano-delivery of salvianolic acid B induces the quiescence of tumor-associated fibroblasts via interfering with TGF-β1/Smad signaling to facilitate chemo- and immunotherapy in desmoplastic tumor. *Int J Pharm* (2022) 623:121953. doi: 10.1016/j.ijpharm.2022.121953

104. Yi M, Zheng X, Niu M, Zhu S, Ge H, Wu K. Combination strategies with PD-1/PD-L1 blockade: current advances and future directions. *Mol Cancer* (2022) 21(1):28. doi: 10.1186/s12943-021-01489-2

105. Anderson AC, Joller N, Kuchroo VK. Lag-3, tim-3, and TIGIT: co-inhibitory receptors with specialized functions in immune regulation. *Immunity* (2016) 44 (5):989–1004. doi: 10.1016/j.immuni.2016.05.001

106. Prendergast GC, Malachowski WJ, Mondal A, Scherle P, Muller AJ. Indoleamine 2,3-dioxygenase and its therapeutic inhibition in cancer. *Int Rev Cell Mol Biol* (2018) 336:175–203. doi: 10.1016/bs.ircmb.2017.07.004

107. Liu Y, Zhou N, Zhou L, Wang J, Zhou Y, Zhang T, et al. IL-2 regulates tumor-reactive CD8 T cell exhaustion by activating the aryl hydrocarbon receptor. *Nat Immunol* (2021) 22(3):358–69. doi: 10.1038/s41590-020-00850-9

108. De Ridder K, Locy H, Piccioni E, Zuazo MI, Awad RM, Verhulst S, et al. TNF-α-secreting lung tumor-infiltrated monocytes play a pivotal role during anti-PD-L1 immunotherapy. *Front Immunol* (2022) 13:811867. doi: 10.3389/fimmu.2022.811867

109. Ai L, Xu A, Xu J. Roles of PD-1/PD-L1 pathway: signaling, cancer, and beyond. *Adv Exp Med Biol* (2020) 1248:33–59. doi: 10.1007/978-981-15-3266-5_3

110. Liu S, Wang H, Shao X, Chen H, Chao S, Zhang Y, et al. Advances in PD-1 signaling inhibition-based nano-delivery systems for tumor therapy. *J Nanobiotechnol* (2023) 21(1):207. doi: 10.1186/s12951-023-01966-4

111. Wang S, Zhou X, Zeng Z, Sui M, Chen L, Feng C, et al. Atovaquone-HSA nano-drugs enhance the efficacy of PD-1 blockade immunotherapy by alleviating hypoxic tumor microenvironment. *J Nanobiotechnol* (2021) 19(1):302. doi: 10.1186/s12951-021-01034-9

112. Wang J, Sanmamed MF, Datar I, Su TT, Ji L, Sun J, et al. Fibrinogen-like protein 1 is a major immune inhibitory ligand of LAG-3. *Cell* (2019) 176(1-2):334–47. doi: 10.1016/j.cell.2018.11.010

113. Wan WJ, Huang G, Wang Y, Tang Y, Li H, Jia CH, et al. Coadministration of iRGD peptide with ROS-sensitive nanoparticles co-delivering siFGL1 and siPD-L1 enhanced tumor immunotherapy. *Acta Biomater* (2021) 136:473–84. doi: 10.1016/j.actbio.2021.09.040

114. Ogbechi J, Huang YS, Clanchy F, Pantazi E, Topping LM, Darlington LG, et al. Modulation of immune cell function, IDO expression and kynurenine production by the quorum sensor 2-heptyl-3-hydroxy-4-quinolone (PQS). *Front Immunol* (2022) 13:1001956. doi: 10.3389/fimmu.2022.1001956

115. Guo Y, Liu Y, Wu W, Ling D, Zhang Q, Zhao P, et al. Indoleamine 2,3-dioxygenase (Ido) inhibitors and their nanomedicines for cancer immunotherapy. *Biomaterials* (2021) 276:121018. doi: 10.1016/j.biomaterials.2021.121018

116. Yang C, He B, Zheng Q, Wang D, Qin M, Zhang H, et al. Nano-encapsulated tryptanthrin derivative for combined anticancer therapy via inhibiting indoleamine 2,3-dioxygenase and inducing immunogenic cell death. *Nanomed (Lond)* (2019) 14 (18):2423–40. doi: 10.2217/nnm-2019-0074

frontiers | Frontiers in Immunology

TYPE Review
PUBLISHED 12 January 2024
DOI 10.3389/fimmu.2023.1324744

OPEN ACCESS

EDITED BY
Björn L. Frendéus,
BioInvent, Sweden

REVIEWED BY
Kaïdre Bendjama,
Transgene, France
Lance Hellman,
Nevada State College, United States
Arash Arashkia,
Pasteur Institute of Iran (PII), Iran

*CORRESPONDENCE
Pengju Wang
wangpengju@zzu.edu.cn
Yujing Xuan
yujing_xuan@126.com

RECEIVED 20 October 2023
ACCEPTED 29 December 2023
PUBLISHED 12 January 2024

CITATION
Xu L, Sun H, Lemoine NR, Xuan Y and Wang P (2024) Oncolytic vaccinia virus and cancer immunotherapy.
Front. Immunol. 14:1324744.
doi: 10.3389/fimmu.2023.1324744

Oncolytic vaccinia virus and cancer immunotherapy

Lihua Xu[1], Huihui Sun[1], Nicholas R. Lemoine[1,2], Yujing Xuan[1]* and Pengju Wang[1]*

[1]Sino-British Research Centre for Molecular Oncology, National Centre for International Research in Cell and Gene Therapy, State Key Laboratory of Esophageal Cancer Prevention & Treatment, School of Basic Medical Sciences, Academy of Medical Sciences, Zhengzhou University, Zhengzhou, China, [2]Centre for Biomarkers & Biotherapeutics, Barts Cancer Institute, Queen Mary University of London, London, United Kingdom

Oncolytic virotherapy (OVT) is a promising form of cancer treatment that uses genetically engineered viruses to replicate within cancer cells and trigger anti-tumor immune response. In addition to killing cancer cells, oncolytic viruses can also remodel the tumor microenvironment and stimulate a long-term anti-tumor immune response. Despite achieving positive results in cellular and organismal studies, there are currently only a few approved oncolytic viruses for clinical use. Vaccinia virus (VACV) has emerged as a potential candidate due to its ability to infect a wide range of cancer cells. This review discusses the mechanisms, benefits, and clinical trials of oncolytic VACVs. The safety and efficacy of different viral backbones are explored, as well as the effects of oncolytic VACVs on the tumor microenvironment. The potential combination of oncolytic VACVs with immunotherapy or traditional therapies is also highlighted. The review concludes by addressing prospects and challenges in the field of oncolytic VACVs, with the aim of promoting further research and application in cancer therapy.

KEYWORDS

oncolytic virotherapy, vaccinia virus, cancer immunotherapy, combination therapy, tumor microenvironment

1 Introduction

Oncolytic virotherapy (OVT) is an emerging tumor treatment modality that is based on naturally or genetically engineered oncolytic viruses (OVs) to selectively lyse tumor cells while sparing healthy cells (1). The history of OVs include three stages: the discovery and application of wild-type viruses (before 1990), the research and development of genetically engineered viruses (1991–2000), and the insertion of therapeutic genes in viruses and synergistic therapies (21st century) (2). In 1991, Martuza et al. first reported a genetically engineered herpes simplex virus (HSV)-1 (dlsptk) for inhibiting glioma growth in nude mice, which accelerated the field of OVT (3). With deeper insight into the anti-tumor mechanisms, OVs have been deemed to not only lyse tumor cells selectively, but activate

anti-tumor immunity and remodel the tumor microenvironment (TME), making them promising as oncologic therapeutic agents (4).

According to their genomic characteristics, OVs are divided into two categories, DNA viruses (e.g., adenovirus, vaccinia virus (VACV), herpesvirus) and RNA viruses [e.g., reovirus, measles virus, New Castle disease virus (NDV), vesicular stomatitis virus (VSV)], in which DNA oncolytic viruses are superior to other viruses due to their larger genome, genetic stability, and high replication ability (5). Larger genome allows for more flexibility for the expression of recombinant payloads. Most of the currently approved OVs that include Rigvir (enteric cytopathic human orphan virus approved in Latvia for melanoma in 2004), Oncorine (adenovirus approved in China for head and neck cancer in 2005), T-VEC (HSV approved in the United States for melanoma in 2015), and DELYTACT (HSV approved in Japan for glioblastoma in 2021) are DNA viruses. Besides the above approved OVs, many other candidate OVs show promising pre-clinical evidence of anti-tumor activity, and increasing clinical trials are currently underway to determine the efficacy of OVs in different cancer patients (6). However, the number of approved OVs and the applicable cancer types remain very rare in the clinic. Intratumor administration is one of the most important limiting factors. The presence of preexisting antiviral neutralizing antibodies or their development during viral therapy render repeat systemic treatments of OVs ineffective, limiting the application in some cancer types with metastases or unable to be administrated *in situ*. For instance, T-VEC is only approved in patient without visceral metastases. The development of novel and more potent oncolytic viruses is urgently needed.

As one kind of DNA virus, VACV is a large DNA prototypic poxvirus that replicates exclusively in the cytoplasm, and it is therefore fully nonintegrative. VACV has been used as a smallpox vaccine for many years with relatively low adverse reactions (7). Recent preclinical results and clinical data about different engineered oncolytic VACVs [e.g., Pexa-Vec (JX-594)] also show its potential for intravenous infusion and tumor therapy *via* highly and stably expressing many therapeutic genes (8). According to the phase 1b trial results of biweekly intravenous Pexa-Vec in colorectal cancer, no patients developed Pexa-Vec infusion-related reactions. The common adverse effects mainly include headache, nausea, anorexia, rash, and vomiting (9). Hence, VACVs are expected to be safe candidates for OVT.

This review outlines the characteristics, viral backbones and clinical trials of oncolytic VACVs. The anti-tumor mechanisms and effects on tumor microenvironment are also discussed. In addition, the potential combination treatments with immunotherapy or traditional therapies are highlighted. The prospects and challenges of oncolytic VACVs are also addressed to promote the further research and application in cancer treatment.

2 Characteristics and anti-tumor mechanisms of oncolytic VACVs

2.1 Characteristics of oncolytic VACVs

VACV is an enveloped double stranded DNA orthopoxvirus, in which the most widely used experimental strains include Lister, Western Reserve (WR), Wyeth strains, Copenhagen strains, Ankara (also known as MVA), and Tiantan stains etc (10). MVA and Tiantan stains are non-replicative strains of VACVs for cancer vaccine, while the other strains are replication competent viruses. During replication, VACVs produce four infectious forms which differ in their outer membranes: intracellular mature virion (IMV), the intracellular enveloped virion (IEV), the cell-associated enveloped virion (CEV) and the extracellular enveloped virion (EEV) (11). The IMV is the most abundant infectious form, responsible for spread between host, while the CEV and EEV are responsible for cell-to-cell transfer and long-range dissemination within the host organism, respectively (12, 13).

Compared with other virus vectors, VACVs have many advantages in OVT. 1) VACVs replicate exclusively in the cytoplasm, with no integration of viral DNA into the host genome, indicating its safety (14). 2) VACVs have a large genome (~190 kb), capable of inserting and stably expressing exogenous therapeutic genes of at least 25 kb in a single vector (15). 3) VACVs own natural tumor tropism, potential for systemic administration (16). 4) VACVs have a rapid and lytic replication cycle. The first viruses can be released from the cells within 8 h after infection, and the infected cells can be destroyed after 48-72 h of infection. 5) VACVs can replicate in hypoxic conditions (17). 6) Because of no limitation on receptors during entry, VACVs exhibit high infectivity not only in various host species but also in a large range of tissues, beneficial for preclinical researches (18, 19).

In addition, like other oncolytic viruses, oncolytic VACVs can exert anti-tumor effect *via* oncolysis and activation of anti-tumor immune responses. To date, several studies have shown that deletion of some endogenous genes enhances the oncolysis of oncolytic VACVs. The key VACV genes and corresponding oncolytic functions are listed in the Table 1. Deletion those genes can improve the antitumor efficacy through multiple ways such as increasing the tumor selectivity, safety and anti-tumor immune response.

Based on the above advantages, oncolytic VACV is an alternative virus vector for OVT.

2.2 Anti-tumor mechanisms of oncolytic VACVs

Oncolytic VACVs primarily destroy tumor tissues *via* three mechanisms: direct oncolysis of tumor cells, disrupting tumor vasculature (tumor-associated endothelial cells lysis-mediated vascular collapse, neutrophils accumulation-mediated thrombosis) and activating anti-tumor immunity (Figure 1). In the following sections, we explore the detailed anti-tumor mechanisms of oncolytic VACVs.

2.2.1 Selective self-replication and oncolysis in tumor cells

Unlike some viruses such as adenoviruses, VACVs have inherent tumor tropism. As one kind of invasive viruses, oncolytic VACVs infect host tumor cells in several steps (20).

TABLE 1 Oncolytic functions of key VACV genes.

Gene name	Corresponding protein function	Oncolytic function after gene deletion	PMID
TK	Key enzymes for DNA replication	Increase tumor selectivity and safety	10678358
VGF	Polypeptide with amino acid sequence homology to epidermal growth factor and transforming growth factor alpha	Attenuate virulence and increase safety	3339716, 30420785, 2739561
B18R	Bind and remove secreted type-I IFNs	Enable IFN-dependent tumor selectivity and increase safety	18162040
F1L	Bind and inhibit the NLR family member NLRP1 as an apoptosis inhibitor	Increase safety and oncolysis	23603272, 31428674
N1L	Inhibit apoptosis and NF-κB activity	Enhance $CD8^+$ T-cell memory and natural killer cell response	22194685, 25382035, 32217766, 18931086
B2R	Viral cGAMP-specific nuclease	Enhance IRF3 phosphorylation and type I IFN expression, improving antitumor immune response	30728498, 37016144
E5R	cGAS inhibitor	Induce much higher levels of type I IFN, improving antitumor immune response	37217469, 37145142

Firstly, oncolytic VACVs use distinct forms of macropinocytosis for host-cell entry, independent on receptors. A study from Helenius's group demonstrated that mature virions (MVs) from both the WR strain and the International Health Department-J (IHD-J) strain entered host cells by macropinocytosis due to virion-exposed phosphatidylserine. However, different macropinocytic mechanisms were possible in the same cell line through subtle differences in the activating ligand. The results showed that MVs from the WR strain entered HeLa cells by activating transient plasma membrane blebbing, while MVs from the IHD-J strain induced rapid formation (and lengthening) of filopodia (19). Next, DNA and proteins for oncolytic VACVs replication are synthesized in the cytoplasm instead of the cell nucleus. Last, progeny of VACVs released from lysed tumor cells spread to surrounding uninfected tumor cells, leading to amplification of their oncolytic activity and inducing tumor cell death. The selective oncolysis of oncolytic VACVs mainly lies on the differences between tumor cells and normal cells. On the one hand, various tumor suppressor genes (e.g., p53, RAS, and PTEN) and antiviral signals (such as type I interferon (IFN) pathway) are significantly downregulated, which make it easier for oncolytic VACVs to survive and replicate in the tumor cell (21). On the other hand, most of oncolytic VACVs are constructed by deletion of some viral genes [e.g., thymidine kinase (TK)] that overexpressed in tumor cells (22). In the healthy cell, oncolytic VACVs cannot replicate due to the deletion of some viral genes that are essential for VACV replication. Once exposure of oncolytic VACV genome in the cytoplasm, cyclic GMP-AMP synthase (cGAS)/stimulator of interferon gene (STING) pathway is activated followed by the production of antiviral cytokines such as type I IFN, further inhibiting oncolytic VACV replication. Subsequently, the genome and proteins of oncolytic VACVs are degraded by DNA and protein-degrading enzymes.

2.2.2 Disrupting tumor vasculature

In general, the peripheral region of a tumor contains enriched vasculature which is primarily composed of endothelial cells, and affects tumor growth and metastasis (23). Targeting the neovasculature is an alternative approach to eradication of tumor cells *via* starving and suffocating tumors. For the first time, Kirn and coworkers found that the oncolytic VACV (JX-594) could induce cytokines and chemokines-mediated neutrophils accumulation in blood vessels, leading to intravascular thrombosis (24). Soon afterwards, they revealed that JX-594, with deletion of TK genes, was able to specifically target and infect tumor-associated endothelial cells and efficiently replicate due to increased vascular endothelial growth factors (VEGF) signaling-mediated TK overexpression, contributing to vascular collapse (25). After intravenous injection of oncolytic VACVs, tumor perfusion in patient biopsy decreased from magnetic resonance imaging results, and no clinical signs of damage to normal vasculature were observed. Another research from Bell's group revealed that VEGF/VEGFR2 signaling in remodeling vessels could also sensitize the tumor vasculature to oncolytic VACVs infection by PRD1-BF1/Blimp1-mediated antiviral immune suppression (26). However, Santry et al. considered that despite many potential benefits by oncolytic VACV-mediated tumor vascular collapse such as leukomonocyte recruitment, shutting off blood vessels may also limit oncolytic VACVs spread and obstruct the delivery of subsequent therapeutic agents, and the entry of immunological effector cells (27).

2.2.3 Activating anti-tumor immune response and remodeling TME

Early the anti-tumor mechanism of OVT was recognized as direct oncolysis of OVs. With the development of tumor immunotherapy, the impact of OVT on the immune response to tumors has become widely studied. It is widely acknowledged that oncolytic VACVs can activate innate and adaptive immune systems in tumors, and further remodel tumor immunosuppressive microenvironment.

Generally, after infection by oncolytic VACVs, pathogen-associated molecular patterns (PAMPs) and progeny viruses are released and sensed by pattern recognition receptors (PRRs) on innate immune cells. Subsequently, chemokines (e.g., CCL3, CCL5, CXCL8, CXCL9) and proinflammatory cytokines (e.g., type I IFNs, interleukin (IL)-12, GM-CSF, TNF-α) are released to recruit and activate more innate immune cells such as macrophages, neutrophils, dentritic cells (DCs) and T-cells in the TME to eliminate the infected tumor cells, which can further stimulate the production of proinflammatory cytokines and chemokines to amplify the initial innate response (28).

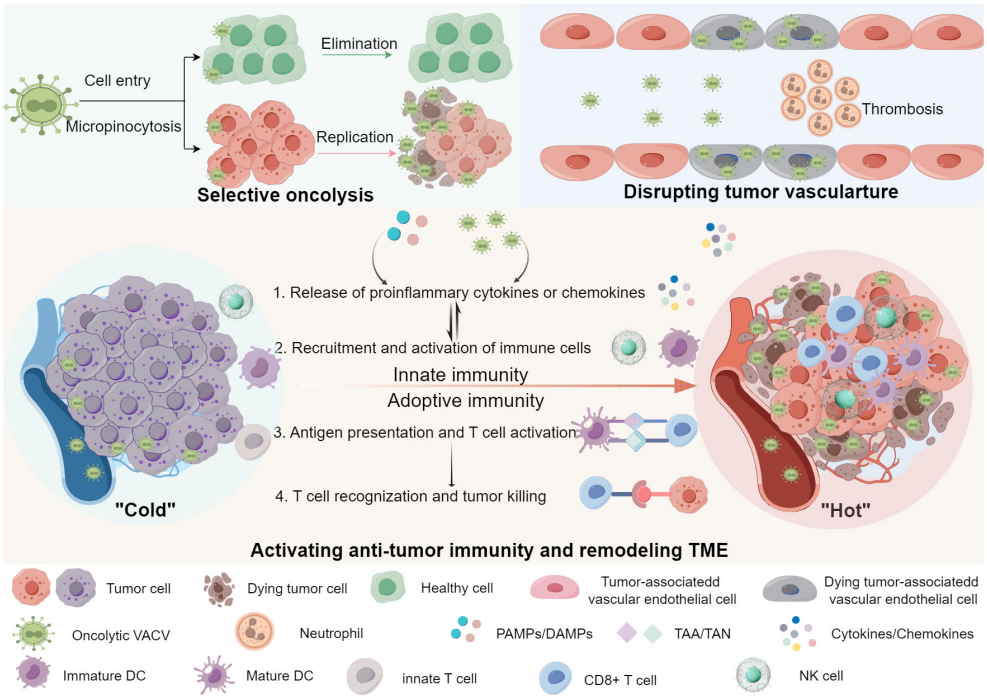

FIGURE 1
Anti-tumor mechanisms of oncolytic VACVs. Oncolytic VACVs can kill cancer cells *via* a variety of mechanisms. First, they directly infect, replicate and lyse tumor cells sparing normal cells. Released virions can infect neighbor tumor cells and so forth. Second, oncolytic VACVs can infect and lyse tumor associated vascular endothelial cells, meanwhile recruiting neutrophile cells and inducing thrombosis. Third, they can remodel the "cold" TME to "hot" by activating innate and adoptive anti-tumor immunity. The release of progeny viruses and PAMPs/DAMPs can promote the innate immune cells to produce proinflammatory cytokines and chemokines, which in turn lead to the recruitment and activation of more immune cells, thus innate immune responses are activated. With the activation of antigen presentation cells, DCs can present the released TAA/TAN to T-cells, enhancing the tumor recognition and killing ability of $CD8^+$ T-cells, inducing a tumor-specific adoptive immune response. PAMPs, Pathogen-associated molecular patterns; DAMPs, Damage-associated molecular pattern; TAA, Tumor-associated antigens; TAN, Tumor-associated neoantigens; DC, Dendritic cell; NK cell, Natural killer cell. The figure is drawn by FigDraw.

In addition, accumulating evidences suggest that oncolytic VACVs induce immunogenic cell death (ICD) in infected cancer cells with the release of damage-associated molecular pattern molecules (DAMPs), such as the "danger" signals high mobility group box 1 (HMGB1), the "find me" signal adenosine triphosphate (ATP) and the "eat me" signal calreticulin (CRT) (29). The DAMPs can activate the immature DC (iDC) into the mature DC (mDC). mDCs are the main antigen presentation cells that present the released tumor-associated antigens (TAAs), and tumor-associated neoantigens (TANs) after oncolysis to T-cells, resulting in activation, proliferation and differentiation of T-cells (30). Effector T-cells exert specific tumor killing, meanwhile memory T-cells are responsible for long-term and distant anti-tumor effect. Thus, adaptive immune responses to oncolytic VACV-infected tumor cells are activated.

It can be seen from the clinical data reported by Samson et al. that JX-594 infusion contributed to a significant increase of IFN and neutralizing antibodies in plasma for viral clearance. Meanwhile, many other proinflammatory and chemokines such as IL12, CXCL10, CXCL2 also increased, leading to the activation of natural killer (NK) cells, and the recruitment and activation of T-cells and DCs (31).

As stated above, oncolytic VACV acts as a bait in the tumor to increase the number of immune cells and proinflammatory cytokines and chemokines in the TME, resulting in the amplification of the anti-tumor immune response and remodeling immunologically "cold" tumors into "hot" tumors. However, immune cells in the TME may be detrimental to effectiveness of OVT by eliminating virally infected cells. Antiviral immunity is a double-edged sword that needs to be well-balanced in tumor therapy (32). It is reflected not only in the tumor tissues, but in the blood circulation when intravenously administrating reovirus or coxsackievirus according to the study from Berkeley et al. (33). They found that neutralizing antibodies had an actual beneficial effect on OVT by forming virus/neutralizing antibody complexes which can be internalized by monocytes and delivered to tumor sites in spite of viral clearance. This finding is very exciting and beneficial for the understanding and application of OVT in future. However, whether this phenomenon exist in the oncolytic VACVs treatment still needs to be explored.

3 Construction of oncolytic VACV backbones

Compared with non-replicative VACVs, replication competent VACVs retain their ability to lyse tumor cells and spread through tumor tissues while the lower safety and efficacy limited the

application. With the ever-increasing knowledge in the fields of molecular virology and cancer cell biology, engineered oncolytic VACVs can be obtained through the DNA recombinant technology (e.g., CRISPR-Cas9 system) (34). The multiple safe and efficacious tumor-targeted oncolytic VACV backbones have been developed in recent years *via* genome editing. Based on the function of the deletion genes, they are mainly classified into three types: viral replication-related, viral dissemination-related and antiviral immune evasion-related. The functions of some VACV genes are listed in the Table 2.

Targeting the overexpressed proteins [e.g., TK and ribonucleotide reductase (RR)] in tumor cells that are necessary for viral replication is the common method to increase the safety of oncolytic VACVs (22, 35). JX-594 is a typical TK-deleted oncolytic VACV with confirmed safety in phase I clinical trials (e.g., NCT02977156 and NCT01394939). Double deletion of TK and RR also showed enhanced safety and selective replication in the preclinical studies (48).

Deletion of viral virulence genes can further enhance the safety of oncolytic VACVs. VACV virulence is related to viral replication, dissemination, and antiviral immune evasion. Viral growth factors (VGF) is an EGF homologue that activates EGFR-Ras pathway to promote cell proliferation. Studies have shown that deletion of VGF contributes to low replication and virulence (49, 50). Double deletion of TK and VGF led to significantly attenuated virulence in resting cells *in vitro* and tumor-specific replication *in vivo* (51). As mentioned previously, EEV and CEV forms of VACVs are responsible for viral dissemination *in vivo*. Deletion of the vaccinia virus F13L gene results in a highly attenuated virus that is defective in EEV and CEV generation and plaque formation (36).

Antagonizing antiviral immunity is an important way for oncolytic VACVs to potentiate virulence. cGAS/STING pathway plays a central role in immune defense against tumors and viral infections, where TANK-binding kinase 1 (TBK1) recruitment to STING further activates both NF-κB and interferon regulatory factor 3 (IRF3) (52). cGAS is a DNA sensor for host defense against VACV infection. Vaccinia B2R gene was recently discovered to encode a cytosolic cGAMP nuclease that obstruct the cGAS signal. Vaccinia E5 is another virulence factor that inhibits cGAS by abolishing cGAMP production. Studies showed that deletion of B2R or E5R gene made the virulence of VACVs attenuated and anti-tumor immunity enhanced (53, 54).

In addition, inhibition of NF-κB signaling and/or IFR signaling cannot only reduce viral virulence, but enhance anti-tumor immunity. F14 is a selective NF-κB inhibitor in the nucleus by disrupting the binding of p65 to its co-activator CBP and reducing acetylation of p65-K310 and a VACV strain lacking F14 has reduced virulence in a mouse model (37). There are many other proteins that show antagonism of NF-κB activation with different action sites. For instance, B14 interacts directly with IκB kinase β to inhibit its activation, and A49 inhibits NF-κB activation by binding to β-TrCP, contributing to virus virulence (38–40). Additionally, N2 is a nuclear virulence factor that inhibits activation of IFNβ promoter by inhibiting IRF3 activation, deletion of which reduced virulence of VACVs (41). Interestingly, some proteins (e.g., N1 and K7) have dual functions of inhibiting NF-κB and IRF activation (42, 55). Studies proved that deletion of the N1L gene reduced virulence and inhibited VACV replication, meanwhile it improved the generation of immediate and long-term memory $CD8^+$ T-cell responses and induced a stronger NK cell response to infection (56, 57). Moreover, deletion of B8R or B18R that directly binds to several species of IFN and neutralizes the antiviral activity also makes oncolytic VACV attenuated for mice (43, 58).

The activation of complement system is another key innate immune defense against viral infection through classical and alternative pathways. Isaacs and coworkers demonstrated that VACV complement-control protein (VCP) could prevent antibody-dependent complement-enhanced neutralization of infectivity and contribute to virulence, as VCP gene (C21L) knockout viruses were attenuated in an intradermal rabbit model (44).

Notably, one gene may be involved in complex biological processes. For example, the VACV A56 protein with haemagglutination activity is able to bind two other viral proteins, a serine protease inhibitor (K2) and VCP, and express them at the surface of the infected cell. The A56–K2 complex binds to the

TABLE 2 Functions of some VACV genes[a].

Classification	Gene name	Function	Reference
Viral replication-related	RR	Key enzymes for DNA replication	(35)
Viral dissemination-related	F13L	EEV and CEV generation and plaque formation	(36)
Anti-tumor immune evasion-related	F14L	Disrupt the binding of p65 to its co-activator CBP and reduce acetylation of p65-K310, inhibiting NF-κB	(37)
	B14R	Inhibit IκB kinase β and NF-κB activation	(38, 39)
	A49R	Inhibit NF-κB activation by binding to β-TrCP	(40)
	N2L	Inhibit activation of IFNβ promoter by inhibiting IRF3 activation	(41)
	K7R	Inhibit NF-κB and IRF activation	(42)
	B18R	Bind and remove secreted type-I IFNs, including IFN-β	(43)
	C21L	Inhibit complements activity	(44)
Multifunctional	A56R	Reduce superinfection and prevent cell–cell fusion of infected cells by forming A56-K2 complex, protect infected cells from complement attack by forming A56-VCP complex, and have haemagglutination activity	(45–47)

[a]The functions of omitted genes such as TK, VGF, B2R et al. were listed in Table 1.

entry–fusion machinery of VACV; reducing superinfection and preventing cell–cell fusion of infected cells, while the A56–VCP complex protects infected cells from complement attack (45, 46). However, the deletion of A56R did not attenuate VACVs in some cases according to the summary from DeHaven and coworkers (47). Given that A56R gene is non-essential for viral replication, it still can be used as a region of VACV genome suitable for exogenous gene insertion. GL-ONC1 is a typical VACV that inserts β-glucuronidase into the A56R loci of VACV genome. The increasing understanding of the multiple functions of VACV genes is conducive to optimize the VACV backbones.

4 Oncolytic VACV-based immune-related combination therapies

OVT is an effective form of immunotherapy that has been used to treat cancer. As previously mentioned, OVs can selectively kill tumor cells, activate anti-tumor immunity and remodel the "cold" TME to "hot". However, OV-based monotherapy has restricted ability to activate anti-tumor immunity, given the potential antiviral machinery induced by activation of the IFN signaling pathway and the highly variable heterogeneity of malignant cells. In this section, strategies augmenting anti-tumor immune responses *via* synergistic therapies are summarized (Figure 2).

4.1 Oncolytic VACVs encoding immunostimulatory genes

With the ever-increasing knowledge of immune regulation mechanisms in tumor tissues, some immunostimulatory genes have been inserted into the genome of VACVs to amplify the anti-tumor immunity of oncolytic VACVs. Anti-tumor immunostimulatory factors include cytokines, chemokines, co-stimulatory factors and so on. Inflammatory cytokines are soluble proteins with the function of regulating innate and adoptive immunity, including pro-inflammatory and anti-inflammatory cytokines.

Arming pro-inflammatory cytokines is a usual way to enhance OVT by recruiting, activating immune cells and inhibiting immunosuppressive cells. GM-CSF is one of the most widely used cytokines that improve OVT. It recruits both DCs and NK cells to promote the maturation of DCs, which in turn, activates anti-tumor immunity (59). T-VEC, a GM-CSF armed HSV, has been approved in the United States for melanoma in 2015. JX-594, a genetically modified VACV that inserts the GM-CSF gene also has shown promising anti-tumor ability in clinical trials. IL-21 arming potentiated the anti-tumor activity of oncolytic VACVs by increasing effector $CD8^+$ T-cell populations (60, 61). Some pro-inflammatory cytokines (e.g., IL-12, IL-23, IL-15) armed oncolytic VACVs showed stronger anti-tumor immune response by enhancing T-cell and NK cell activation and cytotoxicity in

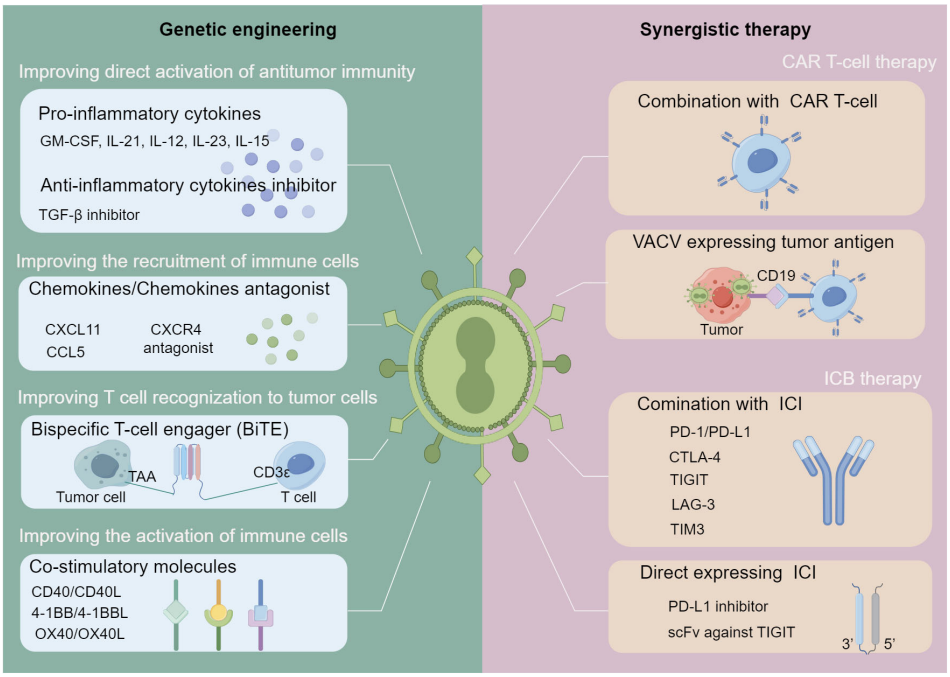

FIGURE 2
Strategies for oncolytic VACV-based immune-related combination therapies. Strategies are divided into two main categories: genetic engineering of oncolytic VACVs and combination with other immunotherapies. In terms of genome engineering (left), various immunostimulatory genes can be inserted into the genome of oncolytic VACVs, including those can activate the anti-tumor immunity directly, improve the T-cells recognition to cancer cells, recruit and activate immune cells. In terms of synergistic immunotherapies (right), oncolytic VACVs can be combined with CAR T-cell or ICI molecules directly or express CAR or ICI to enhance the synergistic therapies. oncolytic VACV, Oncolytic vaccinia virus; TAA, Tumor associated antigen; BiTE, Bispecific T-cell engager; CAR, Chimeric antigen receptor; ICI, Immune checkpoint inhibitor; scFv, Single chain variable fragment. The figure is drawn by FigDraw.

addition to increasing the production of IFN-γ (62–64). Other cytokines that have been used to engineer oncolytic viruses such as adenovirus and HSV may also enhance the anti-tumor effect of oncolytic VACVs through rational design (65). What is noteworthy is that assessment of actual exposure to potential payloads and management of safety issues that may arise from these payloads need to be considered when engineering oncolytic VACVs.

Owing to the important role of anti-inflammatory cytokines (e.g., TGF−β, IL-10) in host immune response, they are also designed to improve the therapeutic efficacy of OVT. Delgoffe and coworkers found that oncolytic VACV-delivered TGFβ inhibitor could overcome the immunosuppressive tumor microenvironment by blocking the immunosuppressive function of TGF−β, and increasing the sensitivity to INF-γ (66). The IL-10 is a recognized immunosuppressive cytokine that inhibits the production of pro-inflammatory cytokines such as IL-12 and INF-γ (67). Hickman and coworkers demonstrated that locally produced IL-10 after VACVs infection limited VACVs replication and dissemination (68). Another study from Wang and coworkers revealed IL-10 could also enhance the anti-tumor efficacy of oncolytic VACVs in pancreatic cancer by dampening antiviral immune response, and prolonging viral persistence in tumors (69).

Chemokines are secreted chemotactic cytokines that attract immune cells into tumor lesions and mediate anti-tumor immune effects. Bartlett's group demonstrated that oncolytic VACVs encoding CCL5 or CXCL11 elicited potent anti-tumor immunity and enhanced therapeutic efficacy by attracting activated immune cells such as T (Th1) and NK cells (70, 71). Generally, chemokine receptors (e.g., CXCR4) help activate the immune system, while the regulation imbalance of signaling pathway promote the tumor growth and metastasis. CXCR4 antagonist armed oncolytic VACVs showed the ability of TME modulation such as inhibiting intratumoral accumulation of immunosuppressive myeloid-derived suppressor cells (MDSCs) and regulatory T-cells (Tregs) (72).

In addition, oncolytic viruses can be modified to express co-stimulatory molecules of T-cell, thereby enhancing T-cell-mediated anti-tumor immunity. ONCOLYTIC VACVs expressing co-stimulatory molecules (e.g., CD40L, 4-1BBL, OX40L) boosted anti-tumor immune responses by activating antigen presentation cells and T lymphocytes, and reprogramming Treg (73–75). Bispecific T-cell engager (BiTE) further improved the anti-tumor activity of oncolytic VACVs by expressing tumor specific antigen in tumor cells and redirecting T-cells to the tumor (76).

Apart from the immune stimulators, some genes associated with other signal pathways are also found to activate anti-tumor immunity. For example, expression of DNA-dependent activator of IFN-regulatory factors (DAI, a cytosolic dsDNA sensor) by an oncolytic VACV boosted innate immune activation and enhanced anti-tumor immunity (77). Oncolytic VACVs expressing White-Spotted Charr Lectin not only induced type I IFN production to elicit anti-tumor activity, but also inhibited IFN-induced ISG production, helping oncolytic VACVs escape elimination (78).

Taken together, oncolytic VACVs encoding genes that induce anti-tumor immune responses have the potential to promote stronger anti-tumor effect.

4.2 Oncolytic VACVs and chimeric antigen receptor (CAR) T-cell therapy

CAR T-cell therapy is a kind of adoptive immunotherapy aimed at augmenting the anti-tumor immune responses of T-cell. In CAR T-cell therapy, one or more CARs are expressed for both antigen-binding and T-cell activating, bypassing the antigen processing and presentation (79). Currently, two products targeting CD19-CAR (Tisagenlecleucel and Axicabtagene Ciloleucel) have been approved to treat hematologic malignancies, and many other CARs are being developed for solid tumors (80). However, the application of CAR T-cells in solid tumors faces several challenges, such as the reduced persistence and expansion of CAR T-cells in immunosuppressive TME and the antigen loss/escape (81, 82).

It is now recognized that oncolytic VACVs can activate the anti-tumor immune response and remodel the "cold" TME to "hot". The enhanced type I IFN signature and the released DAMPs and cytokines in the TME after oncolysis of oncolytic VACVs can further support the priming, proliferation, clonal expansion, effector function and/or memory formation of $CD8^+$ T-cells, enabling the anti-tumor effect of CAR T-cells (83). For example, the combination of HER-2-CAR T-cell and oncolytic VACV with deletion of TK and VGF showed a significant enhancement of tumor killing in the murine breast cancer (D2F2) cell line (84).

To enhance the tumor targeting of CAR T-cells, Priceman's group designed an oncolytic VACV (OV19t) encoding a non-signaling, truncated human CD19 (CD19t) protein in which highly expressed CD19t on the surface of tumor cells worked as a specific tumor antigen to enable the tumor targeting of CD19-CAR T-cells (85). The combination therapy of OV19t/oncolytic viruses encoding the murine CD19t (OVm19t) protein and CD19-CAR T-cells showed durable and effective anti-tumor effects in MDA-MB-468/U251T bearing human tumor xenograft models and a MC38 bearing immunocompetent murine syngeneic tumor models. Another study from Aalipour et al. also demonstrated that the combination therapy of CD19 encoding oncolytic VACVs with CD19-CAR T-cells significantly reduced tumor growth and improved median survival achieved the similar results in an immunocompetent model of B16 melanoma (86). In addition, oncolytic VACVs encoding CXCL11 can further enhance the anti-tumor effect of mesothelin-CAR T-cell therapy *via* CXCL11-mediated recruitment of T-cells (87).

Taken together, oncolytic VACVs can boost the CAR T-cell therapy by the expression of tumor antigen or immunostimulatory factors and activation of anti-tumor immune responses themselves.

4.3 Oncolytic VACVs and immune checkpoint blockade therapy(ICB)

ICB therapy is an emerging immunotherapy aiming at blocking immunosuppressive tumor signals and restoring anti-tumor immune responses by targeting checkpoint receptors or ligands such as PD-1/PD-L1, CTLA-4, TIGIT, LAG-3, TIM3, among which PD-1/PD-L1 is the most common research object. To date, several

immune checkpoint inhibitors (ICIs) have been approved for tumor treatment, including PD-1 inhibitors (nivolumab, pembrolizumab, cemiplimab), PD-L1 inhibitors (avelumab, durvalumab, atezolizumab), and CTLA-4 inhibitors (ipilimumab). However, the efficiency of ICIs is restricted by the immunosuppressive TME and low expression of immune checkpoint molecules.

Oncolytic VACVs cannot only recruit immune cells into immunodeficient tumors and remodel the "cold" TME to "hot", but increase the expression of ICIs such as PD-L1, CTLA-4 or TIGIT inhibitors, sensitizing tumors to ICB therapy. The combination of CXCL11 encoded oncolytic VACV and PD-L1 blockade synergistically enhanced the therapeutic efficacy by increasing T-cell infiltration into the tumor and upregulating the expression of PD-L1 (88). The manganese superoxide dismutase (MnSOD) or immunostimulatory cytokines (such as IL-21, IL-15) expressing oncolytic VACVs could also improve PD-1/PD-L1 inhibition outcome by remodeling the suppressive tumor microenvironment (89–91). In addition, oncolytic VACVs have been engineered to directly express ICIs. For instance, oncolytic VACVs encoding a single chain variable fragment against TIGIT induced effective anti-tumor immunity and achieved a profound remodeling of the inhibitory tumor microenvironment from a "cold" state to a "hot" state synergizing with PD-1 or LAG-3 blockade (92). Oncolytic VACVs co-expressing ICIs and immune stimulatory cytokines exhibited synergistic anti-tumor ability. Oncolytic VACVs expressing PD-L1 inhibitors and GM-CSF activated tumor neoantigen-specific T-cell responses by synergistic action of VACV replication, GM-CSF stimulation, and PD-L1 inhibition on tumor cells and immune cells (93). Oncolytic VACVs expressing CTLA-4 inhibitors and GM-CSF elicited robust systemic $CD8^+$ T-cell-dependent anti-tumor immunity and long-lasting anti-tumor immunity by expanding peripheral effector $CD8^+$ T-cells and reducing Tregs and exhausted $CD8^+$ T-cells (94).

Despite potential synergistic effect of oncolytic VACVs and ICIs, it is worth noting that ICIs may stimulate OVs clearance by activating host immune response. Thus, the optimal administration timing should be considered. Nguyen and coworkers concluded that OV lead-in → anti-PD-1 or OV lead-in → concurrent therapy could be the treatment option for tumor regression and eradication according to PubMed literature search results (95).

5 Other oncolytic VACV-based combination therapies

5.1 Oncolytic VACVs and radiotherapy (RT)

Radiotherapy (RT) is a type of conventional treatment for cancer by inducing DNA damage and apoptosis. With continuous exploration, combination of RT and oncolytic VACVs are recognized as a potent treatment modality for cancer. Focally irradiation in tumor tissues can facilitate the replication of systemically delivered oncolytic VACVs (96). In turn, VACVs encoding the sodium iodide symporter (NIS) can transfer radioactive iodine into virus-infected cancer cells, contributing to enhanced anti-tumor effects of RT in pancreatic cancer and breast cancer (97). Inspired by the theory of peptide-receptor radiotherapy (PRRT), and the ability of selected replication and exogenous gene expression of oncolytic VACVs, McCart and coworkers found that VACVs encoding somatostatin receptor (SSTR) led to virus-directed tumor-specific accumulation of radiopeptides, enabling the imaging and improved treatment of intraperitoneal CRC tumors using ^{177}Lu-DOTATOC (98). In addition, studies have shown that radiation combined with oncolytic VACVs displayed considerably superior anti-tumor efficacy in several tumor models such as glioblastoma and pancreatic cancer (99, 100). For the synergistic mechanisms, a study from Chen et al. showed that RT combined with oncolytic VACVs could trigger tumor cell necroptosis and modify macrophages through the release of DAMPs, generating potent anti-tumor immunity and enhanced anti-tumor efficacy (101). Another study from Kyula et al. illustrated that synergistic cytotoxicity of radiation and oncolytic Lister strain VACV in V600D/E BRAF mutant melanoma depended on JNK and TNF-α signaling (102). Beside preclinical studies, phase II study about the combination of oncolytic VACV (GL-ONC1) with radiation and chemotherapy is warranted after phase I study in patients with locoregionally advanced head and neck carcinoma (103). All above studies proved the potential of the combination of RT and oncolytic VACVs.

5.2 Oncolytic VACVs and chemotherapy

Chemotherapy is the most widely used approach for tumor therapy due to the efficiency and broad spectrum. Chemotherapeutic drugs are cytotoxic agents that act primarily by inhibiting DNA replication or disrupting microtubule structures (104). Some of these cytotoxic agents have been extensively studied in combination with oncolytic VACVs and achieved many positive results. Yu and coworkers found that the anti-tumor efficacy of oncolytic VACV (GLV-1h68) was enhanced by cisplatin or gemcitabine with several potential mechanisms such as the changes in apoptosis, nucleotide pools and DNA repair pathways (105). As seen from the results of a phase II non-randomized clinical trial (NCT05281471) in patients with platinum-resistant or platinum-refractory ovarian cancer (PRROC), oncolytic VACV (Olvi-Vec) in combination with platinum-based chemotherapy demonstrated a favorable objective response rate (ORR) and progression-free survival (PFS) with a manageable safety profile in patients, and that patients are being recruited for phase III trial (NCT05281471) (106, 107). Cyclophosphamide (CPA) enhanced the replication of oncolytic VACVs by transiently suppressing the anti-viral immune response, while another study revealed that the enhanced anti-tumor efficacy of combining oncolytic VACV (GLV-1h68) with CPA was due to an effect on the vasculature rather than an immunosuppressive action of CPA (108, 109). In addition, Thorne's group for the first time revealed that oncolytic VACVs could further sensitize tumor cells to chemotherapy such as anti-

microtubule agent paclitaxel by inducing the release of several cytokines including type I IFN and HMGB1 (110). Some other chemotherapeutic drugs might boost OVT by synergistically activating ICD-mediated anti-tumor immunity such as doxorubicin (111).

Arming VACVs with a prodrug-activator gene is another approach to augment synergistic anti-tumor effects of OVT and chemotherapy with less systemic toxicity. Seubert and coworker demonstrated that GLV-1h68, an engineered oncolytic VACVs encoding β-galactosidase, exhibited enhanced oncolysis and tumor shrinkage with a β-galactosidase-activatable prodrug (112). GLV-1h94 encoding supercytosine deaminase (SCD) increased the cell specific-sensitivity of chemotherapeutic compound 5-fluorouracil (5-FU) by converting the prodrug 5-fluorocytosine (5-FC) to 5-FU only in the oncolytic VACV infected tumor cells (113). The addition of 5-FC made 85% of the cell lines highly sensitive to the combination treatment, none of which tested exhibited a "highly resistant" pattern. Nevertheless, the converted 5-FU reduced the replication of GLV-1h94 in tumor cells. The balance between cell line-specific susceptibility to GLV-1h94-induced oncolysis and 5-FU sensitivity should be taken into consideration.

5.3 Oncolytic VACVs and molecular targeted therapy

Different from chemotherapy, molecular targeted therapy, also known as "bio-missile", is aimed at precisely killing tumor cells by targeted selection of blockers for certain key molecules that are overexpressed in tumor cells but not in normal cells. Given the lower toxicity, molecular targeted therapy has become a promising approach for tumor treatment.

Studies have shown that molecular targeted therapy can amplify the anti-tumor efficacy of oncolytic VACVs through several mechanisms such as evading antiviral immunity and increasing anti-tumor immunity. Inhibition of MEK-ERK pathway enhanced oncolytic VACVs accumulation in doxorubicin-resistant ovarian cancer by abrogating cytosolic DNA sensing and viral defense (114). Transient inhibition of PI3Kδ or COX-2 enabled repeated administration of oncolytic VACVs *via* inhibiting the monocyte uptake of VACVs or decreasing the production of neutralizing antibodies against oncolytic VACVs, with no effect on virus replication, respectively, enhancing the anti-tumor efficacy of IV-delivered oncolytic VACVs (115, 116). Histone deacetylase inhibitors (HDIs) and STAT3 inhibitors were found to enhance the spread and replication of oncolytic VACVs selectively and effectively in tumor cells by dampening innate antiviral immune response (117). What's more, addition of a multitargeted receptor tyrosine kinase inhibitor sunitinib also amplified the anti-tumor effects of JX-594, by improving anti-tumor immune responses such as increasing $CD8^+$ T-cell recruitment and decreasing Tregs and MDSCs (118). It is worth mentioning that the administration sequence should be considered because some drugs influence viral replication. For example, if given simultaneously *in vitro*, sorafenib could inhibit JX-594 replication (119). Hence, in the phase III trial of JX-594, sorafenib was administrated after JX-594 to avoid its antiviral effect. Oncolytic VACVs encoding GLAF-1 exhibited significantly enhanced therapeutic efficacy by directing against VEGF (120).

In a word, the combination of molecular targeted therapy and oncolytic VACVs will be a promising new anticancer therapy. More available molecules for tumor targeting and corresponding drugs need to be developed to enhance OVT.

6 Clinical trials with oncolytic VACVs

As the exciting anti-tumor research results increase, some potential engineered Oncolytic VACVs are warranted for clinical trials. The current clinical trials about replication-competent oncolytic VACVs are found from the website of https://clinicaltrials.gov, and listed in the Table 3. TK gene deletion is the most common way to increase the selectivity of oncolytic VACVs and different therapeutic genes are inserted for better anti-tumor effect. Pexa-Vec and GL-ONC1 are the only two oncolytic VACVs that are already in phase III clinical trials, indicating the safety and efficacy in some cancer patients. Unfortunately, the phase III trial of Pexa-Vec for hepatocellular carcinoma was declared a failure because the interim analysis of the study showed that it was unlikely to prolong the overall survival of patients with Pexa-Vec treatment. Perhaps other combination therapies such as ICB with OVT will exert promising anti-tumor effects.

7 Delivery route of oncolytic VACVs

Up to now, all the approved OVs are intratumorally injected, which renders them ineffective for cancers that are difficult for *in situ* administration or have been already metastatic. Developing intravenous OVs is essential to broaden the clinical applications of OVs. The data about 97 independent clinical trials reporting OV studies from 2000 to 2020 showed that the most common route was intratumoral delivery used in 48 of the clinical trials (49.5%) followed by intravenous delivery used in 34 of the clinical trials (35%) (121). In the clinical trials, intravenous oncolytic VACVs exhibit good safety and potential anti-tumor activity. Different from adenoviruses, oncolytic VACVs can be administrated once *via* intravenous injection because there are no preexisting neutralizing antibodies in most of human bodies. However, after oncolytic VACV treatment, neutralizing antibodies generation occurred, limiting the repeated systematic delivery.

Recently, researchers are dedicated to developing diverse approaches to realize the efficient tumor treatment by repeated administration of intravenous oncolytic VACVs. Ferguson et al. found that transient inhibition of PI3Kδ by the PI3Kδ-selective inhibitor IC87114 or the clinically approved idelalisib (CAL-101) prior to intravenous delivery of a tumor-tropic VACV could inhibit

TABLE 3 Current clinical trials with replication-competent oncolytic VACVs.

Strain	Virus name	Deletion gene	Insertion gene	Cancer type	Combination therapy	Phase	Status	NCT number
Wyeth	Pexa-Vec/JX594	TK	GM-CSF	Colorectal cancer	Durvalumab +Tremelimumab (anti-PD-L1 + anti-CTL-4 antibody)	I/II	Active, not recruiting	NCT03206073
				Metastatic/advanced solid tumor	Ipilimumab (anti-CTL-4 antibody)	I	Completed	NCT02977156
				Colorectal carcinoma	Irinotecan (chemotherapy)	I/II	Completed	NCT01394939
				Metastatic melanoma	ZKAB001 (Anti-PD-L1 antibody)	I/II	Recruiting	NCT04849260
				Renal cell carcinoma	Cemiplimab (anti-PD-1 antibody)	I/II	Active, not recruiting	NCT03294083
				Peritoneal carcinomatosis of ovarian cancer origin		II	Withdrawn	NCT02017678
				Hepatic carcinoma		I	Completed	NCT00629759
				Hepatocellular carcinoma		II	Completed	NCT00554372
				Hepatocellular carcinoma		II	Completed	NCT01387555
				Hepatocellular carinoma		II	Completed	NCT01636284
				Hepatocellular carcinoma	Sorafenib (chemotherapy)	II	Completed	NCT01171651
				Hepatocellular carcinoma	Sorafenib (chemotherapy)	III	Completed	NCT02562755
				Breast cancer, Soft-tissue sarcoma	Cyclophosphamide + Avelumab (chemotherapy + anti-PD-L1 antibody))	I/II	Recruiting	NCT02630368
				Melanoma, Lung cancer, Renal cell carcinoma, Squamous cell carcinoma of the head and neck		I	Completed	NCT00625456
				Metastatic/refractory colorectal carcinoma	Recombinant Vaccinia GM-CSF	I	Completed	NCT01380600
				Metastatic/refractory colorectal carcinoma		I	Completed	NCT01469611
				Neuroblastoma, Rhabdomyosarcoma, Lymphoma, Wilm's Tumor, Ewing's sarcoma		I	Completed	NCT01169584
				Melanoma		I/II	Completed	NCT00429312
Lister	GL-ONC1/ Olvi-Vec	TK, F145L, HA	Luc-GFP, β-glucuronidase, β-galactosidase	Ovarian cancer, Peritoneal carcinomatosis, Fallopian tube cancer	Bevacizumab (anti-VEGF antibody)	I/II	Completed	NCT02759588

(Continued)

10.3389/fimmu.2023.1324744

TABLE 3 Continued

Strain	Virus name	Deletion gene	Insertion gene	Cancer type	Combination therapy	Phase	Status	NCT number
				Peritoneal carcinomatosis		I/II	Completed	NCT01443260
				Advanced solid tumors		I	Completed	NCT00794131
				Solid organ cancers		I	Terminated	NCT02714374
				Cancer of head and neck		I	Completed	NCT01584284
				Lung cancer		I	Active, not recruiting	NCT01766739
				Platinum-resistant ovarian cancer, Fallopian tube cancer, Primary peritoneal cancer, High-grade serous ovarian cancer, Endometrioid ovarian cancer, Ovarian clear cell carcinoma	carboplatin or cisplatin (chemotherapy), Bevacizumab (anti-VEGF antibody)	III	Recruiting	NCT05281471
	VV-GMCSF-Lact	TK, VGF	GM-CSF, Lact	Recurrent/refractory metastatic breast cancer		I	Recruiting	NCT05376527
	ASP9801	VGF, O1L	IL7, IL-12	Advanced/metastatic solid tumors	Pembrolizumab (anti-PD-1 antibody)	I	Active, not recruiting	NCT03954067
Copenhagen	TG6050	TK、RR	CTLA-4, IL-12	Non-small cell lung cancer		I	Recruiting	NCT05788926
	BT-001	TK、RR	CTLA-4, GM-CSF	Metastatic cancer, Soft tissue sarcoma, Merkel cell carcinoma, Melanoma, Triple negative breast cancer, Non-small cell lung cancer	Pembrolizumab (anti-PD-1 antibody)	I/II	Recruiting	NCT04725331
	TG6002/T601	TK、RR	FCU1	Glioblastoma	5-flucytosine (chemotherapy)	I	Unknown status	NCT03294486
				Advanced solid tumors	5-flucytosine (chemotherapy)	I/II	Unknown status	NCT04226066
WR	RGV004	TK	CD19BiFTE	Relapsed or refractory B-cell lymphoma		I	Recruiting	NCT04887025
	vvDD/JX-929	TK, VGF	CD/SMR	Melanoma, Breast cancer, Head and neck squamous cell cancer, Liver cancer, Colorectal cancer, Pancreatic adenocarcinoma		I	Completed	NCT00574977

10.3389/fimmu.2023.1324744

viral attachment to, but not internalization by, systemic macrophages through perturbation of signaling pathways involving RhoA/ROCK, AKT, and Rac, thus potentiating intravenous delivery of oncolytic VACVs to tumors (115). In addition, COX-2 inhibitor treatment can enhance the long-term protective anti-tumor effects generated by oncolytic VACVs *via* inhibiting the generation of neutralizing antibodies against oncolytic VACVs infection, enabling the repeated administration of oncolytic VACVs (116). Another study from McCart's group demonstrated that CP40 (a complement inhibitor) pretreatment elicited an average 10-fold increase in infectious titer in the blood early after the JX-594 infusion by preventing oncolytic VACVs neutralization, beneficial for repeated intravenous administration of oncolytic VACVs (122). The expression of human CD55 protein by oncolytic VACVs could also prolonged viral survival by protecting against complement-mediated lysis and evading neutralization by VACV-specific antibodies, improving intravenous efficacy (123). All above approaches are theoretically and clinically feasible *via* antiviral inhibitors treatment prior to intravenous injection of oncolytic VACVs.

Besides inhibition of antiviral immunity, direct oncolytic VACVs shielding is another alternative to enhance the anti-tumor efficacy of intravenous oncolytic VACVs. As a non-enveloped virus, adenovirus has been delivered by many kinds of cell carriers (e.g., mesenchymal stem cells, erythrocytes), nanomaterials (e.g., liposomes, exosomes) or polymers (e.g., poly(ethylene glycol) (PEG), polyamidoamine) to improves the pharmacokinetics (124, 125). Hill et al. found that polymer (Chol-PEG(10K)-NHS) coating reduced the binding of neutralizing anti-VACV antibodies and oncolytic VACVs and increased the circulation time *in vivo*, although VACV is an enveloped virus (126). These results showed that VACV coating may be an effective way to improve the systematic delivery of oncolytic VACVs. Many other kinds of methods for VACV coating need to be developed.

8 Conclusions and prospects

With the continuous improvement of gene function and anti-tumor mechanism of oncolytic VACVs, a variety of genetically functional VACVs have been constructed and shown safety and efficacy in preclinical and clinical studies. In addition, VACV-based OVT has been acknowledged as a potential adjuvant immunotherapy when combining with traditional anti-tumor therapies. However, challenges remain in the clinical application of engineered oncolytic VACVs. Firstly, failure of the phase III trial about JX-594 reminds us the importance of selecting proper combination therapy, and ensuring the administration sequence and timing. In addition, the two sides of oncolytic VACV-mediated antiviral immunity should be overall considered during the construction of VACV backbones and gene engineering of oncolytic VACVs. Another challenge is repeated intravenous injection of oncolytic VACVs with lower dosages. It is acknowledged that natural tumor tropism and none of initial neutralizing antibodies make VACVs potential for a single intravenous injection, while repeated administration can activate strong antiviral immunity to eliminate VACVs, indicating that higher dosage is needed to achieve anti-tumor effect. With the discovery of diverse signal pathways that are related to antiviral immunity, some drugs show the positive effect on the VACVs circulation *in vivo*, facilitating the progress of VACVs systematic administration. While much work remains, lots of studies have shown the enormous potential of VACV-based OVT. We believe it will not be long before oncolytic VACVs are approved for clinical anti-tumor therapy.

Author contributions

LX: Conceptualization, Writing – original draft. HS: Writing – review & editing. NL: Writing – review & editing. YX: Writing – review & editing, Supervision. PW: Supervision, Writing – review & editing, Conceptualization, Funding acquisition, Project administration.

Funding

The author(s) declare financial support was received for the research, authorship, and/or publication of this article. This research was supported by the Natural Science Foundation of Henan Province for Excellent Young Scholars (202300410360, PW), the National Natural Science Foundation of China (81872486, PW), and the National Key Research and Development Program of China (2019YFC1316101, PW).

Acknowledgments

The authors would like to thank Home for Researcher for preparation of Figures 1, 2 (www.home-for-researchers.com).

Conflict of interest

The authors declare that the research was conducted in the absence of any commercial or financial relationships that could be construed as a potential conflict of interest.

Publisher's note

References

1. Ma R, Li Z, Chiocca EA, Caligiuri MA, Yu J. The emerging field of oncolytic virus-based cancer immunotherapy. *Trends Cancer* (2023) 9(2):122–39. doi: 10.1016/j.trecan.2022.10.003

2. Tian Y, Xie D, Yang L. Engineering strategies to enhance oncolytic viruses in cancer immunotherapy. *Signal Transduction Targeted Ther* (2022) 7(1):117. doi: 10.1038/s41392-022-00951-x

3. Martuza RL, Malick A, Markert JM, Ruffner KL, Coen DM. Experimental therapy of human glioma by means of a genetically engineered virus mutant. *Science* (1991) 252 (5007):854–6. doi: 10.1126/science.1851332

4. Wang L, Chard Dunmall LS, Cheng Z, Wang Y. Remodeling the tumor microenvironment by oncolytic viruses: beyond oncolysis of tumor cells for cancer treatment. *J Immunother Cancer* (2022) 10(5):e004167. doi: 10.1136/jitc-2021-004167

5. Kaufman HL, Kohlhapp FJ, Zloza A. Oncolytic viruses: A new class of immunotherapy drugs. *Nat Rev Drug Discovery* (2015) 14(9):642–62. doi: 10.1038/nrd4663

6. Duan S, Wang S, Qiao L, Yu X, Wang N, Chen L, et al. Oncolytic virus-driven biotherapies from bench to bedside. *Small* (2023) 19(23):e2206948. doi: 10.1002/smll.202206948

7. Thèves C, Crubézy E, Biagini P. History of smallpox and its spread in human populations. *Microbiol Spectr* (2016) 4(4). doi: 10.1128/microbiolspec.PoH-0004-2014

8. Haddad D. Genetically engineered vaccinia viruses as agents for cancer treatment, imaging, and transgene delivery. *Front Oncol* (2017) 7:96. doi: 10.3389/fonc.2017.00096

9. Park SH, Breitbach CJ, Lee J, Park JO, Lim HY, Kang WK, et al. Phase 1b trial of biweekly intravenous pexa-vec (Jx-594), an oncolytic and immunotherapeutic vaccinia virus in colorectal cancer. *Mol Ther* (2015) 23(9):1532–40. doi: 10.1038/mt.2015.109

10. Kirn DH, Thorne SH. Targeted and armed oncolytic poxviruses: A novel multi-mechanistic therapeutic class for cancer. *Nat Rev Cancer* (2009) 9(1):64–71. doi: 10.1038/nrc2545

11. Guo ZS, Lu B, Guo Z, Giehl E, Feist M, Dai E, et al. Vaccinia virus-mediated cancer immunotherapy: cancer vaccines and oncolytics. *J Immunother Cancer* (2019) 7 (1):6. doi: 10.1186/s40425-018-0495-7

12. Blasco R, Moss B. Role of cell-associated enveloped vaccinia virus in cell-to-cell spread. *J Virol* (1992) 66(7):4170–9. doi: 10.1128/jvi.66.7.4170-4179.1992

13. Payne LG. Significance of extracellular enveloped virus in the *in vitro* and *in vivo* dissemination of vaccinia. *J Gen Virol* (1980) 50(1):89–100. doi: 10.1099/0022-1317-50-1-89

14. Greseth MD, Czarnecki MW, Bluma MS, Traktman P, Sandri-Goldin RM. Isolation and characterization of Vδi3 confirm that vaccinia virus ssb plays an essential role in viral replication. *J Virol* (2018) 92(2):e01719–17. doi: 10.1128/jvi.01719-17

15. Smith GL, Moss B. Infectious poxvirus vectors have capacity for at least 25 000 base pairs of foreign DNA. *Gene* (1983) 25(1):21–8. doi: 10.1016/0378-1119(83)90163-4

16. Yu YA, Shabahang S, Timiryasova TM, Zhang Q, Beltz R, Gentschev I, et al. Visualization of tumors and metastases in live animals with bacteria and vaccinia virus encoding light-emitting proteins. *Nat Biotechnol* (2004) 22(3):313–20. doi: 10.1038/nbt937

17. Hiley CT, Yuan M, Lemoine NR, Wang Y. Lister strain vaccinia virus, a potential therapeutic vector targeting hypoxic tumours. *Gene Ther* (2009) 17(2):281–7. doi: 10.1038/gt.2009.132

18. Moss B. Poxvirus cell entry: how many proteins does it take? *Viruses* (2012) 4 (5):688–707. doi: 10.3390/v4050688

19. Mercer J, Knébel S, Schmidt FI, Crouse J, Burkard C, Helenius A. Vaccinia virus strains use distinct forms of macropinocytosis for host-cell entry. *Proc Natl Acad Sci* (2010) 107(20):9346–51. doi: 10.1073/pnas.1004618107

20. Greseth MD, Traktman P. The life cycle of the vaccinia virus genome. *Annu Rev Virol* (2022) 9(1):239–59. doi: 10.1146/annurev-virology-091919-104752

21. de Queiroz NMGP, Xia T, Konno H, Barber GN. Ovarian cancer cells commonly exhibit defective sting signaling which affects sensitivity to viral oncolysis. *Mol Cancer Res* (2019) 17(4):974–86. doi: 10.1158/1541-7786.Mcr-18-0504

22. Puhlmann M, Brown CK, Gnant M, Huang J, Libutti SK, Alexander HR, et al. Vaccinia as a vector for tumor-directed gene therapy: biodistribution of a thymidine kinase-deleted mutant. *Cancer Gene Ther* (2000) 7(1):66–73. doi: 10.1038/sj.cgt.7700075

23. Nasri D, Manwar R, Kaushik A, Er EE, Avanaki K. Photoacoustic imaging for investigating tumor hypoxia: A strategic assessment. *Theranostics* (2023) 13(10):3346–67. doi: 10.7150/thno.84253

24. Liu T-C, Hwang T, Park B-H, Bell J, Kirn DH, Hu Y-C. The targeted oncolytic poxvirus jx-594 demonstrates antitumoral, antivascular, and anti-hbv activities in patients with hepatocellular carcinoma. *Mol Ther* (2008) 16(9):1637–42. doi: 10.1038/sj.mt.6300236

25. Breitbach CJ, Arulanandam R, De Silva N, Thorne SH, Patt R, Daneshmand M, et al. Oncolytic vaccinia virus disrupts tumor-associated vasculature in humans. *Cancer Res* (2013) 73(4):1265–75. doi: 10.1158/0008-5472.Can-12-2687

26. Arulanandam R, Batenchuk C, Angarita Fernando A, Ottolino-Perry K, Cousineau S, Mottashed A, et al. Vegf-mediated induction of prd1-bf1/blimp1 expression sensitizes tumor vasculature to oncolytic virus infection. *Cancer Cell* (2015) 28(2):210–24. doi: 10.1016/j.ccell.2015.06.009

27. Santry LA, van Vloten JP, Knapp JP, Matuszewska K, McAusland TM, Minott JA, et al. Tumour vasculature: friend or foe of oncolytic viruses? *Cytokine Growth Factor Rev* (2020) 56:69–82. doi: 10.1016/j.cytogfr.2020.07.007

28. Gujar S, Pol JG, Kim Y, Lee PW, Kroemer G. Antitumor benefits of antiviral immunity: an underappreciated aspect of oncolytic virotherapies. *Trends Immunol* (2018) 39(3):209–21. doi: 10.1016/j.it.2017.11.006

29. Ma J, Ramachandran M, Jin C, Quijano-Rubio C, Martikainen M, Yu D, et al. Characterization of virus-mediated immunogenic cancer cell death and the consequences for oncolytic virus-based immunotherapy of cancer. *Cell Death Dis* (2020) 11(1):48. doi: 10.1038/s41419-020-2236-3

30. Yaghchi CA, Zhang Z, Alusi G, Lemoine NR, Wang Y. Vaccinia virus, a promising new therapeutic agent for pancreatic cancer. *Immunotherapy* (2015) 7 (12):1249–58. doi: 10.2217/imt.15.90

31. Samson A, West EJ, Carmichael J, Scott KJ, Turnbull S, Kuszlewicz B, et al. Neoadjuvant intravenous oncolytic vaccinia virus therapy promotes anticancer immunity in patients. *Cancer Immunol Res* (2022) 10(6):745–56. doi: 10.1158/2326-6066.Cir-21-0171

32. Marelli G, Howells A, Lemoine NR, Wang Y. Oncolytic viral therapy and the immune system: A double-edged sword against cancer. *Front Immunol* (2018) 9:866. doi: 10.3389/fimmu.2018.00866

33. Berkeley RA, Steele LP, Mulder AA, van den Wollenberg DJM, Kottke TJ, Thompson J, et al. Antibody-neutralized reovirus is effective in oncolytic virotherapy. *Cancer Immunol Res* (2018) 6(10):1161–73. doi: 10.1158/2326-6066.Cir-18-0309

34. Yuan M, Zhang W, Wang J, Al Yaghchi C, Ahmed J, Chard L, et al. Efficiently editing the vaccinia virus genome by using the crispr-cas9 system. *J Virol* (2015) 89 (9):5176–9. doi: 10.1128/jvi.00339-15

35. Aye Y, Li M, Long MJC, Weiss RS. Ribonucleotide reductase and cancer: biological mechanisms and targeted therapies. *Oncogene* (2015) 34(16):2011–21. doi: 10.1038/onc.2014.155

36. Vliegen I, Yang G, Hruby D, Jordan R, Neyts J. Deletion of the vaccinia virus F13l gene results in a highly attenuated virus that mounts a protective immune response against subsequent vaccinia virus challenge. *Antiviral Res* (2012) 93(1):160–6. doi: 10.1016/j.antiviral.2011.11.010

37. Albarnaz JD, Ren H, Torres AA, Shmeleva EV, Melo CA, Bannister AJ, et al. Molecular mimicry of nf-κb by vaccinia virus protein enables selective inhibition of antiviral responses. *Nat Microbiol* (2022) 7(1):154–68. doi: 10.1038/s41564-021-01004-9

38. Chen RAJ, Jacobs N, Smith GL. Vaccinia virus strain western reserve protein B14 is an intracellular virulence factor. *J Gen Virol* (2006) 87(6):1451–8. doi: 10.1099/vir.0.81736-0

39. Buller ML, Chen RAJ, Ryzhakov G, Cooray S, Randow F, Smith GL. Inhibition of Iκb kinase by vaccinia virus virulence factor B14. *PloS Pathog* (2008) 4(2):e22. doi: 10.1371/journal.ppat.0040022

40. Neidel S, Ren H, Torres AA, Smith GL. Nf-κb activation is a turn on for vaccinia virus phosphoprotein A49 to turn off nf-κb activation. *Proc Natl Acad Sci* (2019) 116 (12):5699–704. doi: 10.1073/pnas.1813504116

41. Ferguson BJ, Benfield CTO, Ren H, Lee VH, Frazer GL, Strnadova P, et al. Vaccinia virus protein N2 is a nuclear irf3 inhibitor that promotes virulence. *J Gen Virol* (2013) 94(9):2070–81. doi: 10.1099/vir.0.054114-0

42. Benfield CTO, Ren H, Lucas SJ, Bahsoun B, Smith GL. Vaccinia virus protein K7 is a virulence factor that alters the acute immune response to infection. *J Gen Virol* (2013) 94(7):1647–57. doi: 10.1099/vir.0.052670-0

43. Kirn DH, Wang Y, Boeuf FL, Bell J, Thorne SH. Targeting of interferon-beta to produce a specific, multi-mechanistic oncolytic vaccinia virus. *PloS Med* (2007) 4(12): e353. doi: 10.1371/journal

44. Isaacs SN, Kotwal GJ, Moss B. Vaccinia virus complement-control protein prevents antibody-dependent complement-enhanced neutralization of infectivity and contributes to virulence. *Proc Nati Acad Sci* (1992) 89:628–32. doi: 10.1073/pnas.89.2.628

45. Wagenaar TR, Moss B. Expression of the A56 and K2 proteins is sufficient to inhibit vaccinia virus entry and cell fusion. *J Virol* (2009) 83(4):1546–54. doi: 10.1128/jvi.01684-08

46. DeHaven BC, Girgis NM, Xiao Y, Hudson PN, Olson VA, Damon IK, et al. Poxvirus complement control proteins are expressed on the cell surface through an intermolecular disulfide bridge with the viral A56 protein. *J Virol* (2010) 84(21):11245–54. doi: 10.1128/jvi.00372-10

47. DeHaven BC, Gupta K, Isaacs SN. The vaccinia virus A56 protein: A multifunctional transmembrane glycoprotein that anchors two secreted viral proteins. *J Gen Virol* (2011) 92:1971–80. doi: 10.1099/vir.0.030460-0

48. Delaunay T, Nader J, Grard M, Farine I, Hedwig V, Foloppe J, et al. High oncolytic activity of a double-deleted vaccinia virus copenhagen strain against

Malignant pleural mesothelioma. *Mol Ther–Oncolytics* (2020) 18:573–8. doi: 10.1016/j.omto.2020.08.011

49. Beerli C, Yakimovich A, Kilcher S, Reynoso GV, Fläschner G, Müller DJ, et al. Vaccinia virus hijacks egfr signalling to enhance virus spread through rapid and directed infected cell motility. *Nat Microbiol* (2019) 4(2):216–25. doi: 10.1038/s41564-018-0288-2

50. Lai ACK, Pogo BGT. Attenuated deletion mutants of vaccinia virus lacking the vaccinia growth factor are defective in replication *in vivo*. *Microb Pathog* (1989) 6 (3):219–26. doi: 10.1016/0882-4010(89)90071-5

51. McCart JA, Ward JM, Lee J, Hu Y, Alexander HR, Libutti SK, et al. Systemic cancer therapy with a tumor-selective vaccinia virus mutant lacking thymidine kinase and vaccinia growth factor genes. *Cancer Res* (2001) 61(24):8751–7.

52. Yum S, Li M, Fang Y, Chen ZJ. Tbk1 recruitment to sting activates both irf3 and nf-κb that mediate immune defense against tumors and viral infections. *Proc Natl Acad Sci* (2021) 118(14):e2100225118. doi: 10.1073/pnas.2100225118

53. Riederer S, del Canizo A, Navas J, Peter MG, Link EK, Sutter G, et al. Improving poxvirus-mediated antitumor immune responses by deleting viral cgamp-specific nuclease. *Cancer Gene Ther* (2023) 30(7):1029–39. doi: 10.1038/s41417-023-00610-5

54. Yang N, Wang Y, Dai P, Li T, Zierhut C, Tan A, et al. Vaccinia E5 is a major inhibitor of the DNA sensor cgas. *Nat Commun* (2023) 14(1):2898. doi: 10.1038/s41467-023-38514-5

55. Barry M, Maluquer de Motes C, Cooray S, Ren H, Almeida GMF, McGourty K, et al. Inhibition of apoptosis and nf-κb activation by vaccinia protein N1 occur via distinct binding surfaces and make different contributions to virulence. *PloS Pathog* (2011) 7(12):e1002430. doi: 10.1371/journal.ppat.1002430

56. Jacobs N, Bartlett NW, Clark RH, Smith GL. Vaccinia virus lacking the bcl-2-like protein N1 induces a stronger natural killer cell response to infection. *J Gen Virol* (2008) 89(11):2877–81. doi: 10.1099/vir.0.2008/004119-0

57. Ahmed J, Chard LS, Yuan M, Wang J, Howells A, Li Y, et al. A new oncolytic vaccinia virus augments antitumor immune responses to prevent tumor recurrence and metastasis after surgery. *J Immunother Cancer* (2020) 8(1):e000415. doi: 10.1136/jitc-2019-000415

58. Verardi PH, Jones LA, Aziz FH, Ahmad S, Yilma TD. Vaccinia virus vectors with an inactivated gamma interferon receptor homolog gene (B8r) are attenuated *in vivo* without a concomitant reduction in immunogenicity. *J Virol* (2001) 75(1):11–8. doi: 10.1128/jvi.75.1.11-18.2001

59. Papatriantafyllou M. Gm-csf in focus. *Nat Rev Immunol* (2011) 11(6):370–1. doi: 10.1038/nri2996

60. Wang N, Wang J, Zhang Z, Cao H, Yan W, Chu Y, et al. A novel vaccinia virus enhances anti-tumor efficacy and promotes a long-term anti-tumor response in a murine model of colorectal cancer. *Mol Ther–Oncolytics* (2021) 20:71–81. doi: 10.1016/j.omto.2020.11.002

61. Chen T, Ding X, Liao Q, Gao N, Chen Y, Zhao C, et al. Il-21 arming potentiates the anti-tumor activity of an oncolytic vaccinia virus in monotherapy and combination therapy. *J Immunother Cancer* (2021) 9(1):e001647. doi: 10.1136/jitc-2020-001647

62. Chen L, Chen H, Ye J, Ge Y, Wang H, Dai E, et al. Intratumoral expression of interleukin 23 variants using oncolytic vaccinia virus elicit potent antitumor effects on multiple tumor models via tumor microenvironment modulation. *Theranostics* (2021) 11(14):6668–81. doi: 10.7150/thno.56494

63. Shakiba Y, Vorobyev PO, Yusubalieva GM, Kochetkov DV, Zajtseva KV, Valikhov MP, et al. Oncolytic therapy with recombinant vaccinia viruses targeting the interleukin-15 pathway elicits a synergistic response. *Mol Ther–Oncolytics* (2023) 29:158–68. doi: 10.1016/j.omto.2023.05.002

64. Ge Y, Wang H, Ren J, Liu W, Chen L, Chen H, et al. Oncolytic vaccinia virus delivering tethered il-12 enhances antitumor effects with improved safety. *J Immunother Cancer* (2020) 8(1):e000710. doi: 10.1136/jitc-2020-000710

65. Pearl TM, Markert JM, Cassady KA, Ghonime MG. Oncolytic virus-based cytokine expression to improve immune activity in brain and solid tumors. *Mol Ther–Oncolytics* (2019) 13:14–21. doi: 10.1016/j.omto.2019.03.001

66. DePeaux K, Rivadeneira DB, Lontos K, Dean VG, Gunn WG, Watson MJ, et al. An oncolytic virus–delivered tgfβ Inhibitor overcomes the immunosuppressive tumor microenvironment. *J Exp Med* (2023) 220(10):e20230053. doi: 10.1084/jem.20230053

67. Ouyang W, O'Garra A. Il-10 family cytokines il-10 and il-22: from basic science to clinical translation. *Immunity* (2019) 50(4):871–91. doi: 10.1016/j.immuni.2019.03.020

68. Sigal LJ, Cush SS, Reynoso GV, Kamenyeva O, Bennink JR, Yewdell JW, et al. Locally produced il-10 limits cutaneous vaccinia virus spread. *PloS Pathog* (2016) 12(3): e1005493. doi: 10.1371/journal.ppat.1005493

69. Chard LS, Maniati E, Wang P, Zhang Z, Gao D, Wang J, et al. A vaccinia virus armed with interleukin-10 is a promising therapeutic agent for treatment of murine pancreatic cancer. *Clin Cancer Res* (2015) 21(2):405–16. doi: 10.1158/1078-0432.Ccr-14-0464

70. Li J, O'Malley M, Urban J, Sampath P, Guo ZS, Kalinski P, et al. Chemokine expression from oncolytic vaccinia virus enhances vaccine therapies of cancer. *Mol Ther* (2011) 19(4):650–7. doi: 10.1038/mt.2010.312

71. Liu Z, Ravindranathan R, Li J, Kalinski P, Guo ZS, Bartlett DL. Cxcl11-armed oncolytic poxvirus elicits potent antitumor immunity and shows enhanced therapeutic efficacy. *OncoImmunology* (2015) 5(3):e1091554. doi: 10.1080/2162402x.2015.1091554

72. Komorowski M, Tisonczyk J, Kolakowska A, Drozdz R, Kozbor D. Modulation of the tumor microenvironment by cxcr4 antagonist-armed viral oncotherapy enhances the antitumor efficacy of dendritic cell vaccines against neuroblastoma in syngeneic mice. *Viruses* (2018) 10(9):455. doi: 10.3390/v10090455

73. Parviainen S, Ahonen M, Diaconu I, Hirvinen M, Karttunen Å, Vähä-Koskela M, et al. Cd40 ligand and tdtomato-armed vaccinia virus for induction of antitumor immune response and tumor imaging. *Gene Ther* (2013) 21(2):195–204. doi: 10.1038/gt.2013.73

74. Hinterberger M, Giessel R, Fiore G, Graebnitz F, Bathke B, Wennier S, et al. Intratumoral virotherapy with 4-1bbl armed modified vaccinia ankara eradicates solid tumors and promotes protective immune memory. *J Immunother Cancer* (2021) 9(2): e001586. doi: 10.1136/jitc-2020-001586

75. Yang N, Wang Y, Liu S, Tariq SB, Luna JM, Mazo G, et al. Ox40l-expressing recombinant modified vaccinia virus ankara induces potent antitumor immunity via reprogramming tregs. *J Exp Med* (2023) 220(8):e20221166. doi: 10.1084/jem.20221166

76. Yu F, Wang X, Guo ZS, Bartlett DL, Gottschalk SM, Song X-T. T-cell engager-armed oncolytic vaccinia virus significantly enhances antitumor therapy. *Mol Ther* (2014) 22(1):102–11. doi: 10.1038/mt.2013.240

77. Hirvinen M, Capasso C, Guse K, Garofalo M, Vitale A, Ahonen M, et al. Expression of dai by an oncolytic vaccinia virus boosts the immunogenicity of the virus and enhances antitumor immunity. *Mol Ther–Oncolytics* (2016) 3:16002. doi: 10.1038/mto.2016.2

78. Wang X, Zhou N, Liu T, Jia X, Ye T, Chen K, et al. Oncolytic vaccinia virus expressing white-spotted charr lectin regulates antiviral response in tumor cells and inhibits tumor growth *in vitro* and *in vivo*. *Mar Drugs* (2021) 19(6):292. doi: 10.3390/md19060292

79. Sadelain M, Brentjens R, Rivière I. The basic principles of chimeric antigen receptor design. *Cancer Discovery* (2013) 3(4):388–98. doi: 10.1158/2159-8290.Cd-12-0548

80. Choi T, Kang Y. Chimeric antigen receptor (Car) T-cell therapy for multiple myeloma. *Pharmacol Ther* (2022) 232:108007. doi: 10.1016/j.pharmthera.2021.108007

81. Brown CE, Mackall CL. Car T cell therapy: inroads to response and resistance. *Nat Rev Immunol* (2019) 19(2):73–4. doi: 10.1038/s41577-018-0119-y

82. Liu L, Qu Y, Cheng L, Yoon CW, He P, Monther A, et al. Engineering chimeric antigen receptor T cells for solid tumour therapy. *Clin Transl Med* (2022) 12(12):e1141. doi: 10.1002/ctm2.1141

83. Miyakoda M, Honma K, Kimura D, Akbari M, Kimura K, Matsuyama T, et al. Differential requirements for irf4 in the clonal expansion and homeostatic proliferation of naive and memory murine cd8+ T cells. *Eur J Immunol* (2018) 48(8):1319–28. doi: 10.1002/eji.201747120

84. VanSeggelen H, Tantalo DGM, Afsahi A, Hammill JA, Bramson JL. Chimeric antigen receptor–engineered T cells as oncolytic virus carriers. *Mol Ther–Oncolytics* (2015) 2:15014. doi: 10.1038/mto.2015.14

85. Park AK, Fong Y, Kim S-I, Yang J, Murad JP, Lu J, et al. Effective combination immunotherapy using oncolytic viruses to deliver car targets to solid tumors. *Sci Transl Med* (2020) 12(559):eaaz1863. doi: 10.1126/scitranslmed.aaz1863

86. Aalipour A, Le Boeuf F, Tang M, Murty S, Simonetta F, Lozano AX, et al. Viral delivery of car targets to solid tumors enables effective cell therapy. *Mol Ther–Oncolytics* (2020) 17:232–40. doi: 10.1016/j.omto.2020.03.018

87. Moon EK, Wang L-CS, Bekdache K, Lynn RC, Lo A, Thorne SH, et al. Intra-tumoral delivery of cxcl11 via a vaccinia virus, but not by modified T cells, enhances the efficacy of adoptive T cell therapy and vaccines. *OncoImmunology* (2018) 7(3): e1395997. doi: 10.1080/2162402x.2017.1395997

88. Liu Z, Ravindranathan R, Kalinski P, Guo ZS, Bartlett DL. Rational combination of oncolytic vaccinia virus and pd-L1 blockade works synergistically to enhance therapeutic efficacy. *Nat Commun* (2017) 8(1):14754. doi: 10.1038/ncomms14754

89. Lou J, Dong J, Xu R, Zeng H, Fang L, Wu Y, et al. Remodeling of the tumor microenvironment using an engineered oncolytic vaccinia virus improves pd-L1 inhibition outcomes. *Biosci Rep* (2021) 41(6):BSR20204186. doi: 10.1042/bsr20204186

90. Sun Y, Zhang Z, Zhang C, Zhang N, Wang P, Chu Y, et al. An effective therapeutic regime for treatment of glioma using oncolytic vaccinia virus expressing il-21 in combination with immune checkpoint inhibition. *Mol Ther–Oncolytics* (2022) 26:105–19. doi: 10.1016/j.omto.2022.05.008

91. Kowalsky SJ, Liu Z, Feist M, Berkey SE, Ma C, Ravindranathan R, et al. Superagonist il-15-armed oncolytic virus elicits potent antitumor immunity and therapy that are enhanced with pd-1 blockade. *Mol Ther* (2018) 26(10):2476–86. doi: 10.1016/j.ymthe.2018.07.013

92. Zuo S, Wei M, Xu T, Kong L, He B, Wang S, et al. An engineered oncolytic vaccinia virus encoding a single-chain variable fragment against tigit induces effective antitumor immunity and synergizes with pd-1 or lag-3 blockade. *J Immunother Cancer* (2021) 9(12):e002843. doi: 10.1136/jitc-2021-002843

93. Wang G, Kang X, Chen KS, Jehng T, Jones L, Chen J, et al. An engineered oncolytic virus expressing pd-L1 inhibitors activates tumor neoantigen-specific T cell responses. *Nat Commun* (2020) 11(1):1395. doi: 10.1038/s41467-020-15229-5

94. Semmrich M, Marchand J-B, Fend L, Rehn M, Remy C, Holmkvist P, et al. Vectorized treg-depleting αctla-4 elicits antigen cross-presentation and cd8+ T cell immunity to reject 'Cold' Tumors. *J Immunother Cancer* (2022) 10(1):e003488. doi: 10.1136/jitc-2021-003488

95. Nguyen H-M, Bommareddy PK, Silk AW, Saha D. Optimal timing of pd-1 blockade in combination with oncolytic virus therapy. *Semin Cancer Biol* (2022) 86:971–80. doi: 10.1016/j.semcancer.2021.05.019

96. Advani SJ, Buckel L, Chen NG, Scanderbeg DJ, Geissinger U, Zhang Q, et al. Preferential replication of systemically delivered oncolytic vaccinia virus in focally irradiated glioma xenografts. *Clin Cancer Res* (2012) 18(9):2579–90. doi: 10.1158/1078-0432.Ccr-11-2394

97. Mansfield DC, Kyula JN, Rosenfelder N, Chao-Chu J, Kramer-Marek G, Khan AA, et al. Oncolytic vaccinia virus as a vector for therapeutic sodium iodide symporter gene therapy in prostate cancer. *Gene Ther* (2016) 23(4):357–68. doi: 10.1038/gt.2016.5

98. Ottolino-Perry K, Mealiea D, Sellers C, Acuna SA, Angarita FA, Okamoto L, et al. Vaccinia virus and peptide-receptor radiotherapy synergize to improve treatment of peritoneal carcinomatosis. *Mol Ther–Oncolytics* (2023) 29:44–58. doi: 10.1016/j.omto.2023.04.001

99. Storozynsky QT, Agopsowicz KC, Noyce RS, Bukhari AB, Han X, Snyder N, et al. Radiation combined with oncolytic vaccinia virus provides pronounced antitumor efficacy and induces immune protection in an aggressive glioblastoma model. *Cancer Lett* (2023) 562:216169. doi: 10.1016/j.canlet.2023.216169

100. Dai MH, Liu SL, Chen NG, Zhang TP, You L, Q. Zhang F, et al. Oncolytic vaccinia virus in combination with radiation shows synergistic antitumor efficacy in pancreatic cancer. *Cancer Lett* (2014) 344(2):282–90. doi: 10.1016/j.canlet.2013.11.007

101. Chen W-Y, Chen Y-L, Lin H-W, Chang C-F, Huang B-S, Sun W-Z, et al. Stereotactic body radiation combined with oncolytic vaccinia virus induces potent anti-tumor effect by triggering tumor cell necroptosis and damps. *Cancer Lett* (2021) 523:149–61. doi: 10.1016/j.canlet.2021.09.040

102. Kyula JN, Khan AA, Mansfield D, Karapanagiotou EM, McLaughlin M, Roulstone V, et al. Synergistic cytotoxicity of radiation and oncolytic lister strain vaccinia in V600d/ebraf mutant melanoma depends on jnk and tnf-α Signaling. *Oncogene* (2014) 33(13):1700–12. doi: 10.1038/onc.2013.112

103. Mell LK, Brumund KT, Daniels GA, Advani SJ, Zakeri K, Wright ME, et al. Phase I trial of intravenous oncolytic vaccinia virus (Gl-onc1) with cisplatin and radiotherapy in patients with locoregionally advanced head and neck carcinoma. *Clin Cancer Res* (2017) 23(19):5696–702. doi: 10.1158/1078-0432.Ccr-16-3232

104. Wennier ST, Liu J, McFadden G. Bugs and drugs: oncolytic virotherapy in combination with chemotherapy. *Curr Pharm Biotechnol* (2012) 13(9):1817–33. doi: 10.2174/138920112800958850

105. Yu YA, Galanis C, Woo Y, Chen N, Zhang Q, Fong Y, et al. Regression of human pancreatic tumor xenografts in mice after a single systemic injection of recombinant vaccinia virus glv-1h68. *Mol Cancer Ther* (2009) 8(1):141–51. doi: 10.1158/1535-7163.Mct-08-0533

106. Holloway RW, Thaker P, Mendivil AA, Ahmad S, Al-Niaimi AN, Barter J, et al. A phase iii, multicenter, randomized study of olvimulogene nanivacirepvec followed by platinum-doublet chemotherapy and bevacizumab compared with platinum-doublet chemotherapy and bevacizumab in women with platinum-resistant/refractory ovarian cancer. *Intl J Gynecol Cancer* (2023) 33(9):1458–63. doi: 10.1136/ijgc-2023-004812

107. Holloway RW, Mendivil AA, Kendrick JE, Abaid LN, Brown JV, LeBlanc J, et al. Clinical activity of olvimulogene nanivacirepvec–primed immunochemotherapy in heavily pretreated patients with platinum-resistant or platinum-refractory ovarian cancer: the nonrandomized phase 2 viro-15 clinical trial. *JAMA Oncol* (2023) 9 (7):903–8. doi: 10.1001/jamaoncol.2023.1007

108. Lun XQ, Jang J-H, Tang N, Deng H, Head R, Bell JC, et al. Efficacy of systemically administered oncolytic vaccinia virotherapy for Malignant gliomas is enhanced by combination therapy with rapamycin or cyclophosphamide. *Clin Cancer Res* (2009) 15(8):2777–88. doi: 10.1158/1078-0432.Ccr-08-2342

109. Hofmann E, Weibel S, Szalay AA. Combination treatment with oncolytic vaccinia virus and cyclophosphamide results in synergistic antitumor effects in human lung adenocarcinoma bearing mice. *J Transl Med* (2014) 12:197. doi: 10.1186/1479-5876-12-197

110. Huang B, Sikorski R, Kirn DH, Thorne SH. Synergistic anti-tumor effects between oncolytic vaccinia virus and paclitaxel are mediated by the ifn response and hmgb1. *Gene Ther* (2010) 18(2):164–72. doi: 10.1038/gt.2010.121

111. Zhao X, Yang K, Zhao R, Ji T, Wang X, Yang X, et al. Inducing enhanced immunogenic cell death with nanocarrier-based drug delivery systems for pancreatic cancer therapy. *Biomaterials* (2016) 102:187–97. doi: 10.1016/j.biomaterials.2016.06.032

112. Seubert CM, Stritzker J, Hess M, Donat U, Sturm JB, Chen N, et al. Enhanced tumor therapy using vaccinia virus strain glv-1h68 in combination with a β-galactosidase-activatable prodrug seco-analog of duocarmycin sa. *Cancer Gene Ther* (2010) 18(1):42–52. doi: 10.1038/cgt.2010.49

113. Berchtold S, Beil J, Raff C, Smirnow I, Schell M, D'Alvise J, et al. Assessing and overcoming resistance phenomena against a genetically modified vaccinia virus in selected cancer cell lines. *Int J Mol Sci* (2020) 21(20):7618. doi: 10.3390/ijms21207618

114. Lee S, Yang W, Kim DK, Kim H, Shin M, Choi KU, et al. Inhibition of mek-erk pathway enhances oncolytic vaccinia virus replication in doxorubicin-resistant ovarian cancer. *Mol Ther–Oncolytics* (2022) 25:211–24. doi: 10.1016/j.omto.2022.04.006

115. Ferguson MS, Chard Dunmall LS, Gangeswaran R, Marelli G, Tysome JR, Burns E, et al. Transient inhibition of pi3kδ Enhances the therapeutic effect of intravenous delivery of oncolytic vaccinia virus. *Mol Ther* (2020) 28(5):1263–75. doi: 10.1016/j.ymthe.2020.02.017

116. Chang C-L, Ma B, Pang X, Wu TC, Hung C-F. Treatment with cyclooxygenase-2 inhibitors enables repeated administration of vaccinia virus for control of ovarian cancer. *Mol Ther* (2009) 17(8):1365–72. doi: 10.1038/mt.2009.118

117. Jin D-Y, MacTavish H, Diallo J-S, Huang B, Stanford M, Le Boeuf F, et al. Enhancement of vaccinia virus based oncolysis with histone deacetylase inhibitors. *PloS One* (2010) 5(12):e14462. doi: 10.1371/journal.pone.0014462

118. Kim M, Nitschké M, Sennino B, Murer P, Schriver BJ, Bell A, et al. Amplification of oncolytic vaccinia virus widespread tumor cell killing by sunitinib through multiple mechanisms. *Cancer Res* (2018) 78(4):922–37. doi: 10.1158/0008-5472.Can-15-3308

119. Heo J, Breitbach CJ, Moon A, Kim CW, Patt R, Kim MK, et al. Sequential therapy with jx-594, a targeted oncolytic poxvirus, followed by sorafenib in hepatocellular carcinoma: preclinical and clinical demonstration of combination efficacy. *Mol Ther* (2011) 19(6):1170–9. doi: 10.1038/mt.2011.39

120. Frentzen A, Yu YA, Chen N, Zhang Q, Weibel S, Raab V, et al. Anti-vegf single-chain antibody glaf-1 encoded by oncolytic vaccinia virus significantly enhances antitumor therapy. *Proc Natl Acad Sci* (2009) 106(31):12915–20. doi: 10.1073/pnas.0900660106

121. Macedo N, Miller DM, Haq R, Kaufman HL. Clinical landscape of oncolytic virus research in 2020. *J Immunother Cancer* (2020) 8:e001486. doi: 10.1136/jitc-2020-001486

122. Evgin L, Acuna SA, de Souza CT, Marguerie M, Lemay CG, Ilkow CS, et al. Complement inhibition prevents oncolytic vaccinia virus neutralization in immune humans and cynomolgus macaques. *Mol Ther* (2015) 23(6):1066–76. doi: 10.1038/mt.2015.49

123. Lee N, Jeon Y-H, Yoo J, Shin S-k, Lee S, Park M-J, et al. Generation of Novel Oncolytic Vaccinia Virus with Improved Intravenous Efficacy through Protection against Complement-Mediated Lysis and Evasion of Neutralization by Vaccinia Virus-Specific Antibodies. *J ImmunoTherapy Cancer* (2023) 11(1):e006024. doi: 10.1136/jitc-2022-006024

124. Ban W, Guan J, Huang H, He Z, Sun M, Liu F, et al. Emerging systemic delivery strategies of oncolytic viruses: A key step toward cancer immunotherapy. *Nano Res* (2022) 15(5):4137–53. doi: 10.1007/s12274-021-4031-6

125. Yokoda R, Nagalo BM, Vernon B, Oklu R, Albadawi H, DeLeon TT, et al. Oncolytic virus delivery: from nanopharmacodynamics to enhanced oncolytic effect. *Oncolytic Virother* (2017) 6:39–49. doi: 10.2147/OV.S145262

126. Hill C, Grundy M, Bau L, Wallington S, Balkaran J, Ramos V, et al. Polymer stealthing and mucin-1 retargeting for enhanced pharmacokinetics of an oncolytic vaccinia virus. *Mol Ther–Oncolytics* (2021) 21:47–61. doi: 10.1016/j.omto.2021.03.011

frontiers | Frontiers in Immunology

TYPE Review
PUBLISHED 22 February 2024
DOI 10.3389/fimmu.2024.1343378

OPEN ACCESS

EDITED BY
Yaohe Wang,
Queen Mary University of London,
United Kingdom

REVIEWED BY
Zong Sheng Guo,
University at Buffalo, United States
Hung Jen Liu,
National Chung Hsing University, Taiwan

*CORRESPONDENCE
Hadi Esmaeili Gouvarchin Ghaleh
h.smaili69@yahoo.com

RECEIVED 23 November 2023
ACCEPTED 09 February 2024
PUBLISHED 22 February 2024

CITATION
Zarezadeh Mehrabadi A, Tat M, Ghorbani Alvanegh A, Roozbahani F and Esmaeili Gouvarchin Ghaleh H (2024) Revolutionizing cancer treatment: the power of bi- and tri-specific T-cell engagers in oncolytic virotherapy.
Front. Immunol. 15:1343378.
doi: 10.3389/fimmu.2024.1343378

Revolutionizing cancer treatment: the power of bi- and tri-specific T-cell engagers in oncolytic virotherapy

Ali Zarezadeh Mehrabadi[1], Mahdi Tat[1], Akbar Ghorbani Alvanegh[2], Fatemeh Roozbahani[3] and Hadi Esmaeili Gouvarchin Ghaleh[1*]

[1]Applied Virology Research Center, Baqiyatallah University of Medical Sciences, Tehran, Iran, [2]Human Genetics Research Center, Baqiyatallah University of Medical Sciences, Tehran, Iran, [3]Department of Microbiology and Virology, Faculty of Medicine, Mazandaran University of Medical Sciences, Sari, Iran

Bi- or tri-specific T cell engagers (BiTE or TriTE) are recombinant bispecific proteins designed to stimulate T-cell immunity directly, bypassing antigen presentation by antigen-presenting cells (APCs). However, these molecules suffer from limitations such as short biological half-life and poor residence time in the tumor microenvironment (TME). Fortunately, these challenges can be overcome when combined with OVs. Various strategies have been developed, such as encoding secretory BiTEs within OV vectors, resulting in improved targeting and activation of T cells, secretion of key cytokines, and bystander killing of tumor cells. Additionally, oncolytic viruses armed with BiTEs have shown promising outcomes in enhancing major histocompatibility complex I antigen (MHC-I) presentation, T-cell proliferation, activation, and cytotoxicity against tumor cells. These combined approaches address tumor heterogeneity, drug delivery, and T-cell infiltration, offering a comprehensive and effective solution. This review article aims to provide a comprehensive overview of Bi- or TriTEs and OVs as promising therapeutic approaches in the field of cancer treatment. We summarize the cutting-edge advancements in oncolytic virotherapy immune-related genetic engineering, focusing on the innovative combination of BiTE or TriTE with OVs.

KEYWORDS

cancer immunotherapy, oncolytic viruses, bi-specific t cell engagers, tri-specific t cell engagers, combination therapy

1 Introduction

Cancer is one of the most significant public health issues globally (1). According to the GLOBOCAN 2020 study, the estimated number of cancer cases worldwide in 2020 exceeded 19 million patients, while the number of cancer-related deaths approached about ten million cases (2). Therefore, developing an efficient health system to improve preventive and therapeutic interventions is imperative for dealing with this challenge.

To date, a range of therapeutic approaches have been developed for managing malignancies. Surgery is widely recognized as an essential and prevalent treatment for solid tumors, although accompanied by numerous risks such as cancer metastasis (3, 4). Alongside surgery, chemotherapy and radiotherapy represent two prominent procedures employed in cancer treatment. Despite their unavoidable benefits, these approaches are not successful in eradicating tumors in many cases (5, 6). Therefore, novel and less complicated cancer therapies such as monoclonal antibodies have become developed, particularly due to the systemic adverse effects of traditional treatments on healthy tissues and organs (2, 7). Bi- and Tri-specific T cell engagers (BiTEs and TriTEs) as well as OVs are two innovative therapeutic approaches that are currently the subject of numerous ongoing clinical trials due to their promising therapeutic potential (8–10).

OVs-mediated immunotherapy exhibits a targeted strategy by specifically targeting cancer cells, infecting and lysing them, while refraining from infecting not malignant cells. The OVs encompass both wild type viruses and genetically engineered variants derived from wild viruses (11). Furthermore, beyond to their oncolytic activities, OVs have demonstrated considerable efficacy in inducing inflammation and triggering immune responses against both the viruses and the tumor cells. Nevertheless, the immune response's outcome is accompanied by some complications; the anti-tumor immunity facilitated by OVs mediated cancer immunotherapy eventually appears to be efficient (12, 13).

OVs serve as an appropriate platform for the delivery of therapeutic genes, facilitating the development of different mechanisms of action (14, 15). There are several categories of Trans genes that can be integrated to OV vectors. These genes have the potential to produce cytokines that induce cellular immunity, such as IL-2, IL-12, and IL-15 (16–18). Furthermore, genes involved in the production of proteins that trigger apoptosis and necrosis in malignant cells, such as TRAIL and TNF-α, are also employed in the development of engineered OVs (18, 19). In addition to these genes that have been applied in preclinical and clinical studies, there has been a new focus on genes encoding antibodies with the ability to identify immune cell-associated antigens and tumor-associated antigens that are readily accessible. These therapeutic approaches known as BiTEs and TriTEs which are considered as an innovative class of immunotherapeutic agents (20).

BiTE is a recombinant bispecific antibody with two linked single-chain fragment variables (scFvs) derived from separate antibodies, one targeting a specific cell-surface molecule on T cells while the other scFv targets antigens present on the surface of cancer cells (21). TriTEs are capable of identifying three distinct targeted antigens. A heterologous scFv employed to recognize one or two tumor antigens, which then be linked to another scFv specify for T or NK cell antigens (22).

In this review, our primary focus lies on the application of OVs as a vector to produce bi- or tri-specific antibodies that are facilitate interactions between tumor cells and T or NK cells. This interaction ultimately leads to the activation of immune cells and triggering of tumoricidal activity. Recent findings in pre-clinical and clinical studies involving OVs armed with various BiTEs and TriTEs antibodies for cancer immunotherapy will be discussed.

2 Overview of the bi- and tri-specific T cell engagers and cancer immunotherapy

The concept of using molecules with multiple binding sites for improving their biological functionality back to early 60s, when first bispecific molecule were developed through a combination of antigen-binding fragments derived from distinct polyclonal sera (23). The production of bispecific antibodies was significant progress in the 1970s and 1980s by the advancement of chemical conjugation methods for combining two distinct antigen-specific monoclonal antibodies, as well as the fusing of hybridoma cell lines (quadromas) that are suitable for producing these molecules (24–26). Nevertheless, early formats of these recombinant proteins had restricted therapeutic effectiveness, with advancements in genetic engineering, there are already More than one hundred polyspecific antibody formats under clinical evaluation (27, 28). Although the initial focus was placed on hematological malignancies, there are ongoing researches for the treatment of solid tumors.

The bispecific T cell engager antibody (BiTE) with a small molecular size is a subtype of recombinant bispecific antibodies with two linked single-chain fragment variables (scFvs) derived from two distinct antibodies, one of which targets a pan T cell marker, In most cases CD3, and the other of which targets surface tumor-associated antigens (TAAs) (Figure 1) (29, 30). In cellular models, BiTEs has been found to exhibit significantly higher efficacy in tumor cell lysis compared to monoclonal IgG antibodies as well as other bispecific antibodies. The effectiveness of BiTE is reported to be Up to hundreds of times greater, even when the ratio of T cells to target tumor cells is limited (31). The production of BiTE has proven to be advantageous due to its ability to be generated in significant amounts by mammalian cell lines. This offers a relatively straightforward and efficient production process when compared to time-consuming and difficult methods like CAR T cells (21, 32).

One of the primary benefits of BiTE and TriTE molecules is their ability to provide "specificity" to polyclonally-activated populations of T cells, resulting in resistance to tumor immune evasion strategies, such as the downregulation of Major histocompatibility complex (MHC) molecules (33). MHC molecules play a crucial role in the presentation of TAAs. TAAs are processed by antigen-presenting cells such as dendritic cells and presents to the T-cell receptor (TCR) on T cells by MHC molecules.

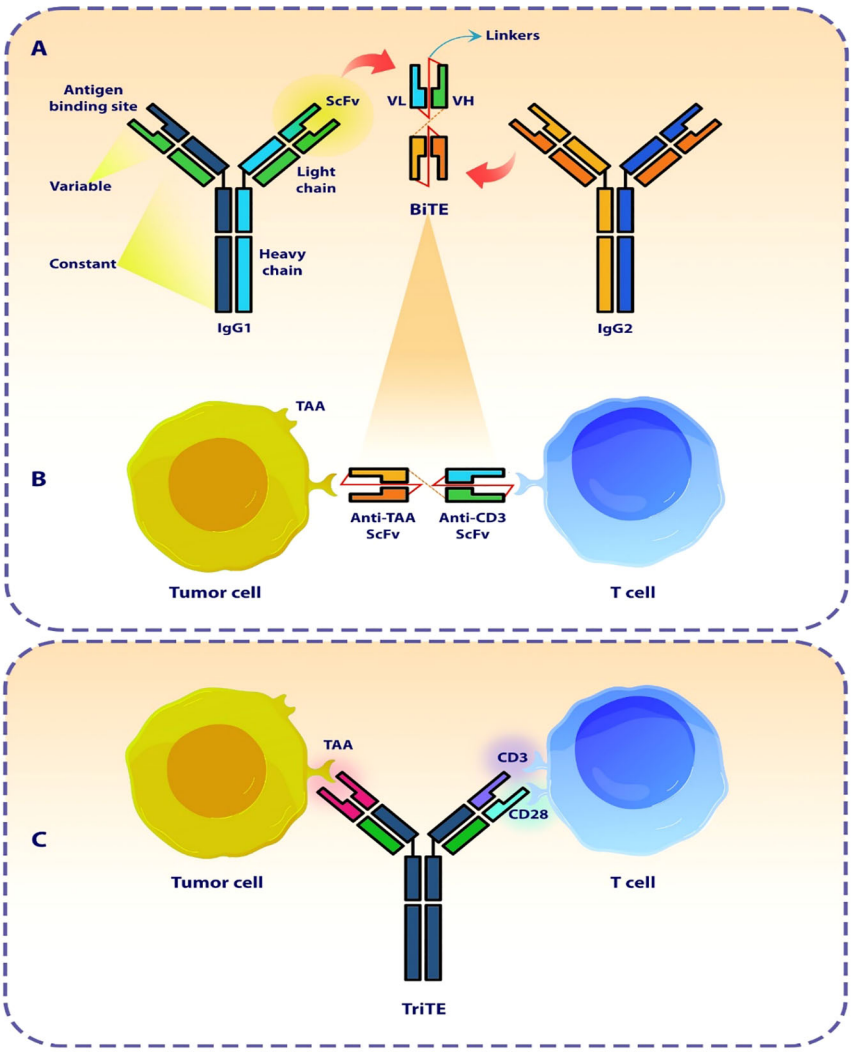

FIGURE 1
The design of a bi- and tri-specific T cell engager antibody (BiTEs and TriTE). **(A)** The Schematic represents the structure and origin of a BiTE molecule that are derived from two distinct antibodies, one specific for a T cell activation molecule and the other specific for a TAA. **(B)** The BiTE molecule organizes the formation of an immunologic synapse by concurrently interacting with a tumor cell via TAA and a T cell through CD3. **(C)** The Schematic represents the conceptualization and design of a TriTE antibody, demonstrating its mechanism of action in establishing a link between T cells and cancer cells. SCFV, single chain fragment variant; VH, Heavy chain variable region; VL, Light chain variable region; TAA, Tumor-associated antigen.

This interaction leads to the activation of T cells, resulting in eliminate of cancer cells. This process is commonly known as MHC restriction (34). The intrinsic resistance to immunotherapies, such as immune checkpoint inhibitors therapy, can be attributed to the impairment or loss of the ability to present antigens for MHC molecules (35, 36). This is a significant factor that impedes the effectiveness of these therapeutic approaches. In addition, it is important to note that the activation of T-cells and the subsequent immune response relies on the presence of costimulatory signals such as CD28 signaling (37, 38).

BiTE has the ability to bridge the gap between cytotoxic T cells and cancer cells, even in the absence of MHC restriction and costimulatory signals. By acting as a biological bridge, BiTE facilitates the activation and proliferation of T cells, regardless of MHC restriction, finally leading to the formation of the immunologic synapse (33, 39). Additionally, BiTE is not dependent on costimulatory signals for T-cell activation. Costimulatory signals, are typically required to fully activate T cells. However, BiTE can independently trigger T-cell activation, making it an adjustable mechanism in cancer immunotherapy (21, 40). Table 1 shows some of the ongoing cancer clinical trials related to BiTEs and TriTEs.

The administration of BiTEs as a novel therapeutic approach for cancer treatment, similar to other procedures, is not without its disadvantages (Figure 2). One characteristic commonly observed in BiTEs/TriTEs is their short biologic half-lives and rapid blood clearance. This means that these molecules are rapidly metabolized. Additionally, they exhibit fast off-rates, which refers to their ability to dissociate from their target molecules quickly (46–48). Another important aspect to consider is the poor retention

10.3389/fimmu.2024.1343378

TABLE 1 Clinical trials about bi- and tri-specific T cell engagers.

BiTE/ TriTE Name	Targeted antigens	Condition	Phase of study	NCT	Status
AMG330	CD33 x CD3	AML	I	[NCT02520427]	Terminated
AMG673	Anti-CD33 with Fc domain	AML	I	[NCT03224819]	Terminated with results
JNJ-63709178	CD123 x CD3	AML	I	[NCT02715011]	Completed
MCLA-117	CLEC12AxCD3	AML	I	[NCT03038230]	Not applicable
AMG420 (BI836909)	BCMA	Multiple Myeloma	I	[NCT02514239]	Completed with results
Solitomab (AMG110, MT110)	Anti-EpCAM	Several solid tumors	I	[NCT00635596]	Completed
AMG211 (MEDI-565)	Anti-CEA	Gastrointestinal Adenocarcinomas	I	[NCT01284231]	Completed
AMG757	DLL3 x CD3	Small Cell Lung Cancer	I	[NCT03319940]	Recruiting with publication (41)
AMG596	EGFRvIII x CD3	Glioblastoma	I	[NCT03296696]	Completed with publication (42)
BAY2010112	PSMA x CD3	Prostate Cancer	I	[NCT01723475]	Completed
BI 764532	DLL3 x CD3	small-cell lung cancer and neuroendocrine carcinomas	I	[NCT04429087]	Recruiting with publication (43)
Tebentafusp	HLA-A*02:01 x CD3	Uveal Melanoma	II/III	[NCT03070392]	Active, not recruiting with publication (44, 45)
SAR442257	CD3xCD28xCD38	Multiple Myeloma, Non-Hodgkin lymphoma	I	[NCT04401020]	Recruiting

times of BiTEs/TriTEs in targeted tumor sites (48). While BiTEs have demonstrated efficiency in numerous cases of relapsed or refractory hematological malignancies, there is a subgroup of patients with hematological malignancies who do not exhibit a response to BiTEs therapy. To enhance the effectiveness of BiTEs, it is imperative to conduct more research regarding tumor escaping mechanisms.

The term of antigen loss refers to the absence of antigen expression and the inability of targeted antibodies or cells to bind to antigens. The occurrence of either or both of these conditions can result in a relapse characterized by the absence of CD19 expression in B-cell lymphoma as well as ALL (49–51). Targeted antigen loss has been identified as a significant factor in patients who have not responded to anti-CD19 CAR T cell treatment. This observation highlights the crucial role that antigen loss contributes in the development of resistance to T-cell based immunotherapies for tumors (50, 51). In a study conducted by Braig et al., the scientists studied patients with ALL who had received blinatumomab and subsequently experienced relapse characterized by the absence of CD19 expression (49). Thus, employing of multi-targeted approaches could prove advantageous for tackling antigen loss. This may involve the development of a singular pharmaceutical agent capable of simultaneously targeting several TAAs, or alternatively, the combination of diverse immunotherapeutic modalities, each targeting distinct TAAs.

The impaired function of the immune system, particularly T cells suppression, constitutes an important variable contributing to this phenomenon (52). For instance BiTE resistance may be related to PD-1/PD-L1 axis. Köhnke et al. in a case study on one B-precursor ALL patient who was resistant to treatment with blinatumomab (a CD19/CD3 bsAb antibody) demonstrated that, after blinatumomab treatment, PD-L1 expression was increased on the tumor cells, suggesting combination of BiTE therapy with programmed cell death protein 1/programmed death-ligand 1 (PD-1/PD-L1) inhibitors could be beneficial for managing tumor immune escaping mechanism (53). Further studies confirmed that the upregulation of immune checkpoints, particularly PD-L1, was observed following BiTE treatment in AML cells and among patients with diverse hematologic neoplasms. This suggests that the combination of immune checkpoint inhibitors with BiTE therapy represents an appropriate strategy to enhance BiTE-induced cytotoxicity (54, 55).

These issues are also observed in BiTEs Therapy for solid tumors as a result of the immunosuppressive tumor microenvironment such as dominance of immunosuppressive myeloid cells and increasing levels of Tregs (56–59). Also various types of solid tumor cells express the immune checkpoint proteins, which binds to the inhibitory receptors on T cells, consequently compromising the effectiveness of cellular immune responses (60). These obstacles go hand in hand, and consequently the efficacy of T cell-based immunotherapies, such as CAR T cell therapies and BiTE therapy, is compromised.

BiTE therapy, similar to other T-Cell based immunotherapies such as CAR-T cell therapy, has been associated with an elevated risk of toxicity as one of its adverse effects. Among the various adverse effects associated with BiTE therapy, two particularly concerning ones are cytokine release syndrome (CRS) and neurotoxicity (61–63). These adverse effects have been identified

FIGURE 2
Schematic represents the disadvantages and challenges of BiTEs and TriTEs in pre-clinical and clinical cancer studies. BiTE, Bi-specific T Cell Engager; TriTE, Tri-specific T Cell Engager; TME, Tumor micro-environment.

as having dose-limiting toxicities (DLTs), meaning that they can become severe enough to limit the dosage of the treatment (63). CRS is a pathological condition characterized by the upregulation of pro-inflammatory cytokines such as IL-6, and interferon-gamma (IFN-γ). The clinical and laboratory findings demonstrate a range of symptoms, including a mild cold-like symptomatology to a severe multi-organ failure, which has the potential to result in mortality (64).

The occurrence of neurological adverse effects can be related to the redistribution of activated T cells. The activation of T lymphocytes stimulated by BiTE results in their adherence to cerebral blood vessels and subsequent migration to the cerebrospinal fluid. The process of T cell sedimentation leads to the impairment of microcirculation and the development of local ischemia, finally giving rise to neurological symptoms (65).

In summary, despite the presence of both notable benefits and drawbacks associated with this innovative therapeutic approach, there exists considerable potential for further development of this category of molecules that orchestrate immune responses against malignancies. These molecules hold promise as cancer immunotherapeutic agents, particularly when applied in combination with OVs to overcome BiTEs/TriTEs monotherapy limitations.

3 Overview of the oncolytic viruses and cancer immunotherapy

Since the 19th century, there have been several case reports of tumor regressions occurring simultaneously with natural viral infections. These patients primarily had hematological malignancies, such as leukemia or lymphoma, which are known to cause significant impairment of the immune system (66). During the 1950s and 1960s, our understanding of viruses greatly increased due to the substantial progress made in cell culture techniques. Virotherapy had attracted significant interest, with viruses such as hepatitis, West Nile, and Epstein-Barr virus commonly employed in cancer treatment at that time. Despite the varying and disputed outcomes (67–69), these reports yielded useful information. During the 1970s and 1980s, the use of viruses as a strategy for combating cancer was disregarded. However, after two decades, this type of treatment resurfaced and became known as “oncolytic viruses” (66). OVs, represent a pioneering category of cancer therapeutic approaches that facilitate the eradication of tumor cells while simultaneously enhancing the innate immune response and the tumor-specific adaptive immune response. OVs have been observed to induce cell death in cancer cells by multiple mechanisms,

including direct virus-mediated cytotoxicity and the activation of cytotoxic immune system pathways (70, 71). The activation of the immune system occurs due to the release of cell debris and viral substances within the tumor's surrounding environment. The selectivity of cancer cells in OV treatment is influenced by multiple parameters. One of these ways involves the entry of the virus into cells through specialized receptors that are specific to the virus. (Figure 3) (70, 72). It has been observed that Tumor cells have a propensity to express elevated levels of specific receptors such as CD46, ICAM-1, DAF, CD155, and integrins. These receptors play an essential role for OVs entry into the malignant cells within TME. For instance, in the case of glioblastoma multiform expressing the human poliovirus receptor CD155, administration of an oncolytic recombinant poliovirus (PVS-RIPO) through intrathecal delivery demonstrated a significant elevation in the median survival time among transgenic mice (73). Nevertheless, there are additional efforts to enhance the specificity of tumor targeting by redirecting OVs for entering cells via receptors that are specific to tumors. Furthermore, the rapid proliferation of tumor cells, characterized by elevated metabolic and replicative functions, may facilitate enhanced viral replication in comparison to normal, quiescent cells. Also, tumor-driver mutations notably enhance the virus replication in the cancer cells (74, 75). In addition, a large percentage of malignant cells demonstrate deficiencies in the signaling of antiviral type I interferon, hence promoting the replication of certain viruses (76).

Adenovirus (AdV), coxsackievirus, herpes simplex virus (HSV), Maraba virus, measles virus, Newcastle disease virus, parvovirus, reovirus, vaccinia virus (VACV), and vesicular stomatitis virus (VSV) are a few of the interesting OV platforms that are currently being tested in pre-clinical and clinical settings (77). OVs with DNA genome, demonstrate notable advantages due to their larger genome size, durable polymerase enzyme, genomic consistency, and strong proliferation capacity. RNA viruses, alternatively, exhibit outstanding compatibility for the purpose of selectively targeting tumor cells growths within the central nervous system, because of their smaller sizes and remarkable capacity to penetrate the blood-brain barrier (69).

The efficacy of OV immunotherapy depends on two pivotal factors: the capacity to selectively target neoplastic cells and the triggering of systemic immune system responses. OVs have the potential to exploit the unique susceptibilities of malignant cells,

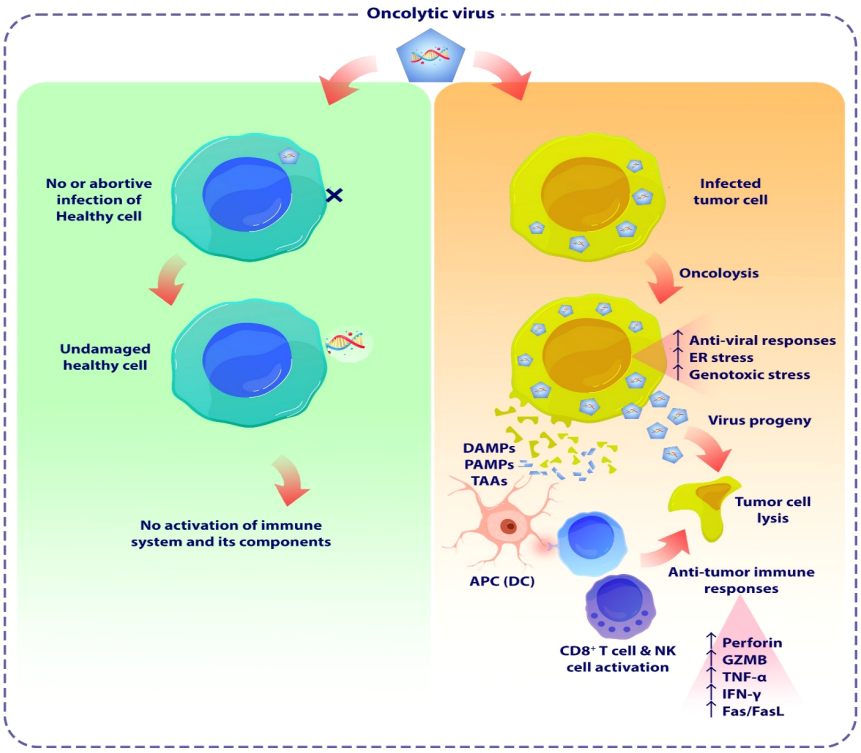

FIGURE 3
The schematic demonstrates the oncolytic viruses mediated tumor lysis. OVs are a novel class of cancer therapeutics that have the potential to eliminate tumor cells and enhance both the innate and adaptive immune responses specific to the tumor. OVs have been proven to trigger apoptosis, necroptosis, and autophagic cell death in malignant cells by many methods, encompassing both direct virus-mediated cytotoxicity and the stimulation of cytotoxic immune system pathways. OVs induce pro-inflammatory responses by enhancing the release of tumor antigens, leading to subsequent immune activation. OVs induce cellular damage and stimulate the release of DAMPs and PAMPs from lysed cancer cells. These substances activate PRRs in NK cells and macrophages, triggering them to secrete inflammatory cytokines such as IFN-γ, and TNF-α. Furthermore, the release of TAAs or TSAs from damaged tumor cells, subsequent presentation by APCs, stimulates adaptive immune responses, including the activation of antigen-specific CD4+ and CD8+ T cells. As a result, these T cells that preferentially target tumors can cause immunogenic cell death in cancer cells. OV, Oncolytic virus; DAMP, Damage-associated molecular patterns; PAMP, Pathogen-associated molecular patterns; TAAs, Tumor-associated antigens; TSAs, tumor-specific antigens; APC, Antigen presenting cell.

including their abnormal stress responses, signaling pathways, and homeostasis processes (78). These abnormalities, which have a possibility to impair the effective functioning of viral clearance mechanisms such as interferon (IFN), toll-like receptor (TLR), Janus kinase-signal transducer and activator of transcription (JAK-STAT), and protein kinase R (PKR) pathways, frequently make cancer cells vulnerable to OV invasion and replication, while protecting healthy cells from adverse effects (79).

OVs frequently trigger immunogenic cell death in cancer cells, and they have the potential to directly engage with immune cells, thereby initiating an anticancer immune response (80, 81). These viruses interact with the immune system while they begin replication within solid tumors (80, 82). OVs cause cellular damage and promote the release of pathogen- and damage-associated molecular patterns (PAMPs and DAMPs) from lysed malignant cells (20). These molecules stimulate innate immune responses in NK cells and macrophages through pattern recognition receptors (PRRs), leading to the secretion of inflammatory cytokines like IFN-α, IFN-γ, TNF-α, IL-6, and IL-12 from these cells (83). Moreover, the release of tumor-associated antigens (TAAs) or tumor-specific antigens (TSAs) from damaged tumor cells and their subsequent presentation by antigen-presenting cells (APCs) stimulate adaptive immune responses, which involve the activation of antigen-specific CD4+ and CD8+ T cells (84, 85). Subsequently, these T cells that specifically target tumors can trigger immunogenic cell death in tumor cells, as confirmed in a preclinical investigation (86, 87).

The emphasis of early virotherapy studies on the inherent mechanism of oncolysis has led to the discovery of tumor-selective virus-mediated apoptosis, which presents an attractive alternative method of cancer therapy in the form of OVs. The reproduction capacity of OVs in healthy cells is limited, whereas the virus can selectively replicate in cancerous cells, leading to their lysis (88, 89). In addition to induction of apoptosis, cellular autophagy mechanisms is influenced by OVs in infected tumor cells. Upon viral infection, OVs interfere with the autophagy machinery in various tumor cells, impacting the self-degradation process (90). These mechanism suggest that inducing the autophagic process alongside virotherapy can improve anti-tumor efficacy in different types of cancer, including lymphoma, myeloma, leukemia, and brain cancers (87, 91, 92).

Nevertheless, it is important to note that although OVs can induce immune responses against cancer, an excessive antiviral response could impair the replication of OVs and may significantly reduce the efficacy of this therapeutic approach (73). Therefore, it is imperative to establish an equilibrium between the immune system responses and the oncolytic activities within the tumor microenvironment.

Currently, there are only two approved OVs for clinical use worldwide. Oncorine (H101) received approval from Chinese authorities in 2005 for treating nasopharyngeal carcinoma in combination with chemotherapy. In 2015, the FDA approved T-VEC (Talimogene laherparepvec) for the treatment of advanced melanoma patients in the United States (93, 94). Several OVs, including HF10 (Canerpaturev), CVA21 (CAVATAK), and Pexa-Vec (a vaccinia virus), are currently undergoing phase II/III clinical trials either as monotherapy or in combination with immune checkpoint inhibitors for several malignancies (70, 95–97). Moreover, there is provisional regulatory approval in Japan for the HSV-based OV called Delytact (Teserpaturev/G47Δ), which is a genetically modified third-generation herpes simplex virus type 1 (HSV-1) with triple mutations, primarily for treating malignant gliomas (98, 99). These advancements represent notable progress in the field of OV therapy.

The utilization of OVs in cancer therapy poses several challenges, including the issues of Limited Virus Penetration, patient selection, passive targeting, immune responses and hypoxia (100–102). In order to overcome these challenges that OV monotherapy is facing, today the attention of scientists in this field has been drawn to the genetic engineering of these viruses in order to express cytokines, chemokines, and also recombinant antibodies. These changes can significantly increase the efficiency of this novel therapeutic approach.

4 The applications of oncolytic viruses for the delivery of immunotherapies

Traditionally, the primary treatment methods employed in cancer management have mainly limited and consisted of combinations of chemo-radiotherapy, surgical intervention, and targeted therapies. Despite the continuous progress achieved in developing various therapeutic strategies, reducing the risk of adverse effects resulting from these procedures still poses considerable issues (69). It has been determined that immunotherapy, particularly via the application of immune checkpoint inhibitors (ICIs), CAR-T cells, monoclonal antibodies (mAb), and bispecific molecules, is not exempt from this concept (Table 2). Numerous patients experience significant adverse effects, such as auto-inflammatory disorders and autoimmunity, which develop from the non-specific stimulation of the immune system and unintended impacts on non-targeted tissues. Therefore, there exists considerable potential for the application of OVs to enhance the safety and specificity of addressed therapeutic interventions, primarily by precisely and exclusively conducting these antibodies toward the tumor site (69, 105, 106). Table 2 presents a brief summary of mentioned immunotherapies currently used for cancer treatment, highlighting the challenges associated with monotherapy as well as the numerous advantages associated with the application of modified OVs. The table also includes the cancer clinical trials on these OVs.

5 The incorporation of bi- and tri-specific t cell engagers into oncolytic virotherapy

As described in previous sections, T cell engagers including BiTEs and TriTEs has attracted considerable interest among physicians and scientists. However, their short serum half-life mandates continuous infusion, and systemic administration can lead to severe and fatal side effects. Also, efficacy of this therapeutic approach against solid tumors is constrained by tumor barriers and immune-suppressive microenvironments (9, 107–109). One of the approaches that

TABLE 2 Summary of immunotherapies in cancer treatment: monotherapy challenges, modified oncolytic viruses, and related clinical trials.

Type of immunotherapy	Description	Disadvantages of monotherapy	Advantages of modified OVs	Clinical trials
Therapeutic antibodies	Therapeutic antibodies, such as ICIs, function by blocking homeostatic signals, such as CTLA-4 and PD-1, with the aim of triggering immune responses against tumor cells (103).	- Limited efficacy in some patients - ICIs are less effective in treating "cold" tumors - Pulmonary and Gastrointestinal toxicities - Neurologic and ocular complications - Rheumatologic complications - Dermatological toxicities	- Enhanced therapeutic response - OVs modulate TME to make "cold" tumors susceptible to immune checkpoint inhibitors. - Improved tumor lymphocyte infiltration - Improved tumor penetration - Reduced side effects through local delivery	- NCT05788926 (Recruiting/Phase I): TG6050 (CTLA-4 antibody) is an oncolytic vaccinia viruses/Non-small cell lung cancer - NCT04336241 (Recruiting/Phase I), NCT05733611 (Active, Not recruiting, Phase II): RP2 (CTLA-4 antibody) is a genetically modified HSV-1/Metastatic Colorectal Cancer - NCT05081492 (Active, Not recruiting, Phase I): CF33 (hNIS/Anti-PD-L1 antibody) is a genetically modified Orthopoxvirus/Metastatic Triple Negative Breast Cancer - NCT05733611 (Active, Not Recruiting, Phase II), NCT05733598 (Not yet recruiting, Phase II), NCT05743270 (Withdrawn, Phase II), NCT04735978 (Active, Not yet recruiting, Phase I): RP3 (CTLA-4 antibody) is a genetically modified HSV-1/Metastatic Colorectal Cancer, Squamous Cell Carcinoma of Head and Neck, and Hepatocellular Carcinoma - NCT03852511(Completed, Phase I): NG-350A (Anti-CD40 antibody) is a genetically modified Adenovirus/ Advanced Epithelial Tumors
CAR T cells	CAR T cell therapy is a form of cancer immunotherapy wherein T cells, undergo genetic engineering to enhance their ability to identify and eliminate tumor cells with improved efficacy (104).	- Limited success in solid tumors - Antigen escape - Limited tumor infiltration - Tumor heterogeneity - CAR-T cell toxicity (e.g. CRS and ICANS) - T cell exhaustion - On-target off-tumor effects - Immunosuppressive TME limited the efficiency of CAR T cell	- Increased CAR T cell infiltration - Reducing tumor immune escaping - Increase the T cells activity to suppress tumors and increase the lifespan - Improved efficacy by combination therapy with cytokine-armed OVs (e.g., IL-2, IFNs) - OV-mediated delivery of tumor-selective surface antigens enhances the antitumor efficacy of CAR T-cells - OVs modulate the TME via enhancing the expression of immune checkpoint costimulatory receptors and ligands. (e.g., OX40, OX40L, 4-1BB, 4-1BBL)	- NCT03740256 (Recruiting): CAdVEC/A First in Human Phase I Trial of Binary Oncolytic Adenovirus in Combination With HER2-Specific Autologous CAR T Cells in Patients With Advanced HER2 Positive Solid Tumors
Bi- and Tri-specific molecules	BiTE is a recombinant bispecific antibody containing two linked scFvs derived from distinct antibodies. One scFv targets a T cell-surface molecule, while the other targets cancer cell antigens. TriTEs are capable of identifying three distinct targeted antigens (21, 22).	- Short biological lifespan - Poor tumor retention - Antigen escape - Limited memory immune response - toxicity such as CRS	- Activated T/NK cells for tumor lysis - Enhanced tumor specific targeting - Enhanced tumor cytotoxicity both *in vitro* and *in vivo* - Significant reduction in tumor growth *in vivo* - Prolonged remission of tumors without recurrence in animal models	- NCT05938296 (Recruiting/Phase I): BS006 (PD-L1/CD3-BsAb) is a genetically modified HSV-2/Metastatic Solid Tumors

ICI, Immune checkpoint inhibitor; OV, Oncolytic virus; HSV, Herpes simplex virus; TME, Tumor micro-environment; CRS, Cytokine release syndrome; ICANS, Immune effector cell-associated neurotoxicity syndrome; IFN, Interferon.

received considerable interest in the field of cancer immunotherapy to address these limitations is oncolytic virotherapy.

The combination of BiTEs/TriTEs with OVs holds the potential for mutual advantages. The infection caused by OV triggers a localized inflammatory response and attracts T cells to the tumor site. These T cells can be guided towards tumor cells by the administration of BiTEs (Figure 4) (71, 73, 110–112). Furthermore, the use of OVs for encoding BiTEs/TriTEs is an opportunity to address the limitations associated with BiTEs/TriTEs therapy. This delivery method has the potential to enhance the concentration of this therapeutic molecules specifically at the site of the tumor and facilitate its penetration into solid tumors, all the while minimizing its distribution within the body and systemic exposure (113–115). Consequently, this approach enhances the therapeutic efficacy by improving the range of doses that could be safely administered.

Typically, the production stages for engineered OVs employed as vectors for expressing BiTEs and TriTEs in Studies in this field adhere to a standardized approach. These OVs contain transgenic cassettes that encodes bi- or tri-specific T cell engagers. Typically, the BiTEs/TriTEs sequences are composed of scFvs that are developed to specifically bind to CD3, together with either a TAA or antigens expressed on cancer-associated fibroblasts or tumor-associated macrophages (116–118). Regulatory domains such as promoters and leader sequences encoding secretory signaling peptides derived from immunoglobulins are commonly found upstream of transgenes (113). Subsequently, the viral vectors and transgenic products are subjected to characterization. The assessment of viral replication kinetics and the potential for direct tumor cell killing involves quantifying progeny and employing several cell viability assays, including metabolic, impedance, or flow cytometry-based evaluations. The confirmation of the expression and secretion of BiTEs/TriTEs is achieved through SDS-PAGE and immunoblotting procedures on the cell-free supernatant obtained from virus-infected cells. In order to determine the binding specificity of BiTEs/TriTEs towards their target antigens and cells expressing the antigens, researchers used ELISA and/or flow cytometry tests. Furthermore, the functionality of BiTEs/TriTEs is explored through *in vitro* co-culture experiments involving target cells and immune effector cells (117, 119–123). In Table 3, engineered OVs expressing BiTEs/TriTEs and targeted antigens along with the results and observations of each study are summarized.

This type of combination therapy is a recent innovation that originated within the past ten years. In 2014, Yu et al. conducted a pioneering study wherein they employed an oncolytic Vaccinia virus (VV) that harbored a T cell engager specifically designed to target EphA2 (EphA2-TEA-VV) (117). This BiTE construct had previously demonstrated a capability to selectively target and effectively suppress tumor growth (133). The study was carried out on a lung cancer mouse models, which expressing the tumor antigen EphA2. Administration of this therapeutic construct resulted in the significant inhibition of tumors growth, whereby such outcomes were simultaneously associated to the upregulation of effector cytokines. Tumor cells that were infected with EphA2-TEA-VV induced the activation of T cells, as indicated by the release of IFN-γ and IL-2. The results of *in vivo* experiments demonstrated that the application of EphA2-TEA-VV, in

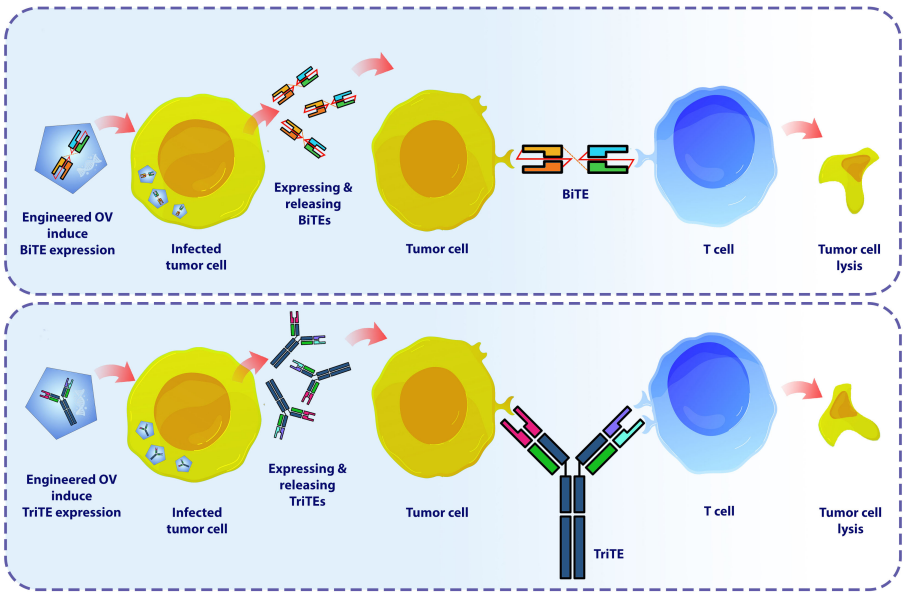

FIGURE 4
The schematic demonstrates how OV-BiTEs/TriTES work against cancer cells. The production stages (Not shown) for engineered OVs employed as vectors for expressing BiTEs and TriTEs in Studies in this field adhere to a standardized approach. These OVs contain transgenic cassettes that encode bi- or tri-specific T cell engagers. Oncolytic-modified viruses possess the ability to selectively target and damage cancer cells. Infected tumor cells secrete BiTEs and TriTEs antibodies, which serve as attractants for T lymphocytes, hence facilitating their recruitment to the tumor microenvironment. In the context of this therapeutic approach, alongside the viral-mediated lysis of tumor cells, the trigger of tumor cells killing is also attributed to the presence of specific T lymphocytes. BiTE, Bi-specific T cell engager; TriTE, Tri-specific T cell engager.

TABLE 3 BiTE- and TriTE-armed OVs for cancer immunotherapy in pre-clinical studies.

OV type	OV-BiTEs name	Targeted Antigen (s)	Results and observations	References
AdV	OAd-MUC16-BiTE	CD3 x MUC16	- MUC16-BiTE mediated T cell activation and target cancer cells specially. - OAd-MUC16-BiTE–mediated enhanced T-cell–mediated tumor cell killing and bystander effect. - OAd-MUC16-BiTE enhanced infiltration of CTLs and reversed the immunosuppressive TME. - Promoted T cell trafficking to the tumor by increasing pro-inflammatory factors and decreasing anti-inflammatory factors. - Local administration lowered toxicity and systemic exposure.	(119)
	ICOVIR-15K-cBiTE	CD3 x EGFR	- ICOVIR-15K-cBiTE mediated robust T cell activation, proliferation, and bystander cell-mediated cytotoxicity. - ICOVIR-15K-cBiTE Increased TIL durability and accumulation *in vivo*. - ICOVIR-15K-cBiTE Improved antitumor activity when coupled with PBMCs or T cells.	(116)
	ICOVIR-15K-cBiTE	CD3 x EGFR	- ICOVIR-15K-cBiTE mediated robust T cell activation, proliferation, and cytotoxicity. - ICOVIR-15K-cBiTE increased antitumor effectiveness when combined with PBMCs or T cells in xenograft models. Mesenchymal stem cells are being employed as carriers to enhance delivery.	(120)
	EnAdV	CD3 x EpCAM	- EpCAM-BiTE mediated activation of CD4+ and CD8+ T-cell populations. - EnAdV increased TIL infiltration and mediated long-lasting antitumor immunity. EnAdV- EpCAM BiTE overcome immunosuppressive environment and enhanced activation of endogenous T cells.	(121)
	EnAd-FAP-BiTE	CD3 x FAP	- EnAd-FAP-BiTE mediated T cell activation, their subsequent proliferation, and the induction of cytotoxicity in cancer cells. - EnAd-FAP-BiTE induces repolarization of resident TAMs in ascites samples. - EnAd-FAP-BiTE increased infiltration of T cells.	(124)
	ICO15K-FBiTE	CD3 x FAP	- Supernatants from ICO15K-FBiTE-infected cells triggers the activation and proliferation of T lymphocytes. - ICO15K-FBiTE promoted tumor T-cell retention and accumulation *in vivo*. - ICO15K-FBiTE is more effective in combatting tumors than the parental virus.	(125)
	–	- CD3ϵ x (CD206 or FRβ) - CD3ϵ x CD3ϵ x CD206 - CD3ϵ x CD28 x CD206	- Selective elimination of M2-polarized autologous macrophages as opposed to M1-polarized autologous macrophages. - A TriTE, possessing bivalent CD3ϵ binding, showed enhanced efficacy while maintaining its selectivity towards target cells. In contrast, a TriTE containing CD28 has induced non-specific activation of T cells. - Enhanced activation of endogenous T cells and IFN-γ production upon exposure to both free and EnAd-encoded T cell engagers.	(122)
	ICO15K-cBiTE	CD3 x EGFR	- ICO15K-cBiTE –mediated oncolysis enhances activation and proliferation of CAR-T cells. - CAR-T cells in combination with ICO15K-cBiTE enhances antitumor efficacy and T cell activation *in vivo*.	(126)
	CAdTrio	CD3ϵ x CD44v6	- CAdTrio Enables T Cells to Kill Tumor Cells *In Vitro*. - CAdTrio Increases the Anti-tumor Activity of HER2.CAR-T Cells.	(127)
VV	OVV-CD19 BiTE	CD3 x CD19	- Supernatants from OVV-CD19 BiTE -infected cells induces the activation and proliferation of T lymphocytes. - Long-term tumor remissions without recurrence noted. - OVV-CD19 BiTE triggers T cells proliferation and recruited this lymphocytes to the tumor sites. - OVV-CD19 BiTE has higher anticancer activity than parental virus and blinatumomab.	(128)
	EphA2-TEA-VV	CD3 x EphA2	- EphA2-TEA-VV infected tumor cells induced T cell activation. - EphA2-TEA-VV redirects T lymphocytes to EphA2-positive cancer cells. - EphA2-TEA-VV induces bystander killing of non-infected tumor cells and enhanced antitumor activity *in vivo*.	(117)
	mFAP-TEA-VV	CD3 x mFAP	- mFAP-TEA-VV replicated within tumor cells and induced oncolysis similarly to the unmodified VV. - mFAP-TEA-VV demonstrates significant anticancer efficacy in an immunocompetent B16 melanoma model.	(118)
	VV-EpCAM BiTE	CD3 x EpCAM	- The secretion of EpCAM BiTE has been shown to effectively promote activation of T cells. - The VV-EpCAM BiTE demonstrates enhanced antitumor activity in EpCAM-expressing breast cancer. - Both VV-EpCAM BiTE and VV-Ctrl exhibit similar anticancer properties in the EpCAM-negative carcinoma model.	(129)

(Continued)

TABLE 3 Continued

OV type	OV-BiTEs name	Targeted Antigen (s)	Results and observations	References
Measles viruses	MV-BiTE	CD3 x (CEA or CD20)	- Therapeutic efficacy of MV-BiTE in combatting malignancies in immunocompetent mice. - An association between the efficacy of anti-tumor agents and the enhanced presence of TIL.	(123)
HSV	oHSV-1 PD-L1 BiTE	CD3 x PD-L1	- PD-L1 BiTE does not increases killing of activated T cells. - oHSV-1 PD-L1 BiTE overcome immune-suppressive ascites fluids environment and have toxic effect for tumor cells. - oHSV-1 PD-L1 BiTE polarized M2-like macrophages. - oHSV-1 PD-L1 BiTE activate endogenous T cells.	(130)
	OV-mOX40L	CD3 x OX40L	- OV-mOX40L inhibited tumor growth *in vivo* - Local treatment of OV-mOX40L stimulated intratumoral immune cells. - OV-mOX40L activated CD4+ T cells and CD8+ cytotoxic T cells and reduced Treg proportion leading to switching the TME to a more pro-inflammatory state.	(131)
	- oHSV2-BiTEs-PD-L1 - oHSV2-mBiTEs-CD19	- CD3 x PD-L1 - CD3 x CD19	- oHSV2-BiTEs-PD-L1 mediated T cell activation boosting T cell cytotoxicity. - oHSV2-BiTEs-PD-L1 strengthens antitumor activity.	(132)

AdV, Adenovirus; VV, Vacina virus; HSV, Herpes simplex virus; OV, Oncolytic virus; BiTE, Bi-specific T cell engager; MUC-16, Mucin 16; EGFR, Epidermal growth factor receptor; TME, Tumor micro environment; TIL, Tumor infiltrated lymphocyte; PBMC, peripheral blood mononuclear cells; EpCAM, Epithelial cellular adhesion molecule; TAM, Tumor associated macrophage; FAP, Fibroblast activation protein; FRβ, Folate receptor-β; EphA2, Ephrin type-A receptor 2; CEA, carcinoembryonic antigen; PD-L1, Programmed death-ligand 1; OX40L, OX40 ligand.

combination with the adoptive transfer of human T cells, resulted in significantly enhanced antitumor efficacy compared to the control group receiving VV plus T cells. Hence, the application of BiTE-armed OVs is a highly encouraging strategy to enhance the efficacy of oncolytic immunotherapy (117). Nevertheless, the methodology still requires evaluation in models that closely resemble clinical conditions, wherein the presence of intratumoral T cell infiltration and immunosuppressive TME are commonly evaluated (134).

In another research published three years after the initial study ICOVIR-15K-cBiTE, an oncolytic adenovirus (AdV) expressing a BiTE targeting the epidermal growth factor receptor (EGFR), was examined (116). Fajardo et al. used a scFv made from and FDA approved monoclonal antibody cetuximab, which is effective against metastatic colorectal cancer (116, 135). ICOVIR-15K-cBiTE has demonstrated significant oncolytic properties, leading to the activation and proliferation of T cells. Furthermore, this approach has also been found to facilitate bystander cell-mediated cytotoxicity, thereby enhancing its therapeutic potential. *In vivo* studies demonstrated a significant increase in the tumor-infiltrated lymphocytes (TILs) and retardation in tumor growth in tumor xenograft models treated with ICOVIR-15K-cBiTE, in comparison to mice given the primary virus and the control group. The immunohistochemical assessments demonstrated comparable levels of viral proteins in all groups that were treated with the virus, irrespective of the administration of peripheral blood mononuclear cells (PBMCs). This suggests that the virus remains present at the tumor site despite the existence of effector T cells. Also, the cBiTE-mediated cancer cell death does not have any negative impact on the virus's capacity to persist in the tumor, as observed in the animal models (116). Generally, the results of this study reveals that BiTE-armed oncolytic adenoviruses possess distinct characteristics that can stimulate targeted and redirected immune responses against tumors. This approach demonstrates a capacity to address significant constraints in oncolytic virotherapy. Another research has provided more evidence that an EGFR-targeted BiTE armed OV can be effectively delivered into the TME by utilizing mesenchymal stem cells (MSCs) as carriers, resulting in enhanced therapeutic effectiveness and systemic availability of ICOVIR-15K-cBiTE. The findings of the study demonstrate the successful production of cBiTE from OAd-infected MSCs, resulting in enhanced cytotoxicity both *in vitro* and *in vivo*. These results confirm the effectiveness of the synergistic effect of OAd, cBiTE, and MSCs in controlling tumor growth. The comparison of *in vivo* antitumor efficacy between the cBiTE-expressing and non-expressing OAdv in combination with MSCs is of particular significance to this study. While the group treated with MSCs/ICOVIR15-cBiTE showed a significant reduction in tumor growth compared to other treatment groups, MSCs/ICOVIR15 also demonstrated improved tumor growth control compared to the ICOVIR15 groups (ICOVIR15, ICOVIR15-cBiTE) and untreated mice. These findings indicate that using ICOVIR15-cBiTE in combination with MSCs may present a promising strategy for cancer treatment that warrants further investigation in clinical trials (120).

In the study published by Wang et al., researchers made modifications to the parental Oncolytic Adenovirus by expressing a MUC16-targeting BiTE antibody. This modified variant, known as OAd-MUC16-BiTE, demonstrated that it maintained its oncolytic properties and ability to replicate *in vitro*. The BiTE molecule, released by tumor cells, accumulates within the TME. It has the ability to bind MUC16 located on targeted cells, subsequently forming connections with CD3 receptors present on T cells. This interaction triggers a series of events, including the activation, proliferation, and damaging effects of T cells against tumor cells that express MUC16. In ex vivo tumor cultures that were obtained from patients with ovarian cancer, OAd-MUC16-

BiTE, successfully overcame the immunosuppressive TME. As a result, it displayed enhanced cytotoxicity compared to the wild type virus. Furthermore, in the context of cell-derived xenograft and patient-derived xenograft models, OAd-MUC16-BiTE demonstrated heightened antitumor efficacy and a notable augmentation in CTLs, as compared to the primary virus. In summary, the combined use of OVs and MUC16-BiTE provides a synergistic effect that overcomes its drawbacks. This approach offers a new and innovative therapeutic option for ovarian cancer. In addition, it can be utilized in combination with diverse cancer treatments, including immune checkpoint inhibitors, chemotherapy, and VEGF inhibitors; nevertheless, investigations evaluating clinical efficacy are necessary (119).

The OV-BiTE strategy has yet to be demonstrated to be effective in more realistic immunological context models. Freedman et al. applied modifications to the oncolytic group B adenovirus EnAdenotucirev (EnAdV) in order to facilitate its capacity to express an additional BiTE. The BiTE construct has been engineered to exhibit dual binding affinity for EpCAM+ tumor cells and CD3+ T cells, leading to the formation of clusters and subsequent activation of CD4+ and CD8+ T cells alongside with cancer cells. In this study, the regulation of BiTE transcription is mediated by the primary late promoter of the virus, hence confining its expression to cancer cells that are capable of supporting virus replication. This methodology has the potential to enhance the cytotoxic effects of EnAd. This report showcases the application of this approach in primary pleural effusions and peritoneal malignant ascites, where the infection of cancer cells with BiTE-expressing EnAd triggers the activation of endogenous T cells. Consequently, these activated T cells are able to effectively eliminate endogenous tumor cells, even in the presence of an immunosuppressive TME. Overall, EnAd has the ability to encode bispecific T-cell engagers without compromising its oncolytic pathogenicity, thus showcasing its transgenic packaging capability. The transgene will not have any impact on the physicochemical characteristics of the viral particles. Therefore, the modified viruses are expected to exhibit identical clinical pharmacokinetics as their parental agent. Additionally, they will preferentially express the encoded BiTE specifically in tumors located throughout the body. The clinical studies of this novel and promising systemically targeted cancer immunotherapy should be given priority (121).

In another study Min Wei et al. engineered an oncolytic vaccinia virus expressing EpCAM Bispecific T-Cell Engager. The VV-EpCAM BiTE has demonstrated notable efficacy in the infection, replication, and lysis of tumor cells. The EpCAM BiTE molecule effectively formed a binding interaction between EpCAM-positive tumor cells and CD3ϵ receptors on T cells, subsequently initiating the activation of naive T cells and the subsequent release of various pro-inflammatory factors, including IFN-γ, IL2, IL6, and IL10. The administration of intratumoral injection of VV-EpCAM BiTE demonstrated a significant enhancement in the efficacy of tumor suppression within EpCAM-positive tumor models, when compared to the administration of wild type of vaccinia virus. Furthermore, there was a significant enhancement in the infiltration of immune cells within the TME in the group that received VV-EpCAM BiTE (129). The findings of this study provide evidence that BiTE-armored oncolytic VVs possess distinct characteristics that can stimulate targeted and redirected immune responses against tumors. The implementation of this particular strategy demonstrates the capacity to effectively overcome significant constraints in the application of oncolytic virotherapy and BiTE therapies within solid tumors. Consequently, it serves as a catalyst for the continued assessment and advancement of these therapeutic approaches.

In a separate investigation, cancer cells were treated by an engineered oncolytic measles virus expressing MV-BiTEs designed to target the tumor antigens CEA and CD20. As a result, the cancer cells were shown to release BiTE antibodies that exhibited functional properties. Significantly, the researchers demonstrated the therapeutic efficacy of MV-BiTE in combatting well-established malignancies in mice with completely functional immune systems. The present model demonstrate an association between the efficacy of anti-tumor agents and the enhanced presence of TIL, as well as the production of durable protective antitumor immune responses. Moreover, the therapeutic efficacy of MV-BiTE in xenograft spheroid models of patient-derived primary colorectal cancer was demonstrated when delivered in combination with human PBMCs. This study reveals the prolonged remission of tumors without recurrence and the development of immune protection following MV-BiTE therapy. This study demonstrates the feasibility of employing an oncolytic vector to express targeted BiTE, showing effectiveness against solid tumors (123).

Instead of directly focusing on cancer cells, BiTEs have the potential to be engineered in a manner that enables T cells to be directed towards pro-tumorigenic factors within the TME. Fibroblast activation protein-α (FAP) demonstrate an elevated expression level in CAFs, which serve as the predominant component of the tumor stroma. As a result, numerous researchers have employed FAP as a focal point for BiTE engineering (118, 136). CAFs exhibit diverse immune-modulating and pro-tumorigenic features, which encompass the secretion of transforming growth factor beta (TGF-β). These CAFs can be effectively addressed by targeting FAP which is known to be expressed on fibroblast cells that are involved in the natural healing process of wounds and tissue remodeling. Nevertheless, the delivery of FAP-BiTEs specifically to tumors by developing engineering OVs may offer an opportunity for minimizing any potential toxicities associated with non-selective targeting. A Vaccinia-based vector, known as mFAP-TEA-VV, was produced in a manner similar to the methodology employed for the development of EphA2-TEA-VV as discussed in the previous study (117, 118). In an immunocompetent melanoma model, mFAP-TEA-VV revealed significant anticancer activity when compared to control VVs and exhibited robust expansion in tumor sites. It is important to note that the increased viral spread caused by mFAP-TEA-VV had a favorable association with the elimination of tumor stroma. To summarize, this study offers preclinical evidence supporting the therapeutic advantages of TEA −VVs that target FAP on CAF. This study demonstrates that mFAP-TEA-VVs significantly increased the replication of viruses within tumors and exhibited potent anticancer effects in a mouse model of melanoma with an optimally functioning immune system (118).

Following this similar concept, Freedman et al. developed an EnAd-derived OV vector encoding a FAP-specific BiTE, capable of concomitantly targeting malignant and immunosuppressive stromal cells. This T-cell Engager shows a high affinity for FAP-expressed CAFs and CD3ϵ expressed on T cells. This interaction triggers a cascade of events, including the induction of fibroblast cell death and the efficient activation of T cells. In summary, EnAd-FAP-BiTE, in contrast to control vectors, resulted in enhanced activation of T cells and cytotoxicity. This led to the decrease of FAP-positive cells and subsequent reductions in TGF-β levels in ascites cultures. The mentioned effects were not detected in patient samples without cancer cells, thereby suggesting enhanced safety attributable to the vector's precise tumor-directed ability. EnAd-SA-FAP-BiTE demonstrated a remarkable ability to enhance T cell-associated chemokines and effector molecules, while concurrently increasing the expression of genes implicated in dendritic cell maturation and antigen presentation across multiple biopsies. This observation implies the possibility of antigen dissemination and subsequent activation of diverse endogenous T cells, thereby facilitating the development of persistent anti-tumor immune responses. Furthermore, the administration of EnAd-SA-FAP-BiTE has been observed to induce the reprogramming of TAMs by altering their phenotypic expression from pro-tumorigenic M2 macrophages to a more pro-inflammatory M1 phenotype. Furthermore, the administration of this FAP-BiTE-encoding OV to freshly collected clinical biopsies, such as malignant peritoneal ascites and solid prostate cancer tissue, resulted in the upregulation of PD-1 expression on TILs, followed by the destruction of CAFs. In conclusion, EnAd blood stability and systemic bioavailability make it a potential virus platform for targeted BiTE expression in tumors. This approach to trigger proinflammatory cell death and reverse TME-mediated immunosuppression may be required to transform uncompromising, stromal-rich carcinomas into immunotherapeutic targets (124).

Another evaluation of CAF-targeting through applying of the ICOVIR oncolytic adenovirus platform was conducted in order to explore the efficacy of OV-BiTE (125). The two studies conducted by Freedman et al. and de Sostoa et al. elucidate similar methodologies and concepts (124, 125). In contrast to the EnAd-FAP-BiTE research, the study conducted by de Sostoa et al. included immunodeficient mouse models instead of clinical samples in order to assess efficacy (125). The evaluation of T cell biological distribution and efficacy against tumors has been conducted *in vivo*. The interaction between FBiTE and CD3+ effector T cells, as well as FAP+ targeted cells, resulted in the activation of T cells, their subsequent proliferation, and the induction of cytotoxicity leading to the death of FAP-positive A549 tumor cell lines. In the Hu-SCID tumor models, the expression of FBiTE in OVs was found to augment the intratumoral retention and accumulation of T cells while concurrently reducing the level of FAP expression in the treated tumors. The anti-cancer beneficial effects of the FBiTE-armed OV exhibited a notable superiority over the unmodified viral strain (125). Taken together, the findings from these studies indicate that BiTE-armed OVs have the ability to selectively target malignant cells as well as the stroma associated with tumors, hence encouraging improved therapeutic effectiveness.

Scott et al. designed a research experiment wherein they successfully developed BiTE-armed Ad viruses as well as TriTE-armed Ad viruses. The study demonstrated the efficacy of these viruses in the eradication of TAMs in samples obtained from patients suffering from several malignancies such as melanoma, ovarian cancer, breast cancer and gastrointestinal cancers. In the present study, a comprehensive assortment of bi- and tri-valent T cell engagers was precisely constructed, with the primary objective of targeting CD3ϵ on T cells and CD206 or folate receptor β (FRβ) on M2-like macrophages. T-cell engagers were genetically integrated into the genome of EnAd, a viral vector, and subsequently evaluated for their oncolytic activity and secretion of BiTE in the presence of tumor cells. Overall, this study designed an oncolytic adenovirus, EnAd, to express TAM-targeting T cell engagers without affecting its oncolytic activity, developing a multi-prolonged therapeutic approach to target cancer cells and immunosuppressive TAMs. In summary, this study predicts that eliminating cancer-promoting TAMs, along with the immune-boosting effects of BiTEs and OVs, will offer a potent treatment strategy for overcoming obstacles to anti-tumor immunity in cancer patients (122).

The T lymphocytes, upon activation by the CD206 and FRβ-targeting BiTEs/TriTEs, demonstrate a preference for the selective elimination of M2-polarized autologous macrophages as opposed to M1-polarized autologous macrophages. A novel TriTE, possessing bivalent CD3ϵ binding, showed enhanced efficacy while maintaining its selectivity towards target cells. In contrast, a TriTE containing CD28 has induced non-specific activation of T cells. In immunosuppressive malignant ascites, the activation of endogenous T cells and the production of IFN-γ were observed upon exposure to both free and EnAd-encoded T cell engagers. This resulted in a notable expansion of T cell populations and a reduction in the presence of CD11b+CD64+ ascites macrophages. Remarkably, the macrophages that succeeded to survive demonstrated a notable elevation in the expression of M1 markers. This observation indicates a potential shift in the microenvironment towards a state of pro-inflammatory response (122). The results of this study suggest that there is significant potential in the field of viral vectors and BiTE/TriTE molecule engineering for the development of safer and more effective cancer immunotherapy. However, further investigation into the mechanisms underlying the OV-BiTE therapeutic approach is recommended.

The treatment landscape for recurrent or refractory (R/R) B-cell malignancies has been significantly impacted by the substantial advancements achieved in CD19-based immunotherapy in recent years (137, 138). Blinatumomab, a BiTE targeting CD19 and CD3, has received approval for use in the relapsed/refractory (R/R) B-cell precursor ALL. This approval is based on evidence gathered from the Phase III TOWER study, which demonstrated notable enhancements in overall survival and remission rates when compared to the conventional chemotherapy (139). Nevertheless, NHL patients who demonstrate extramedullary involvement may

display greater resistance towards BiTE therapy, indicating a potential constraint in the ability of BiTEs to infiltrate the tumor sites. Additional limitations include the relatively brief half-life of blinatumomab, necessitating a continuous infusion spanning a duration of 6 to 8 weeks. This temporal constraint represents a significant challenge to its clinical application. Furthermore, a notable feedback is that a majority of patients who received this therapeutic agent experienced rate 3 or greater adverse events (139, 140). To address these problems, Wen et al. developed an oncolytic vaccinia virus (OVV) that encodes a CD19-specific BiTE (OVV-CD19BiTE). The findings indicate that the replication and oncolytic properties of OVV-CD19BiTE were comparable to those of its parental counterpart. The induction of activation and proliferation of human T cells, as well as the bystander effect of the virus, were observed upon exposure to supernatants derived from OVV-CD19BiTE-infected cells. The *in vivo* investigation demonstrated that OVV-CD19BiTE displayed selective replication within the tumor tissue, resulting in a notably augmented proportion of CD3, CD8, and naïve CD8 T subpopulations within the tumor, as compared to blinatumomab. Furthermore, it is of utmost significance to note that the administration of OVV-CD19BiTE, both *in vitro* and in animal models, exhibited remarkable efficacy in combating tumor growth when compared to the control group receiving control OVs or blinatumomab (128). This research presents compelling evidence regarding the therapeutic advantages of CD19-targeting BiTE expression through Oncolytic Vaccinia Virus. This novel OVV has the potential to overcome the limitations observed in current BiTE therapy, leading to significant therapeutic benefits in the management of B-cell lymphomas. Furthermore, it recommends the possibility of evaluating that therapeutic approach in clinical trials.

In several recent studies, the herpes simplex virus has been employed as an efficient vector for BiTEs. A study has revealed that the administration of oncolytic herpes simplex virus type 1 (HSV-1) has the ability to reprogram the TME with immunosuppressive characteristics into a state that is more proinflammatory. Specifically, it has been observed that the presence of oncolytic HSV-1 leads to a significant decrease in the population of anti-inflammatory macrophages in the TME (141). Furthermore, the administration of CD40L-expressing HSV-1 therapy demonstrated the ability to induce dendritic cell maturation and activate cytotoxic T cells. This therapeutic intervention substantially extended the lifespan of mice suffering from pancreatic ductal adenocarcinoma (PDAC) (142). The results of this study have strengthened the hypothesis of the effectiveness of oHSV-CD40L when combined with ICIs in targeting the PD-1/PD-L1 pathway for overcoming PDAC. Moreover, clinical trials are currently underway to study the potential of HSV Type 2 in treating a variety of solid cancers, including melanoma (**NCT03866525**). These studies provide evidence of the therapeutic potential of HSV in the treatment of various malignancies.

Khalique et al. conducted a study wherein they armed oncolytic herpes simplex virus-1 (oHSV-1) with PD-L1 BiTE. The objective was to evaluate the efficacy of this combination in delivering targeted cytotoxicity in unpurified cultures of malignant ascites obtained from diverse cancer patients. The findings of the study demonstrate that PD-L1 BiTE exhibits notable efficacy as an immunotherapy agent for killing PD-L1-positive tumor cells and macrophages, while concurrently preserving the integrity of T lymphocytes. Using an OV for the purpose of local expression of PD-L1 BiTE not only helps prevent the occurrence of systemic toxicities associated with 'on-target off-tumor' effects but also have the ability to overcome the TME immunosuppressive conditions (130). In another study Shiyu Liu et al. developed a murine OX40L BiTE-armed oHSV-1 (OV-mOX40L). The administration of OV-mOX40L resulted in the transformation of the immunosuppressive tumor immunological environment into a state of elevated activation, accompanied by the restructuring of the stromal matrix and stimulation of T cell response. The administration of OV-mOX40L demonstrated a significant increase in the lifespan of mice with pancreatic ductal PDAC, whether used as a monotherapy or in combination with complementary antibodies that exhibited synergistic effects (131). The results of this study offer significant evidence supporting the effectiveness of OV-mOX40L treatment. These results have the potential to make valuable contributions to the development of OV-mOX40L as a monotherapy or as part of a combination therapy for PDAC.

Jing Jin and colleagues performed a study in which they developed BiTEs targeting PD-L1 or CD19 (oHSV2-BiTEs-PD-L1 or oHSV2-mBiTEs-CD19). The findings of their study indicate that the oHSV2-BiTEs showed enhanced oncolytic potency both *in vitro* and *in vivo*. The oHSV2-BiTEs-PD-L1 construct has the ability to trigger oncolysis in tumor cells that have been infected. Additionally, it can stimulate PBMCs by releasing BiTEs-PD-L1, which leads to the PBMCs-mediated elimination of tumor cells that express PD-L1, irrespective of the level of PD-L1 expression. Furthermore, it has been shown that both oHSV2 and PBMCs have the ability to enhance the expression of PD-L1 on tumor cells. oHSV2-BiTEs-PD-L1 and oHSV2-mBiTEs-CD19 demonstrated an elevated oncolytic effect both *in vitro* and *in vivo* when compared to the control group, which involved the backbone virus oHSV2-GFP (132). The study's findings indicate that the oHSV2, armed with BiTEs molecules, possesses the capability to transform T cells into potent tumor-killing cells, thereby enhancing the effectiveness of antitumor treatment. This suggests that it holds great potential as a potential therapy for future cancer clinical trials.

6 Combination therapy: CAR-T cells and OV-armed BITEs

Tumor antigen heterogeneity poses a significant challenge in the context of therapeutic interventions involving chimeric antigen receptor (CAR) T cells and bi- or Tri-specific T-cell engagers armed with OVs (104). In order to address this significant concern, two studies have been designed employing BiTE-OVs in combination with the adoptive transfer of CAR-T cells.

In a study published by Wing et al., it was demonstrated that CAR-T cells armed against FR-α effectively infiltrated tumors. However, these CAR T cells were unable to achieve robust responses, likely attributable to the existence of FR-α-negative malignant cells induced by tumor evasion. Through the

combination of ICO15K-cBiTE AdV, which encodes an EGFR-targeting BiTE, with FR-α-specific CAR T cells, the objective of this study was to address the issue of tumor heterogeneity and the potential loss of tumor antigens. The findings revealed that Ad-BiTE-mediated oncolysis indicated a noteworthy enhancement in the activation and proliferation of CAR-T cells. Additionally, it led to an enhancement in cytokine production and cytotoxicity, thereby displaying a favorable safety profile *in vitro* when compared to CAR-T cell-armed EGFR. BiTEs are synthesized and released by cells that have been infected which have the ability to redirect CAR-T cells towards epidermal EGFR, even without the presence of FR-α. This redirection of CAR-T cells plays a crucial role in addressing the heterogeneity of tumors. The secretion of BiTE additionally directs CAR-negative, non-specific T cells that are present in CAR-T cell preparations towards cancer cells. The implementation of a combination methodology exhibited enhanced antitumor efficacy and long-term survival in mouse cancer models, in contrast to the monotherapies. This favorable outcome can be attributed to an enhanced activation of T-cells mediated by BiTE within the TME (126).

In these concept, Porter et al. applied an OV designed for simultaneously producing IL-12, an anti-programmed cell death ligand-1 (PD-L1) antibody, and a CD44 variant6-targeting BiTE, thereby creating a combined agent stated as CAdTrio (127). Given the significant expression of CD44v6 on tumor tissue and its absence in normal tissue, it is noteworthy that the administration of a CD44v6 antibody to patients suffering from cancers has been associated with reduced adverse effects (127, 143, 144). The CD44v6 BiTE, when expressed from CAdTrio, facilitated the cytotoxicity of HER2-specific CAR-T cells against various CD44v6+ cancer cell lines. Additionally, it resulted in a more expedited and prolonged treatment of disease in orthotopic HER2+ and HER2− CD44v6+ tumor cells. The administration of CAdTrio, in combination with HER2.CAR T cells, facilitated the achievement of dual targeting of two tumor antigens through the engagement of separate receptor classes (CAR and native receptor [TCR]), thereby enhancing therapeutic outcomes (127). In summary, the findings of this studies indicate that simultaneous administration of a BiTE-expressing OVand adoptive CAR-T cell therapy effectively addresses the fundamental drawbacks of CAR-T cells and BiTEs when used as monotherapy for solid tumors. These results provide compelling evidence to support the demand for further research of this combined approach in clinical trials.

7 Concluding remarks

The rapid advancements in molecular biotechnology have facilitated the development of innovative approaches for harnessing the immune system for the management of cancer. At now, several methodologies, such as adoptive cell treatments, monoclonal antibodies, checkpoint inhibitors, and OVs, are considered major advancements in the field of cancer treatment. These approaches have demonstrated the ability to deliver long-lasting and efficient clinical outcomes to cancer patients. Nevertheless, it is imperative to note that currently, the therapeutic advantages of immunotherapy are confined to a restricted subset of patients who undergo treatment. Solid tumors often possess a tumor microenvironment that is characterized by its ability to decrease the activity of T cells and facilitate tumor development. Furthermore, the emergence of novel immunotherapy treatments has given rise to the appearance of previously unobserved immunological adverse effects, such as cytokine storm and autoimmune disorders. Given these drawbacks, it is imperative to make additional modifications to these therapeutic procedures. In addition to novel immunotherapeutic approaches, it is imperative to enhance our knowledge of a patient's immune contexts in order to improve patient benefits.

FDA and EuEU authorities have approved armed OVs, including T-VEC, in the treatment of patients diagnosed with advanced-stage melanoma. This approval has established armed OVs as a prominent example for the ongoing development of OVs. Regarding BiTEs, it is worth noting that blinatumomab, a dual-specific antibody targeting CD19 and CD3, has demonstrated enhanced efficacy in treating patients diagnosed with B cell lymphoma.

Due to the OVs and BiTEs/TriTEs limitations in solid tumor treatments, the use of BiTE- or TriTE-armed OVs poses an attractive and efficient approach for addressing this unresolved clinical requirement, especially when employed in combination with supplementary methods aimed at mitigating the immunosuppressive tumor microenvironment. These efforts are expected to result in the creation of innovative anti-cancer therapeutic approaches, such as enhanced T cell engagers. This particular goal is recognized as one of the most significant challenges in the field of cancer immunology. The OV-BiTE/TriTE methodology serves as a prime instance in this context. Based on the reliable rationale for science, numerous preclinical research have substantiated the proof-of-concept for this particular approach. Therefore, it is imperative for OV-BiTEs to exhibit both practicality and effectiveness in a clinical setting.

Author contributions

AZ: Conceptualization, Investigation, Validation, Visualization, Writing – original draft, Writing – review & editing. MT: Writing – original draft. AG: Writing – original draft. FR: Writing – original draft. HE: Conceptualization, Supervision, Validation, Writing – review & editing.

Funding

The author(s) declare that no financial support was received for the research, authorship, and/or publication of this article.

Conflict of interest

The authors declare that the research was conducted in the absence of any commercial or financial relationships that could be construed as a potential conflict of interest.

Publisher's note

References

1. Bray F, Laversanne M, Weiderpass E, Soerjomataram I. The ever-increasing importance of cancer as a leading cause of premature death worldwide. *Cancer*. (2021) 127:3029–30. doi: 10.1002/cncr.33587.

2. Sung H, Ferlay J, Siegel RL, Laversanne M, Soerjomataram I, Jemal A, et al. Global cancer statistics 2020: GLOBOCAN estimates of incidence and mortality worldwide for 36 cancers in 185 countries. *CA: Cancer J Clin*. (2021) 71:209–49. doi: 10.3322/caac.21660.

3. Tohme S, Simmons RL, Tsung A. Surgery for cancer: a trigger for metastases. *Cancer Res*. (2017) 77:1548–52. doi: 10.1158/0008-5472.CAN-16-1536.

4. Goldfarb Y, Ben-Eliyahu S. Surgery as a risk factor for breast cancer recurrence and metastasis: mediating mechanisms and clinical prophylactic approaches. *Breast disease*. (2007) 26:99–114. doi: 10.3233/BD-2007-26109.

5. Bidram E, Esmaeili Y, Ranji-Burachaloo H, Al-Zaubai N, Zarrabi A, Stewart A, et al. A concise review on cancer treatment methods and delivery systems. *J Drug Deliv Sci Technol*. (2019) 54:101350. doi: 10.1016/j.jddst.2019.101350.

6. Madmoli M. Evaluation of chemotherapy complications in patients with cancer: A systematic review. *Int J Res Stud Sci Eng Technol*. (2018) 5:59–64.

7. Scott AM, Allison JP, Wolchok JD. Monoclonal antibodies in cancer therapy. *Cancer immun*. (2012) 12:14. doi: 10.1038/nrc3236.

8. Cook M, Chauhan A. Clinical application of oncolytic viruses: a systematic review. *Int J Mol Sci*. (2020) 21:7505. doi: 10.3390/ijms21207505.

9. Goebeler M-E, Bargou RC. T cell-engaging therapies—BiTEs and beyond. *Nat Rev Clin Oncol*. (2020) 17:418–34. doi: 10.1038/s41571-020-0347-5.

10. Huehls AM, Coupet TA, Sentman CL. Bispecific T-cell engagers for cancer immunotherapy. *Immunol Cell Biol*. (2015) 93:290–6. doi: 10.1038/icb.2014.93.

11. Hemminki O, Hemminki A. A century of oncolysis evolves into oncolytic immunotherapy. *Oncoimmunology*. (2016) 5:e1074377. doi: 10.1080/2162402X.2015.1074377.

12. Sadri M, Najafi A, Rahimi A, Behranvand N, Kazemi MH, Khorramdelazad H, et al. Hypoxia effects on oncolytic virotherapy in Cancer: Friend or Foe? *Int Immunopharmacol*. (2023) 122:110470. doi: 10.1016/j.intimp.2023.110470.

13. Chaurasiya S, Fong Y, Warner SG. Oncolytic virotherapy for cancer: clinical experience. *Biomedicines*. (2021) 9:419. doi: 10.3390/biomedicines9040419.

14. Guo ZS, Bartlett DL. Oncolytic viruses as platform for multimodal cancer therapeutics: a promising land. *Cancer Gene Ther*. (2014) 21:261–3. doi: 10.1038/cgt.2014.31.

15. Twumasi-Boateng K, Pettigrew JL, Kwok YE, Bell JC, Nelson BH. Oncolytic viruses as engineering platforms for combination immunotherapy. *Nat Rev Cancer*. (2018) 18:419–32. doi: 10.1038/s41568-018-0009-4.

16. Wong RJ, Chan M-K, Yu Z, Ghossein RA, Ngai I, Adusumilli PS, et al. Angiogenesis inhibition by an oncolytic herpes virus expressing interleukin 12. *Clin Cancer Res*. (2004) 10:4509–16. doi: 10.1158/1078-0432.CCR-04-0081.

17. Kowalsky SJ, Liu Z, Feist M, Berkey SE, Ma C, Ravindranathan R, et al. Superagonist IL-15-armed oncolytic virus elicits potent antitumor immunity and therapy that are enhanced with PD-1 blockade. *Mol Ther*. (2018) 26:2476–86. doi: 10.1016/j.ymthe.2018.07.013.

18. Watanabe K, Luo Y, Da T, Guedan S, Ruella M, Scholler J, et al. Pancreatic cancer therapy with combined mesothelin-redirected chimeric antigen receptor T cells and cytokine-armed oncolytic adenoviruses. *JCI Insight*. (2018) 3:e99573. doi: 10.1172/jci.insight.99573.

19. Sova P, Ren X-W, Ni S, Bernt KM, Mi J, Kiviat N, et al. A tumor-targeted and conditionally replicating oncolytic adenovirus vector expressing TRAIL for treatment of liver metastases. *Mol Ther*. (2004) 9:496–509. doi: 10.1016/j.ymthe.2003.12.008.

20. Guo ZS, Lotze MT, Zhu Z, Storkus WJ, Song X-T. Bi-and tri-specific T cell engager-armed oncolytic viruses: next-generation cancer immunotherapy. *Biomedicines*. (2020) 8:204. doi: 10.3390/biomedicines8070204.

21. Zhou S, Liu M, Ren F, Meng X, Yu J. The landscape of bispecific T cell engager in cancer treatment. *biomark Res*. (2021) 9:38. doi: 10.1186/s40364-021-00294-9.

22. Yao Y, Hu Y, Wang F. Trispecific antibodies for cancer immunotherapy. *Immunology*. (2023) 169:389–99. doi: 10.1111/imm.13636.

23. Nisonoff A MMR. Recombination of a mixture of univalent antibody fragments of different specificity. *Arch Biochem biophys*. (1961) 93:460–2. doi: 10.1016/0003-9861(61)90296-X.

24. Staerz UD, Kanagawa O, Bevan MJ. Hybrid antibodies can target sites for attack by T cells. *Nature*. (1985) 314:628–31. doi: 10.1038/314628a0.

25. Karpovsky B, Titus JA, Stephany DA, Segal DM. Production of target-specific effector cells using hetero-cross-linked aggregates containing anti-target cell and anti-Fc gamma receptor antibodies. *J Exp Med*. (1984) 160:1686–701. doi: 10.1084/jem.160.6.1686.

26. Perez P, Hoffman RW, Shaw S, Bluestone JA, Segal DM. Specific targeting of cytotoxic T cells by anti-T3 linked to anti-target cell antibody. *Nature*. (1985) 316:354–6. doi: 10.1038/316354a0.

27. Spiess C, Zhai Q, Carter PJ. Alternative molecular formats and therapeutic applications for bispecific antibodies. *Mol Immunol*. (2015) 67:95–106. doi: 10.1016/j.molimm.2015.01.003.

28. Segués A, Huang S, Sijts A, Berraondo P, Zaiss DM. Opportunities and challenges of bi-specific antibodies. *Int Rev Cell Mol Biol*. (2022) 369:45–70. doi: 10.1016/bs.ircmb.2022.05.001

29. Runcie K, Budman DR, John V, Seetharamu N. Bi-specific and tri-specific antibodies-the next big thing in solid tumor therapeutics. *Mol Med*. (2018) 24:50. doi: 10.1186/s10020-018-0051-4.

30. Baeuerle PA, Reinhardt C. Bispecific T-cell engaging antibodies for cancer therapy. *Cancer Res*. (2009) 69:4941–4. doi: 10.1158/0008-5472.CAN-09-0547.

31. Wolf E, Hofmeister R, Kufer P, Schlereth B, Baeuerle PA. BiTEs: bispecific antibody constructs with unique anti-tumor activity. *Drug Discovery Today*. (2005) 10:1237–44. doi: 10.1016/S1359-6446(05)03554-3.

32. Löffler A, Kufer P, Lutterbüse R, Zettl F, Daniel P, Schwenken-becher J, et al. A re-combinant bispecific single-chain antibody, CD19 x CD3, induces rapid and high lymphoma-directed cytotoxicity by unstimulated T lymphocytes. *Blood*. (2000) 95:2098–103. doi: 10.1182/blood.V95.6.2098

33. Offner S, Hofmeister R, Romaniuk A, Kufer P, Baeuerle PA. Induction of regular cytolytic T cell synapses by bispecific single-chain antibody constructs on MHC class I-negative tumor cells. *Mol Immunol*. (2006) 43:763–71. doi: 10.1016/j.molimm.2005.03.007.

34. La Gruta NL, Gras S, Daley SR, Thomas PG, Rossjohn J. Understanding the drivers of MHC restriction of T cell receptors. *Nat Rev Immunol*. (2018) 18:467–78. doi: 10.1038/s41577-018-0007-5.

35. Alspach E, Lussier DM, Miceli AP, Kizhvatov I, DuPage M, Luoma AM, et al. MHC-II neoantigens shape tumour immunity and response to immunotherapy. *Nature*. (2019) 574:696–701. doi: 10.1038/s41586-019-1671-8.

36. DuPage M, Mazumdar C, Schmidt LM, Cheung AF, Jacks T. Expression of tumour-specific antigens underlies cancer immunoediting. *Nature*. (2012) 482:405–9. doi: 10.1038/nature10803.

37. Lim SA, Su W, Chapman NM, Chi H. Lipid metabolism in T cell signaling and function. *Nat Chem Biol*. (2022) 18:470–81. doi: 10.1038/s41589-022-01017-3.

38. Daniels MA, Luera D, Teixeiro E. NFκB signaling in T cell memory. *Front Immunol*. (2023) 14:1129191. doi: 10.3389/fimmu.2023.1129191.

39. Klinger M, Benjamin J, Kischel R, Stienen S, Zugmaier G. Harnessing T cells to fight cancer with BiTE® antibody constructs–past developments and future directions. *Immunol Rev*. (2016) 270:193–208. doi: 10.1111/imr.12393.

40. Dreier T, Lorenczewski G, Brandl C, Hoffmann P, Syring U, Hanakam F, et al. Extremely potent, rapid and costimulation-independent cytotoxic T-cell response against lymphoma cells catalyzed by a single-chain bispecific antibody. *Int J cancer*. (2002) 100:690–7. doi: 10.1002/ijc.10557.

41. Paz-Ares L, Champiat S, Lai WV, Izumi H, Govindan R, Boyer M, et al. Tarlatamab, a first-in-class DLL3-targeted bispecific T-cell engager, in recurrent Small-cell lung cancer: An open-label, phase I study. *J Clin Oncol*. (2023) 41:2893. doi: 10.1200/JCO.22.02823.

42. Sternjak A, Lee F, Thomas O, Balazs M, Wahl J, Lorenczewski G, et al. Preclinical assessment of AMG 596, a bispecific T-cell engager (BiTE) immunotherapy targeting the tumor-specific antigen EGFRvIII. *Mol Cancer Ther*. (2021) 20:925–33. doi: 10.1158/1535-7163.MCT-20-0508.

43. Wermke M, Felip E, Gambardella V, Kuboki Y, Morgensztern D, Hamed ZO, et al. Phase I trial of the DLL3/CD3 bispecific T-cell engager BI 764532 in DLL3-positive small-cell lung cancer and neuroendocrine carcinomas. *Future Oncol*. (2022) 18:2639–49. doi: 10.2217/fon-2022-0196.

44. Hua G, Carlson D, Starr JR. Tebentafusp-tebn: A novel bispecific T-cell engager for metastatic uveal melanoma. *J Adv Practition Oncol*. (2022) 13:717. doi: 10.6004/jadpro.

45. Nathan P, Hassel JC, Rutkowski P, Baurain J-F, Butler MO, Schlaak M, et al. Overall survival benefit with tebentafusp in metastatic uveal melanoma. *N Engl J Med*. (2021) 385:1196–206. doi: 10.1056/NEJMoa2103485.

46. Brinkmann U, Kontermann RE. The making of bispecific antibodies. *MAbs*. (2017) 9:182–212. doi: 10.1080/19420862.2016.1268307.

47. Zhang X, Yang Y, Fan D, Xiong D. The development of bispecific antibodies and their applications in tumor immune escape. *Exp Hematol Oncol*. (2017) 6:12. doi: 10.1186/s40164-017-0072-7.

48. Runcie K, Budman DR, John V, Seetharamu N. Bi-specific and tri-specific antibodies-the next big thing in solid tumor therapeutics. *Mol Med*. (2018) 24:50–65. doi: 10.1186/s10020-018-0051-4.

49. Braig F, Brandt A, Goebeler M, Tony H-P, Kurze A-K, Nollau P, et al. Resistance to anti-CD19/CD3 BiTE in acute lymphoblastic leukemia may be mediated by disrupted CD19 membrane trafficking. *Blood J Am Soc Hematol*. (2017) 129:100–4. doi: 10.1182/blood-2016-05-718395.

50. Yu H, Sotillo E, Harrington C, Wertheim G, Paessler M, Maude SL, et al. Repeated loss of target surface antigen after immunotherapy in primary mediastinal large B cell lymphoma. *Am J hematol*. (2017) 92:E11. doi: 10.1002/ajh.24594.

51. Bukhari A, El Chaer F, Koka R, Singh Z, Hutnick E, Ruehle K, et al. Rapid relapse of large B-cell lymphoma after CD19 directed CAR-T-cell therapy due to CD-19 antigen loss. *Am J hematol*. (2019) 94:E273–E5. doi: 10.1002/ajh.25591.

52. Dunn GP, Bruce AT, Ikeda H, Old LJ, Schreiber RD. Cancer immunoediting: from immunosurveillance to tumor escape. *Nat Immunol*. (2002) 3:991–8. doi: 10.1038/ni1102-991.

53. Köhnke T, Krupka C, Tischer J, Knösel T, Subklewe M. Increase of PD-L1 expressing B-precursor ALL cells in a patient resistant to the CD19/CD3-bispecific T cell engager antibody blinatumomab. *J Hematol Oncol*. (2015) 8:111. doi: 10.1186/s13045-015-0213-6.

54. Krupka C, Kufer P, Kischel R, Zugmaier G, Lichtenegger F, Köhnke T, et al. Blockade of the PD-1/PD-L1 axis augments lysis of AML cells by the CD33/CD3 BiTE antibody construct AMG 330: reversing a T-cell-induced immune escape mechanism. *Leukemia*. (2016) 30:484–91. doi: 10.1038/leu.2015.214.

55. Feucht J, Kayser S, Gorodezki D, Hamieh M, Döring M, Blaeschke F, et al. T-cell responses against CD19+ pediatric acute lymphoblastic leukemia mediated by bispecific T-cell engager (BiTE) are regulated contrarily by PD-L1 and CD80/CD86 on leukemic blasts. *Oncotarget*. (2016) 7:76902. doi: 10.18632/oncotarget.v7i47.

56. Jackson CM, Choi J, Lim M. Mechanisms of immunotherapy resistance: lessons from glioblastoma. *Nat Immunol*. (2019) 20:1100–9. doi: 10.1038/s41590-019-0433-y.

57. Duell J, Dittrich M, Bedke T, Mueller T, Eisele F, Rosenwald A, et al. Frequency of regulatory T cells determines the outcome of the T-cell-engaging antibody blinatumomab in patients with B-precursor ALL. *Leukemia*. (2017) 31:2181–90. doi: 10.1038/leu.2017.41.

58. Ghiringhelli F, Larmonier N, Schmitt E, Parcellier A, Cathelin D, Garrido C, et al. CD4+ CD25+ regulatory T cells suppress tumor immunity but are sensitive to cyclophosphamide which allows immunotherapy of established tumors to be curative. *Eur J Immunol*. (2004) 34:336–44. doi: 10.1002/eji.200324181.

59. Perez C, Botta C, Zabaleta A, Puig N, Cedena M-T, Goicoechea I, et al. Immunogenomic identification and characterization of granulocytic myeloid-derived suppressor cells in multiple myeloma. *Blood J Am Soc Hematol*. (2020) 136:199–209. doi: 10.1182/blood.2019004537.

60. Cherkassky L, Morello A, Villena-Vargas J, Feng Y, Dimitrov DS, Jones DR, et al. Human CAR T cells with cell-intrinsic PD-1 checkpoint blockade resist tumor-mediated inhibition. *J Clin Invest*. (2016) 126:3130–44. doi: 10.1172/JCI83092.

61. Frey NV, Porter DL. Cytokine release syndrome with novel therapeutics for acute lymphoblastic leukemia. *Hematol 2014 Am Soc Hematol Educ Program Book*. (2016) 2016:567–72. doi: 10.1182/asheducation-2016.1.567.

62. Stein AS, Schiller G, Benjamin R, Jia C, Zhang A, Zhu M, et al. Neurologic adverse events in patients with relapsed/refractory acute lymphoblastic leukemia treated with blinatumomab: management and mitigating factors. *Ann Hematol*. (2019) 98:159–67. doi: 10.1007/s00277-018-3497-0.

63. Li H, Er Saw P, Song E. Challenges and strategies for next-generation bispecific antibody-based antitumor therapeutics. *Cell Mol Immunol*. (2020) 17:451–61. doi: 10.1038/s41423-020-0417-8.

64. Fitzgerald JC, Weiss SL, Maude SL, Barrett DM, Lacey SF, Melenhorst JJ, et al. Cytokine release syndrome after chimeric antigen receptor T cell therapy for acute lymphoblastic leukemia. *Crit Care Med*. (2017) 45:e124. doi: 10.1097/CCM.0000000000002053.

65. Klinger M, Zugmaier G, Nägele V, Goebeler M-E, Brandl C, Stelljes M, et al. Adhesion of T cells to endothelial cells facilitates blinatumomab-associated neurologic adverse events. *Cancer Res*. (2020) 80:91–101. doi: 10.1158/0008-5472.CAN-19-1131.

66. Kelly E, Russell SJ. History of oncolytic viruses: genesis to genetic engineering. *Mol Ther*. (2007) 15:651–9. doi: 10.1038/sj.mt.6300108.

67. Gey G. Tissue culture studies of the proliferative capacity of cervical carcinoma and normal epithelium. *Cancer Res*. (1952) 12:264–5.

68. Weller TH, Robbins FC, Enders JF. Cultivation of poliomyelitis virus in cultures of human foreskin and embryonic tissues. *Proc Soc Exp Biol Med*. (1949) 72:153–5. doi: 10.3181/00379727-72-17359.

69. Zarezadeh Mehrabadi A, Roozbahani F, Ranjbar R, Farzanehpour M, Shahriary A, Dorostkar R, et al. Overview of the pre-clinical and clinical studies about the use of CAR-T cell therapy of cancer combined with oncolytic viruses. *World J Surg Oncol*. (2022) 20:16. doi: 10.1186/s12957-021-02486-x.

70. Mishra AK, Ali A, Dutta S, Banday S, Malonia SK. Emerging trends in immunotherapy for cancer. *Diseases*. (2022) 10:60. doi: 10.3390/diseases10030060.

71. Seymour LW, Fisher KD. Oncolytic viruses: finally delivering. *Br J cancer*. (2016) 114:357–61. doi: 10.1038/bjc.2015.481.

72. Huang Q, Cai W-Q, Han Z-W, Wang M-Y, Zhou Y, Cheng J-T, et al. Bispecific T cell engagers and their synergistic tumor immunotherapy with oncolytic viruses. *Am J Cancer Res*. (2021) 11:2430–55.

73. Shi T, Song X, Wang Y, Liu F, Wei J. Combining oncolytic viruses with cancer immunotherapy: establishing a new generation of cancer treatment. *Front Immunol*. (2020) 11:683. doi: 10.3389/fimmu.2020.00683.

74. Aghi M, Visted T, Depinho R, Chiocca E. Oncolytic herpes virus with defective ICP6 specifically replicates in quiescent cells with homozygous genetic mutations in p16. *Oncogene*. (2008) 27:4249–54. doi: 10.1038/onc.2008.53.

75. Coffey MC, Strong JE, Forsyth PA, Lee PW. Reovirus therapy of tumors with activated Ras pathway. *Science*. (1998) 282:1332–4. doi: 10.1126/science.282.5392.1332.

76. Stojdl DF, Lichty B, Knowles S, Marius R, Atkins H, Sonenberg N, et al. Exploiting tumor-specific defects in the interferon pathway with a previously unknown oncolytic virus. *Nat Med*. (2000) 6:821–5. doi: 10.1038/77558.

77. Martin NT, Bell JC. Oncolytic virus combination therapy: killing one bird with two stones. *Mol Ther*. (2018) 26:1414–22. doi: 10.1016/j.ymthe.2018.04.001.

78. Adair RA, Roulstone V, Scott KJ, Morgan R, Nuovo GJ, Fuller M, et al. Cell carriage, delivery, and selective replication of an oncolytic virus in tumor in patients. *Sci Transl Med*. (2012) 4:138ra77. doi: 10.1126/scitranslmed.3003578.

79. Fend L, Yamazaki T, Remy C, Fahrner C, Gantzer M, Nourtier V, et al. Immune checkpoint blockade, immunogenic chemotherapy or IFN-α blockade boost the local and abscopal effects of oncolytic virotherapy. *Cancer Res*. (2017) 77:4146–57. doi: 10.1158/0008-5472.CAN-16-2165.

80. Workenhe ST, Mossman KL. Oncolytic virotherapy and immunogenic cancer cell death: sharpening the sword for improved cancer treatment strategies. *Mol Ther*. (2014) 22:251–6. doi: 10.1038/mt.2013.220.

81. Guo ZS, Liu Z, Bartlett DL. Oncolytic immunotherapy: dying the right way is a key to eliciting potent antitumor immunity. *Front Oncol*. (2014) 4:74. doi: 10.3389/fonc.2014.00074.

82. Mardi A, Shirokova AV, Mohammed RN, Keshavarz A, Zekiy AO, Thangavelu L, et al. Biological causes of immunogenic cancer cell death (ICD) and anti-tumor therapy; combination of oncolytic virus-based immunotherapy and CAR T-cell therapy for ICD induction. *Cancer Cell Int*. (2022) 22:168. doi: 10.1186/s12935-022-02585-z.

83. Li Q, Tan F, Wang Y, Liu X, Kong X, Meng J, et al. The gamble between oncolytic virus therapy and IFN. *Front Immunol*. (2022) 13:168. doi: 10.3389/fimmu.2022.971674.

84. Harrington K, Freeman DJ, Kelly B, Harper J, Soria J-C. Optimizing oncolytic virotherapy in cancer treatment. *Nat Rev Drug Discov*. (2019) 18:689–706. doi: 10.1038/s41573-019-0029-0.

85. Ma W, He H, Wang H. Oncolytic herpes simplex virus and immunotherapy. *BMC Immunol*. (2018) 19:40. doi: 10.1186/s12865-018-0281-9.

86. Angelova AL, Grekova SP, Heller A, Kuhlmann O, Soyka E, Giese T, et al. Complementary induction of immunogenic cell death by oncolytic parvovirus H-1PV and gemcitabine in pancreatic cancer. *J virol*. (2014) 88:5263–76. doi: 10.1128/JVI.03688-13.

87. Wu Y-Y, Sun T-K, Chen M-S, Munir M, Liu H-J. Oncolytic viruses-modulated immunogenic cell death, apoptosis and autophagy linking to virotherapy and cancer immune response. *Front Cell infect Microbiol*. (2023) 13:1142172. doi: 10.3389/fcimb.2023.1142172.

88. Li J, Meng Q, Zhou X, Zhao H, Wang K, Niu H, et al. Gospel of Malignant Glioma: Oncolytic virus therapy. *Gene*. (2022) 818:146217. doi: 10.1016/j.gene.2022.146217.

89. Kalyanasundram J, Hamid A, Yusoff K, Chia SL. Newcastle disease virus strain AF2240 as an oncolytic virus: A review. *Acta tropica*. (2018) 183:126–33. doi: 10.1016/j.actatropica.2018.04.007.

90. Meng S, Xu J, Wu Y, Ding C. Targeting autophagy to enhance oncolytic virus-based cancer therapy. *Expert Opin Biol Ther*. (2013) 13:863–73. doi: 10.1517/14712598.2013.774365.

91. Lei W, Wang S, Xu N, Chen Y, Wu G, Zhang A, et al. Enhancing therapeutic efficacy of oncolytic vaccinia virus armed with Beclin-1, an autophagic Gene in leukemia and myeloma. *Biomed Pharmacother*. (2020) 125:110030. doi: 10.1016/j.biopha.2020.110030.

92. Botta G, Passaro C, Libertini S, Abagnale A, Barbato S, Maione AS, et al. Inhibition of autophagy enhances the effects of E1A-defective oncolytic adenovirus dl 922–947 against glioma cells in *vitro* and in vivo. *Hum Gene Ther*. (2012) 23:623–34. doi: 10.1089/hum.2011.120.

93. Johnson DB, Puzanov I, Kelley MC. Talimogene laherparepvec (T-VEC) for the treatment of advanced melanoma. *Immunotherapy*. (2015) 7:611–9. doi: 10.2217/imt.15.35.

94. Liang M. Oncorine, the world first oncolytic virus medicine and its update in China. *Curr Cancer Drug targets*. (2018) 18:171–6. doi: 10.2174/1568009618666171129221503.

95. Yokota K, Isei T, Uhara H, Fujisawa Y, Takenouchi T, Kiyohara Y, et al. Final results from phase II of combination with canerpaturev (formerly HF10), an oncolytic viral immunotherapy, and ipilimumab in unresectable or metastatic melanoma in second-or later line treatment. *Ann Oncol*. (2019) 30:v557. doi: 10.1093/annonc/mdz255.053.

96. Annels NE, Mansfield D, Arif M, Ballesteros-Merino C, Simpson GR, Denyer M, et al. Phase I trial of an ICAM-1-targeted immunotherapeutic-coxsackievirus A21 (CVA21) as an oncolytic agent against non muscle-invasive bladder cancer. *Clin Cancer Res*. (2019) 25:5818–31. doi: 10.1158/1078-0432.CCR-18-4022.

97. Kim S-G, Hwang T. Phase 2 trial of Pexa-Vec (pexastimogene devacirepvec; JX-594), an oncolytic and immunotherapeutic vaccinia virus, in patients with metastatic, refractory renal cell carcinoma (RCC). *Eur J Cancer*. (2015) 51:S510. doi: 10.1016/S0959-8049(16)31415-0.

98. Frampton JE. Teserpaturev/G47Δ: first approval. *BioDrugs*. (2022) 36:667–72. doi: 10.1007/s40259-022-00553-7.

99. Maruyama Y, Sakurai A, Noda S, Fujiwara Y, Okura N, Takagi T, et al. Regulatory issues: PMDA–review of sakigake designation products: oncolytic virus therapy with delytact injection (Teserpaturev) for Malignant glioma. *Oncol*. (2023) 28:664–70. doi: 10.1093/oncolo/oyad041.

100. Abd-Aziz N, Poh CL. Development of oncolytic viruses for cancer therapy. *Trans Res*. (2021) 237:98–123. doi: 10.1016/j.trsl.2021.04.008.

101. Hong J, Yun C-O. Overcoming the limitations of locally administered oncolytic virotherapy. *BMC Biomed Eng*. (2019) 1:17. doi: 10.1186/s42490-019-0016-x.

102. Guo ZS. The impact of hypoxia on oncolytic virotherapy. *Virus Adapt Treat*. (2011) 3:71–82. doi: 10.2147/VAAT.

103. Park Y-J, Kuen D-S, Chung Y. Future prospects of immune checkpoint blockade in cancer: from response prediction to overcoming resistance. *Exp Mol Med*. (2018) 50:109. doi: 10.1038/s12276-018-0130-1.

104. Mehrabadi AZ, Ranjbar R, Farzanehpour M, Shahriary A, Dorostkar R, Hamidinejad MA, et al. Therapeutic potential of CAR T cell in Malignancies: A scoping review. *Biomed Pharmacother*. (2022) 146:112512. doi: 10.1016/j.biopha.2021.112512.

105. Boland P, Pavlick AC, Weber J, Sandigursky S. Immunotherapy to treat Malignancy in patients with pre-existing autoimmunity. *J immunother cancer*. (2020) 8:e000356. doi: 10.1136/jitc-2019-000356.

106. Linardou H, Gogas H. Toxicity management of immunotherapy for patients with metastatic melanoma. *Ann Trans Med*. (2016) 4:272. doi: 10.21037/atm.

107. Yu S, Li A, Liu Q, Yuan X, Xu H, Jiao D, et al. Recent advances of bispecific antibodies in solid tumors. *J Hematol Oncol*. (2017) 10:155. doi: 10.1186/s13045-017-0522-z.

108. Esfahani K, Roudaia L, Buhlaiga N, Del Rincon S, Papneja N, Miller W. A review of cancer immunotherapy: from the past, to the present, to the future. *Curr Oncol*. (2020) 27:87–97. doi: 10.3747/co.27.5223.

109. Waldman AD, Fritz JM, Lenardo MJ. A guide to cancer immunotherapy: from T cell basic science to clinical practice. *Nat Rev Immunol*. (2020) 20:651–68. doi: 10.1038/s41577-020-0306-5.

110. Achard C, Surendran A, Wedge M-E, Ungerechts G, Bell J, Ilkow CS. Lighting a fire in the tumor microenvironment using oncolytic immunotherapy. *EBioMedicine*. (2018) 31:17–24. doi: 10.1016/j.ebiom.2018.04.020.

111. Oh C-M, Chon HJ, Kim C. Combination immunotherapy using oncolytic virus for the treatment of advanced solid tumors. *Int J Mol Sci*. (2020) 21:7743. doi: 10.3390/ijms21207743.

112. Ribas A, Dummer R, Puzanov I, VanderWalde A, Andtbacka RH, Michielin O, et al. Oncolytic virotherapy promotes intratumoral T cell infiltration and improves anti-PD-1 immunotherapy. *Cell*. (2017) 170:1109–19.e10. doi: 10.1016/j.cell.2017.08.027

113. Heidbuechel JPW, Engeland CE. Oncolytic viruses encoding bispecific T cell engagers: a blueprint for emerging immunovirotherapies. *J Hematol Oncol*. (2021) 14:63. doi: 10.1186/s13045-021-01075-5.

114. Song X-T. Combination of virotherapy and T-cell therapy: arming oncolytic virus with T-cell engagers. *Discov Med*. (2013) 16:261–6.

115. Scott EM, Duffy MR, Freedman JD, Fisher KD, Seymour LW. Solid tumor immunotherapy with T cell engager-armed oncolytic viruses. *Macromol Biosci*. (2018) 18:1700187. doi: 10.1002/mabi.201700187.

116. Fajardo CA, Guedan S, Rojas LA, Moreno R, Arias-Badia M, De Sostoa J, et al. Oncolytic adenoviral delivery of an EGFR-targeting T-cell engager improves antitumor efficacy. *Cancer Res*. (2017) 77:2052–63. doi: 10.1158/0008-5472.CAN-16-1708.

117. Yu F, Wang X, Guo ZS, Bartlett DL, Gottschalk SM, Song X-T. T-cell engager-armed oncolytic vaccinia virus significantly enhances antitumor therapy. *Mol Ther*. (2014) 22:102–11. doi: 10.1038/mt.2013.240.

118. Yu F, Hong B, Song X-T. A T-cell engager-armed oncolytic vaccinia virus to target the tumor stroma. *Cancer Trans Med*. (2017) 3:122–32. doi: 10.4103/ctm.ctm_13_17.

119. Wang Q, Ma X, Wu H, Zhao C, Chen J, Li R, et al. Oncolytic adenovirus with MUC16-BiTE shows enhanced antitumor immune response by reversing the tumor microenvironment in PDX model of ovarian cancer. *Oncoimmunology*. (2022) 11:2096362. doi: 10.1080/2162402X.2022.2096362.

120. Barlabé P, Sostoa JD, Fajardo CA, Alemany R, Moreno R. Enhanced antitumor efficacy of an oncolytic adenovirus armed with an EGFR-targeted BiTE using menstrual blood-derived mesenchymal stem cells as carriers. *Cancer Gene Ther*. (2020) 27:383–8. doi: 10.1038/s41417-019-0110-1.

121. Freedman JD, Hagel J, Scott EM, Psallidas I, Gupta A, Spiers L, et al. Oncolytic adenovirus expressing bispecific antibody targets T-cell cytotoxicity in cancer biopsies. *EMBO Mol Med*. (2017) 9:1067–87. doi: 10.15252/emmm.201707567.

122. Scott EM, Jacobus EJ, Lyons B, Frost S, Freedman JD, Dyer A, et al. Bi-and tri-valent T cell engagers deplete tumour-associated macrophages in cancer patient samples. *J ImmunoTher Cancer*. (2019) 7:320. doi: 10.1186/s40425-019-0807-6.

123. Speck T, Heidbuechel JP, Veinalde R, Jaeger D, Von Kalle C, Ball CR, et al. Targeted BiTE expression by an oncolytic vector augments therapeutic efficacy against solid tumors. *Clin Cancer Res*. (2018) 24:2128–37. doi: 10.1158/1078-0432.CCR-17-2651.

124. Freedman JD, Duffy MR, Lei-Rossmann J, Muntzer A, Scott EM, Hagel J, et al. An oncolytic virus expressing a T-cell engager simultaneously targets cancer and immunosuppressive stromal cells. *Cancer Res*. (2018) 78:6852–65. doi: 10.1158/0008-5472.CAN-18-1750.

125. de Sostoa J, Fajardo CA, Moreno R, Ramos MD, Farrera-Sal M, Alemany R. Targeting the tumor stroma with an oncolytic adenovirus secreting a fibroblast activation protein-targeted bispecific T-cell engager. *J immunother cancer*. (2019) 7:19. doi: 10.1186/s40425-019-0505-4.

126. Wing A, Fajardo CA, Posey AD Jr, Shaw C, Da T, Young RM, et al. Improving CART-cell therapy of solid tumors with oncolytic virus–driven production of a bispecific T-cell engager. *Cancer Immunol Res*. (2018) 6:605–16. doi: 10.1158/2326-6066.CIR-17-0314.

127. Porter CE, Shaw AR, Jung Y, Yip T, Castro PD, Sandulache VC, et al. Oncolytic adenovirus armed with BiTE, cytokine, and checkpoint inhibitor enables CAR T cells to control the growth of heterogeneous tumors. *Mol Ther*. (2020) 28:1251–62. doi: 10.1016/j.ymthe.2020.02.016.

128. Lei W, Ye Q, Hao Y, Chen J, Huang Y, Yang L, et al. CD19-targeted bite expression by an oncolytic vaccinia virus significantly augments therapeutic efficacy against B-cell lymphoma. *Blood Cancer J*. (2022) 12:35. doi: 10.1038/s41408-022-00634-4.

129. Wei M, Zuo S, Chen Z, Qian P, Zhang Y, Kong L, et al. Oncolytic vaccinia virus expressing a bispecific T-cell engager enhances immune responses in EpCAM positive solid tumors. *Front Immunol*. (2022) 13:1017574. doi: 10.3389/fimmu.2022.1017574.

130. Khalique H, Baugh R, Dyer A, Scott EM, Frost S, Larkin S, et al. Oncolytic herpesvirus expressing PD-L1 BiTE for cancer therapy: exploiting tumor immune suppression as an opportunity for targeted immunotherapy. *J immunother cancer*. (2021) 9:e001292. doi: 10.1136/jitc-2020-001292.

131. Liu S, Li F, Ma Q, Du M, Wang H, Zhu Y, et al. OX40L-armed oncolytic virus boosts T-cell response and remodels tumor microenvironment for pancreatic cancer treatment. *Theranostics*. (2023) 13:4016. doi: 10.7150/thno.83495.

132. Jin J, Wang R, Yang J, Hu H, Wang D, Cai L, et al. BiTEs expressed by an oncolytic herpes simplex virus type 2 can transform heterologous T cells into uniform tumor killer cells. *Hum Gene Ther*. (2022) 33:649–63. doi: 10.1089/hum.2021.277.

133. Hammond SA, Lutterbuese R, Roff S, Lutterbuese P, Schlereth B, Bruckheimer E, et al. Selective targeting and potent control of tumor growth using an EphA2/CD3-Bispecific single-chain antibody construct. *Cancer Res*. (2007) 67:3927–35. doi: 10.1158/0008-5472.CAN-06-2760.

134. Albelda SM, Thorne SH. Giving oncolytic vaccinia virus more BiTE. *Mol Ther*. (2014) 22:6–8. doi: 10.1038/mt.2013.271.

135. Wong S-F. Cetuximab: an epidermal growth factor receptor monoclonal antibody for the treatment of colorectal cancer. *Clin Ther*. (2005) 27:684–94. doi: 10.1016/j.clinthera.2005.06.003.

136. Chen X, Song E. Turning foes to friends: targeting cancer-associated fibroblasts. *Nat Rev Drug Discov*. (2019) 18:99–115. doi: 10.1038/s41573-018-0004-1.

137. Locke FL, Go WY, Neelapu SS. Development and use of the anti-CD19 chimeric antigen receptor T-cell therapy axicabtagene ciloleucel in large B-cell lymphoma: a review. *JAMA Oncol*. (2020) 6:281–90. doi: 10.1001/jamaoncol.2019.3869.

138. Frigault MJ, Maus MV. State of the art in CAR T cell therapy for CD19+ B cell Malignancies. *J Clin Invest*. (2020) 130:1586–94. doi: 10.1172/JCI129208.

139. Kantarjian H, Stein A, Gökbuget N, Fielding AK, Schuh AC, Ribera J-M, et al. Blinatumomab versus chemotherapy for advanced acute lymphoblastic leukemia. *N Engl J Med*. (2017) 376:836–47. doi: 10.1056/NEJMoa1609783.

140. Aldoss I, Song J, Stiller T, Nguyen T, Palmer J, O'Donnell M, et al. Correlates of resistance and relapse during blinatumomab therapy for relapsed/refractory acute lymphoblastic leukemia. *Am J hematol*. (2017) 92:858–65. doi: 10.1002/ajh.24783.

141. Zhang L, Wang W, Wang R, Zhang N, Shang H, Bi Y, et al. Reshaping the immune microenvironment by oncolytic herpes simplex virus in murine pancreatic ductal adenocarcinoma. *Mol Ther*. (2021) 29:744–61. doi: 10.1016/j.ymthe.2020.10.027.

142. Wang R, Chen J, Wang W, Zhao Z, Wang H, Liu S, et al. CD40L-armed oncolytic herpes simplex virus suppresses pancreatic ductal adenocarcinoma by facilitating the tumor microenvironment favorable to cytotoxic T cell response in the syngeneic mouse model. *J immunother cancer*. (2022) 10:e003809. doi: 10.1136/jitc-2021-003809.

143. Tijink BM, Buter J, De Bree R, Giaccone G, Lang MS, Staab A, et al. A phase I dose escalation study with anti-CD44v6 bivatuzumab mertansine in patients with incurable squamous cell carcinoma of the head and neck or esophagus. *Clin Cancer Res*. (2006) 12:6064–72. doi: 10.1158/1078-0432.CCR-06-0910.

144. Rupp U, Schoendorf-Holland E, Eichbaum M, Schuetz F, Lauschner I, Schmidt P, et al. Safety and pharmacokinetics of bivatuzumab mertansine in patients with CD44v6-positive metastatic breast cancer: final results of a phase I study. *Anti-cancer Drugs*. (2007) 18:477–85. doi: 10.1097/CAD.0b013e32801403f4.

frontiers | Frontiers in Immunology

TYPE Original Research
PUBLISHED 15 March 2024
DOI 10.3389/fimmu.2024.1360063

OPEN ACCESS

EDITED BY
Monika Semmrich,
BioInvent, Sweden

REVIEWED BY
Urska Kamensek,
Institute of Oncology Ljubljana, Slovenia
Matthias Bozza,
Vector BioPharma, Switzerland

*CORRESPONDENCE
Frederik H. Igney
frederik.igney@boehringer-ingelheim.com
Matthias Klugmann
matthias.klugmann@boehringer-ingelheim.com

†These authors have contributed equally to this work

RECEIVED 22 December 2023
ACCEPTED 14 February 2024
PUBLISHED 15 March 2024

CITATION
Düchs MJ, Kratzer RF, Vieyra-Garcia P, Strobel B, Schönberger T, Groß P, Aljayyoussi G, Gupta A, Lang I, Klein H, Morilla SM, Hopf S, Park J, Kreuz S, Klugmann M and Igney FH (2024) Riboswitch-controlled IL-12 gene therapy reduces hepatocellular cancer in mice. *Front. Immunol.* 15:1360063. doi: 10.3389/fimmu.2024.1360063

Riboswitch-controlled IL-12 gene therapy reduces hepatocellular cancer in mice

Matthias J. Düchs[1], Ramona F. Kratzer[2], Pablo Vieyra-Garcia[3], Benjamin Strobel[4], Tanja Schönberger[4], Peter Groß[4], Ghaith Aljayyoussi[4], Aradhana Gupta[5], Isabel Lang[1], Holger Klein[6], Sandra Martinez Morilla[7], Stefan Hopf[3], John Park[2], Sebastian Kreuz[1], Matthias Klugmann[1*†] and Frederik H. Igney[2*†]

[1]Research Beyond Borders, Boehringer Ingelheim Pharma GmbH & Co. KG, Biberach an der Riss, Germany, [2]Cancer Immunology and Immune Modulation, Boehringer Ingelheim Pharma GmbH & Co. KG, Biberach an der Riss, Germany, [3]Cancer Immunology and Immune Modulation, Boehringer Ingelheim RCV GmbH & Co. KG, Vienna, Austria, [4]Drug Discovery Sciences, Boehringer Ingelheim Pharma GmbH & Co. KG, Biberach an der Riss, Germany, [5]Nonclinical Drug Safety, Boehringer Ingelheim Pharmaceuticals, Inc., Ridgefield, CT, United States, [6]Global Computational Biology and Digital Sciences, Boehringer Ingelheim Pharma GmbH & Co. KG, Biberach an der Riss, Germany, [7]Cancer Immunology and Immune Modulation, Boehringer Ingelheim RCV GmbH & Co. KG, Ridgefield, CT, United States

Hepatocellular carcinoma (HCC) and solid cancers with liver metastases are indications with high unmet medical need. Interleukin-12 (IL-12) is a proinflammatory cytokine with substantial anti-tumor properties, but its therapeutic potential has not been realized due to severe toxicity. Here, we show that orthotopic liver tumors in mice can be treated by targeting hepatocytes via systemic delivery of adeno-associated virus (AAV) vectors carrying the murine IL-12 gene. Controlled cytokine production was achieved *in vivo* by using the tetracycline-inducible K19 riboswitch. AAV-mediated expression of IL-12 led to STAT4 phosphorylation, interferon-γ (IFNγ) production, infiltration of T cells and, ultimately, tumor regression. By detailed analyses of efficacy and tolerability in healthy and tumor-bearing animals, we could define a safe and efficacious vector dose. As a potential clinical candidate, we characterized vectors carrying the human IL-12 (huIL-12) gene. In mice, bioactive human IL-12 was expressed in a vector dose-dependent manner and could be induced by tetracycline, suggesting tissue-specific AAV vectors with riboswitch-controlled expression of highly potent proinflammatory cytokines as an attractive approach for vector-based cancer immunotherapy.

KEYWORDS

il-12, cancer, immunotherapy, aptazyme riboswitch, inducible gene expression, regulatable gene therapy, AAV, Tet-ON

Introduction

Hepatocellular carcinoma (HCC) is the most common form of liver cancer and the third most common cause of all cancer-related deaths worldwide (1, 2). In patients with colorectal carcinoma (CRC) the liver is the most frequent site of metastasis, and fewer than 20% of patients diagnosed with metastatic CRC survive more than 5 years (3). Despite marked improvements in the management of these diseases, there is still a high unmet medical need, specifically to enable long-term tumor control.

IL-12 is a cytokine with strong immune-stimulating activity and has a key function in the induction and enhancement of cell-mediated immunity (4, 5). It is mainly produced by dendritic cells, monocytes, macrophages and B cells, and is involved in the induction of Th1 cell differentiation, activation of T and NK cells, and reprogramming of immunosuppressive cells. IL-12 is comprised of two subunits, p35 and p40, that are linked by disulfide bonds to form a p70 heterodimer. The IL-12 signaling pathway leads to phosphorylation of the transcription factor STAT4, which induces the proinflammatory and anti-tumor cytokine interferon-γ (IFNγ).

In preclinical studies, robust anti-tumor activity of IL-12 has been observed (4, 5). Clinical trials with systemically administered recombinant human IL-12 have caused severe toxicities, including on-study deaths (4–7). Therefore, several approaches to target the protein to tumors while minimizing systemic exposure are under evaluation (6, 7). Local delivery of the genes encoding IL-12 represents an ideal strategy for achieving sustained intratumoral IL-12 levels and reduction of side-effects (6).

Viral platforms, including adenovirus (Ad) or adeno-associated virus (AAV) vectors, have been used for local and sustained expression of IL-12. Intratumoral delivery is a pre-requisite for the reported efficacy following Ad.IL-12 gene therapy in a variety of preclinical cancer models [reviewed by (6)].

The ecdysone receptor-based RheoSwitch® Therapeutic System (RTS) incorporated in Ad-RTS-hIL-12 has extended survival in a mouse glioma model (7). The RTS gene switch relies on constitutively expressed transcription factors that are activated by oral administration of the synthetic small molecule veledimex. Patients with recurrent high-grade glioma who were treated by injection of this vector into the resection cavity wall and subsequent induction of IL-12 expression presented with inflammatory infiltrates at the tumor site, and indications of survival prolongation were observed (8). Severe adverse events reversed upon withdrawal of veledimex.

Hepatotropic AAVs carrying the IL-12 gene for constitutive expression can be administered systemically and were shown to reduce tumor burden and increase survival time in an orthotopic HCC model, suggesting that transduced hepatocytes produce IL-12 that stimulate anti-tumoral hepatic lymphocytes (9). In a technically more sophisticated approach, a liver-specific tetracycline (tet)-On system (10) was employed for regulatable AAV-mediated IL-12 expression following intravenous administration in a model of CRC (11). Induction of IL-12 transgene expression was achieved by oral doxycycline which prevented the establishment of liver metastases and induced a T-cell memory response to tumor cells without obvious side effects. A common feature of these gene switches is that they utilize protein-based systems that activate transcription upon ligand-binding. Ligand-dependent riboswitches, in contrast, function via mRNA-self-cleavage independently of co-expressed foreign proteins and inherently lack any immunogenicity risk.

The concept of this study was to transduce hepatocytes and have them express IL-12 that leads to activation of T and NK cells that infiltrate and attack tumor cells in the vicinity. We employed the previously described tet-dependent riboswitch K19 (12, 13) that allows potent regulation of AAV-based transgene expression (12) for controlling IL-12 expression in mice bearing orthotopic liver tumors. K19 is a synthetic hammerhead switch previously identified from a rationally designed riboswitch library (13) based on the Cb28 tetracycline aptamer (14) and the full-length hammerhead ribozyme N79 from Schistosoma mansoni (15). AAV8 was used as gene delivery vector due to its established hepatocyte tropism (16, 17). Vectorized IL-12 led to IFNγ production, infiltration of T cells and, ultimately, to tumor regression. We also optimized vectors carrying the human IL-12 gene in healthy mice and provide a pharmacokinetic/pharmacodynamic (PK/PD) model that can be used to predict safe and efficacious doses. In summary, these data demonstrate that riboswitch-enabled IL-12 gene therapy can be controlled in a spatio-temporal manner for a safe and efficient immunomodulatory effect using a rational combination of AAV serotype, vector dose, and tet dosing regimen.

Materials and methods

Expression constructs

DNA sequences encoding murine or human single-chain IL-12 were derived from previously described constructs IL-12.p40.L.Ap35 and IL-12.p35.L.Ap40 using the $(Gly4Ser)_3$ linker (18). The human IgG signal peptide coding sequence was introduced by PCR and cloned into pCR-TOPOP3.3. Constructs harboring the liver-specific LP1 promoter (19) to express IL-12 or a control anti-FITC scFv antibody (12), were obtained by restriction enzyme-mediated cloning utilizing published plasmid backbones (12) or by full gene synthesis (GeneArt, Thermo Fisher). The K19 riboswitch sequence flanked by $(CAAA)_3$ spacers has been described previously [(13)]. AAV-cis plasmids carried expression cassettes with SV40 poly-adenylation (pA) signal and were flanked by AAV2 inverted terminal repeats (ITRs). A set of optimized AAV constructs was designed and synthesized to express huIL-12 or mIL-12 driven by the LP1 promoter with the SV40 intron and a bovine growth hormone (bGH) polyadenylation (pA) signal. For these optimized constructs, coding sequences were modified to deplete CpG motifs in order to reduce the risk of uncontrolled immune response via Toll-like receptor 9 (TLR9) (20). These constructs also included 30-nt sequences (insulators) between the expression cassette and the ITRs in order to limit potential influence of the inherent transcriptional activity of the ITRs (21) The insulators were designed to avoid splice sites or transcription factor binding sites. Separately, the presence of C.G-rich tails

immediately outside the ITRs in the plasmid backbone has been shown to exert a destabilizing effect that can lead to diminished AAV producibility (22). To address this, we replaced these sequences with 30-nt sequences according to the insulator design.

Production of recombinant AAV vectors

Production and quantification of AAVs has been described previously (23). Briefly, AAVs were packaged in transiently transfected HEK293 cells and purified by PEG-precipitation, iodixanol-gradients and ultrafiltration. Genomic titers were determined by ddPCR. The three co-transfected plasmid constructs were as follows: One plasmid encoding the AAV cap gene; The AAV cis-plasmid containing the expression cassette flanked by ITRs; and a pHelper plasmid (AAV Helper-free system, Agilent).

Animals, treatments, and tumor model

8-10 week-old female C57BL/6NCrl mice used in this study were purchased from Charles River laboratories. AAVs were diluted to the desired concentration in PBS and administered into the tail vein in a volume of 100 µL per mouse, under isoflurane anesthesia (3.5-5 volume %). Tetracycline (tet) was formulated in 2-hydroxypropyl beta-cyclodextrin solution (HP-ß-CD, Sigma Aldrich) and administered as described previously (12). Preparation of tet hydrocholoride solution formulation in 20% Kolliphor HS15 was done as follows: 1M NaOH was added to tet HCl (Sigma Aldrich, CAS No.: 64-75-5) and the mixture was ultrasonicated for eight minutes to yield a light-yellow suspension.

Then, a 40% (w/v) solution of Kolliphor HS15 (Sigma Aldrich, CAS No.: 70142-34-6) and was added and again the formulation was ultrasonicated for eight minutes to yield a yellow solution. The pH was adjusted to 5 with 1M NaOH. Finally, deionized water was added resulting in final concentration of 20% (w/v) Kolliphor HS15 and the solution was sterile filtered.

20 µL of blood was collected by puncturing the *Saphenous vein* using K3-EDTA Microvette POCT 20 µL capillary microtubes (Sarstedt) followed by centrifugation. Blood plasma was used for quantitative measurements of biomarkers and IL-12. At the final blood draw, additional serum samples were prepared for the assessment of liver enzymes. For necropsy, animals were anaesthetized with isoflurane (3.5-5 volume %) and then euthanized via cervical dislocation. Organs of interest were dissected and snap-frozen in liquid nitrogen for DNA extraction or the preparation of protein tissue lysates. For tumor-cell application and spleen resection mice received Meloxicam (1.0 mg/kg in 10.0 ml/kg) subcutaneously 1 - 2 hours before surgery with a repetition 24 hours later. Then mice were anaesthetized with isoflurane (3.5-5 volume %) and luciferase-expressing Hepa1-6 tumor cells (1.0 x 10^6 cells in 50µL PBS) were injected into the spleen of each mouse and allowed to migrate into the liver for 5 min via splenic vein. Thereafter the spleen was resected. All animal experiments in this study were approved by the local German authorities and conducted in compliance with the German and European Animal Welfare Acts.

Bioluminescence imaging

Tumor volumes were determined by *in vivo* bioluminescence using an IVIS® Lumina III BLI system (Perkin Elmer) with a CCD-camera. For this purpose, 150 mg/kg (7.5 mL/kg) D-Luciferin in aqua dest. was injected *i.p.* 8 min before anesthetization. Light emission was measured 10 min post injection. Tumor-bearing mice were block-randomized according to tumor sizes measured by the *in vivo* BLI of the same day. For block-randomization, a robust automated random number generation within individual blocks was used (MS-Excel 2016).

Preparation of protein tissue lysates

Snap-frozen tissue samples were homogenized in 100 µL MSD lysis buffer (R60TX-2), using a Precellys-24 homogenizer (KT03961-1-009.2, VWR). Following addition of 900 µL lysis buffer, a second homogenization was carried out. Samples were then centrifuged. 700 µL of supernatant was recovered and protein concentration was determined using a BCA assay (Promega).

Determination of IL-12 and inflammatory biomarkers

Expression of IL-12, IL-15, IL-18, CXCL10, TNFα, and IFNγ was analyzed using the Mouse IL-12p70 Kit and the Proinflammatory Panel 1 Mouse Kit (K152ARB and K15048D, MSD) or the Human IL-12p70 Kit (K151QVD, MSD). The lowest standard of provided IL-12p70 was taken as lower limit of detection (LLOD). STAT4 and pSTAT4 were quantified using the respective MSD Kits (K150O and K150P).

Assessment of AST, ALT and GLDH enzyme activity

All measurements were performed using the Konelab PRIME 60 fully automated clinical chemistry analyzer and test kits from Thermo Scientific (according to the Konelab Chemistry Information Manual 12A/2003, March 2003) and spectrophotometrical assessment at 340 nm. Aspartate aminotransferase (AST) activity was measured by an enzymatic rate method (24) without pyridoxal-5'-phosphate for AST activation. Alanine aminotransferase (ALT) activity was measured by an enzymatic rate method based on the International Federation of Clinical Chemistry (IFCC) method (25) without adding pyridoxal-5'-phosphate. The removal of NADH was measured spectrophotometrically at 340 nm. Glutamate dehydrogenase (GLDH) activity was measured by an enzymatic rate method, using a kit supplied by Roche Diagnostics.

IL-12 *in vitro* bioactivity reporter assays

A HEK-Blue™ assay was used to prove IL-12 bioactivity *in vitro*. HEK-Blue™ IL-12 cells (InvivoGen, #hkb-il12) are designed to detect bioactive human and murine IL-12. To show *in vitro* bioactivity of IL-12 derived from AAV plasmids or AAV vectors, cells were cultured, transfected with plasmids or transduced with AAV vectors, and a reporter assay carried out according to manufacturer's instructions. To show bioactivity of IL-12 expressed from the AAVs *in vivo*, plasma obtained from AAV-injected mice was examined in the HEK-Blue™ assay.

Quantification of AAV vector genomes in tissue

Tissue samples were snap-frozen immediately after dissection. For DNA isolation, samples were homogenized in 900 µL RLT buffer (79216, Qiagen) + ß-mercapto-EtOH (1%), using a Precellys-24 homogenizer. Afterwards, samples were immediately placed on ice and subjected to Phenol-chloroform-isoamyl alcohol (77617, Sigma Aldrich) extraction. DNA was purified using the KingFisher (ThermoFisher) with the MagMAX DNA Multi-Sample Ultra 2.0 Kit (A45721). AAV vector genomes were detected after DNA extraction via singleplex ddPCR using the Automated Droplet Generator, QX200 Droplet Digital PCR System, and QX200 Droplet Reader (all Bio-rad). A custom TaqMan gene expression assay (#APDJ4HP; Thermo Scientific) was used as to detect the target region in the LP1 promoter. Oligonucleotide primers 5′-GGGAATGACTCCTTTCGGTAAGTG-3′ (forward) and 5′-CGCCCGCCTACGCT-3′ (reverse) and 5′-CCTGGGCAGTGT ACAGCT-3′ (probe) were utilized for this assay.

Histology and immunohistochemistry

Tissue samples of mouse livers were fixed in 4% PFA and paraffin embedded (i.e., formalin-fixed and paraffin embedded, FFPE). 3 µm thick sections of FFPE tissue on HistoBond+ slides (Marienfeld GmbH, Germany) slides were deparaffinized and rehydrated by serial passage through changes of xylene and graded ethanol for subsequent hematoxylin-eosin (H&E) and immunohistochemistry (IHC) staining. H&E staining was performed according to standard protocols (26). For the tolerability and efficacy study IHC was carried out on the automated Leica Bond™ platform (Leica Biosystems, Melbourne, Australia). Antigen retrieval was performed by incubating the sections in Leica Bond Epitope Retrieval Solution 1 (Citrate based, pH6, Cat# AR9961) for 30 minutes at 95°C for staining of CD45 and CD3 positive cells. For detection of CD8a positive cells antigen retrieval with Leica Bond Epitope Retrieval Solution 2 (EDTA based, pH9, Cat# AR9640) for 20 minutes at 95°C was performed. Sections were incubated with an anti-CD45 antibody (abcam, ab10558, rabbit polyclonal), anti- CD3 (abcam, ab5690, rabbit polyclonal), or an anti-CD8a antibody (abcam, ab209775, rabbit monoclonal, clone EPR20305), respectively. The antibodies were diluted (1:400, 1:200, or 1:1000, respectively) with Leica Primary Antibody Diluent (AR9352; Leica Biosystems, Nussloch, Germany) and incubated for 30 min at room temperature. In the experiment assessing the immune response induced by AAV.RS-mIL-12-noCpG, anti-CD8 detection was done on the Leica Bond RX using ER2 antigen retrieval, using D4W2Z clone at 1:800 dilution. anti-pSTAT4 IHC was done on the Ventana Discovery Ultra, using CC1 as antigen retrieval, using D2E4 clone at 1:400 dilution. Bond Polymer Refine Detection Kit (Cat# DS9800) was used for detection (3,3′Diaminobenzidine as chromogen, DAB) and counterstaining (hematoxylin).

Image analysis

For analysis, liver sections were scanned with an Axio Scan.Z1 whole slide scanner (Carl Zeiss Microscopy GmbH, Jena, Germany) using an 20x objective (0.22 µm/px) in bright field illumination. Tumor sizes were calculated on HE stained sections using the image processing software HALO® (Indica Labs, Corrales, NM, USA). A classifier based on DenseNET (27) was trained with sample regions from background, healthy and cancer tissue. For quantitative analysis of infiltrating cells, the percentage of the cells positive for CD45, CD3, CD8a, or pSTAT4, was calculated using the image processing software HALO 3.1 with CytoNuclear v2.0.9 module. Cell count analysis was then used to determine immunoreactive cells in tumor areas and normal tissue segmented in a pre-processing step using the trained classifier.

Transfection and transduction of cell lines

HEK293H and HepG2 cells were cultured in DMEM + GlutaMAX + 10% FCS at 37°C. 25,000 HEK293 cells per 96-well were seeded 24 h prior to transfection using the Lipofectamine-3000 kit (Invitrogen). Transduction of HepG2 cells was performed at MOI 100,000 and the media was not replaced before the end of the experiment (72 h). Tetracycline (Tet-HCl, Sigma-Aldrich) was added to the cells 1-2 h after transfection and simultaneously to AAV addition in case of transduction.

Pharmocokinetics/ pharmacodynamics modeling

The dynamics of AAV, tet and tumor growth were fitted using a compartmental model that was run in three sequential steps. The first step was fitting the pharmacokinetic (PK) parameters of tet. In the second step, the effect of tet upon the activation of IL-12 was modeled by fitting the data for multiple doses of AAV given in the presence and absence of tet including both the constitutively active

10.3389/fimmu.2024.1360063

and riboswitch-controlled types of the AAVs. Finally, the IL-12 tumor dynamics were fitted by fixing the tet and tet-specific parameters in the full model while estimating the growth rate, kill rate and EC50 of riboswitch-controlled IL-12 against the tumor as shown in the equations below. The final model was constituted of 10 differential equations as follows (Equations 1–10):

$$\frac{d_{AAVDose}}{d} = AAVDose * 0 \quad (1)$$

$$\frac{d_{gut}}{dt} = -k_{abs} \cdot gut \quad (2)$$

$$\frac{d_{plasma}}{dt} = k_{abs} \cdot gut - plasma \cdot \left(\frac{CL/F + Q_1/F}{V_c/F}\right) + \frac{Q_1/F}{V_{p1}/F} \cdot periph \quad (3)$$

$$\frac{d_{periph}}{dt} = plasma \cdot \frac{Q_1/F}{V_c/F} - \frac{Q_1/F}{V_{p1}/F} \cdot periph \quad (4)$$

$$TET_{conc} = \frac{plasma}{V_c/F} \quad (5)$$

$$Tet_{effect} = TET_{conc}^{h} \frac{TETconc^{h}}{TETconc^{h} + EC_{50}Tet^{h}} \quad (6)$$

$$\frac{dIL12\_a}{dt} = \frac{AAVDose \cdot kin}{AAVDose + EC_{50}(off)} + \frac{AAVDose \cdot kin}{AAVDose + EC_{50}(on)} \cdot Tet_{effect} - k_{out} \cdot IL12\_a \quad (7)$$

$$IL12 = IL12\_A + background \quad (8)$$

$$\frac{d_{effectcomp}}{dt} = k_{ein} \cdot IL12 - k_{eout} \cdot effectcomp \quad (9)$$

$$\frac{d_{cancer}}{dt} = k_{growth} \cdot cancer \cdot \frac{1 - cancer}{10^5} - \frac{E_{max} \cdot effectcomp}{EC_{50}cancer + effectcomp} \cdot cancer \quad (10)$$

Where *AAVDose* is the dose of AAV administered in the mouse; *gut* is representing the mass of administered tet in the gut; k_{abs} is the rate of absorption of tet to plasma per hour; *CL/F* is the estimated oral clearance of Tet from the systematic circulation; V_c/F is the volume of distribution of tet; V_{p1}/F *and* Q_1/F are the peripheral volume of distribution and intercompartmental clearance of tet, respectively; *periph* represents the mass of tet in the peripheral compartment; TET_{conc} is the concentration of tet in plasma; k_{in} is the maximal rate of generation of IL-12 and k_{out} represents the natural elimination rate of IL-12; $EC_{50}tet$ is the concentration of tet required to illicit 50% of the maximum stimulation of IL-12 production in the presence of the AAV; EC_{50} *(on)* and EC_{50} *(out)* are the concentrations of AAV required to achieve maximal stimulation of IL-12; k_{growth} represents the growth rate of the tumor per hour; k_{kill} is the maximal rate of tumor size reduction per hour; $EC_{50}cancer$ is half of the IL-12 concentration required to illicit the maximal kill rate; k_{ein} is the transfer parameter of drug to the effect compartment; and k_{eout} is the movement of drug back from the effect compartment to plasma. Data was fitted using RxODE/nlmixr within R(4.1.2). Data visualization was also performed via R using the ggplot2 package (3.4.0).

Statistical analysis

Statistical evaluations were performed utilizing GraphPad Prism Version 9.5.0 (GraphPad Software, LCC). All data are expressed as mean ± SEM. A normal distribution for all variables and equal variances across groups was assumed, and an unpaired two-tailed t-test against the specified group for statistical comparisons was executed. No alpha correction was implemented. The significance level (alpha) was set at 0.05, thus p-values less than 0.05 were considered statistically significant and marked with *, ** and, *** for $p < 0.05$, < 0.01 and < 0.001 respectively.

Results

Tetracycline-dependent control of IL-12 expression *in vitro* and *in vivo*

We have previously shown that the tet-dependent ribozyme K19 has the potential to control AAV-mediated reporter gene expression in mice using a hepatotropic AAV capsid and the hepatocyte-specific LP1 promoter (12). Features of this riboswitch-based expression control system include potent regulation, reversibility, and repeatable induction. Given the high liver exposure of tet, we hypothesized that this gene switch would enable liver-directed, inducible IL-12 expression following AAV-mediated gene delivery and allow for fine-tuned local immunotherapy of liver cancer. Figure 1A illustrates that vectorized IL-12 mRNA is stabilized following binding of tet by K19, resulting in onset of gene expression and subsequent therapeutic effects. In the absence of the ligand, basal expression is reduced due to K19 auto-cleavage and mRNA degradation. In a pilot experiment, we transfected HEK293 cells with plasmids expressing codon-optimized single-chain mIL-12 p40-linker-p35 or the p35-linker-p40 orientation and confirmed presence of bioactive IL-12 in the supernatant from either transfectant (Figure 1B). The p40-linker-p35 orientation has a superior stability (18) and was therefore used in all further experiments. We then cloned the mIL-12 gene into an AAV construct with the LP1 promoter and the K19 riboswitch in the 3'-UTR, and packaged the entire cassette into AAV9 (AAV9.RS-mIL-12). A control vector harboring mIL-12 and a catalytically inactive K19 switch (AAV9.mIL-12), was used to achieve constitutive IL-12 expression. We then transduced the human liver cancer cell line HepG2 with AAV9.RS-mIL-12 and observed that the highest tet-dose induced a 4.8-fold increase in mIL-12 production, reaching

10.3389/fimmu.2024.1360063

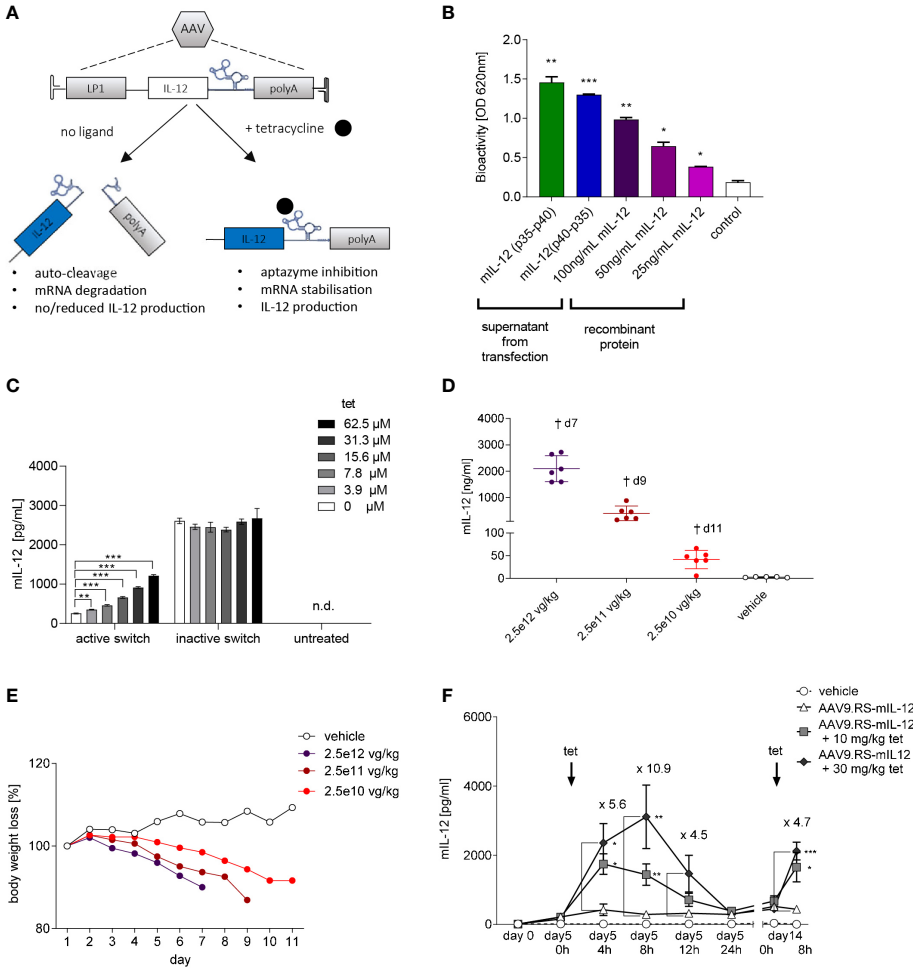

FIGURE 1
Riboswitch-controlled expression of single chain IL-12. **(A)** Schematic of AAV-mediated and tet-controlled expression of IL-12. **(B)** Bioactivity of single-chain murine IL-12 protein (mIL-12) produced by transfected HEK293 cells. Statistical analysis was conducted comparing groups to non-transfected HEK293 cells (control). **(C)** Tet concentration-dependent mIL-12 production in Hep G2 liver cells. Hep G2 cells were transduced with AAV9 harboring riboswitch-controlled mIL-12 cassette = active switch. Activation of riboswitch was assessed by comparing groups to no tet control (active switch, 0 µm). N= 3 biological replicates. **(D)** Application of mice with AAV9 for constitutive expression of murine IL-12 led to AAV dose-dependent increase of mIL-12 in plasma and **(E)** weight loss of mice. N= 6 animals per group. **(F)** Tet exposure-dependent mIL-12 production in C57BL/6NCrl mice. Mice were treated with either vehicle or 10^9 vg/kg body weight of AAV9 delivering riboswitch-controlled mIL-12 sequence (AAV9.RS-mIL-12). On day 5 and day 14 riboswitch was activated with 10 or 30 mg/kg tet and mIL-12 levels were assessed at the indicated time points in plasma. Statistical analysis was performed comparing to AAV group receiving no tet (AAV9.RS-mIL12). N= 5 animals per group.

45% of the expression levels mediated by the constitutively active AAV9.mIL-12 control (Figure 1C).

The encouraging *in vitro* biopotency data were the basis for a pilot *in vivo* dose-response study using AAV9.mIL-12. In this experiment, we delivered three different doses ($2.5x10^{10}$, $2.5x10^{11}$, $2.5x10^{12}$ vg/kg) to achieve constitutive mIL-12 expression and plasma exposure in C57BL/6NCrl mice. All mice in the AAV9.mIL-12 groups lost body weight in a dose-dependent manner that correlated with IL-12 levels (Figures 1D, E). The low-dose group displayed 48 ng/mL IL-12 in plasma, which was not tolerated, suggested by body weight loss starting five days following vector administration. Body weight loss can be interpreted as a pathological consequence of circulating IL-12 levels that originate from hepatocytes, and show the need for a gene switch with low background expression. The low vector dose of $2.5x10^{10}$ vg/kg was selected for a PK study on tet-induced IL-12 expression in naïve mice (Figure 1F). The study design included three groups of mice receiving AAV9.RS-mIL-12 or saline, and tet at 10 mg/kg or 30 mg/kg, on day 5 and day 14 (tet re-challenge) following vector delivery. At 8 h after the tet re-challenge, tet concentrations in plasma were 100 nM and 750 nM in the 10 mg and 30 mg tet groups, respectively. The plasma IL-12 levels showed tet dose-dependent induction. 30 mg/kg tet induced IL-12 almost 11-fold after 8 h over background levels (day 5, 0 h). Following the fast on-kinetic, IL-12 levels had returned to baseline after 24 h. The tet re-challenge induced IL-12 at a lower level of 4.7-fold, and the absolute IL-12 concentrations ranged between 2-3 ng/mL. In summary, these data showed repeatable and quick ON and OFF kinetics for tet-induced IL-12 expression *in vivo* following systemic AAV9.RS-mIL-12 delivery.

10.3389/fimmu.2024.1360063

AAV9.RS-mIL-12 dose finding in healthy mice

Next, we investigated RS-controlled IL-12 expression by multi-day tet exposure (Figure 2A). The aim of this study was to identify a vector dose that allowed for tet-dependent sustained induction of relevant IL-12 levels in plasma during tet administration, but full reversal to background levels upon tet retraction. Weight loss and liver enzymes were monitored as a measure of toxicity. The study design entailed delivery of AAV9.RS-mIL-12 at doses from $2.5x10^9$-$2.5x10^{12}$ vg/kg. Half of the animals of each group were subjected to twice daily (b.i.d.) tet applications for 5 consecutive days, while the other half received no tet. The body weight development was normal for all groups except the highest AAV9.RS-mIL-12 dose groups (with or without tet) and the constitutive AAV9.mIL-12 group (Figure 2B). This observation suggests that tolerated IL-12 levels were achieved in most dose groups. IL-12 levels in plasma showed vector dose-dependency during and after tet-induction (Figures 2C, D). Importantly, in the $2.5x10^{10}$ vg/kg dose group that had received tet, IL-12 levels had returned to background three days after the final tet exposure (Figure 2E). The same treatment group showed elevated levels of IFNγ, the key effector of IL-12-induced T-cell activation (Figure 2F). Liver enzymes of animals that received the $2.5x10^{10}$ vg/kg dose were not elevated at any time point of our investigation, independent of tet treatment (Figures 2G–I). In summary, the dose of $2.5x10^{10}$ vg/kg had the best combination of PK and safety.

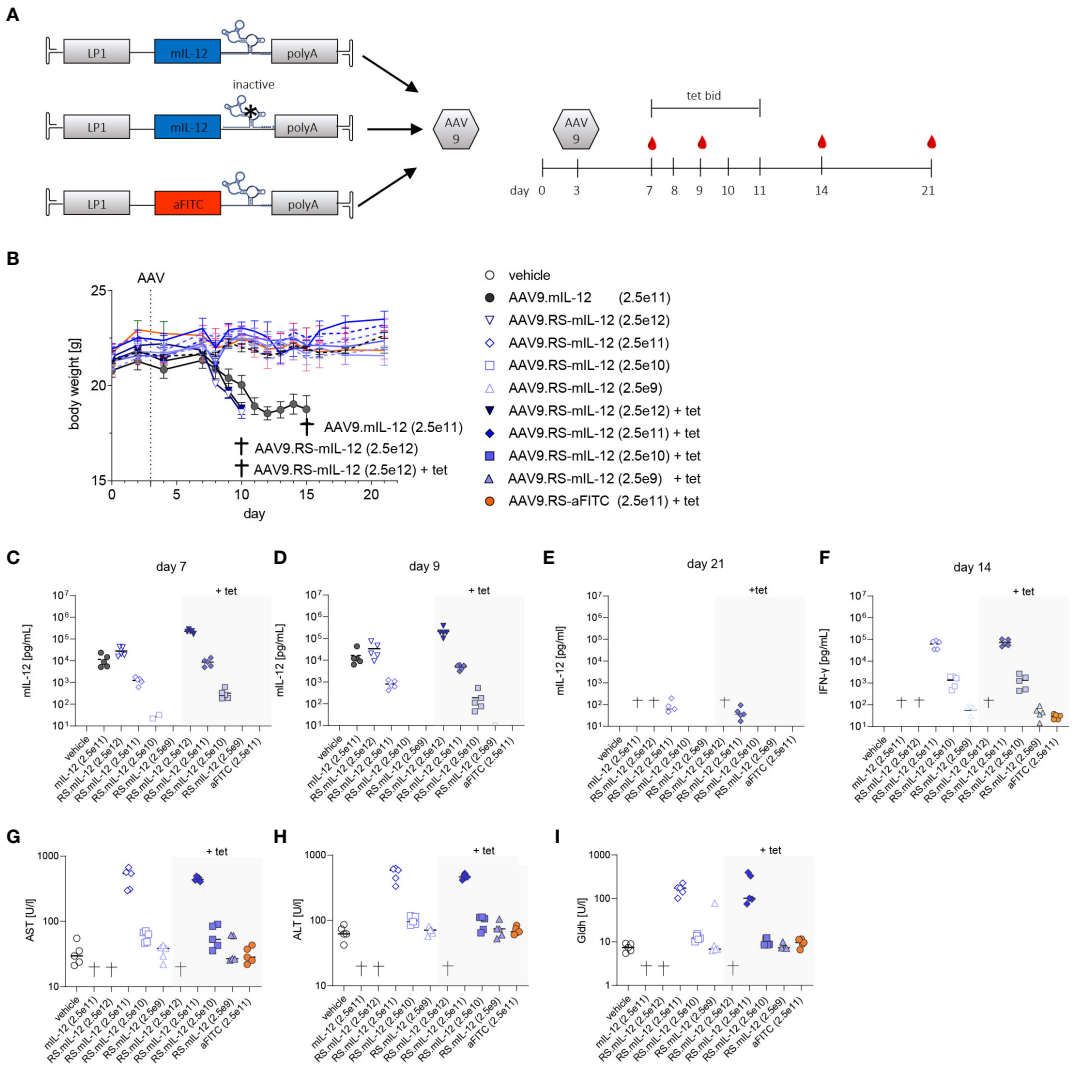

FIGURE 2
In vivo dose finding for AAV9-mediated and tetracycline-controlled mIL-12. **(A)** Schematic designs of applied cassettes; active (AAV9.RS-mIL-12), inactive switch (AAV9.mIL-12) and aFITC nanobody harboring vector control (AAV9.RS-aFITC) and experimental schedule for application of AAV, tet, blood sampling (red droplet). **(B)** Body weight development of AAV +/- tet treated C57BL/6NCrl mice. Groups that reached pre-defined humane endpoints are indicated by †. Weights are given as mean of groups and AAV doses are presented in vg/kg body weight. **(C-E)** Development of mIL-12 levels in plasma was assessed on days 7 **(C)**, 9 **(D)** and 21 **(E)**. **(F)** IFNγ levels in plasma were measured on day 14. **(G-I)** Level of liver enzymes – aspartate aminotransferase (AST), alanine aminotransferases (ALT) and glutamate dehydrogenase (GLDH) were assessed on final day of experiment. AAV doses are given as vg/kg body weight, N= 5 animals per group, tet bid = tet twice daily 30 mg/kg, Symbols shown only for values >10 pg/ml.

10.3389/fimmu.2024.1360063

Riboswitch-controlled IL-12 is safe and efficacious in a murine liver cancer model

To test whether HCC can effectively be treated with AAV9.RS-mIL-12, we used an orthotopic HCC mouse model. For this model, we generated a Hepa1-6 tumor cell line that stably expressed luciferase, so that tumor growth could be monitored by BLI *in vivo* over time. These tumor cells were injected on day 0 to form tumor nodules in the liver (Figure 3A). On day 3, virus preparations were injected intravenously. To induce transgene expression, tet was administered twice daily from day 7 to 11. Animals were kept for another week without tet and were euthanized for analysis on day 18.

To control for transgene induction, blood samples were taken and IL-12 levels in plasma were determined. Constitutive expression with $2.5x10^{11}$ vg/kg of AAV9.mIL-12 resulted in IL-12 plasma levels above 10 ng/ml at all time-points (Figure 3B). Like in the previous study in healthy mice, these levels led to body weight loss, starting around day 11 (Supplementary Figure 1), and 7 out of 12 mice were euthanized prematurely in this group over the course of the study. In animals treated with $2.5x10^{11}$ vg/kg of AAV9.RS-mIL-12, tet-induced IL-12 expression reached 7.5 ng/ml in plasma on day 7 which dropped below 1 ng/ml on days 14 and 18 after stopping tet administration. In this group, no body weight loss was observed except for one animal, indicating the increased safety profile of riboswitch-controlled IL-12 expression. In animals treated

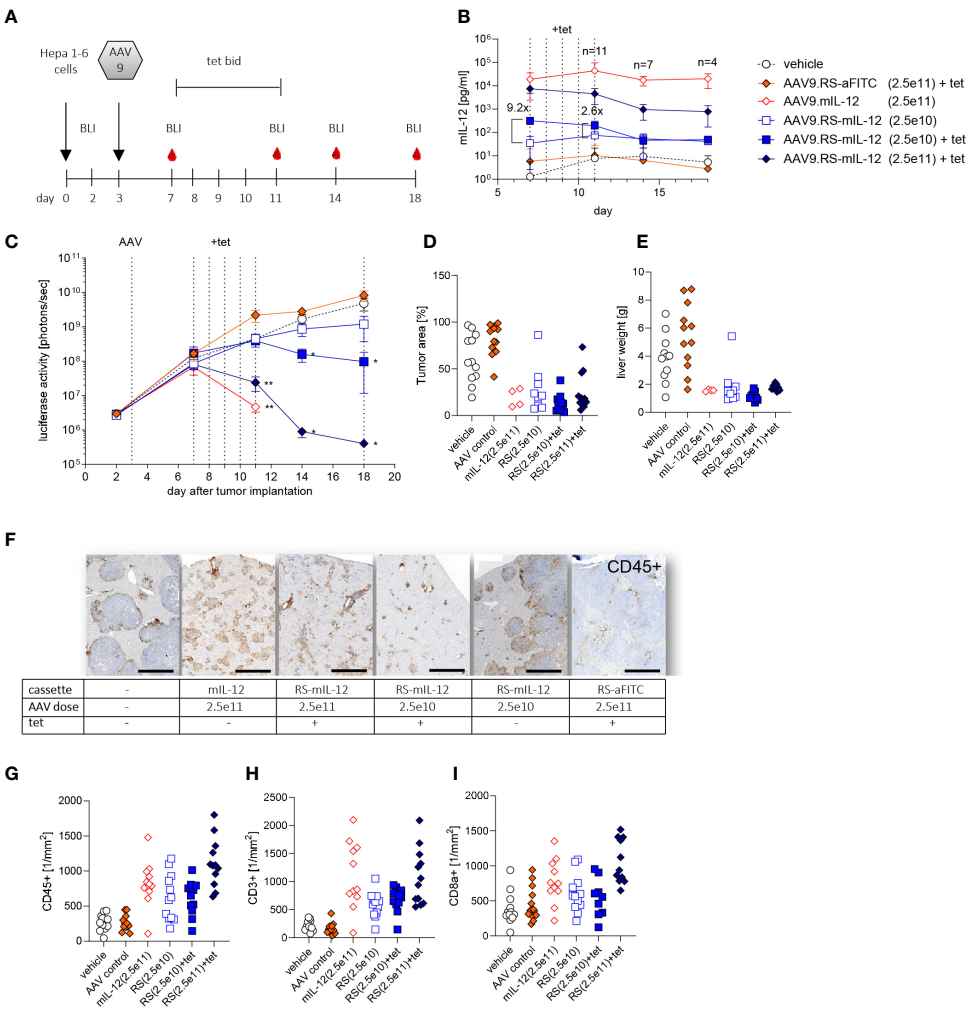

FIGURE 3
Tolerability and efficacy of riboswitch-controlled mIL-12 expression in murine liver cancer model. **(A)** Schedule of treatment and sample collection in mouse tumor study. On day 0 all animals received luciferase expressing Hepa 1-6 tumor cells, on day 3 AAVs were applied. BLI = time point of bioluminescence measurement for assessment of Hepa 1-6 tumor cell growth, tet bid = tet twice daily with 30 mg/kg, N=12 per group at start of experiment. **(B)** mIL-12 levels were assessed in plasma; indicated is the fold increase of mIL-12 after tet activation comparing the two groups receiving $2.5x10^{10}$ vg/kg of AAV9.RS-mIL-12 with or without activation by tet. AAV doses given as vg/kg body weight. **(C)** Tumor growth was analyzed via BLI over 18 days and treatment effects were assessed by comparison to vehicle group receiving no AAV. **(D)** Tumor growth was further assessed by histological analysis of liver tissue sections on final day of experiment. **(E)** As additional indicator for tumor growth total weights of livers were assessed. **(F)** Cellular immune response to treatment was assessed. Representative liver tissue sections stained for CD45+ cells are shown. Scale bar = 1 mm **(G-I)** Quantification of immune cells was conducted for CD45+ **(G)**, CD3+ **(H)**, and CD8+ **(I)** cells in liver sections.

10.3389/fimmu.2024.1360063

with a ten-fold lower vector dose ($2.5x10^{10}$ vg/kg of AAV9.RS-mIL-12), basal expression of around 50 pg/ml IL-12 was observed in the absence of tet, which remained constant over time. Tet administration raised IL-12 levels to 318 pg/ml, which dropped to ~50 pg/ml after ceasing tet treatment. In the control groups (vehicle or AAV9.RS-aFITC), IL-12 levels remained below 10 pg/ml. These data confirmed that the IL-12 level was dependent on the vector dose and could be induced by tet in animals treated with AAV9.RS-mIL-12.

Tumor growth was monitored by BLI (Figure 3C). In control groups, tumor burden increased continuously. In animals with constitutive IL-12 expression, after initial tumor growth, tumor size declined until the animals had to be euthanized due to body weight loss. Similarly, induction by tet on day 7 in animals with riboswitch-controlled IL-12 led to an AAV-dose-dependent reduction of tumor burden with almost complete regression in the high dose group. In the absence of tet, only a moderate effect on tumor growth inhibition was observed.

At the end of the experiment, tumor burden was also determined by quantifying the tumor area in histological liver sections (Figure 3D) and by measuring liver organ weight, comprised of liver and tumor tissue (Figure 3E). These data were in line with the BLI measurements.

Immunohistological analysis of liver sections revealed that IL-12 expression resulted in an increase of immune cells (Figures 3F–I). The number of cells depended on the IL-12 expression level. A large fraction of the infiltrated cells were $CD3^+$ and $CD8^+$ T cells.

Taken together, these results suggest that IL-12 expression led to recruitment of cytotoxic T cells, which controlled tumor growth, and that riboswitch-regulated IL-12 was safe and efficacious.

Optimization of human IL-12 AAV vector

We then performed AAV cassette optimization by combining genetic elements that have been reported to result in beneficial AAV-mediated transgene expression in hepatocytes of both animals and human subjects (19, 28, 29). The introduction of an intron and a 5'-UTR element to the AAV cassette increases transgene product levels *in vivo* (29). Therefore, we adopted a clinically validated cassette design including the LP1 promoter, an SV40 intron (19), the coding sequence of huIL-12 (p40-linker-p35), the K19 Tet-switch, and the bovine growth hormone pA sequence (pAAV.RS-huIL-12) (Figure 4A). The cellular Toll-like receptor 9 (TLR9) recognizes unmethylated cytosine-phosphate-guanosine motifs (CpG) motifs in the therapeutic expression cassettes packaged in an AAV capsid and induces innate and adaptive immunity, thereby limiting the duration of gene therapy (20). We therefore created an equivalent AAV-construct to pAAV.RS-huIL-12 in which CpGs of the IL-12 coding sequence were depleted (pAAV.RS-huIL-12-noCpG). AAV8 shows less extrahepatic biodistribution than AAV9 (30). Therefore, it is more suitable for liver-restricted gene delivery, which is required for our concept of vectorized IL-12 immunotherapy. To characterize both designs, AAV.RS-huIL-12 and AAV.RS-huIL-12-noCpG were packaged as AAV8 vectors and delivered to C57BL/6NCrl mice at a single dose that resulted in tet-dependent induction of bioactive huIL-12 (Figure 4B). We then performed a dose escalation study using both AAV8.RS-huIL-12 and AAV8.RS-huIL-12-noCpG in C57BL/6NCrl mice and observed no difference in the performance of the two designs as assessed by the huIL-12 levels in plasma (Figure 4C). Vector genome analysis in liver confirmed comparable transduction of dose-matched groups

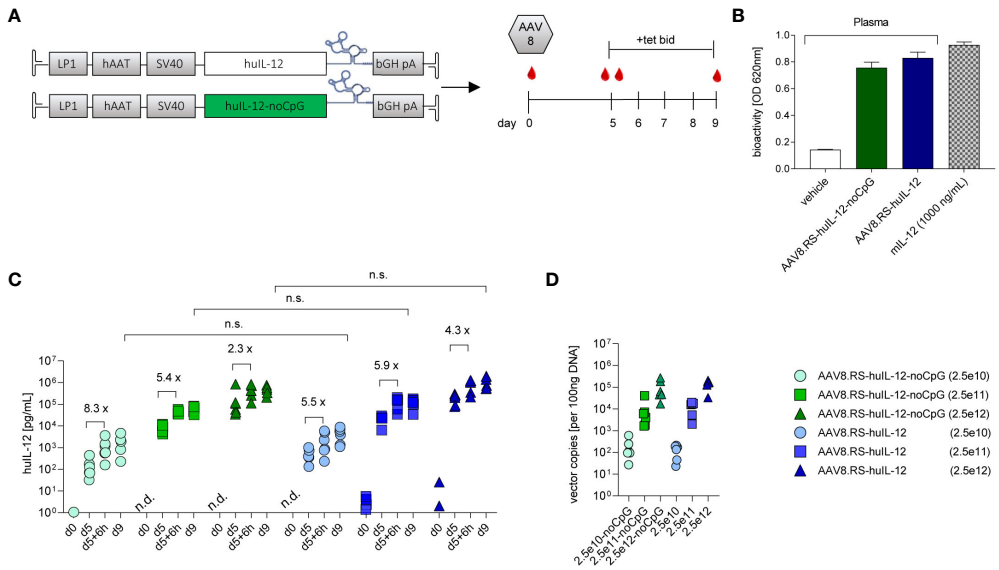

FIGURE 4
Optimization of human IL-12 (huIL-12) AAV vector candidate. **(A)** Schematic of CpG containing (huIL-IL12) and CpG-depleted (huIL-12-noCpG) riboswitch-controlled expression cassettes for human IL-12 (huIL-12), and respective study design for their comparison in C57BL/6NCrl mice. **(B)** Bioactivity measurement of IL-12 in plasma of mice injected with AAV8.RS-huIL-12-noCpG or AAV8.RS-huIL-12. **(C)** Expression efficacy of optimized sequences were compared by measurement of huIL-12 protein levels in plasma on day 9, 6h after tet activation. n.s., non-significant. Riboswitch activation effects were assessed comparing huIL-12 levels before and 6h after tet treatment on day 5. Symbols shown only for values >1 pg/ml. n.d. not detectable. **(D)** Transduction efficacy was assessed by quantification of vector genomes in liver tissue. AAV doses = vg/kg body weight, tet bid = tet twice daily 30 mg/kg, N=6 per group,.

10.3389/fimmu.2024.1360063

(Figure 4D). Based on these data, we nominated AAV8.RS-huIL-12-noCpG as the lead candidate and used the mouse surrogate (AAV8.RS-mIL-12-noCpG) for subsequent pre-clinical PK/PD experiments as huIL-12 does not act on murine cells (31).

AAV8.RS-mIL-12-noCpG is efficacious, and IL-12 levels correlate with efficacy

To confirm the efficacy of the mouse surrogate of the lead candidate and to determine efficacious doses, we titrated AAV8.RS-mIL-12-noCpG in the orthotopic HCC mouse model (Figure 5A). All animals received tet from day 7 to 11 after tumor implantation. The level of induced IL-12 in plasma was dependent on the AAV dose and dropped to pre-tet levels after ceasing tet administration (Supplementary Figure 2). Tumor growth inhibition depended on the AAV dose with complete responses in all animals of the highest dose group (Figure 5B). Doses above $5.0x10^{10}$ vg/kg resulted in >90% of tumor growth inhibition with all animals responding. Treatment with $1.5x10^{10}$ vg/kg resulted in tumor growth inhibition of ~50%. In the lowest dose group ($5.0x10^{9}$ vg/kg), only minimal IL-12 expression was detected with almost no tumor growth inhibition. Tumor burden was also determined by measuring liver organ weight (Figure 5C) which confirmed the BLI measurements. Because of the variability between animals of the same dose group, we analyzed the relationship of IL-12 levels and tumor growth in individual animals (Figure 5D). Interestingly, there was a clear correlation between the level of IL-12 induced by tet and the reduction of tumor BLI signal. In general, induction of IL-12 to more than 100 pg/ml in plasma resulted in tumor regression, whereas tumors continued to grow in animals with lower levels. To investigate the T cell response, immunohistological analysis of liver sections was performed at the end of the study. The number of $CD3^+$ T cells was quantified separately within or outside of the tumor area (Figures 5E, F). In the vehicle-treated group, a low number of T cells was seen inside and outside of the tumor. Induction of IL-12 by tet from days 7-11 in the riboswitch-controlled group resulted in dose-dependent increase of intratumoral $CD3^+$ cells on day 15, suggesting the activation of an anti-tumor T cell response. Importantly, outside of the tumor tissue (in liver parenchyma), $CD3^+$ cell numbers remained low in all groups. These results confirmed that the mouse surrogate of the lead candidate (AAV8.RS-mIL-12-CpG) showed efficacy at doses $\geq 1.5x10^{10}$ vg/kg and that IL-12 levels correlated with tumor growth inhibition.

IL-12 induces T cell infiltration preferentially into the tumor and persistently activates the immune response

To analyze the immune response in more detail, we performed a dedicated study with AAV8.RS-mIL-12-noCpG in the orthotopic HCC model with the same schedule as before and euthanized animals for specimen collection at three different time-points: on day 7 (after first tet administration), day 8, and day 14 (three days after the last tet dose). The tumor area was quantified in histopathological liver sections (Figure 6A). As in the previous experiment, IL-12 – either expressed constitutively or induced by tet – resulted in reduction of tumor size. In the lower AAV dose group

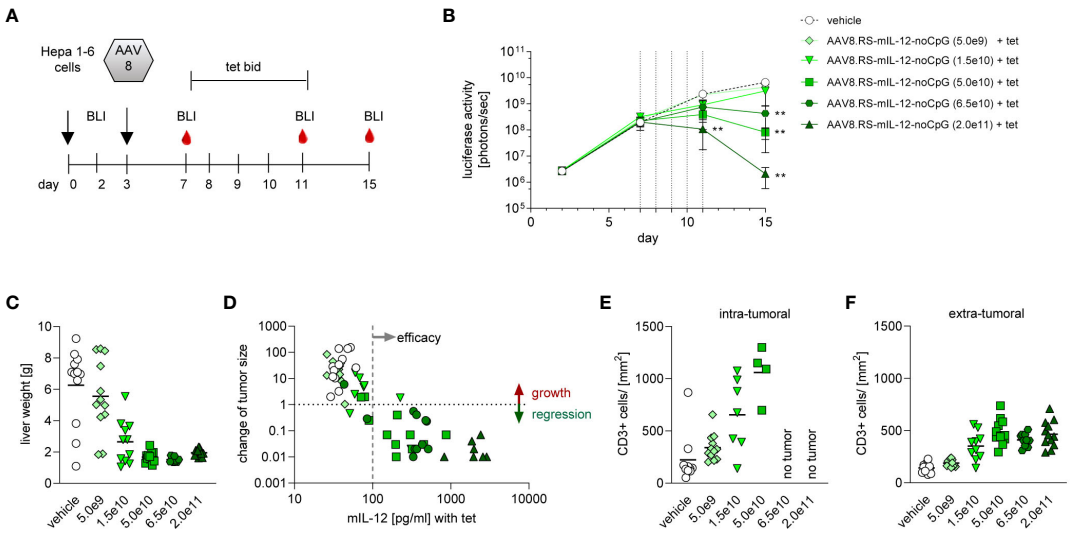

FIGURE 5
Dose finding with AAV8.RS-mIL-12-noCpG in HCC model. **(A)** Treatment and sampling schedule for analysis of AAV8.RS-mIL-12-noCpG in C57BL/6NCrl mice. Animals were treated with luciferase expressing Hepa 1-6 tumor cell on day 0, AAV was administered on day 3 and riboswitch was activated with 30 mg/kg body weight of tet from day 7 to 11, twice daily. **(B)** Tumor growth was assessed via luciferase activity measurement on day 3, 7, 11 and 15. Statistical effects were assessed comparing signals of treatment group to signals of vehicle treated group. N=12 per group. **(C)** As a second indicator for tumor growth liver weight was measured. **(D)** Effects of mIL-12 levels on tumor growth were visualized by plotting mIL-12 plasma levels vs changes of tumor size for individual animals. Change of tumor size was calculated by comparing luciferase signal on day 15 (end of experiment) vs day 7 (start of tet treatment). **(E, F)** Quantitative analysis of CD3 staining of liver tissue sections; CD3+ cells in tumor tissue **(E)**, and in non-tumor liver tissue **(F)**.

10.3389/fimmu.2024.1360063

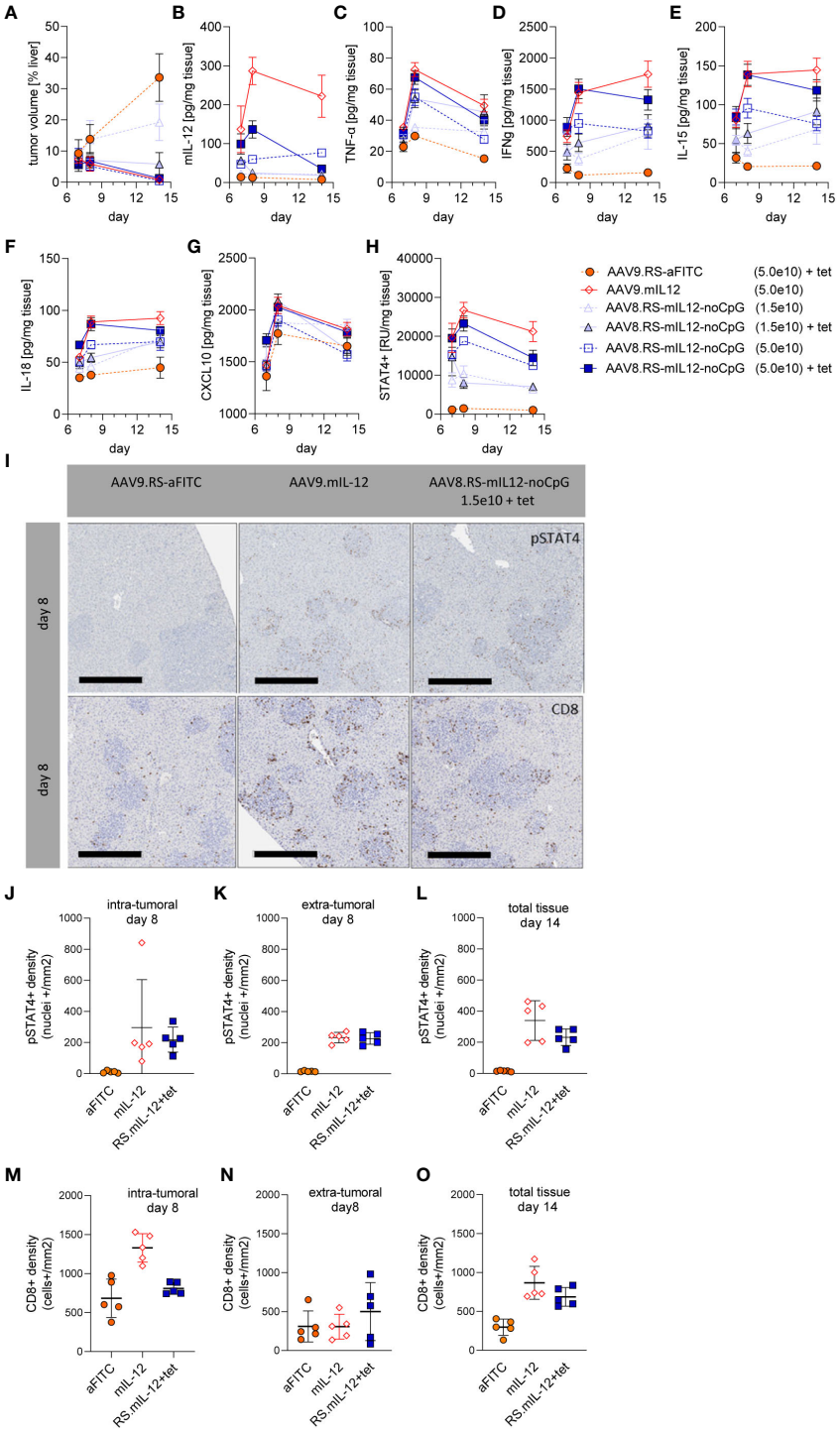

FIGURE 6
Immune response induced by AAV8.RS-mIL-12-noCpG in HCC model. In the HCC model, mice were treated with tumor cells on day 0, AAVs on day 3, and 30 mg/kg tet twice daily on days 7-11. Groups of mice were euthanized for analyses on day 7, 8 or 14 after tumor inoculation and **(A)** tumor volume, and levels of **(B)** mIL-12, **(C)** TNF-α, **(D)** IFNγ, **(E)** IL-15, **(F)** IL-18, **(G)** CXCL10 and **(H)** pSTAT4 were assessed in liver tissue. **(I)** Representative pictures of immunohistologically stained liver sections for pSTAT4+ cells (upper row) or CD8+ cells (lower row), 8 days post tumor inoculation, scale bar = 400 µm. Quantitative analysis of histological stained liver tissue for pSTAT4+ nuclei on day 8 **(J)** intra-, or **(K)** extra-tumoral, and **(L)** of total tissue on day 14. Analysis of liver tissue stained for CD8+ cells on day 8 **(M)** intra-, or **(N)** extra-tumoral or **(O)** of total tissue on day 14. N=5 per group and time point, AAV doses = vg/kg body weight.

(1.5x10^9 vg/kg), induction was necessary for efficacy, whereas in the higher dose group (5.0x10^9 vg/kg) basal IL-12 expression already induced tumor reduction. Quantification of IL-12 levels in plasma confirmed highest IL-12 levels by constitutive expression, AAV dose dependency and inducibility of IL-12 levels by tet (Supplementary Figure 3). Cytokines were also quantified in liver lysates (Figures 6B–G). Without tet induction, IL-12 tissue levels remained constant over time and depended on the AAV dose as in

plasma. Both the constitutive expression and the high dose group with tet displayed elevated IL-12 tissue levels on day 7, which further increased on day 8. Ceasing tet administration led to reduction of IL-12 tissue levels in the riboswitch-controlled group on day 14 as expected. The low dose AAV8-RS-mIL-12-noCpG group confirmed these patterns on days 7 and 14. However, the value on day 8 was unexpectedly low, which might be explained be a technical problem in the virus injection in these animals or the preparation of samples for analysis.

We confirmed that IL-12 expression induced IL-12 receptor signaling by determining the amount of phosphorylated STAT4 (pSTAT4) which was in line with IL-12 levels (Figure 6H). Interestingly, IFNγ, one of the downstream mediators of IL-12, was upregulated and remained high even after ceasing tet administration, suggesting a sustained immune response (Figure 6D). Other proinflammatory cytokines or chemokines followed similar patterns as IL-12 or IFNγ.

To investigate the location of IL-12R signaling, immunohistological analysis of liver sections was performed (Figures 6I–L). Staining for pSTAT4 confirmed that IL-12 induced persistent IL-12 receptor signaling which was absent in the control group at all time points. On day 8, pSTAT4 was detected to a similar degree within or outside of the tumor tissue area. On day 15, the tumor area was too small to quantify the intra- and extratumoral staining separately. To investigate the cytotoxic T cell response, $CD8^+$ T cells were stained and quantified in the liver sections (Figure 6I, M–O). With constitutive IL-12 expression (AAV9.mIL-12) the number of intratumoral $CD8^+$ T cells was increased compared to vector control on day 8. Induction of IL-12 by tet from day 7 in the riboswitch-controlled group did not yet elevate intratumoral $CD8^+$ T cell numbers on day 8 but seemed to require a longer treatment. Although on day 15 tumor area was too small to quantify intra- and extratumoral staining, qualitatively there was a high $CD8^+$ cell density at the regressing tumor lesions while the $CD8^+$ cells in the liver parenchyma remained low.

Tolerability of AAV8.RS-mIL-12-noCpG in healthy mice

As toxicity is a major concern of IL-12 therapy, we analyzed in detail the tolerability of our vectorized and riboswitch-controlled IL-12 by administering a wide range of AAV8.RS-mIL-12-noCpG doses to non-tumor bearing, healthy mice. First, we studied an acute setting in which IL-12 was induced by tet using the same regimen as in the efficacy studies (Figures 7A, B). In the highest dose group ($1.3x10^{12}$ vg/kg), all animals had to be euthanized between day 11 (last day of tet administration) and day 15 due to ataxia and/or poor general condition. These animals exhibited IL-12 levels in plasma above 45 ng/ml after induction (Supplementary Figure 4). Animals in the second highest dose group ($2.5x10^{11}$ vg/kg) had to be euthanized about one week later mainly because of a distended abdomen due to ascites. Tet-induced IL-12 plasma levels were at 6.2 ng/ml, and liver enzymes were increased in most of the animals at the time of euthanasia. All doses $\leq 5x10^{10}$ vg/kg were well tolerated without adverse events. Also, in the long-term follow-up of these animals after stopping tet application, no adverse findings were observed.

As AAV8.RS-mIL-12-noCpG treatment resulted in expression of IL-12 even in the absence of tet, we performed a tolerability study in a chronic setting without induction by tet to determine which basal IL-12 levels were tolerated long-term (Figures 7C–N). Healthy mice were injected with a wide range of AAV8.RS-mIL-12-noCpG doses and monitored for 5 weeks. At the highest AAV dose used ($1.5x10^{12}$ vg/kg), all animals lost body weight over the course of the study (Figure 7C) and had to be euthanized prematurely (Figure 7D). At 5.0 $x10^{11}$ vg/kg and $1.5x10^{11}$ vg/kg, only one animal per group had to be euthanized after more than 3 weeks. All other animals did not display any macroscopic observations.

At the end of the study, several organs were preserved for further analysis. The organ weights of liver, spleen and kidney were determined (Figure 7E). Organ weights were not available for mice that underwent unscheduled early termination. Higher increases in spleen and liver weights were present at $\geq 1.5x10^{11}$ vg/kg in all animals followed by animals at $5.0x10^{10}$ vg/kg, and no changes in weights at $1.5x10^{10}$ vg/kg. Kidney weights were not affected at any dose level. A detailed histopathological examination revealed adverse microscopic findings in spleen, liver, and bone marrow in affected animals. In the liver, microscopic findings included minimal to moderate mixed cell inflammation, minimal to moderate hepatocyte degeneration, minimal to slight single cell necrosis, and minimal thrombosis. The spleen displayed minimal to severe decrease in lymphocyte cellularity, minimal to severe increase in cellularity of stromal cells, minimal thrombosis and minimal to severe extramedullary hematopoiesis. In the bone marrow, adverse microscopic findings were minimal to moderate decrease in erythroid and/or myeloid cellularity and/or minimal to severe necrosis. These findings were more prevalent and more severe in higher dose levels. In the group injected with $1.5x10^{10}$ vg/kg, findings were only of minimal severity grade with low incidences and were considered non-adverse. Liver histopathology changes correlated with an increase in plasma liver enzymes in a dose-dependent manner at the end of the study (Figures 7F–H).

We determined basal expression of IL-12 in the plasma over the course of the study (Figure 7I). Overall, the levels were dependent on the AAV dose as before and showed a small decline from day 5 to day 32. At doses ≤ 5.0 $x10^{10}$ vg/kg, no or only minimal IL-12 plasma levels were detected. At the highest dose ($1.5x10^{12}$ vg/kg), IL-12 levels on day 5 were >10 ng/ml (mean 14 ng/ml) and remained high until the day of early unscheduled termination. In the other groups, surviving animals had IL-12 plasma levels<5 ng/ml. At the end of the study, additional cytokines were increased in plasma dependent on the AAV dose and may indicate immune activation and a potential safety liability (Figures 7J-N).

In summary, we observed that high levels of IL-12 could induce several adverse findings, such as body weight loss, ascites, elevated liver enzymes and plasma cytokines, increased weight of liver and spleen, and histopathological changes in spleen, liver and bone marrow. Safety of AAV8.RS-mIL-12 was dependent on the dose with no findings at $\leq 1.5x10^{10}$ vg/kg and minimal findings at $5.0x10^{10}$ vg/kg.

10.3389/fimmu.2024.1360063

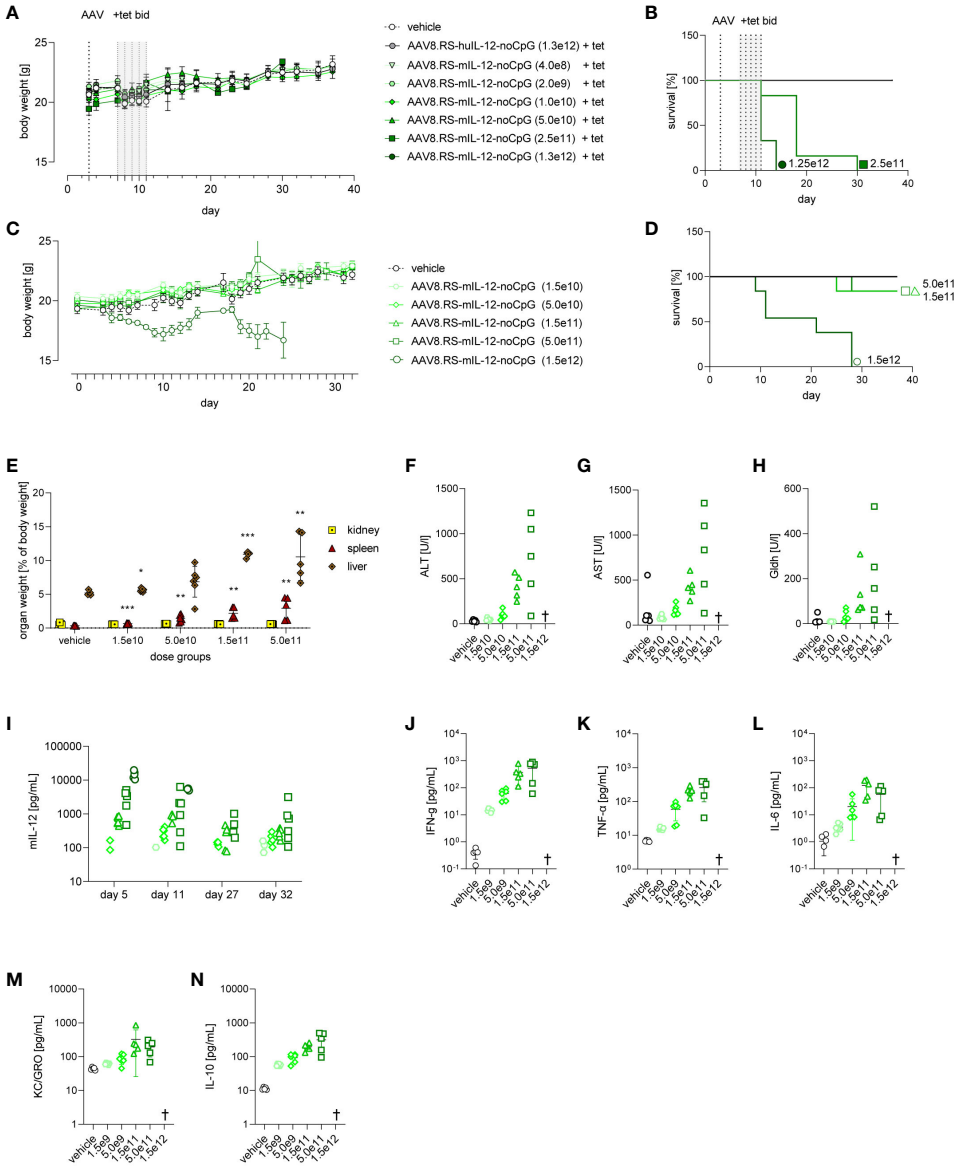

FIGURE 7
Tolerability of AAV8.RS-mIL-12-noCpG in healthy mice with and without tetracycline induction of mIL-12. **(A)** Body weight development of mice receiving $1.5x10^{10}$ to $1.5x10^{12}$ vg/kg of AAV8.RS-mIL-12-noCpG on day 3 and 30 mg/kg of tet twice daily on days 7-11. **(B)** Survival curves of AAV dose groups with tet-induced switch activation. **(C)** Body weight development of mice after AAV application on day 0 receiving no tet. **(D)** Survival curves of AAV dose groups receiving no tet. **(E)** Effects of AAV doses without tet on organ weights of kidney, spleen and liver weights, were assessed and statistically compared with respective organ weight of vehicle group. **(F)** Levels of aspartate aminotransferase (AST), **(G)** alanine aminotransferases (ALT), and **(H)** glutamate dehydrogenase (GLDH) were assessed on day 32 at the end of study. **(I)** mIL-12 plasma levels on day 5, 11, 27 and 32. Symbols shown only for values >10 pg/ml. On final day of study cytokine levels of **(J)** IFNγ **(K)** TNF-α and **(L)** IL-6, **(M)** KC/GRO, **(N)** IL-10, were measured in plasma. AAV doses = vg/kg body weight, tet bid = tet twice daily 30 mg/kg body weight, N=6 per group. † = euthanized groups. *p< 0.05, **p< 0.01; ***p< 0.001.

Increase of tet dose and PK/PD modeling

In our tumor and tolerability studies, tet has been used at a fixed concentration of 30 mg/kg. In Figure 1D we have observed that an increase of the tet dose from 10 mg/kg to 30 mg/kg led to higher IL-12 induction. Therefore, we tested whether an increase of the tet dose to 90 mg/kg would further improve the dynamic range of expression and hence, the induction window (Figure 8A). A clear induction of IL-12 by tet was only observed at the highest vector dose used (5.0×10^{11} vg/kg). Induction from baseline was 4.9-fold for 30 mg/kg tet and 5.6-fold for 90 mg/kg. This moderate difference indicated that at 30 mg/kg tet almost complete aptazyme inhibition and mRNA stabilization was achieved and that higher tet doses would not increase the therapeutic window.

PK/PD modeling was performed to quantify the potency of AAV.RS-mIL-12 + tet in mice and its effect on tumor growth (Figures 8B, C). The modeling allowed for parameterizing the effect of AAV to optimize dosage and to estimate with precision the

10.3389/fimmu.2024.1360063

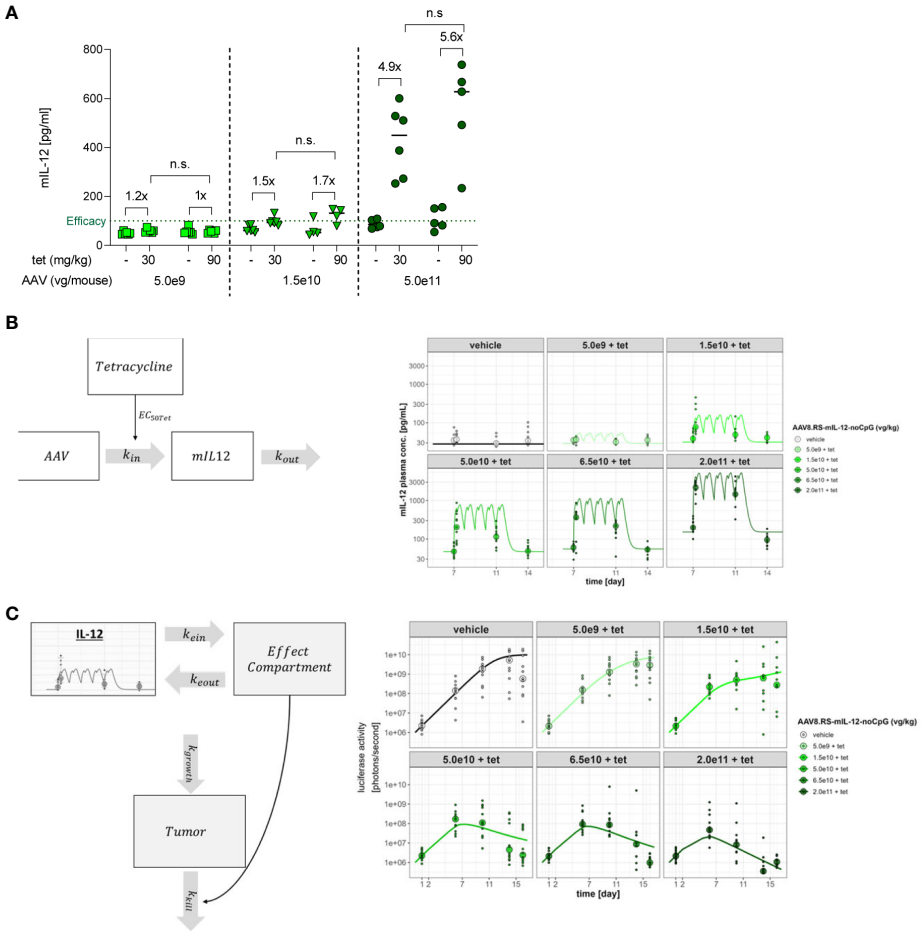

FIGURE 8
Induction of mIL-12 with different tetracycline doses and PK/PD modeling for IL-12 and tumor growth. **(A)** mIL-12 induction after tet doses of 30 or 90 mg/kg in C57BL/6NCrl mice receiving 5.0x10^9, 1.5x10^{10}, or 5.0x10^{11} vg/kg of AAV8.RS-mIL-12-noCpG. Plasma was collected 21 days post AAV application, before and 6 h after tet administration. N=6 per group. n.s., not significant **(B)** PK/PD model. The model is implemented in two stages. The first stage describes the relationship between the AAV dose, tet plasma exposure and levels of generated IL-12 over time according to the dosing intervals of tet. **(C)** The second stage of the model defines the relationship between generated IL-12 levels and tumor elimination. The model assumes an effect compartment to allow for the apparent delayed and prolonged effect of IL-12 upon the tumor where the drug moves to the effect compartment, guided by parameters k_{ein} and k_{eout}. The effect of IL-12 on tumor size was assumed to follow an E_{max} relationship with a hill slope of 1. Growth of the tumor is defined by the capacity limited parameter k_{growth} while the tumor reduction is expressed by the parameter k_{kill} which reflects the maximal rate of tumor elimination. Plots in **(B, C)** are based on the treatment scheme used in tumor studies.

minimum required IL-12 level to achieve activity as well as the level of tet required to fully activate IL-12 expression (Table 1). The required tet exposure was calculated to estimate whether the antibiotic can be given at safe doses in humans given its known clinical PK profile. Modelling showed an EC50 of 348 nM for tet in mice and, thus, demonstrated that safe doses of the drug can be given clinically to activate AAV.RS-IL-12. The modeling also revealed a ~15-fold higher potency of AAV.RS-IL-12 in presence of tet compared to absence of tet, confirming that induction of IL-12 by tet increases efficacy. With this complex PK/PD relationship being established, it is possible to translate the *in vivo* activity in mice to predicted human activity. However, a few caveats remain in the translation which include the uncertainty about the innate turnover levels of IL-12 in mice and humans and any variables that might change the response of a tumor to murine or human IL-12.

Discussion

HCC and CRC with liver metastasis are indications with high unmet medical need. For a long time, the highly proinflammatory cytokine IL-12 has been proposed for anti-tumor therapy, but its therapeutic potential has not been realized due to severe systemic toxicity. Therefore, we aimed to explore whether liver tumors can be treated safely by an AAV-based gene therapy that enables tissue-specific and regulatable expression of IL-12.

Using a combination of hepatotropic AAV8 vectors, the liver-specific promotor LP1 and the K19 riboswitch, we achieved tet-dependent control of IL-12 expression *in vitro* and *in vivo*. In an orthotopic liver tumor model, AAV-mediated expression of IL-12 induced IL-12R signaling (STAT4 phosphorylation), and led to IFN-γ production, infiltration of T cells and to tumor regression in a vector dose-dependent manner. IL-12 activated the immune

10.3389/fimmu.2024.1360063

TABLE 1 Estimated parameters from the models used to fit the PK of tet, the dynamics of tetracycline activation of AAV and the AAV stimulation of IL-12 production and the pharmacodynamic model describing the relationship between IL-12 production in plasma and its effect on tumor size reduction.

Parameter	Value [% RSE]
Tet PK	
k_{abs} $[h^{-1}]$	0.83 [108%]
CL/F $[L/h/kg]$	3.33 [13.6%]
V_c/F $[L/kg]$	1.59 [119%]
V_{p1}/F $[L/kg]$	2.37 [41%]
Q_1/F $[L/h/kg]$	0.605 [46.5%]
Tet/IL-12 dynamics	
k_{out} $[h^{-1}]$	0.208 [20.6%]
$k_{in}[h^{-1}]$	k_{out} x 10^5
$EC50_{tet}$ $[nM]$	348 [19%]
EC_{50} (on) $[AAV\ units]$	25.4 x 10^9 [4.6%]
EC_{50} (off) $[AAV\ units]$	375 x 10^9 [6.6%]
IL-12 - Tumor Dynamics	
k_{growth} $[h^{-1}]$	0.0454 [0.39%]
k_{kill} $[h^{-1}]$	0.0658 [2.7%]
$EC_{50}cancer$ $[pg/mL]$	0.560 [0.45%]
k_{ein} $[h^{-1}]$	0.0728 [2.33%]
k_{eout} $[h^{-1}]$	$k_{ein}/20$

response persistently even after removal of tet and induced T cell infiltration or accumulation preferentially into the tumor, but not into liver parenchyma. Therefore, we hypothesize that IL-12 initiates the immune response, but additional factors are required for a full and sustained anti-tumor response, such as presence of tumor antigens which can stimulate T cells and lead to their proliferation. One limitation of our studies was that the potential of abscopal responses or long-term immunity was not tested in a tumor re-challenge model. However, long-lasting systemic efficacy appears likely, given positive data from several clinical and non-clinical IL-12 gene therapy studies (7, 11, 32). One disadvantage of tet is its antibiotic activity, which potentially comes with side effects. However, our treatment concept embodies a limited tet delivery of days to weeks at a time that will be sufficient to induce sustained proinflammatory and anti-tumor effects downstream of IL-12.

Of note, IL-12 levels were monitored at the protein level and did not distinguish between endogenous and transgenic protein. Therefore, hypothetically AAV.IL-12 could have induced the production of endogenous protein. Such a scenario is not supported by our data, however, as IL-12 levels were strictly AAV-dose and tet-dependent and quickly declined within hours – matching the kinetic of reporter gene expression driven by the K19 switch. Finally, AAV-control treated animals or metastasis control groups did not show increased IL-12 levels.

AAV vectors have emerged as the preferred platform for *in vivo* gene therapy, mostly in the context of gene replacement to treat monogenic diseases. However, innate immune recognition of methylated CpG motifs in the transgene cassette induces antigen-specific CD8+ T cell responses against the payload (33). In the case of liver-targeted gene delivery, T-cell-mediated loss of transduced hepatocytes, leading to lack of sustained transgene expression, has been suggested by clinical and pre-clinical data (34–36). We addressed this by removing all CpG sequences from the IL-12 cassette, a strategy that was recently applied in a pre-clinical non-viral IL-12 gene therapy study (37). This optimization did not alter biological potency of the transgene cassette *in vivo* (Figure 4). We thereby eliminated one factor potentially confounding clinical dose-response relationship. AAV vector genomes are maintained as episomes in transduced cells, and multi-year transgene expression has been documented in clinical trials, leading to FDA approval of the first liver-directed Hemophilia A gene therapy drug (38). Recent data in non-human primates suggest that persistent transgene expression might be caused by vector genome integration in hepatocytes, rather than by concatemerized episomal genomes (39). This observation calls for a very tight IL-12 regulation, i.e. no detectable expression in absence of tet. Also, along the line of long-term safety, we examined the consequences of low levels of residual IL-12 expression that may occur even in the absence of tet.

Our experiments with the tool construct AAV9.RS-mIL-12 indicated that riboswitch-controlled expression of IL-12 was safer than constitutive expression. A dose of $2.5x10^{11}$ vg/kg led to premature euthanasia of animals injected with the constitutive control vector AAV9.mIL-12, but not of animals injected with the regulatable construct (Figures 2C, 3C). With the optimized vector AAV8.RS-mIL-12-noCpG, a detailed analysis of the therapeutic window was conducted. Dose titration revealed that doses $\geq 5x10^{10}$ vg/kg were highly efficacious, including complete tumor regression, and that $1.5x10^{10}$ vg/kg still showed considerable tumor growth inhibition (Figures 5 and 6A). In general, in individual mice, tumor size reduction was achieved after induction of IL-12 to more than 100 pg/ml in plasma (Figure 5D).

To assess safety, we mimicked the treatment protocol of the tumor model in healthy mice and analyzed a wide range of toxicity parameters. Adverse findings depended on the AAV dose, but they were not caused by tet or the vector itself. In a setting with induction of IL-12 by tet, all doses $\leq 5x10^{10}$ vg/kg were well tolerated without adverse events (Figures 7A, B). Analysis of individual mice over all studies performed here indicated that, in general, IL-12 plasma levels >5000 pg/ml resulted in acute toxicity and early unscheduled termination. In principle, an effective IL-12 plasma level of >100 pg/ml and an acutely toxic level >5000 pg/ml represents a sufficient therapeutic window. By varying the tet dose, the IL-12 level may be adjusted to a safe and efficacious level in each individual. Another study (11) reported 200-fold higher IL-12 levels required for efficacy (>20 ng/ml) and toxicity (>1000 ng/ml) in a mouse model. Interestingly, they also observed a 50-fold window between these thresholds. The deviation in absolute values might be explained by technical differences, such as the quantification method, time-point and matrix (serum/plasma). In most other mouse studies, no clear

IL-12 threshold levels for toxicity and efficacy were reported. Maximum tolerated doses observed with recombinant IL-12 protein have only limited relevance for gene therapy, because recombinant IL-12 protein has a short half-life *in vivo*, whereas gene therapy can achieve sustained levels of IL-12. Because of the basal IL-12 expression of AAV8.RS-mIL-12-noCpG in the absence of tet, we analyzed safety without tet induction over 5 weeks (Figures 7C–N). No findings were observed at doses ≤$1.5x10^{10}$ vg/kg and minimal findings at $5.0x10^{10}$ vg/kg, but higher doses resulted in a clear dose-dependent toxicity. Therefore, we defined the range of safe and efficacious AAV doses from $1.5x10^{10}$ vg/kg with no adverse findings and suboptimal efficacy, to $5.0x10^{10}$ vg/kg with excellent efficacy, but first hints of potential toxicity. As cancer immunotherapies generally aim at stimulating the immune system, immune-related side effects may not be completely avoidable and are reported for established immunotherapies, such as anti-PD-1 or CAR-T cells (40, 41). Clinically, they are managed, e.g. by anti-IL-6 therapy or general immune suppression with corticosteroids. For AAV.RS-huIL-12, the approved anti-IL-12/IL-23 antibody ustekinumab might be used as a specific inhibitor.

Intratumorally injected IL-12 mRNA promoted Th1 transformation of the tumor microenvironment and anti-tumor immunity in mouse models (42). In a clinical trial in patients with advanced melanoma, local electroporation of an IL-12-encoding plasmid was combined with pembrolizumab. The combination was associated with a higher-than-expected response rate (43). However, non-viral approaches entailing tumor electroporation are best achieved in accessible cancer types, such as melanoma, and are hampered by low IL-12 levels and limited duration of expression.

A protein-based approach aiming at limiting systemic toxicity is the "immunocytokine" NHS-IL-12 that consists of two molecules of IL-12 fused to an antibody that targets tumor necrosis via binding to DNA (44). In a clinical trial with monotherapy, no objective tumor responses were observed (45). However, the immune system was stimulated, and some patients experienced stable disease. It is questionable whether immunocytokines can avoid systemic toxicity, as the cytokine can also interact with immune cells in circulation. Another targeting approach is the fusion of IL-12 to a domain that masks IL-12. The linker used is cleavable by tumor-associated proteases, thus releasing active IL-12 preferentially at the tumor site. Impressive preclinical results have been published, but clinical data is still missing (46, 47).

Liver fibrosis is a common comorbidity of HCC. The altered liver architecture may have a significant impact on the penetration and transduction efficiency of a systemically delivered therapeutic virus. A report on inferior transgene expression in cirrhotic liver achieved by delivery of hepatotropic AAV1 in the portal vein of rats (48) is supported by data we generated. Indeed, in a preclinical mouse model of liver fibrosis we have found that severe fibrosis reduced the transduction efficiency of AAV8 by the order of a magnitude (data not shown). The variability of fibrosis grades between HCC patients complicates the prediction of the clinical dose, but also speaks for a tightly regulatable system to fine-tune IL-12 expression in each patient individually.

More subtle differences in the AAV dose-response PK relationship were observed in healthy mice vs. tumor-bearing mice. In healthy mice, we determined $2.5.x10^{10}$ vg/kg as the vector dose resulting in no detectable IL-12 levels in plasma without tet administration or 3 days after transient tet exposure (Figures 2C–E). In the HCC model though, the same vector dose led to detectable IL-12 levels even without tet administration (Figure 3B). While these IL-12 levels were safe, they also showed a treatment benefit in tumor-bearing mice. The IL-12 data confirm the potential to fine-tune expression levels of a therapeutic protein *in vivo* by vector titration and adjusting the ligand-dose in a riboswitch context. Our data show that the K19 riboswitch enables versatile and comparable regulation of different transgenes, including reporters (12), and mouse and human IL-12 cDNA employing different AAV serotypes (this study). The reported lack of function of the K19 aptazyme to switch AAV-mediated transgene expression in the mouse eye (49) is likely partially due to the poor tet exposure in this organ (12).

While our approach represents another part in the growing molecular armory to fight liver cancer, the relatively small therapeutic window that we observed indicates the need for further optimization. Using the K19 aptazyme, we observed dynamic ranges of 5 to 11-fold expression levels in this study which is similar to the 19-fold range achieved when driving reporter gene expression (12). Tet-responsive riboswitches showing comparable dynamic ranges were achieved in C. elegans by leveraging the modularity of combining tet-aptamers with exon-skipping expression platforms (50). A recent report suggests that strongly improved regulation can be achieved in the mouse by using a tet switch design with a poly-A signal in the 5'-UTR and including several aptamers (51).

Achieving controllable gene expression at high dynamic ranges is highly desirable, as evident from various protein-based systems that have been investigated recently, including destabilizing domains and inducible promoters as the most advanced approaches (7, 52). The TET-on system was used to regulate IL-12 in mouse model of CRC (11). This system requires bidirectional expression of both IL-12 and the mutated reverse tet transactivator rtTA under the control of the liver-specific albumin promoter. Doxycycline-induced regulation of IL-12 provided anti-tumor efficacy. However, tolerability was not investigated, and optimization of the inducer dose was not performed. These transcriptional control systems, including the Rheoswitch system, Mifepristone, and classic Tet-ON/OFF promoter systems, suffer from a unifying drawback: They require the expression of DNA-binding proteins that enable transcription after being activated by their cognate ligands (8, 11, 53–55). These DNA-binding proteins represent T-cell epitopes that bear an immunogenic risk. Attempts were undertaken to address this risk for the Tet-promoter control system by engineering versions without certain T cell epitopes for HLA0201 (the most common human HLA serotype). If that is even possible –the protein has to retain specific binding to both the Tet repressor, and to tet –humans with other serotypes may still present epitopes from the resulting protein, given lack of immune tolerance to this exogenous protein (56). These data show that genetic

switches with wide dynamic ranges that control transgene expression without additional protein components are required to achieve the full potential of gene therapy technologies.

In conclusion, our data suggest that IL-12 gene therapy can be controlled using an aptazyme approach in a spatio-temporal manner for a safe and efficient immunomodulatory effect using a rational combination of AAV serotype, vector dose, and tet dosing regimen. This approach enabled regulated and repeatable transgene expression in a dose-dependent manner and achieved a defined therapeutic window. As such, the RS-IL-12 approach added safety over non-regulated gene therapy but will require further optimization.

Data availability statement

The original contributions presented in the study are included in the article/Supplementary Material. Further inquiries can be directed to the corresponding authors.

Ethics statement

Ethical approval was not required for the studies on humans in accordance with the local legislation and institutional requirements because only commercially available established cell lines were used. The animal study was approved by Regierungspräsidium Tübingen, Germany, or Regierungspräsidium Freiburg, Germany. The study was conducted in accordance with the local legislation and institutional requirements.

Author contributions

MD: Conceptualization, Investigation, Visualization, Writing – original draft. RK: Conceptualization, Investigation, Methodology, Project administration, Supervision, Writing – review & editing. PV-G: Investigation, Writing – review & editing. BS: Conceptualization, Methodology, Resources, Writing – review & editing. TS: Investigation, Writing – review & editing. PG: Investigation, Writing – review & editing. GA: Formal Analysis, Methodology, Software, Visualization, Writing – original draft. AG: Investigation, Writing – review & editing. IL: Investigation, Writing – review & editing. HK: Methodology, Software, Writing – review & editing. JP: Conceptualization, Writing – review & editing. SK: Conceptualization, Writing – review & editing. MK: Conceptualization, Project administration, Supervision, Writing – original draft, Writing – review & editing. FI: Conceptualization, Project administration, Supervision, Writing – original draft, Writing – review & editing. SM: Investigation, Writing – review & editing. SH: Investigation, Writing – review & editing.

Funding

The author(s) declare that financial support was received for the research, authorship, and/or publication of this article. This research was financially supported by Boehringer Ingelheim. The funder had no role in the study design, data collection and analysis, decision to publish, or preparation of the manuscript.

Acknowledgments

We thank Stefan Michelfelder and Dragica Blazevic for their advice regarding HCC model establishment and IL-12 assays. Birgit Stierstorfer, Charlotte Lempp and Suzanne Segal provided expert histological support. Ines Truebenbach and Silvija Suffrian were instrumental in tet formulation and preparation. Audrey Brenot for advice regarding study design.

Conflict of interest

All authors are employees of Boehringer Ingelheim.

Publisher's note

Supplementary material

The Supplementary Material for this article can be found online at: https://www.frontiersin.org/articles/10.3389/fimmu.2024.1360063/full#supplementary-material

References

1. Llovet JM, Kelley RK, Villanueva A, Singal AG, Pikarsky E, Roayaie S, et al. Hepatocellular carcinoma. *Nat Rev Dis Primers*. (2021) 7:6. doi: 10.1038/s41572-020-00240-3

2. Research IA for C. Cancer Today. Available online at: https://gco.iarc.fr/today/home (Accessed August 12, 2023).

3. Biller LH, Schrag D. Diagnosis and treatment of metastatic colorectal cancer. *JAMA*. (2021) 325:669–85. doi: 10.1001/jama.2021.0106

4. Cirella A, Luri-Rey C, Trani CAD, Teijeira A, Olivera I, Bolaños E, et al. Novel strategies exploiting interleukin-12 in cancer immunotherapy. *Pharmacol Therapeut*. (2022) 239:108189. doi: 10.1016/j.pharmthera.2022.108189

5. Nguyen KG, Vrabel MR, Mantooth SM, Hopkins JJ, Wagner ES, Gabaldon TA, et al. Localized interleukin-12 for cancer immunotherapy. *Front Immunol*. (2020) 11:575597. doi: 10.3389/fimmu.2020.575597

6. Hernandez-Alcoceba R, Poutou J, Ballesteros-Briones MC, Smerdou C. Gene therapy approaches against cancer using in *vivo* and ex vivo gene transfer of interleukin-12. *Immunotherapy*. (2016) 8:179–98. doi: 10.2217/imt.15.109

7. Barrett JA, Cai H, Miao J, Khare PD, Gonzalez P, Dalsing-Hernandez J, et al. Regulated intratumoral expression of IL-12 using a RheoSwitch Therapeutic System® (RTS®) gene switch as gene therapy for the treatment of glioma. *Cancer Gene Ther*. (2018) 25:106–16. doi: 10.1038/s41417-018-0019-0

8. Chiocca EA, Yu JS, Lukas RV, Solomon IH, Ligon KL, Nakashima H, et al. Regulatable interleukin-12 gene therapy in patients with recurrent high-grade glioma: Results of a phase 1 trial. *Sci Transl Med*. (2019) 11:eaaw5680. doi: 10.1126/scitranslmed.aaw5680

9. Lo C, Chang C, Tang S, Pan W, Fang C, Chen Y, et al. Differential antitumor effect of interleukin-12 family cytokines on orthotopic hepatocellular carcinoma. *J Gene Med*. (2010) 12:423–34. doi: 10.1002/jgm.1452

10. Gossen M, Bujard H. Tight control of gene expression in mammalian cells by tetracycline-responsive promoters. *Proc Natl Acad Sci*. (1992) 89:5547–51. doi: 10.1073/pnas.89.12.5547

11. Vanrell L, Scala MD, Blanco L, Otano I, Gil-Farina I, Baldim V, et al. Development of a liver-specific tet-on inducible system for AAV vectors and its application in the treatment of liver cancer. *Mol Ther*. (2011) 19:1245–53. doi: 10.1038/mt.2011.37

12. Strobel B, Düchs MJ, Blazevic D, Rechtsteiner P, Braun C, Baum-Kroker KS, et al. A small-molecule-responsive riboswitch enables conditional induction of viral vector-mediated gene expression in mice. *ACS Synth Biol*. (2020) 9:1292–305. doi: 10.1021/acssynbio.9b00410

13. Beilstein K, Wittmann A, Grez M, Suess B. Conditional control of mammalian gene expression by tetracycline-dependent hammerhead ribozymes. *ACS Synth Biol*. (2015) 4:526–34. doi: 10.1021/sb500270h

14. Berens C, Thain A, Schroeder R. A tetracycline-binding RNA aptamer. *Bioorg Med Chem*. (2001) 9:2549–56. doi: 10.1016/s0968-0896(01)00063-3

15. Yen L, Svendsen J, Lee J-S, Gray JT, Magnier M, Baba T, et al. Exogenous control of mammalian gene expression through modulation of RNA self-cleavage. *Nature*. (2004) 431:471–6. doi: 10.1038/nature02844

16. Davidoff AM, Gray JT, Ng CYC, Zhang Y, Zhou J, Spence Y, et al. Comparison of the ability of adeno-associated viral vectors pseudotyped with serotype 2, 5, and 8 capsid proteins to mediate efficient transduction of the liver in murine and nonhuman primate models. *Mol Ther*. (2005) 11:875–88. doi: 10.1016/j.ymthe.2004.12.022

17. Monahan PE, Sun J, Gui T, Hu G, Hannah WB, Wichlan DG, et al. Employing a gain-of-function factor IX variant R338L to advance the efficacy and safety of hemophilia B human gene therapy: preclinical evaluation supporting an ongoing adeno-associated virus clinical trial. *Hum Gene Ther*. (2015) 26:69–81. doi: 10.1089/hum.2014.106

18. Lieschke GJ, Rao PK, Gately MK, Mulligan RC. Bioactive murine and human interleukin-12 fusion proteins which retain antitumor activity *in vivo*. *Nat Biotechnol*. (1997) 15:35–40. doi: 10.1038/nbt0197-35

19. Nathwani AC, Gray JT, Ng CYC, Zhou J, Spence Y, Waddington SN, et al. Self-complementary adeno-associated virus vectors containing a novel liver-specific human factor IX expression cassette enable highly efficient transduction of murine and nonhuman primate liver. *Blood*. (2006) 107:2653–61. doi: 10.1182/blood-2005-10-4035

20. Martino AT, Suzuki M, Markusic DM, Zolotukhin I, Ryals RC, Moghimi B, et al. The genome of self-complementary adeno-associated viral vectors increases Toll-like receptor 9–dependent innate immune responses in the liver. *Blood*. (2011) 117:6459–68. doi: 10.1182/blood-2010-10-314518

21. Logan GJ, Dane AP, Hallwirth CV, Smyth CM, Wilkie EE, Amaya AK, et al. Identification of liver-specific enhancer–promoter activity in the 3′ untranslated region of the wild-type AAV2 genome. *Nat Genet*. (2017) 49:1267–73. doi: 10.1038/ng.3893

22. Wilmott P, Lisowski L, Alexander IE, Logan GJ. A user's guide to the inverted terminal repeats of adeno-associated virus. *Hum Gene Ther Methods*. (2019) 30:206–13. doi: 10.1089/hgtb.2019.276

23. Strobel B, Miller FD, Rist W, Lamla T. Comparative analysis of cesium chloride- and iodixanol-based purification of recombinant adeno-associated viral vectors for preclinical applications. *Hum Gene Ther Methods*. (2015) 26:147–57. doi: 10.1089/hgtb.2015.051

24. Schumann G, Bonora R, Ceriotti F, Férard G, Ferrero CA, Franck PFH, et al. IFCC primary reference procedures for the measurement of catalytic activity concentrations of enzymes at 37°C. Part 5. Reference procedure for the measurement of catalytic concentration of aspartate aminotransferase. *Clin Chem Lab Med*. (2002) 40:725–33. doi: 10.1515/cclm.2002.125

25. Schumann G, Bonora R, Ceriotti F, Clerc-Renaud P, Ferrero CA, Férard G, et al. IFCC primary reference procedures for the measurement of catalytic activity concentrations of enzymes at 37°C. Part 3. Reference procedure for the measurement of catalytic concentration of lactate dehydrogenase. *Clin Chem Lab Med*. (2002) 40:643–8. doi: 10.1515/cclm.2002.111

26. Romeis. *Mikroskopische Technik*. Spektrum S, editor. München, Wien, Baltimore: Springer Spektrum (2015). p. 201.

27. Huang G, Liu Z, van der Maaten L, Weinberger KQ. Densely connected convolutional networks. *2017 IEEE Conf Comput Vis Pattern Recognit (CVPR)*. (2017), 2261–9. doi: 10.1109/cvpr.2017.243

28. Manno CS, Pierce GF, Arruda VR, Glader B, Ragni M, Rasko JJ, et al. Successful transduction of liver in hemophilia by AAV-Factor IX and limitations imposed by the host immune response. *Nat Med*. (2006) 12:342–7. doi: 10.1038/nm1358

29. Miao CH, Ohashi K, Patijn GA, Meuse L, Ye X, Thompson AR, et al. Inclusion of the hepatic locus control region, an intron, and untranslated region increases and stabilizes hepatic factor IX gene expression in vivo but not in vitro. *Mol Ther*. (2000) 1:522–32. doi: 10.1006/mthe.2000.0075

30. Zincarelli C, Soltys S, Rengo G, Rabinowitz JE. Analysis of AAV serotypes 1–9 mediated gene expression and tropism in mice after systemic injection. *Mol Ther*. (2008) 16:1073–80. doi: 10.1038/mt.2008.76

31. Zou JJ, Schoenhaut DS, Carvajal DM, Warrier RR, Presky DH, Gately MK, et al. Structure-function analysis of the p35 subunit of mouse interleukin 12 (∗). *J Biol Chem*. (1995) 270:5864–71. doi: 10.1074/jbc.270.11.5864

32. Algazi AP, Twitty CG, Tsai KK, Le M, Pierce R, Browning E, et al. Phase II trial of IL-12 plasmid transfection and PD-1 blockade in immunologically quiescent melanoma. *Clin Cancer Res*. (2020) 26:2827–37. doi: 10.1158/1078-0432.ccr-19-2217

33. Bertolini TB, Shirley JL, Zolotukhin I, Li X, Kaisho T, Xiao W, et al. Effect of cpG depletion of vector genome on CD8+ T cell responses in AAV gene therapy. *Front Immunol*. (2021) 12:672449. doi: 10.3389/fimmu.2021.672449

34. Konkle M. BAX 335 hemophilia B gene therapy clinical trial results: potential impact of CpG sequences on gene expression.pdf. *Blood*. (2021) 137(6):763–74. doi: 10.1182/blood.2019004625

35. Wright JF. Codon modification and PAMPs in clinical AAV vectors: the tortoise or the hare? *Mol Ther*. (2020) 28:701–3. doi: 10.1016/j.ymthe.2020.01.026

36. Wright JF. Quantification of cpG motifs in rAAV genomes: avoiding the toll. *Mol Ther*. (2020) 28:1756–8. doi: 10.1016/j.ymthe.2020.07.006

37. Ahn H-H, Carrington C, Hu Y, Liu H, Ng C, Nam H, et al. Nanoparticle-mediated tumor cell expression of mIL-12 via systemic gene delivery treats syngeneic models of murine lung cancers. *Sci Rep*. (2021) 11:9733. doi: 10.1038/s41598-021-89124-4

38. Mahlangu J, Kaczmarek R, von Drygalski A, Shapiro S, Chou S-C, Ozelo MC, et al. Two-year outcomes of valoctocogene roxaparvovec therapy for hemophilia A. *N Engl J Med*. (2023) 388:694–705. doi: 10.1056/nejmoa2211075

39. Greig JA, Martins KM, Breton C, Lamontagne RJ, Zhu Y, He Z, et al. Integrated vector genomes may contribute to long-term expression in primate liver after AAV administration. *Nat Biotechnol*. (2023), 1–11. doi: 10.1038/s41587-023-01974-7

40. Baxi S, Yang A, Gennarelli RL, Khan N, Wang Z, Boyce L, et al. Immune-related adverse events for anti-PD-1 and anti-PD-L1 drugs: systematic review and meta-analysis. *BMJ*. (2018) 360:k793. doi: 10.1136/bmj.k793

41. Maus MV, Grupp SA, Porter DL, June CH. Antibody-modified T cells: CARs take the front seat for hematologic Malignancies. *Blood*. (2014) 123:2625–35. doi: 10.1182/blood-2013-11-492231

42. Hewitt SL, Bailey D, Zielinski J, Apte A, Musenge F, Karp R, et al. Intratumoral IL12 mRNA therapy promotes TH1 transformation of the tumor microenvironment. *Clin Cancer Res*. (2020) 26:6284–98. doi: 10.1158/1078-0432.ccr-20-0472

43. Algazi A, Bhatia S, Agarwala S, Molina M, Lewis K, Faries M, et al. Intratumoral delivery of tavokinogene telseplasmid yields systemic immune responses in metastatic melanoma patients. *Ann Oncol*. (2020) 31:532–40. doi: 10.1016/j.annonc.2019.12.008

44. Fallon J, Tighe R, Kradjian G, Guzman W, Bernhardt A, Neuteboom B, et al. The immunocytokine NHS-IL12 as a potential cancer therapeutic. *Oncotarget*. (2014) 5:1869–84. doi: 10.18632/oncotarget.1853

45. Strauss J, Heery CR, Kim JW, Jochems C, Donahue RN, Montgomery AS, et al. First-in-human phase I trial of a tumor-targeted cytokine (NHS-IL12) in subjects with metastatic solid tumors. *Clin Cancer Res*. (2018) 25:clincanres.1512.2018. doi: 10.1158/1078-0432.ccr-18-1512

46. Mansurov A, Hosseinchi P, Chang K, Lauterbach AL, Gray LT, Alpar AT, et al. Masking the immunotoxicity of interleukin-12 by fusing it with a domain of its receptor via a tumour-protease-cleavable linker. *Nat BioMed Eng*. (2022) 6:819–29. doi: 10.1038/s41551-022-00888-0

47. Xue D, Moon B, Liao J, Guo J, Zou Z, Han Y, et al. A tumor-specific pro-IL-12 activates preexisting cytotoxic T cells to control established tumors. *Sci Immunol*. (2022) 7:eabi6899. doi: 10.1126/sciimmunol.abi6899

48. Sobrevals L, Enguita M, Rodriguez C, Gonzalez-Rojas J, Alzaguren P, Razquin N, et al. AAV vectors transduce hepatocytes in *vivo* as efficiently in cirrhotic as in healthy rat livers. *Gene Ther*. (2012) 19:411–7. doi: 10.1038/gt.2011.119

49. Reid CA, Nettesheim ER, Connor TB, Lipinski DM. Development of an inducible anti-VEGF rAAV gene therapy strategy for the treatment of wet AMD. *Sci Rep*. (2018) 8:11763. doi: 10.1038/s41598-018-29726-7

50. Finke M, Brecht D, Stifel J, Gense K, Gamerdinger M, Hartig JS. Efficient splicing-based RNA regulators for tetracycline-inducible gene expression in human cell culture and C. elegans. *Nucleic Acids Res*. (2021) 49:gkab233–. doi: 10.1093/nar/gkab233

51. Luo L, Jea JD-Y, Wang Y, Chao P-W, Yen L. Control of mammalian gene expression by modulation of polyA signal cleavage at 5′ UTR. *Nat Biotechnol*. (2024). doi: 10.1038/s41587-023-01989-0

52. Santiago CP, Keuthan CJ, Boye SL, Boye SE, Imam AA, Ash JD. A drug-tunable gene therapy for broad-spectrum protection against retinal degeneration. *Mol Ther*. (2018) 26:2407–17. doi: 10.1016/j.ymthe.2018.07.016

53. Das AT, Tenenbaum L, Berkhout B. Tet-on systems for doxycycline-inducible gene expression. *Curr Gene Ther*. (2016) 16:156–67. doi: 10.2174/1566523216666160524144041

54. Gonzalez-Aparicio M, Alzuguren P, Mauleon I, Medina-Echeverz J, Hervas-Stubbs S, Mancheno U, et al. Oxaliplatin in combination with liver-specific expression of interleukin 12 reduces the immunosuppressive microenvironment of tumours and eradicates metastatic colorectal cancer in mice. *Gut*. (2011) 60:341. doi: 10.1136/gut.2010.211722

55. Wang L, HernÁndez-Alcoceba R, Shankar V, Zabala M, Kochanek S, Sangro B, et al. Prolonged and inducible transgene expression in the liver using gutless adenovirus: A potential therapy for liver cancer. *Gastroenterology*. (2004) 126:278–89. doi: 10.1053/j.gastro.2003.10.075

56. Ginhoux F, Turbant S, Gross DA, Poupiot J, Marais T, Lone Y, et al. HLA-A*0201-restricted cytolytic responses to the rtTA transactivator dominant and cryptic epitopes compromise transgene expression induced by the tetracycline on system. *Mol Ther*. (2004) 10:279–89. doi: 10.1016/j.ymthe.2004.05.012

frontiers | Frontiers in Immunology

TYPE Original Research
PUBLISHED 15 May 2024
DOI 10.3389/fimmu.2024.1360436

OPEN ACCESS

EDITED BY
Yaohe Wang,
Queen Mary University of London,
United Kingdom

REVIEWED BY
Hadi Esmaili Gouvarchinghaleh,
Baqiyatallah University of Medical Sciences,
Iran
Gabri Van Der Pluijm,
Leiden University Medical Center (LUMC),
Netherlands

*CORRESPONDENCE
Chae-Ok Yun
chaeok@hanyang.ac.kr

RECEIVED 23 December 2023
ACCEPTED 29 April 2024
PUBLISHED 15 May 2024

CITATION
Yoon A-R, Jiao A, Hong J, Kim B and Yun C-O (2024) Tumor microenvironment-modulating oncolytic adenovirus combined with GSK-3β inhibitor enhances antitumor immune response against bladder cancer. *Front. Immunol.* 15:1360436.
doi: 10.3389/fimmu.2024.1360436

Tumor microenvironment-modulating oncolytic adenovirus combined with GSK-3β inhibitor enhances antitumor immune response against bladder cancer

A-Rum Yoon[1,2,3], Ao Jiao[1], JinWoo Hong[4], Bomi Kim[1] and Chae-Ok Yun[1,2,3,4]*

[1]Department of Bioengineering, College of Engineering, Hanyang University, Seoul, Republic of Korea, [2]Institute of Nano Science and Technology (INST), Hanyang University, Seoul, Republic of Korea, [3]Hanyang Institute of Bioscience and Biotechnology (HY-IBB), Hanyang University, Seoul, Republic of Korea, [4]GeneMedicine Co., Ltd., Seoul, Republic of Korea

Bladder cancer is a common type of cancer around the world, and the majority of patients are diagnosed with non-muscle-invasive bladder cancer (NMIBC). Although low-risk NMIBC has a good prognosis, the disease recurrence rate and development of treatment-refractory disease remain high in intermediate- to high-risk NMIBC patients. To address these challenges for the treatment of NMIBC, a novel combination therapy composed of an oncolytic adenovirus (oAd) co-expressing interleukin (IL)-12, granulocyte-macrophage colony-stimulating factor (GM-CSF), and relaxin (RLX; HY-oAd) and a clinical-stage glycogen synthase kinase (GSK)-3β inhibitor (9-ING-41; elraglusib) was investigated in the present report. Our findings demonstrate that HY-oAd and 9-ING-41 combination therapy (HY-oAd+9-ING-41) exerted superior inhibition of tumor growth compared with respective monotherapy in a syngeneic NMIBC tumor model. HY-oAd+9-ING-41 induced high-level tumor extracellular matrix (ECM) degradation and a more potent antitumor immune response than the respective monotherapy. In detail, HY-oAd+9-ING-41 induced superior accumulation of intratumoral T cells, prevention of immune cell exhaustion, and induction of tumor-specific adaptive immune response compared to either monotherapy. Collectively, these results demonstrate that the combination of HY-oAd and 9-ING-41 may be a promising approach to elicit a potent antitumor immune response against bladder cancer.

KEYWORDS

oncolytic virus, adenovirus, bladder cancer, GSK-3β inhibitor, antitumor immune response

Introduction

Non-muscle-invasive bladder cancer (NMIBC) is the most common genitourinary malignancy and comprises more than 70% of all bladder cancer cases (1). Currently, transurethral resection of bladder tumors and adjuvant intravesical treatments, like chemotherapy or Bacillus Calmette–Guérin (BCG), are widely utilized and demonstrated favorable outcomes for the majority of the patients (2–4). Nevertheless, approximately 40% of these NMIBC patients eventually experience tumor recurrence within a span of 2 years, while 10% of the cases progress to muscle-invasive bladder cancer (MIBC) with a worse prognosis (5).

To address the limitations of conventional therapeutic options, various immunotherapeutics, like cancer vaccines, gene therapies, and immune checkpoint inhibitors (ICIs), have been extensively investigated in both preclinical and clinical environments (6). Recently, gene therapies utilizing adenovirus (Ad) have shown promising clinical efficacy against BCG-unresponsive or advanced NMIBC cases (7). In detail, Adstiladrin, a non-replicating Ad expressing interferon (IFN)-α2b, was approved by the US Food and Drug Administration (FDA) for the treatment of BCG-unresponsive NMIBC patients in 2022 after achieving 51% complete response rate (8). Similarly, CG0070, which is an oncolytic Ad (oAd) expressing granulocyte-macrophage colony-stimulating factor (GM-CSF), has shown promising clinical activity for the treatment of BCG-refractory NMIBC patients in a phase II clinical trial (9). Currently, CG0070 is being evaluated in a phase III trial as monotherapy and in combination with pembrolizumab in a phase II trial for the treatment of BCG-unresponsive high-grade NMIBC patients (10), highlighting the promising nature of Ad-based gene therapy for disease management of NMIBC.

oAds, which can preferentially replicate in and lyse tumor cells (11–15), are more actively evaluated in the clinical environment than replication-incompetent counterparts for the treatment of cancer owing to several advantageous attributes like prolonged biological persistence, higher level of therapeutic gene expression, and superior induction of antitumor immune response (16, 17). Briefly, cancer-specific viral replication and subsequent cytolysis of tumor cells by oAd release tumor-specific antigens and danger-associated signaling molecules that promote tumor-specific immune response. Arming the oAd with immune-stimulatory therapeutic genes, like cytokines and chemokines, further potentiates the antitumor immune response mediated by the virus via exponential amplification of transgene products in a tumor-specific manner (18, 19). Indeed, the majority of the oncolytic viruses under clinical investigations express at least one immune-stimulatory therapeutic gene, with interleukin (IL)-12 and GM-CSF being the most frequently utilized antitumor immune transgene candidates to date (17, 20).

Of the two cytokines, GM-CSF has been more extensively investigated with several different types of oncolytic viruses, including Ad, herpes simplex virus (HSV), and vaccinia virus (VV), expressing GM-CSF (CG0070, Imlygic, and Pexa-vec, respectively) either completing or under ongoing investigation in phase III clinical trials. Although GM-CSF has been extensively investigated in clinical trials as a therapeutic transgene for oncolytic viruses or as a recombinant cytokine for cancer immunotherapy, there are increasing number of evidences that demonstrate the potentially pro-tumorigenic role of GM-CSF and inadequate therapeutic benefit of GM-CSF monotherapy in clinical environment (21–24), suggesting that GM-CSF as sole therapeutic gene may exert suboptimal antitumor immune response. Indeed, there are evidences that suggest that there are better antitumor cytokine candidates, like IL-12, that can exert a superior therapeutic effect compared with GM-CSF for oncolytic virotherapy (25–28). Thus, more recently developed oncolytic viruses in clinical trials have been armed with immune transgenes, like IL-12, IL-15, and IL-21, instead of GM-CSF (17). Alternatively, co-expression of GM-CSF with other immune-stimulatory transgenes, like IL-12, by an oncolytic virus has been shown to exert a superior antitumor effect over the expression of respective immune transgene alone in preclinical setting (26, 27, 29), suggesting that GM-CSF as an adjuvant transgene may warrant further investigations.

One of the major obstacles to effective disease management of NMIBC cases remains innate or acquired resistance to BCG therapy. There are several purported mechanisms, like differential tumor mutation burden or mutation signatures, to patients becoming unresponsive to BCG treatment (30). Recent lines of evidence also suggest that T-cell exhaustion, evidenced by elevated immune checkpoint molecules like PD-1, LAG3, CTLA-4, TIGIT, or TIM-3, is correlated with BCG unresponsiveness of NMIBC patients (30, 31). In line with these findings, PD-1-targeted ICI, pembrolizumab, was shown to exert promising therapeutic efficacy against BCG-unresponsive NMIBC cases, ultimately leading to US FDA approval in 2020 (32, 33), showing that reversal of T-cell exhaustion via checkpoint blockade can be a promising strategy for the treatment of BCG-unresponsive NMIBC.

Based on these backgrounds, the present report investigated a novel combination immunotherapy regimen utilizing oAd co-expressing IL-12, GM-CSF, and relaxin (RLX; HY-oAd) and glycogen synthase kinase (GSK)-3β inhibitor (iGSK3β), 9-ING-41 (34, 35), for the treatment of NMIBC. Clinically evaluated iGSK3β, 9-ING-41, was chosen for combination therapy based on its previously reported function to inhibit the expression of various checkpoint molecules, like PD-1, TIM-3, and TIGIT, on $CD8^+$ T cells (35). As oAd-mediated antitumor immune response has been reported to induce T-cell exhaustion and T-cell exhaustion is associated with BCG unresponsiveness of NMIBC, the present report sought to overcome T-cell exhaustion by combining HY-oAd with iGSK3β to induce synergistic antitumor immune response. To this end, HY-oAd as a single agent induced potent bladder cancer-specific killing efficacy and inhibited tumor growth by inducing a potent antitumor immune response in the syngeneic murine bladder tumor model. The combination of HY-oAd and 9-ING-41 (HY-oAd+9-ING-41) exerted superior anticancer efficacy both *in vitro* and *in vivo* over the respective monotherapy. The superior efficacy of HY-oAd+9-ING-41 was achieved via superior induction of $CD4^+$ and $CD8^+$ T-cell infiltration into tumor tissues, as well as tumor-specific immune response over the respective monotherapy, indicating that combining both oAd and iGSK3β inhibitor can be a promising strategy to overcome T-cell exhaustion and exert potent antitumor immunity against NMIBC.

Results

HY-oAd expresses all three therapeutic genes and elicits bladder cancer-specific cell-killing effect

To overcome the limitations of oncolytic virus expressing GM-CSF as a single therapeutic gene for the treatment of NMIBC, HY-oAd co-expressing single-chain murine IL-12 (scIL-12), murine GM-CSF, and human RLX has been utilized (Figure 1A). As shown in Figure 1B, infection of murine NMIBC cell line MB49 cells with HY-oAd led to a dose-dependent expression of all therapeutic genes, showing that HY-oAd has been properly generated.

Infection of human or murine bladder cancer cell lines with HY-oAd led to a dose-dependent cancer cell-killing effect that was significantly more potent than those observed using control oAd lacking therapeutic transgene (control oAd) (Figure 1C; $^{**}p < 0.01$, $^{***}p < 0.001$). Neither control oAd nor HY-oAd exerted off-target cytopathic effects in murine or human fibroblast cell lines up to 500 or 50 multiplicity of infection (MOI), respectively. Together, these results demonstrate that the three therapeutic genes expressed by HY-oAd enhanced bladder cancer-specific cell-killing effect with no observable off-target activity in normal cell lines.

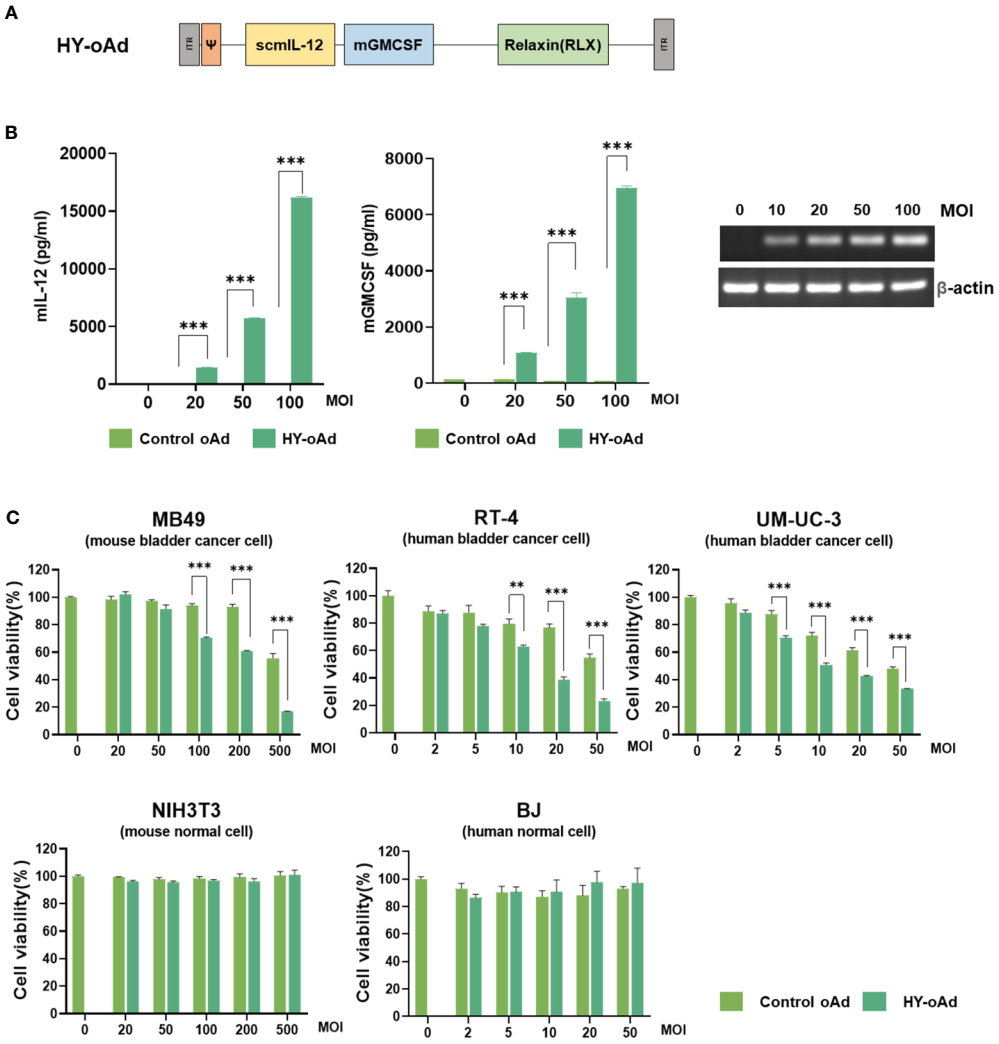

FIGURE 1
Characterization of HY-oAd. **(A)** Schematic representation for the genomic structure of the HY-oAd. **(B)** MB49, a murine bladder cancer cell, was infected with control oAd or HY-oAd at 0 to 100 MOI for 48 h The supernatants were harvested, and then murine IL-12 and GM-CSF expression levels were analyzed by ELISA. Total RNA was extracted from MB49 cell lysates, and then mRNA expression levels of RLX and β-actin were analyzed by conventional reverse-transcriptase PCR. Each cell line was tested at least three times, and the data shown are representative of experiments performed in triplicate. Bars represent mean ± SD. $^{***}p < 0.001$ (n = 3). *p*-Values were determined using Student's *t*-test. **(C)** Murine bladder cancer cell line (MB49), human bladder cancer cell lines (RT-4 and UM-UC-3), murine normal fibroblast (NIH3T3), and human normal fibroblast (BJ) were infected with 0–500 MOI of control oAd or HY-oAd, and then the cell viability was determined by MTT assay. Each cell line was tested at least three times, and the data shown are representative of experiments performed in triplicate. Bars represent mean ± SD. $^{***}p < 0.001$, $^{**}p < 0.01$ (n = 3). *p*-Values were determined using Student's *t*-test. MOI, multiplicity of infection; GM-CSF, granulocyte-macrophage colony-stimulating factor; MTT, 3-(4,5-dimethylthiazol-2-yl)-2,5-diphenyltetrazolium bromide.

HY-oAd induces potent antitumor effect against subcutaneous bladder tumor model

To evaluate the antitumor efficacy of HY-oAd, mice bearing subcutaneous MB49 tumors were intratumorally treated with 2×10^{10} viral particles (VPs) of HY-oAd or an oAd expressing GM-CSF alone on days 0, 2, and 4 along with phosphate-buffered saline (PBS) as negative control (Figure 2A). As shown in Figures 2B, C, the PBS-treated group exhibited rapid tumor growth and reached an average tumor volume of 3,464.2 ± 295.2 mm^3 at day 30 after the initial treatment. In contrast, both oAd expressing GM-CSF alone and HY-oAd induced significant tumor growth inhibition compared to the PBS-treated group (***$p < 0.001$). Importantly, HY-oAd exerted a significantly more potent antitumor effect compared with oAd expressing GM-CSF alone, as evidenced by complete regression of all tumors in six out of six mice compared to three out of six regression, respectively. Together, these findings demonstrated that the expression of multiple therapeutic genes by HY-oAd led to a more potent anticancer effect against NMIBC compared to the expression of GM-CSF as the only therapeutic gene.

9-ING-41 enhances the bladder cancer cell-specific killing effect of HY-oAd

Prior to the evaluation of HY-oAd+9-ING-41 combination therapy, we first sought to investigate the anticancer effect of 9-ING-41 monotherapy against bladder cancer. As shown in Figures 3A and Supplementary Figure S1, treatment of either murine or human bladder cancer cell lines with 9-ING-41 led to dose-dependent cell killing. In normal cell lines (murine or human fibroblasts), 9-ING-41 did not induce a significant cell-killing effect up to 8 μM.

Next, two different HY-oAd+9-ING-41 combination therapy dosing regimens, as shown in Figure 3B, were evaluated to

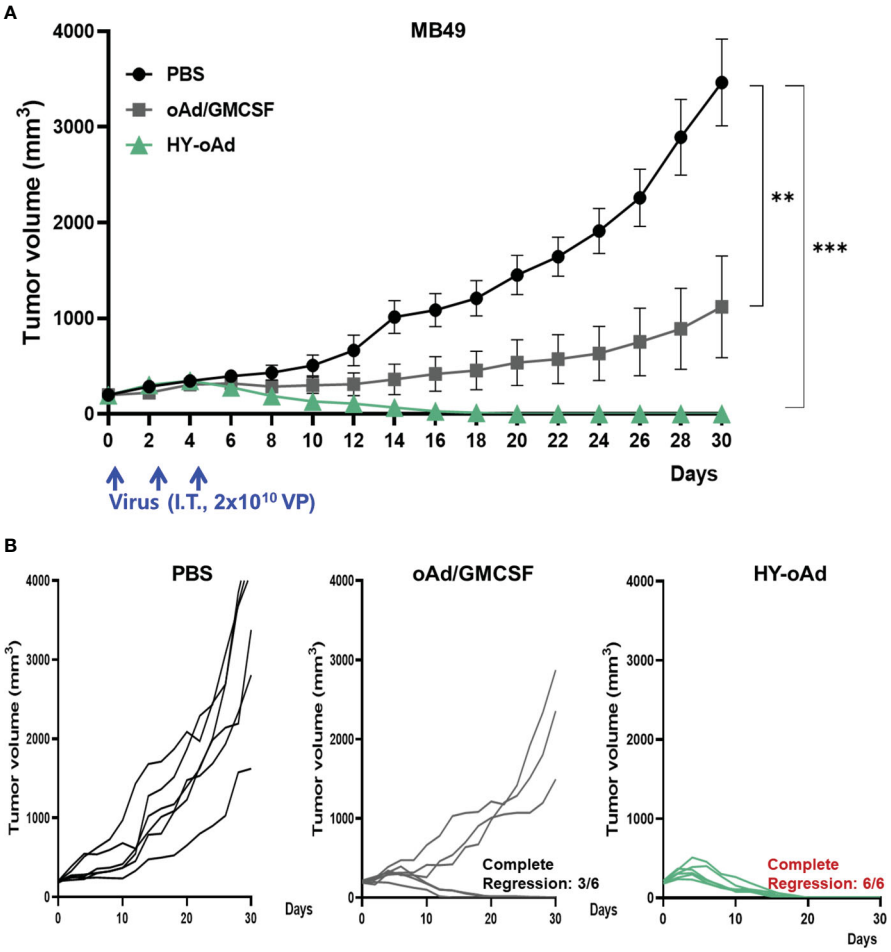

FIGURE 2
Antitumor effect of HY-oAd against MB49 tumor. **(A)** C57BL/6 mice were subcutaneously inoculated with MB49 cells. When the mean tumor volume of MB49 reached 200 mm^3, mice were intratumorally treated three times with 2×10^{10} VPs of HY-oAd or oAd expressing GM-CSF (oAd/GM-CSF) along with PBS as negative control (n = 6 per group). Data are presented as mean ± SEM. *$p < 0.05$ or ***$p < 0.001$. p-Values were determined using the one-way ANOVA. **(B)** The tumor growth of individual MB49 tumor-bearing mice is provided. VPs, viral particles; GM-CSF, granulocyte-macrophage colony-stimulating factor; PBS, phosphate-buffered saline.

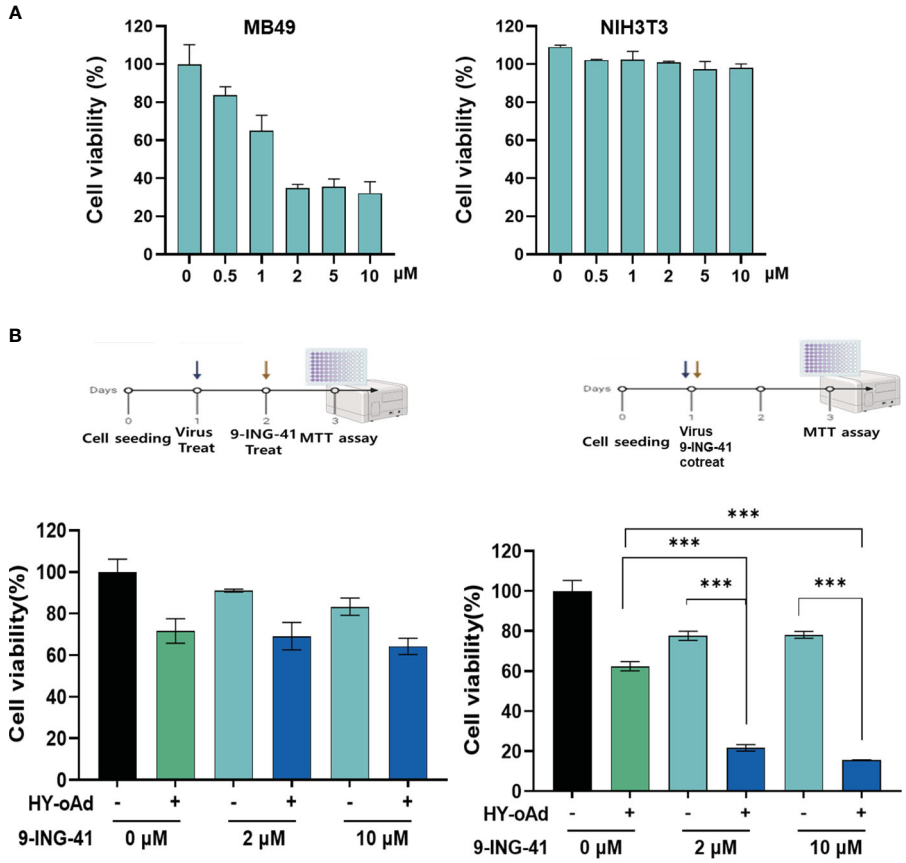

FIGURE 3
Cancer cell-specific killing effect of HY-oAd combined with 9-ING-41. **(A)** Bladder cancer cells (MB49) and normal cells (NIH3T3) were treated with 0–10 μM of 9-ING-41 for 48 h The cell viability was determined by MTT assay. **(B)** MB49 cells were either sequentially treated with 9-ING-41 at 24 h after HY-oAd treatment (left) or simultaneously treated with 9-ING-41 and HY-oAd for 48 h (right). Each cell line was tested at least three times, and the data shown are representative of experiments performed in triplicate. Bars represent mean ± SD. ***$p < 0.001$. p-Values were determined using the two-way ANOVA. MTT, 3-(4,5-dimethylthiazol-2-yl)-2,5-diphenyltetrazolium bromide.

determine the optimal combination therapy administration method. When 9-ING-41 was administered 24 h after HY-oAd administration (left panel), the bladder cancer cell killing effect of the combination therapy was similar to that observed with HY-oAd monotherapy, suggesting an antagonistic relationship of this administration method. In contrast, co-treatment of HY-oAd and 9-ING-41 at the same time point led to combination therapy exerting a significantly superior bladder cancer cell-killing effect compared to respective monotherapy groups (***$p < 0.001$). Based on these findings, all subsequent HY-oAd+9-ING-41 administration was performed by concomitant administration of both therapeutics in the remainder of this study.

Lastly, we investigated whether the synergistic bladder cancer cell killing effect of HY-oAd+9-ING-41 was achieved due to 9-ING-41-mediated enhancement of viral replication. As shown in Supplementary Figure S2, up to 10 μM 9-ING-41 did not affect the overall replication efficiency of HY-oAd in MB49 bladder cancer cells. Together, these results demonstrated that the simultaneous administration of HY-oAd in combination with 9-ING-41 can induce a synergistic bladder cancer-specific cell killing effect with any inhibitory effect against viral replication.

Combination of HY-oAd with 9-ING-41 exerts potent antitumor effect against bladder cancer

To evaluate the combined antitumor efficacy of HY-oAd+9-ING-41, subcutaneous MB49 bladder tumors were established in C57BL/6 mice. When the average tumor volume reached 200 mm^3, the tumor-bearing mice were either intraperitoneally or intratumorally treated with HY-oAd, 9-ING-41, or HY-oAd+9-ING-41, along with PBS as a negative control as described in Figure 4A. As shown in Figure 4B, both PBS-treated groups exhibited rapid growth up to 28 days after the initial treatment. In contrast, 9-ING-41 and HY-oAd induced 42.1% and 51.5% inhibition of tumor growth, respectively. HY-oAd+9-ING-41 treatments induced a significantly more potent antitumor effect

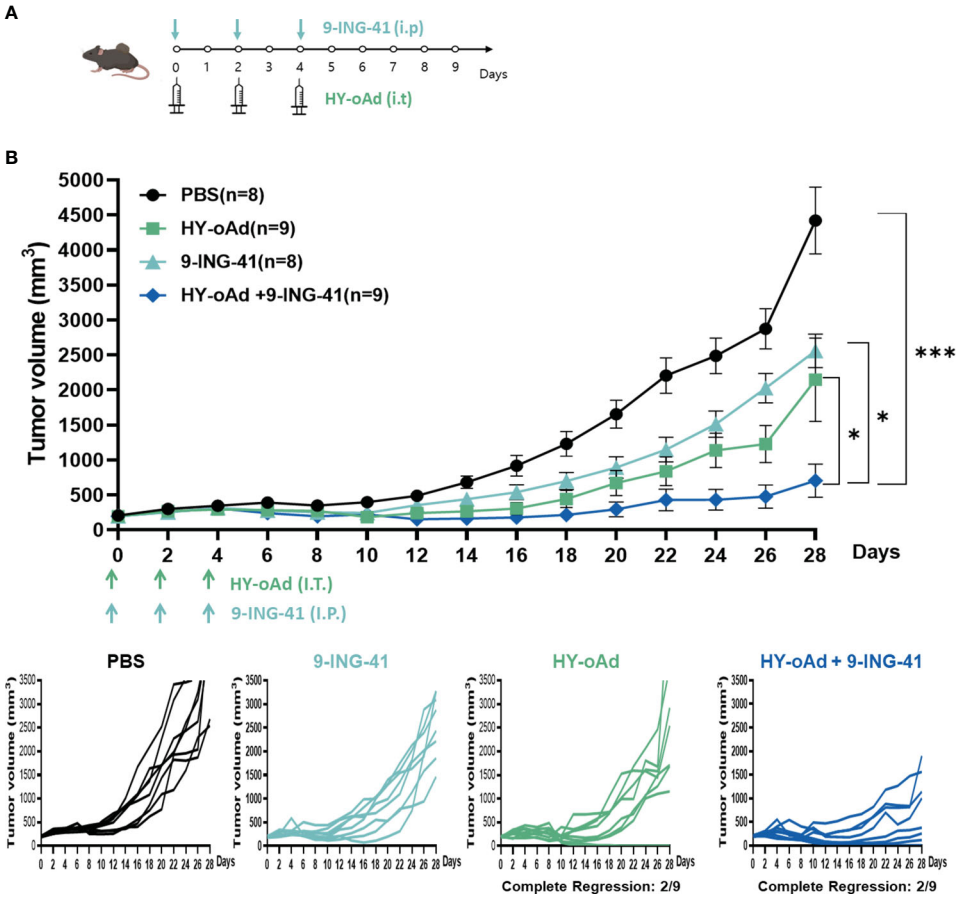

FIGURE 4
Antitumor effect of HY-oAd with 9-ING-41 combination therapy against subcutaneous MB49 tumors. **(A)** Graphical outlay of the treatment schedule and dosing for the combination therapy efficacy evaluation study. When the mean tumor volume of MB49 reached 200 mm^3, mice were intratumorally treated three times with 2×10^{10} VPs of HY-oAd and/or intraperitoneally administered with 10 mg/kg of 9-ING-41 (n = 8–9 per group), along with PBS as negative control. **(B)** The mean tumor volume throughout the course of the study and individual tumor volume of all mice are provided. Data are presented as mean ± SEM (n = 8–9). *$p < 0.05$, ***$p < 0.001$. p-Values were determined using the one-way ANOVA. Individual tumor growth curves in MB49 tumor model treated with PBS, 9-ING-41, HY-oAd, or HY-oAd+ 9-ING-41 were plotted. VPs, viral particles; PBS, phosphate-buffered saline.

compared with either HY-oAd or 9-ING-41 monotherapy (*$p < 0.05$), showing 72.6% and 67.2% superior tumor burden reduction, respectively. Importantly, both HY-oAd and HY-oAd+9-ING-41 treatments exerted robust anti-metastatic effects compared to PBS or 9-ING-41 groups where extensive lung metastasis (>20 metastatic nodules per lung) was observed (Supplementary Figure S3). In detail, 6/6 and 8/8 mice in PBS and 9-ING-41 groups, respectively, showed extensive lung metastasis, whereas 5/9 mice were either free of metastatic nodules or with less than 10 nodules for both HY-oAd monotherapy and HY-oAd+9-ING-41 treatment groups. Notably, HY-oAd+9-ING-41 treatment led to the highest percentage of mice that were nearly absent of metastatic nodules (5/9 for combination therapy versus 3/9 for HY-oAd monotherapy for mice with 0–2 metastatic nodules). None of the treatments induced any significant body weight loss and observable toxicity up to 28 days after the initial treatment (Supplementary Figure S4), indicating negligible systemic toxicity. Taken together, these results suggest that the combination of HY-oAd and 9-ING-41 can effectively control the growth of both in a safe manner.

HY-oAd+9-ING-41 promotes ECM degradation, apoptosis, and viral dispersion in bladder tumor tissue

To further evaluate the therapeutic effect of the combination treatment regimen, histological and immunohistochemical analyses of tumor tissues were performed. As shown in Figure 5A, Masson's trichrome staining revealed that HY-oAd-, 9-ING-41-, and HY-oAd+9-ING-41-treated tumors had significantly attenuated tumor extracellular matrix (ECM) accumulation in comparison to those treated with PBS (***$p < 0.001$), suggesting that either HY-oAd or 9-ING-41 could effectively degrade tumor ECM. Hematoxylin and eosin (H&E) and proliferating cell nuclear antigen (PCNA) staining revealed that tumors treated with HY-oAd+9-ING-41 were nearly devoid of PCNA-positive cell population (Figure 5B; ***$p < 0.001$) and that most of the tumor tissues were necrotic. In line with these results, terminal deoxynucleotidyl transferase dUTP nick end labeling assay (TUNEL) staining revealed that HY-oAd+9-ING-

10.3389/fimmu.2024.1360436

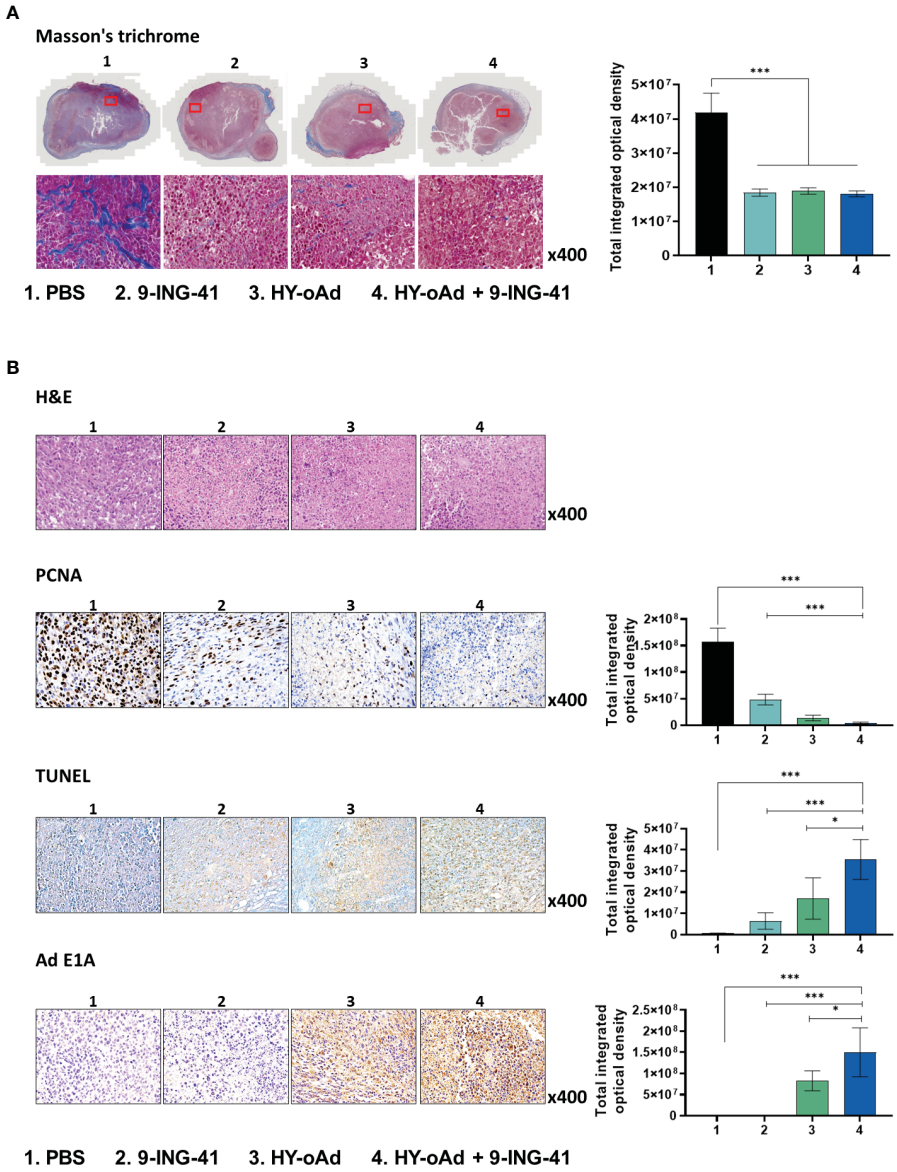

FIGURE 5
ECM degradation, apoptosis, and viral dispersion induced by combination of HY-oAd with 9-ING-41 in bladder tumor tissue. **(A)** MB49 tumor tissues of mice treated with PBS, 9-ING-41, HY-oAd, and HY-oAd+9-ING-41 were stained with Masson's trichrome to assess collagen accumulation in the tumor tissues. Original magnification rate, ×400. The percentage of collagen-occupied area of MB49 tumor tissues was semi-quantitatively analyzed using ImageJ software. Data are presented as mean ± SD (n = 4). ***$p < 0.001$. p-Values were determined using Student's t-test. **(B)** H&E staining, TUNEL staining, and immunohistochemical staining of PCNA and Ad E1A were performed using MB49 tumor sections. Original magnification rate, ×400. Images were semi-quantitatively analyzed using ImageJ software. Data are presented as mean ± SD (n = 4). *$p < 0.05$, ***$p < 0.001$. p-Values were determined using Student's t-test. ECM, extracellular matrix; PBS, phosphate-buffered saline; TUNEL, terminal deoxynucleotidyl transferase dUTP nick end labeling assay; PCNA, proliferating cell nuclear antigen.

41-treated tumor tissues exhibited the highest level of apoptotic cell death over either monotherapy option (***p <0.001, *p <0.05). These results suggested that the combination of HY-oAd+9-ING-41 effectively induced apoptosis and inhibited the proliferation of tumor cells in a synergistic manner. Importantly, HY-oAd+9-ING-41-treated tumors exhibited more robust dispersion of virions and a greater quantity of virion accumulation than HY-oAd in the tumor tissues, suggesting that the potent ECM-degrading and pro-apoptotic effect of the combination could facilitate virus dispersion throughout the bladder tumor.

HY-oAd+9-ING-41 promotes T-cell accumulation in tumor and spleen tissues

To investigate the mechanism behind the antitumor immune response mediated by each treatment, the splenic and intratumoral $CD4^+$ and $CD8^+$ T-cell populations were analyzed. As shown in Figure 6A, the number of $CD4^+$ and $CD8^+$ T-cell populations was unaffected by 9-ING-41 monotherapy in comparison with the PBS control group. In contrast, both HY-oAd monotherapy and its combination with 9-ING-41 led to significantly elevated $CD4^+$ and

10.3389/fimmu.2024.1360436

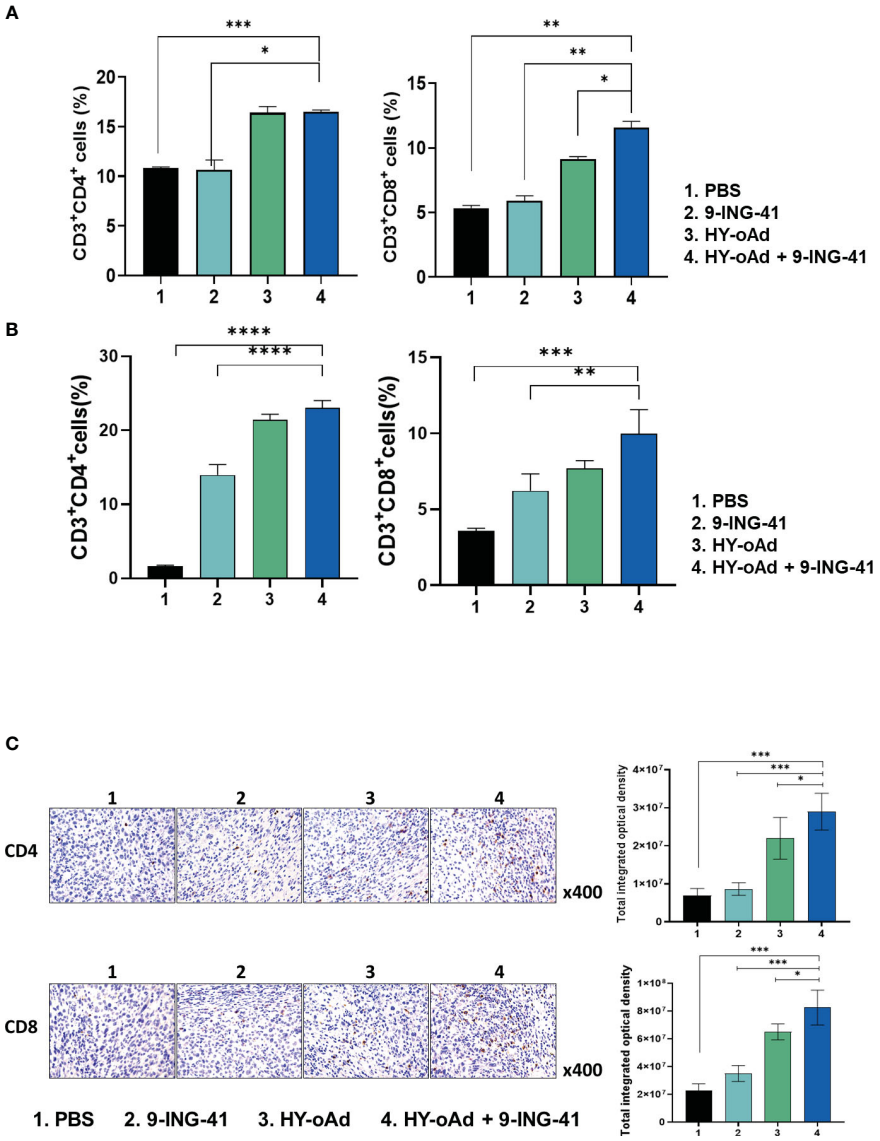

FIGURE 6
Analysis of T-cell accumulation in spleen and tumor tissues after combined treatment using HY-oAd with 9-ING-41. **(A)** The changes to $CD3^+CD4^+$ or $CD3^+CD8^+$ T-cell population in spleen were analyzed using MB49 subcutaneous tumor-bearing mice treated with PBS, 9-ING-41, HY-oAd, and HY-oAd+9-ING-41 via flow cytometry. Data are presented as mean ± SD (n = 4). ***$p < 0.001$, **$p < 0.01$, *$p < 0.05$. p-Values were determined using Student's t-test. **(B)** The infiltration of $CD3^+CD4^+$ or $CD3^+CD8^+$ T cells into the subcutaneous MB49 tumor tissues was analyzed by flow cytometry following treatment with PBS, 9-ING-41, HY-oAd, and HY-oAd+9-ING-41. Data are presented as mean ± SD (n = 4). ***$p < 0.001$, **$p < 0.01$. p-Values were determined using Student's t-test. **(C)** Immunohistochemical staining of $CD4^+$ and $CD8^+$ T cells from subcutaneous MB49 tumor tissue sections obtained after treatment with PBS, 9-ING-41, HY-oAd, and HY-oAd+9-ING-41. Original magnification rate, x400. Images were semi-quantitatively analyzed using ImageJ software. Data are presented as mean ± SD (n=4). *$p < 0.05$, ***$p < 0.001$. p-Values were determined using Student's t-test. PBS, phosphate-buffered saline.

$CD8^+$ T-cell population in comparison with the PBS or 9-ING-41 group (*$p < 0.05$, **$p < 0.01$, or ***$p < 0.001$), suggesting that HY-oAd was integral to induction of T cell-mediated antitumor immune response. Of note, HY-oAd+9-ING-41 combination therapy induced a higher level of $CD8^+$ T-cell accumulation in the spleen with respect to HY-oAd (*$p < 0.05$), whereas the $CD4^+$ T-cell accumulation was similarly high between the two groups, showing that the synergistic effect induced by the combination therapy was more reliant on $CD8^+$ T-cell response. In line with these findings, the analysis of tumor-infiltrating lymphocyte (TIL) population also revealed that both $CD4^+$ and $CD8^+$ T-cell accumulation was significantly elevated in tumor tissues after treatment with HY-oAd monotherapy or its combination with 9-ING-41 in comparison with the PBS control group with extremely low-level T-cell infiltration (less than 5% of total tumor cell population was either CD4+ or CD8+ T cells; ***p < 0.001; Figure 6B). One notable difference between spleen and tumor tissues was that 9-ING-41 significantly elevated $CD4^+$ and $CD8^+$ T-cell infiltration into the tumor tissues in comparison with PBS control, whereas the therapy failed to elevate T-cell recruitment in the spleen tissues, suggesting that systemically administered 9-ING-41 may induce a more pronounced T-cell response in

immunosuppressive tumor microenvironment. Importantly, HY-oAd plus 9-ING-41 combination therapy led to the highest level of both $CD4^+$ and $CD8^+$ T-cell infiltration among all treatment groups (**$p < 0.01$ or ***$p < 0.001$ versus 9-ING-41 monotherapy). Similar results were also obtained by immunohistochemical analysis, as HY-oAd+9-ING-41 induced the highest level of $CD4^+$ and $CD8^+$ T-cell recruitment in the tumor (Figure 6C; *$p < 0.05$ or ***$p < 0.001$ versus HY-oAd or 9-ING-41 monotherapy). Together, these results suggested that the combination therapy induced a potent antitumor effect through robust initiation of T cell-mediated antitumor immune response.

Tumor-specific immune response and prevention of T-cell exhaustion by combination of HY-oAd and 9-ING-41

To further characterize the antitumor immune response induced by HY-oAd+9-ING-41 combination therapy, the splenocytes from tumor-bearing mice treated with PBS, 9-ING-41, 1×10^9 VPs of HY-oAd, and HY-oAd+9-ING-41 were harvested and co-cultured with irradiated MB49 cells to determine IFN-γ-secreting lymphocyte population by IFN-γ ELISpot assay. As shown in Figure 7A, the HY-oAd+9-ING-41 combination group showed a significantly higher number of IFN-γ-secreting lymphocytes over the respective monotherapy (*$p < 0.05$, **$p < 0.01$), suggesting that it could induce a potent tumor-specific adaptive immune response.

Next, we evaluated whether the HY-oAd+9-ING-41 combination therapy abates cytotoxic T-cell exhaustion in the spleen and tumor tissues. As shown in Figure 7B, all treatments (9-ING-41, HY-oAd, or HY-oAd+9-ING-41) elevated frequency of $CD8^+PD1^-$ T-cell subsets in spleen tissues in comparison with the PBS control group (*$p < 0.05$, **$p < 0.01$), suggesting that all three treatments can enhance the accumulation of functional cytotoxic T cells that were not exhausted in the secondary lymphoid organ. In contrast, only HY-oAd+9-ING-41 combination therapy significantly elevated the number of unexhausted $CD8^+PD1^-$ T-cell population in the tumor tissues (***$p < 0.01$), whereas the respective monotherapy could not. In support, immunofluorescence detection of PD-1 expression in MB49 tumor tissues also revealed that the periphery of tumor tissues of mice in the PBS group was enriched with $PD\text{-}1^+$ cells (Figure 7C). Both 9-ING-41 and HY-oAd monotherapy markedly attenuated intratumoral infiltration of $PD\text{-}1^+$ cells in comparison with the PBS control group. Of the two monotherapies, 9-ING-41 exerted superior inhibition of $PD\text{-}1^+$ cell infiltration. Importantly, HY-oAd+9-ING-41 combination therapy showed a markedly lower level of $PD\text{-}1^+$ cell infiltration compared to the HY-oAd monotherapy or PBS control group, suggesting that the potent PD-1 inhibitory effect of 9-ING-41 enabled a synergistic increase in intratumoral infiltration of unexhausted $CD8^+PD1^-$ T cells. Together, these results demonstrate that the HY-oAd+9-ING-41 combination therapy could effectively induce a tumor-specific immune response and enhance the recruitment of unexhausted cytotoxic T cells in the immunosuppressive tumor milieu.

Discussion

BCG has been used as the first-line immunotherapeutic treatment for NMIBC. Despite BCG having long been the standard therapy, its failure occurred in 30% to 50% of patients (36). The response to BCG is often limited by several factors, like activation of the PD-1/PD-L1 signaling axis that induces immune anergy and T-cell exhaustion, which abrogate the efficacy of BCG therapy over the treatment course (31). Currently, oncolytic virus expressing pro-inflammatory cytokine can boost the induction of antitumor immune response and reprogram the immunosuppressive tumor milieu (10, 37–39). Still, the oncolytic viruses' effect on T-cell exhaustion and immune checkpoint regulation within the tumor microenvironment have not been conclusively elucidated: some suggested that T-cell exhaustion can be prevented or reversed by oncolytic virotherapy, while others demonstrated that the virus infection can upregulate PD-L1 expression on the surface of tumor cells and simultaneously increase PD-1 expression on T cells that are suggestive of exhaustion (40–42).

Although the complexity of PD-1 regulation patterns for T cells makes it difficult for PD-1 expression status alone to discriminate between exhausted and activated T cells within the tumor microenvironment (43), our present findings demonstrated that clinical-stage GSK-3β inhibitor, 9-ING-41, which has been reported to activate and transcriptionally attenuate expression of various immune checkpoint molecules of T cells in either preclinical or clinical environment (35, 44, 45), in combination with oAd armed with immune-stimulatory and ECM-degrading therapeutic genes could effectively diminish $PD\text{-}1^+$ cell infiltration into the periphery of the bladder tumor and synergistically enhanced the infiltration and recruitment of $CD8^+PD\text{-}1^-$ T cells in both tumor and spleen (Figures 7B, C). These findings suggested that the potential risk of T-cell exhaustion via activation of PD-1/PD-L1 signaling axis could be effectively mitigated by the rational combination of HY-oAd and 9-ING-41. The combination therapy was also shown to induce the highest level of tumor-specific immune response (Figure 7A), which likely contributed to it inducing the most robust inhibition of lung metastasis (Supplementary Figure S3). These findings are in line with previous publications that highlight the importance of tumor-specific immunity in the initiation of strong abscopal effect and systemic immune response by the therapeutic (46–48). Although these findings showed that PD-1 downregulation by combination may exert an anti-metastatic effect via abscopal effect and systemic immune activation, more in-depth preclinical characterization of the combination therapy regimen across different types of tumors, especially those that are refractory to PD-1/PD-L1 checkpoint inhibitors, is still needed to translate these findings into clinical stages.

Additionally, GM-CSF therapy has been reported to exert conflicting biological functions across different types of tumors, as both pro-tumorigenic and anticancer activity of the cytokine have been reported (22, 49). The inhibition of the GSK-3 signaling pathway has also been reported to exert potentially pro-tumorigenic function, as it can induce anti-inflammatory reactions by suppressing the NF-κB signaling axis (34, 50, 51).

10.3389/fimmu.2024.1360436

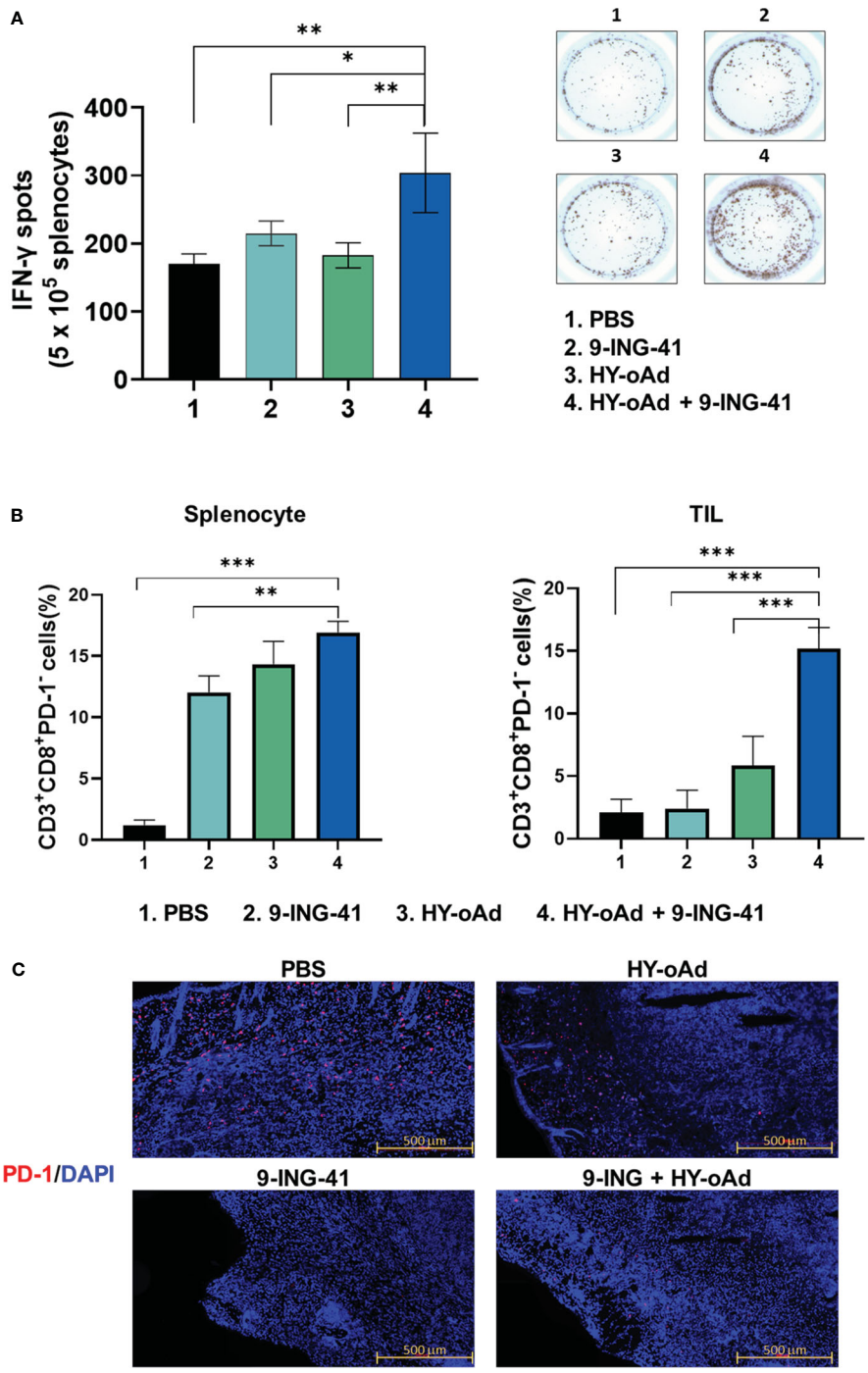

FIGURE 7
Assessment of tumor-specific immune response and prevention of T-cell exhaustion by combination of HY-oAd with 9-ING-41. **(A)** Splenocytes were collected from each group at 12 days following treatment and co-incubated with preirradiated MB49 cells for 24 h IFN-γ ELISPOT assays were then performed. Images are representatives of results from three independent experiments. The number of spots was counted per 1×10^5 splenocytes. Each value represents mean ± SD. $^{**}p < 0.01$, $^{*}p < 0.05$. *p*-Values were determined using Student's *t*-test. **(B)** $CD3^+CD8^+PD\text{-}1^-$ T cells from spleen or tumor tissues of mice that were treated with PBS, 9-ING-41, HY-oAd, and HY-oAd+9-ING-41 were analyzed by flow cytometry. Data are presented as mean ± SD (n = 4). $^{***}p < 0.001$, $^{**}p < 0.01$. *p*-Values were determined using Student's *t*-test. **(C)** Subcutaneous MB49 tumors treated with each group were stained with DAPI (blue fluorescence) or Alexa488-labeled PD-1 (red fluorescence). Scale bar = 500 μm. PBS, phosphate-buffered saline; DAPI, 4′,6-diamidino-2-phenylindole.

These findings demonstrate that further evaluations of HY-oAd and 9-ING-41 in other types of cancers will be necessary in the future to better identify patient demographics that would benefit from this treatment regimen.

Another important clinical feature of both HY-oAd and 9-ING-41 for cancer therapy is that they are capable of degrading aberrant tumor ECM (Figure 5A), which is a well-known barrier against intratumoral penetration and dispersion of various cancer

therapeutics and immune cells (52–54). In line with this literature, effective degradation of tumor ECM by HY-oAd and 9-ING-41 was shown to facilitate $CD4^+$ and $CD8^+$ T-cell infiltration into the tumor tissues (Figures 6B, C, 7B), as well as simultaneously improving HY-oAd dispersion and accumulation throughout the bladder tumor tissues in a viral replication-independent manner (Figures 5B, Supplementary Figure S2). These findings highlighted that degradation of ECM had a critical role in positively reshaping TIL composition within bladder tumors.

There are several studies showing the role of GM-CSF in immune cell homeostasis. These studies illustrate that a small amount of GM-CSF hampers the proper generation of innate immune cells and subsequent activation of the adaptive anticancer immune response, whereas excessive GM-CSF can deplete immune cells and foster cancer growth (22, 49). Additionally, the impact of GM-CSF signaling on cancer progression varied based on cancer type and the tumor microenvironment as well as GM-CSF levels. Even though GM-CSF has a double-edged sword mechanism in cancer immunotherapy, our results show that the strategy of combining 9-ING-41 with HY-oAd-expressing GM-CSF does not negatively affect the eradication of bladder tumors. Nevertheless, for the combination dosing strategy proposed in this study to be applied in the clinic with expanded indications, a serious approach to the effect of GM-CSF on the anticancer immune response is required.

Despite significant advancements made with Ad-based immunotherapy for the treatment of bladder cancer, no oAd treatment has reached clinical approval for the treatment of NMIBC by the US FDA or European Medicines Agency to date. Additionally, there are many patients who still suffer from NMIBC and do not respond to either BCG or ICI treatments, with more recent lines of evidence suggesting that T-cell exhaustion is correlated with BCG unresponsiveness of NMIBC patients (30, 31). To address these challenges, the present report investigated GSK-3β inhibitor, 9-ING-41, rather than PD-1/PD-L1-targeted ICI to pharmacologically inhibit checkpoint upregulation within the tumor milieu and combat T-cell exhaustion in combination with multifunctional HY-oAd. Collectively, our findings demonstrate that oAd armed with multiple immune-stimulatory and ECM-degrading therapeutic genes can outperform those observed using oAd expressing GM-CSF as a single therapeutic gene and that it could synergize with 9-ING-41 to induce robust degradation of tumor ECM and tumor-specific immune response and prevent immune cell exhaustion, ultimately enabling effective control of primary and metastatic bladder tumor growth.

Materials and methods

Cell lines and reagents

MB49 (murine bladder cancer cell line) was kindly gifted by Prof. Chung-Soo Kim (Asan Medical Center, Seoul, South Korea). UM-UC-3, RT4 (human bladder cancer cell lines), NIH3T3 (murine embryonic fibroblast), BJ (human normal fibroblast), and 293A (human embryonic kidney cell) were purchased from the American Type Culture Collection (ATCC; Manassas, VA, USA). RT4 was cultured in RPMI-1640 medium (PAN Biotech, Dorset, UK); MB49, UM-UC-3, NIH3T3, and BJ were cultured in Dulbecco's modified high-glucose Eagle's medium (DMEM; PAN Biotech). All media were supplemented with 1% penicillin-streptomycin (PAN Biotech), and 10% fetal bovine serum (FBS; GIBCO, Grand Island, NY, USA) was used as the culture medium. Cells were maintained at 37°C in a humidified incubator with 5% CO_2.

The GSK-3B inhibitor 9-ING-41 was purchased from MedChemExpress (MCE) (Monmouth Junction, NJ, USA). It was dissolved in dimethyl sulfoxide (DMSO; Sigma-Aldrich, Burlington, MA, USA) and stored as a 10 mM stock solution at −20°C.

Preparation of HY-oAd

To produce HY-oAd, the HY-oAd genome containing plasmid was linearized with *Pac*I and then transfected into 293A cells using JetPrime transfection reagent (Polyplus, Illkirch, France) according to the manufacturer's instruction. The construction and generation of hypoxia- and telomerase-responsive control oAd lacking therapeutic transgene (control oAd) have been described previously (50). All Ads were propagated in A549 cells and purified by CsCl gradient centrifugation. The number of VPs was determined by measuring the optical density at 260 nm, for which an absorbance value of 1 is equivalent to 1.1×10^{12} VPs/mL. Purified viruses were stored at −80°C until use.

Quantification of IL-12, GM-CSF, and RLX expression level

MB49 cells were plated onto 6-well plates at 2×10^5 cells per well overnight and then infected with HY-oAd at a MOI of 20, 50, or 100. At 48 h after infection, the supernatants were harvested. The expression levels of mouse IL-12 and mouse GM-CSF secreted into the supernatants were determined using conventional mouse IL-12p70 (R&D Systems, Minneapolis, MN, USA) and mouse GM-CSF Duo Set ELISA kit (R&D Systems) according to the manufacturer's instructions. For the assessment of the mRNA expression level of RLX, cell lysates were obtained from the same plate as those utilized for ELISA by treating these cells with RNA iso Plus kit (Takara, Otsu, Japan) according to the manufacturer's protocol.

Total RNA was purified from the cell lysates, and cDNA was obtained using a High-Capacity cDNA Reverse Transcription Kit (Applied Biosystems, Foster City, CA, USA) under the following conditions: 25°C for 10 min, 37°C for 120 min, and 85°C for 5 min. RLX mRNA was amplified by PCR with the following primer set: 5′-CCTGGAGCAAAAGGTCTCTG-3′ as the sense primer and 5′-TCTCAGATAGGGCTGCCTTC-3′ as the antisense primer. PCR products were analyzed by gel electrophoresis using 1% agarose gels.

MTT assay

The cancer cell-specific cytotoxicity of HY-oAd was determined by measuring the conversion of the tetrazolium salt 3-(4,5-dimethylthiazol-2-yl)-2,5-diphenyltetrazolium bromide (MTT; Sigma, Livonia, MI, USA) to formazan. The cells were seeded at 5 × 10^3 cells per well in a 96-well plate overnight and then treated with HY-oAd or control oAd at 0–400 MOI (MB49, NIH3T3) or 0–50 MOI (RT-4, UM-UC-3, BJ). The cells were also treated with 9-ING-41 at 0–10 μM. For combination treatment, MB49 were sequentially treated with 9-ING-41 (2 or 10 μM) at 24 h after HY-oAd (100 MOI) treatment or simultaneously treated with 9-ING-41 (2 or 10 μM) and HY-oAd (100 MOI) for 48 h. At 48 h after the infection, 50 μL of MTT in PBS (2 mg/mL) was added to each well, and then cells were incubated at 37°C for 4 h. The supernatant was discarded, and the precipitated formazan was dissolved in 200 μL of DMSO (Sigma). Plates were read on a microplate reader at 540 nm. The absorbance of the PBS-treated well was considered 100% viable. All assays were performed in triplicate.

In vivo antitumor effect

To evaluate the therapeutic effects of HY-oAd, 5 × cells of MB49 were suspended in 50 μL of Hank's balanced salt solution (HBSS; GIBCO) and injected subcutaneously into the right flank of 6-week-old male C57BL/6 mice. When the tumor volume reached approximately 200 mm^2, mice were sorted into groups to receive three intratumoral injections of HY-oAd or oAd expressing GM-CSF (oAd/GM-CSF) at 2 × 10^{10} VPs/dose every other day, along with PBS as negative control (n = 6 per group). To evaluate therapeutic effects by combination of HY-oAd and 9-ING-41, mice were randomly divided into four groups—1) PBS control, 2) HY-oAd (1 × 10^{10} VP, intratumoral injection), 3) 9-ING-41 (10 mg/kg, intraperitoneal injection), and 4) combined HY-oAd and 9-ING-41—administered at the same dose and administration route for single treatments. For individual treatments, mice were treated with HY-oAd and 9-ING-41 every other day for a total of three treatments. At 61 days post-inoculation of the primary tumor, mice with complete regression were rechallenged with MB49 cancer cells. Tumor growth was monitored every other day by measuring the length (L) and width (W) using electronic calipers (Fowler, Inc., Zurich, Switzerland). Tumor volume was calculated using the following formula: volume = $0.523LW^2$.

Histology and immunohistochemistry

For histologic examination and immunohistochemical staining, MB49 tumor tissues were collected from tumor-bearing mice treated with PBS, HY-oAd, 9-ING-41, and HY-oAd plus 9-ING-41 at 3 days after the last treatment, fixed in 4% paraformaldehyde, and embedded in paraffin wax. H&E, Masson's trichrome staining, and TUNEL were performed as previously described (51). The tumor sections were incubated at 4°C overnight with anti-mouse PCNA antibody (DAKO, Glostrup, Denmark), anti-rabbit E1A polyclonal antibody (Abcam, Cambridge, UK), anti-mouse CD4 monoclonal antibody (Invitrogen, Waltham, MA, USA), or CD8a monoclonal antibody (Invitrogen) and then incubated with Streptavidin-HRP (BD Biosciences, Franklin Lakes, NJ, USA) for 1 h at room temperature. Diaminobenzidine/hydrogen peroxidase (DAKO) was treated as the chromogen substrate, using a Peroxidase/DAB Detection kit (Agilent Technologies, Santa Clara, CA, USA). All slides were counterstained with Mayer's hematoxylin. The expression levels of PCNA, E1A, CD4, and CD8a were semi-quantitatively analyzed using ImageJ image analysis software (National Institutes of Health, Bethesda, MD, USA).

Viral production of HY-oAd in MB49 in combination with 9-ING-41

To assess the viral replication of HY-oAd in MB49, cells were seeded in 24-well plates and co-treated with HY-oAd at MOI of 100 and 200 and 9-ING-41 at 0, 5, or 10 μM. After 48 h of incubation, the cell pellets and supernatants were collected and freeze-thawed three times to harvest the virions. Quantitative real-time PCR (TaqMan PCR detection; Applied Biosystems, Waltham, MA, USA) was used to assess the number of viral genomes in each sample as described previously (55). The results are representative of three independent experiments.

Fluorescence-activated cell sorting analysis of immune cell population

MB49 tumor-bearing mice were either intraperitoneally or intratumorally injected with PBS, HY-oAd, 9-ING-41, and HY-oAd plus 9-ING-41. At 7 days after the initial treatment, lymphocytes were isolated from the spleen or tumor as previously reported (56). Before staining, cells were treated with FcR Blocking Reagent, mouse (Miltenyi Biotec, Bergisch Gladbach, Germany) in MACS buffer [0.5% bovine serum albumin (BSA) and 2 mM ethylenediaminetetraacetic acid (EDTA) in PBS]. Then, cells were stained with fluorescent-labeled antibodies. CD3-FITC (BioLegend, San Diego, CA, USA), CD8-BB700 (BD Biosciences), CD4-APC (BioLegend), and PD-1-PE (BD Biosciences) for 1 h at 4°C. After washing three times with MACS buffer, the cells were fixed in 1% paraformaldehyde. Samples were analyzed using a flow cytometry (FACSCanto™ II flow cytometer; BD Biosciences).

IFN-γ ELISPOT assay

After 3 days following the final treatment with PBS, HY-oAd, 9-ING-41, and HY-oAd plus 9-ING-41, spleens were collected aseptically from tumor-bearing mice, and unicellular splenocytes were prepared as described previously (57). Briefly, the splenocytes were co-cultured with irradiated MB49 (6,000 rad) tumor cells for 18 h in the presence of recombinant mouse IL-2 (100 U/mL; R&D Systems). An IFN-γ ELISpot assay (BD Biosciences) was then

carried out as described previously (57). The spots were measured using a computer-based immunospot system (AID ELISpot Reader System version 3.4; Autoimmun Diagnostika GmbH, Strassberg, Germany).

Animal studies

Five-week-old male C57BL/6 mice (DBL Inc., Eumseong, South Korea) were maintained in a laminar airflow cabinet with specific pathogen-free conditions. All facilities have been approved by the Association for Assessment and Accreditation of Laboratory Animal Care International (AAALAC). Animal studies were conducted according to the institutional guidelines established by the Hanyang University Institutional Animal Care and Use Committee.

Statistical analysis

No statistical methods were used to predetermine sample sizes for *in vitro* or *in vivo* experiments. All results are expressed as the mean ± SEM unless indicated otherwise. Comparisons between groups were made using the two-tailed Student's t-test or one-way ANOVA and Tukey's *post-hoc* tests for multiple groups. Statistical significance was denoted as $^{*}p < 0.05$, $^{**}p < 0.01$, and $^{***}p < 0.001$. Statistical analysis was performed in GraphPad Prism 5 (GraphPad, San Diego, CA, USA).

Data availability statement

The original contributions presented in the study are included in the article/Supplementary Material, further inquiries can be directed to the corresponding author/s.

Ethics statement

The animal study was approved by Hanyang University Institutional Animal Care and Use Committee. The study was conducted in accordance with the local legislation and institutional requirements.

Author contributions

A-RY: Conceptualization, Funding acquisition, Project administration, Writing – original draft, Writing – review & editing. AJ: Data curation, Visualization, Writing – original draft, Writing – review & editing. JH: Writing – original draft. BK: Data curation, Writing – original draft. C-OY: Conceptualization, Investigation, Supervision, Writing – original draft, Writing – review & editing.

Funding

The author(s) declare financial support was received for the research, authorship, and/or publication of this article. This work was supported by the National Research Foundation of Korea (2021R1A2C301016611, C-OY; 2021M2E8A1049151, 2022R1I1A1A01071162, A-RY).

Conflict of interest

Author JH is an employee of the company GeneMedicine Co., Ltd. C-OY is the CEO of GeneMedicine, Co., Ltd.

The remaining authors declare that the research was conducted in the absence of any commercial or financial relationships that could be construed as a potential conflict of interest.

Publisher's note

Supplementary material

The Supplementary Material for this article can be found online at: https://www.frontiersin.org/articles/10.3389/fimmu.2024.1360436/full#supplementary-material

References

1. Amling CL. Diagnosis and management of superficial bladder cancer. *Curr Probl Cancer*. (2001) 25:219–78. doi: 10.1067/mcn.2001.117539

2. Kimura T, Ishikawa H, Kojima T, Kandori S, Kawahara T, Sekino Y, et al. Bladder preservation therapy for muscle invasive bladder cancer: the past, present and future. *Jpn J Clin Oncol*. (2020) 50:1097–107. doi: 10.1093/jjco/hyaa155

3. Hadaschik BA, ter Borg MG, Jackson J, Sowery RD, So AI, Burt HM, et al. Paclitaxel and cisplatin as intravesical agents against non-muscle-invasive bladder cancer. *BJU Int*. (2008) 101:1347–55. doi: 10.1111/j.1464-410X.2008.07571.x

4. Taoka R, Matsuoka Y, Kohashiguchi K, Miura T, Tohi Y, Miyauchi Y, et al. Impact of second transurethral resection on recurrence in patients with high-grade Ta bladder cancer. *Int J Urol*. (2020) 27:1130–5. doi: 10.1111/iju.14372

5. Li Y, Youssef SF, Buanz AB. Intravesical combination therapies for non-muscle invasive bladder cancer: Recent advances and future directions. *Eur J Pharmacol*. (2022) 926:175024. doi: 10.1016/j.ejphar.2022.175024

6. Das SK, Menezes ME, Bhatia S, Wang XY, Emdad L, Sarkar D, et al. Gene therapies for cancer: strategies, challenges and successes. *J Cell Physiol*. (2015) 230:259–71. doi: 10.1002/jcp.24791

7. Belete TM. The current status of gene therapy for the treatment of cancer. *Biol: Targets Ther*. (2021) 15:67–77. doi: 10.2147/BTT.S302095

8. Lee A. Nadofaragene firadenovec: first approval. *Drugs*. (2023) 83:353–7. doi: 10.1007/s40265-023-01846-z

9. Grandi P, Darilek A, Moscu A, Pradhan A, Li R. Intravesical infusion of oncolytic virus CG0070 in the treatment of bladder cancer. *Methods Mol Biol.* (2023) 2684:303–17. doi: 10.1007/978-1-0716-3291-8_19

10. Packiam VT, Lamm DL, Barocas DA, Trainer A, Fand B, Davis R, et al. An open label, single-arm, phase II multicenter study of the safety and efficacy of CG0070 oncolytic vector regimen in patients with BCG-unresponsive non-muscle-invasive bladder cancer: Interim results. *Urol Oncol.* (2018) 36:440–7. doi: 10.1016/j.urolonc.2017.07.005

11. Liang M. Oncorine, the world first oncolytic virus medicine and its update in China. *Curr Cancer Drug Targets.* (2018) 18:171–6. doi: 10.2174/1568009618666171129221503

12. Saito Y, Sunamura M, Motoi F, Abe H, Egawa S, Duda DG, et al. Oncolytic replication-competent adenovirus suppresses tumor angiogenesis through preserved E1A region. *Cancer Gene Ther.* (2006) 13:242–52. doi: 10.1038/sj.cgt.7700902

13. Barton KN, Siddiqui F, Pompa R, Freytag SO, Khan G, Dobrosotskaya I, et al. Phase I trial of oncolytic adenovirus-mediated cytotoxic and interleukin-12 gene therapy for the treatment of metastatic pancreatic cancer. *Mol Ther Oncol.* (2021) 20:94–104. doi: 10.1016/j.omto.2020.11.006

14. Yoo JY, Kim JH, Kwon YG, Kim EC, Kim NK, Choi HJ, et al. VEGF-specific short hairpin RNA-expressing oncolytic adenovirus elicits potent inhibition of angiogenesis and tumor growth. *Mol Ther.* (2007) 15:295–302. doi: 10.1038/sj.mt.6300023

15. Havunen R, Siurala M, Sorsa S, Grönberg-Vähä-Koskela S, Behr M, Tähtinen S, et al. Oncolytic adenoviruses armed with tumor necrosis factor alpha and interleukin-2 enable successful adoptive cell therapy. *Mol Ther Oncol.* (2017) 4:77–86. doi: 10.1016/j.omto.2016.12.004

16. Yoon AR, Hong J, Kim SW, Yun CO. Redirecting adenovirus tropism by genetic, chemical, and mechanical modification of the adenovirus surface for cancer gene therapy. *Expert Opin Drug Delivery.* (2016) 13:843–58. doi: 10.1517/17425247.2016.1158707

17. Yun CO, Hong J, Yoon AR. Current clinical landscape of oncolytic viruses as novel cancer immunotherapeutic and recent preclinical advancements. *Front Immunol.* (2022) 13:953410. doi: 10.3389/fimmu.2022.953410

18. Hwang JK, Hong J, Yun CO. Oncolytic viruses and immune checkpoint inhibitors: preclinical developments to clinical trials. *Int J Mol Sci.* (2020) 21:8627. doi: 10.3390/ijms21228627

19. Hemminki O, Dos Santos JM, Hemminki A. Oncolytic viruses for cancer immunotherapy. *J Hematol Oncol.* (2020) 13:84. doi: 10.1186/s13045-020-00922-1

20. Macedo N, Miller DM, Haq R, Kaufman HL. Clinical landscape of oncolytic virus research in 2020. *J ImmunoTher Cancer.* (2020) 8:e001486. doi: 10.1136/jitc-2020-001486

21. Rong Q-x, Wang F, Guo Z-x, Hu Y, An S-n, Luo M, et al. GM-CSF mediates immune evasion via upregulation of PD-L1 expression in extranodal natural killer/T cell lymphoma. *Mol Cancer.* (2021) 20:80. doi: 10.1186/s12943-021-01374-y

22. Kumar A, Taghi Khani A, Sanchez Ortiz A, Swaminathan S. GM-CSF: A double-edged sword in cancer immunotherapy. *Front Immunol.* (2022) 13:901277. doi: 10.3389/fimmu.2022.901277

23. Hong IS. Stimulatory versus suppressive effects of GM-CSF on tumor progression in multiple cancer types. *Exp Mol Med.* (2016) 48:e242. doi: 10.1038/emm.2016.64

24. Su X, Xu Y, Fox GC, Xiang J, Kwakwa KA, Davis JL, et al. Breast cancer–derived GM-CSF regulates arginase 1 in myeloid cells to promote an immunosuppressive microenvironment. *J Clin Invest.* (2021) 131:e145296. doi: 10.1172/JCI145296

25. Varghese S, Rabkin SD, Liu R, Nielsen PG, Ipe T, Martuza RL. Enhanced therapeutic efficacy of IL-12, but not GM-CSF, expressing oncolytic herpes simplex virus for transgenic mouse derived prostate cancers. *Cancer Gene Ther.* (2006) 13:253–65. doi: 10.1038/sj.cgt.7700900

26. Choi KJ, Zhang SN, Choi IK, Kim JS, Yun CO. Strengthening of antitumor immune memory and prevention of thymic atrophy mediated by adenovirus expressing IL-12 and GM-CSF. *Gene Ther.* (2012) 19:711–23. doi: 10.1038/gt.2011.125

27. Jung BK, Ko HY, Kang H, Hong J, Ahn HM, Na Y, et al. Relaxin-expressing oncolytic adenovirus induces remodeling of physical and immunological aspects of cold tumor to potentiate PD-1 blockade. *J Immunother Cancer.* (2020) 8:e000763. doi: 10.1136/jitc-2020-000763

28. de Graaf JF, de Vor L, Fouchier RAM, van den Hoogen BG. Armed oncolytic viruses: A kick-start for anti-tumor immunity. *Cytokine Growth Fact Rev.* (2018) 41:28–39. doi: 10.1016/j.cytogfr.2018.03.006

29. Kim KJ, Moon D, Kong SJ, Lee YS, Yoo Y, Kim S, et al. Antitumor effects of IL-12 and GM-CSF co-expressed in an engineered oncolytic HSV-1. *Gene Ther.* (2021) 28:186–98. doi: 10.1038/s41434-020-00205-x

30. Reike MJ, Ingersoll MA, Müller DC, Zuiverloon TCM, Strandgaard T, Kamat AM, et al. Biology of BCG response in non-muscle invasive bladder cancer - 2021 IBCN Updates Part III. *Urol Oncol.* (2023) 41:211–8. doi: 10.1016/j.urolonc.2022.09.012

31. Strandgaard T, Lindskrog SV, Nordentoft I, Christensen E, Birkenkamp-Demtröder K, Andreasen TG, et al. Elevated T-cell exhaustion and urinary tumor DNA levels are associated with bacillus calmette-guérin failure in patients with non-muscle-invasive bladder cancer. *Eur Urol.* (2022) 82:646–56. doi: 10.1016/j.eururo.2022.09.008

32. Wright KM. FDA approves pembrolizumab for BCG-unresponsive NMIBC. *Oncol (Williston Park).* (2020) 34:44.

33. Balar AV, Kamat AM, Kulkarni GS, Uchio EM, Boormans JL, Roumiguié M, et al. Pembrolizumab monotherapy for the treatment of high-risk non-muscle-invasive bladder cancer unresponsive to BCG (KEYNOTE-057): an open-label, single-arm, multicentre, phase 2 study. *Lancet Oncol.* (2021) 22:919–30. doi: 10.1016/S1470-2045(21)00147-9

34. He R, Du S, Lei T, Xie X, Wang Y. Glycogen synthase kinase 3β in tumorigenesis and oncotherapy (Review). *Oncol Rep.* (2020) 44:2373–85. doi: 10.3892/or

35. Shaw G, Cavalcante L, Giles FJ, Taylor A. Elraglusib (9-ING-41), a selective small-molecule inhibitor of glycogen synthase kinase-3 beta, reduces expression of immune checkpoint molecules PD-1, TIGIT and LAG-3 and enhances CD8(+) T cell cytolytic killing of melanoma cells. *J Hematol Oncol.* (2022) 15:134. doi: 10.1186/s13045-022-01352-x

36. Nazmifar M, Williams C, Naser-Tavakolian A, Heard J, Rosser C, Theodorescu D, et al. Clinical and preclinical therapies for bladder cancer following bacillus calmette-guérin failure. *J Urol.* (2023) 209:32–48. doi: 10.1097/JU.0000000000002957

37. Friedman GK, Johnston JM, Bag AK, Bernstock JD, Li R, Aban I, et al. Oncolytic HSV-1 G207 immunovirotherapy for pediatric high-grade gliomas. *N Engl J Med.* (2021) 384:1613–22. doi: 10.1056/NEJMoa2024947

38. Robinson C, Xu MM, Nair SK, Beasley GM, Rhodin KE. Oncolytic viruses in melanoma. *Front Biosci (Landmark Ed).* (2022) 27:63. doi: 10.31083/j.fbl2702063

39. Wang M, Wang S, Desai J, Trapani JA, Neeson PJ. Therapeutic strategies to remodel immunologically cold tumors. *Clin Transl Immunol.* (2020) 9:e1226. doi: 10.1002/cti2.1226

40. Liu S, Li F, Ma Q, Du M, Wang H, Zhu Y, et al. OX40L-armed oncolytic virus boosts T-cell response and remodels tumor microenvironment for pancreatic cancer treatment. *Theranostics.* (2023) 13:4016–29. doi: 10.7150/thno.83495

41. Crupi MJF, Taha Z, Janssen TJA, Petryk J, Boulton S, Alluqmani N, et al. Oncolytic virus driven T-cell-based combination immunotherapy platform for colorectal cancer. *Front Immunol.* (2022) 13. doi: 10.3389/fimmu.2022.1029269

42. Feola S, Capasso C, Fusciello M, Martins B, Tähtinen S, Medeot M, et al. Oncolytic vaccines increase the response to PD-L1 blockade in immunogenic and poorly immunogenic tumors. *Oncoimmunology.* (2018) 7:e1457596. doi: 10.1080/2162402X.2018.1457596

43. Simon S, Labarriere N. PD-1 expression on tumor-specific T cells: Friend or foe for immunotherapy? *Oncoimmunology.* (2017) 7:e1364828. doi: 10.1080/2162402X.2017.1364828

44. Hsu A, Huntington KE, De Souza A, Zhou L, Olszewski AJ, Makwana NP, et al. Clinical activity of 9-ING-41, a small molecule selective glycogen synthase kinase-3 beta (GSK-3β) inhibitor, in refractory adult T-Cell leukemia/lymphoma. *Cancer Biol Ther.* (2022) 23:417–23. doi: 10.1080/15384047.2022.2088984

45. Huntington KE, Louie AD, Srinivasan PR, Schorl C, Lu S, Silverberg D, et al. GSK-3 inhibitor elraglusib enhances tumor-infiltrating immune cell activation in tumor biopsies and synergizes with anti-PD-L1 in a murine model of colorectal cancer. *Int J Mol Sci.* (2023) 24:10870. doi: 10.3390/ijms241310870

46. Kondo N. Chapter Five - DNA damage and biological responses induced by Boron Neutron Capture Therapy (BNCT). In: Tamanoi F, Yoshikawa K, editors. *The Enzymes*. Cambridge, MA, USA: Academic Press. (2022). p. 65–78.

47. Spitzer MH, Carmi Y, Reticker-Flynn NE, Kwek SS, Madhireddy D, Martins MM, et al. Systemic immunity is required for effective cancer immunotherapy. *Cell.* (2017) 168:487–502.e15. doi: 10.1016/j.cell.2016.12.022

48. Schreiber H. Tumor-specific immune responses. *Semin Immunol.* (2008) 20:265–6. doi: 10.1016/j.smim.2008.10.001

49. Petrina M, Martin J, Basta S. Granulocyte macrophage colony-stimulating factor has come of age: From a vaccine adjuvant to antiviral immunotherapy. *Cytokine Growth Fact Rev.* (2021) 59:101–10. doi: 10.1016/j.cytogfr.2021.01.001

50. Oh E, Hong J, Kwon OJ, Yun CO. A hypoxia- and telomerase-responsive oncolytic adenovirus expressing secretable trimeric TRAIL triggers tumour-specific apoptosis and promotes viral dispersion in TRAIL-resistant glioblastoma. *Sci Rep.* (2018) 8:1420. doi: 10.1038/s41598-018-19300-6

51. Lee WJ, Ahn HM, Na Y, Wadhwa R, Hong J, Yun CO. Mortalin deficiency suppresses fibrosis and induces apoptosis in keloid spheroids. *Sci Rep.* (2017) 7:12957. doi: 10.1038/s41598-017-13485-y

52. Liang S, Dang B, Chen S, Mi H. Prognostic value and immunological role of cathepsin S gene in pan−cancer. *Oncol Lett.* (2024) 27:41. doi: 10.3892/ol.2023.14175

53. Zheng C, Chu Y, Zhang N, Jia T, Li Y, Jiang T, et al. Pan-cancer analysis of the LOX family reveals that LOX affects tumor prognosis by affecting immune infiltration. *Crit Rev Eukaryot Gene Expr.* (2024) 34:87–100. doi: 10.1615/CritRevEukaryotGeneExpr.v34.i2

54. Gu Y, Chen Q, Yin H, Zeng M, Gao S, Wang X. Cancer-associated fibroblasts in neoadjuvant setting for solid cancers. *Crit Rev Oncol Hematol.* (2023) 193:104226. doi: 10.1016/j.critrevonc.2023.104226

55. Yoon AR, Kasala D, Li Y, Hong J, Lee W, Jung SJ, et al. Antitumor effect and safety profile of systemically delivered oncolytic adenovirus complexed with EGFR-targeted PAMAM-based dendrimer in orthotopic lung tumor model. *J Controlled release.* (2016) 231:2–16. doi: 10.1016/j.jconrel.2016.02.046

56. Ahn HM, Hong J, Yun CO. Oncolytic adenovirus coexpressing interleukin-12 and shVEGF restores antitumor immune function and enhances antitumor efficacy. *Oncotarget.* (2016) 7:84965–80. doi: 10.18632/oncotarget.v7i51

57. Lee YS, Kim JH, Choi KJ, Choi IK, Kim H, Cho S, et al. Enhanced antitumor effect of oncolytic adenovirus expressing interleukin-12 and B7–1 in an immunocompetent murine model. *Clin Cancer Res.* (2006) 12:5859–68. doi: 10.1158/1078-0432.CCR-06-0935

frontiers | Frontiers in Immunology

TYPE Original Research
PUBLISHED 21 May 2024
DOI 10.3389/fimmu.2024.1355566

OPEN ACCESS

EDITED BY
Yaohe Wang,
Queen Mary University of London,
United Kingdom

REVIEWED BY
Hadi Esmaili Gouvarchinghaleh,
Baqiyatallah University of Medical Sciences,
Iran
Degao Chen,
Army Medical University, China

*CORRESPONDENCE
Chae-Ok Yun
chaeok@hanyang.ac.kr

†These authors have contributed equally to this work and share first authorship

RECEIVED 14 December 2023
ACCEPTED 06 May 2024
PUBLISHED 21 May 2024

CITATION
Kim I-W, Yoon A-R, Hong J, Kasala D and Yun C-O (2024) Synergistic antitumor immune response mediated by paclitaxel-conjugated nanohybrid oncolytic adenovirus with dendritic cell therapy.
Front. Immunol. 15:1355566.
doi: 10.3389/fimmu.2024.1355566

Synergistic antitumor immune response mediated by paclitaxel-conjugated nanohybrid oncolytic adenovirus with dendritic cell therapy

In-Wook Kim[1,2,3†], A-Rum Yoon[1,2,3†], JinWoo Hong[4], Dayananda Kasala[1] and Chae-Ok Yun[1,2,3,4*]

[1]Department of Bioengineering, College of Engineering, Hanyang University, Seoul, Republic of Korea, [2]Hanyang Institute of Bioscience and Biotechnology (HY-IBB), Hanyang University, Seoul, Republic of Korea, [3]Institute of Nano Science and Technology (INST), Hanyang University, Seoul, Republic of Korea, [4]GeneMedicine CO., Ltd., Seoul, Republic of Korea

Dendritic cell (DC)-based vaccines have emerged as a promising strategy in cancer immunotherapy due to low toxicity. However, the therapeutic efficacy of DC as a monotherapy is insufficient due to highly immunosuppressive tumor environment. To address these limitations of DC as immunotherapeutic agent, we have developed a polymeric nanocomplex incorporating (1) oncolytic adenovirus (oAd) co-expressing interleukin (IL)-12 and granulocyte-macrophage colony-stimulating factor (GM-CSF) and (2) arginine-grafted bioreducible polymer with PEGylated paclitaxel (APP) to restore antitumor immune surveillance function in tumor milieu and potentiate immunostimulatory attributes of DC vaccine. Nanohybrid complex (oAd/APP) in combination with DC (oAd/APP+DC) induced superior expression level of antitumor cytokines (IL-12, GM-CSF, and interferon gamma) than either oAd/APP or DC monotherapy in tumor tissues, thus resulting in superior intratumoral infiltration of both endogenous and exogenous DCs. Furthermore, oAd/APP+DC treatment led superior migration of DC to secondary lymphoid organs, such as draining lymph nodes and spleen, in comparison with either monotherapy. Superior migration profile of DCs in oAd/APP+DC treatment group resulted in more prolific activation of tumor-specific T cells in these lymphoid organs and greater intratumoral infiltration of T cells. Additionally, oAd/APP+DC treatment led to lower subset of tumor infiltrating lymphocytes and splenocytes being immunosuppressive regulatory T cells than any other treatment groups. Collectively, oAd/APP+DC led to superior induction of antitumor immune response and amelioration of immunosuppressive tumor microenvironment to elicit potent tumor growth inhibition than either monotherapy.

KEYWORDS

DC, oncolytic Ad, nanohybrid, therapeutic vaccine, antitumor immune response, T cells, Treg

Introduction

Dendritic cells (DC) are potent antigen-presenting cells (APC) that present tumor-associated antigen (TAA) to naïve T cells, thereby inducing an adaptive antitumor immune response by activation and recruitment of type 1 helper (Th1) cells and cytotoxic T lymphocytes (CTLs). DC-based therapeutic vaccines have emerged as a promising strategy in cancer immunotherapy due to low toxicity and immune stimulatory attributes. Despite these promising attributes of DC-based therapeutic vaccines, the efficacy of DC as monotherapeutic was insufficient in clinical trials due to highly immunosuppressive environment of clinical tumors (1, 2). In specific, tumors secrete various immunosuppressive factors, such as vascular endothelial growth factor (VEGF), transforming growth factor (TGF)-β, and interleukin (IL)-10, resulting in formation of immunosuppressive network that attenuates the therapeutic potency of immunotherapeutics. Accumulation of immunosuppressive molecules in tumor milieu impairs the recruitment and maturation of immune effector cells (3). In this regard, an additional therapeutic adjuvant is required to maximize the potency of DC therapeutic vaccines in immunosuppressive tumor microenvironment.

Cytokine therapy is another promising strategy for treatment of cancer (4). However, recombinant cytokine therapy in clinical trials demonstrated low therapeutic efficacy and toxicity, thus requiring alternative delivery route for efficient treatment of cancer. Oncolytic adenovirus (Ad)-mediated expression of cytokine in tumor tissue is a promising approach to address the limitations of cytokine therapy (5–7). In detail, oncolytic Ad-mediated cytokine expression is tumor-specific, as the virus selectively replicates and amplifies transgene in tumor cells, ultimately changing immunosuppressive tumor microenvironment to be more susceptible to antitumor immunity (6, 8, 9). The antitumor immune response mediated by oncolytic Ad can function in a synergistic manner with the innately pro-inflammatory nature of the virus, as even the unarmed virus can promote type I interferon (IFN) response in infected cells by promoting release tumor-associated antigens and danger- or pathogen-associated molecular patterns (10–14).

To date, IL-12 and granulocyte-macrophage colony-stimulating factor (GM-CSF), which promote Th1 immune response (15) and promote maturation of APCs (16), respectively, have been most extensively investigated immune stimulatory therapeutic gene candidates for oncolytic virotherapy across numerous clinical trials with varying degree of success (17, 18). Briefly, GMCSF-expressing oncolytic herpes simplex virus, Imlygic, was the first clinically approved oncolytic virotherapy by both United States and European Union, while several other oncolytic viruses either expressing IL-12 or GMCSF as therapeutic gene have completed or under ongoing investigation in phase II or phase III clinical trials (11, 19–22), demonstrating the promising nature of oncolytic viruses armed with single immune stimulatory transgene. We had previously demonstrated that antitumor efficacy of oncolytic Ad can be further enhanced by coexpressing IL-12 and GM-CSF (oAd) in a single vector, as this virus exerted superior antitumor immune response over the control virus expressing either IL-12 or GMCSF alone (23). Further, the potent antitumor efficacy of oAd was synergistically augmented when combined with adoptively transferred DCs, showing enhanced infiltration and activation of immune effector cells in tumor tissues and potent induction of systemic antitumor immunity (5).

To increase therapeutic potential of Ad, researchers examined the combination of Ad and chemotherapeutic drugs (24, 25). Since combination of Ad and paclitaxel (PTX) enhances Ad's transduction efficacy in both coxsackie and adenovirus receptor (CAR)-positive and -negative cancer cells while oncolytic Ad chemosensitizes cancer cells to PTX (26), PTX is one of the best chemotherapeutic for combination therapy with Ad. However, PTX, due to its highly hydrophobic nature, has poor solubility and its clinical application is limited by its low water solubility, off-target toxicity, and acquired drug resistance (27, 28). To overcome this limitation of PTX, Nam et al., have developed a PTX-conjugated cationic polymer (APP) by combining arginine-grafted bioreducible polymer (ABP) with PEGylated PTX, which overcome the low solubility and poor penetration of PTX into the tumor tissues (29, 30), resulting in enhanced antitumor efficacy in comparison to PTX (31). We have previously demonstrated that APP-coated p53 variant-expressing oncolytic Ad (oAd-vp53/APP) exerted synergistic antitumor effect against both CAR-positive and -negative breast cancer xenografts via either intratumoral or systemic administration due to enhanced accumulation of both PTX and oncolytic Ad in tumor tissues (32). In our present study, we have utilized APP-complexed oncolytic Ad co-expressing IL-12 and GM-CSF (oAd/APP) in combination with DC to enhance the delivery of PTX and oncolytic Ad to tumor tissue, improve DC function, and subsequently induce potent antitumor effect by conjoining oncolytic Ad, chemotherapeutic, and immunotherapeutic. oAd/APP in combination with DC elicited strong and synergistic antitumor effects via either local or systemic administration, elucidating that oAd/APP can act as a potent adjuvant for optimizing DC vaccination and induction of potent tumor-specific adaptive immunity.

Materials and methods

Cell lines and culture

Murine melanoma cell line (B16-F10) and human embryonic kidney cell line transformed with Ad type 5 E1 gene (HEK293) were purchased from the American Type Culture Collection (ATCC, Manassas, VA). Dulbecco's modified Eagle's medium (DMEM; Gibco BRL, Grand Island, NY) supplemented with 10% fetal bovine serum (FBS; Gibco BRL), L-glutamine (2 mmol/L), penicillin (100 IU/mL), and streptomycin (50 μg/mL) was used as the culture medium. All cell lines were cultured at 37°C in a humidified atmosphere 5% CO_2 and 95% air.

Mice

Six-week-old male C57BL/6 mice were obtained from Orient Bio Inc. (Seongnam, South Korea). Green fluorescent protein (GFP) transgenic mice were purchased from Jackson Laboratories (Bar

Harbor, ME). All animal studies were performed according to the institutionally approved protocols of Hanyang University. During the experiments, all mice were kept in a laminar air flow cabinet under specific pathogen free conditions.

Preparation of oncolytic Ads

The generation and construction of oncolytic Ad coexpressing IL-12 and GM-CSF (oAd) have been described in a previous paper (5). All viruses were propagated in HEK293 cells and purified by CsCl gradient centrifugation (33). oAd was stored at −80°C until use. Numbers of viral particles (VPs) were calculated from optical density measurements at 260 nm (OD_{260}), where 1 absorbance (OD_{260} = 1.0) was equivalent to 1.1×10^{12} viral particles (VP)/mL.

Characterization of oAd and oAd/APP

For the physiochemical characterization of oAd/APP complex, 1×10^{10} VP of oAd particles and APP solution were gently mixed in phosphate-buffered saline (PBS) by pipetting. The mixtures were allowed to electrostatically interact to form oAd/APP polyplex at room temperature for 30 min, generating oAd/APP complex at an Ad:polymer molar ratio of 1: 1.75×10^4, 8.75×10^4, 3.5×10^5, and 8.75×10^5. The average particle sizes and zeta potentials of oAd and oAd/APP complexes were measured by Zetasizer Nano ZS (Malvern Instrument, Inc., Worcestershire, UK) with a He–Ne laser beam (633 nm, fixed scattering angle of 90°) at 25°C. All other experiments utilized optimal oAd: APP molar ratio of 1:3.5 × 10^5 as determined in our previous report (32).

Generation of bone marrow-derived DC

Bone marrow cells were harvested from flushed marrow cavities of femurs and tibias of GFP transgenic mice (Jackson Laboratories) under aseptic conditions. The harvested bone marrow cells were cultured according to a previously reported procedure to isolate GFP-expressing DCs and DCs were subsequently matured by co-incubating with B16-F10 tumor lysates and lipopolysaccharide (5, 9). Immature DCs were prepared in similar manner as mature DCs with only difference being that cells were not exposed to the tumor lysate and lipopolysaccharide.

Quantification of IL-12, GM-CSF, and IFN-γ expression level

At 48 hr after infection of B16-F10 cells with oAd or oAd/APP at a multiplicity of infection (MOI) of 10, 20, or 50, supernatants were harvested and the level of IL-12 and GM-CSF were determined with conventional IL-12 and GM-CSF ELISA kit (R&D systems, Minneapolis, MN) according to manufacturer's instruction. To identify level of cytokine expression in tumor tissue, C57BL/6 mice with subcutaneously established B16-F10 melanoma tumor tissues were harvested from mice at 4 days after final treatment with intratumorally administered DCs (1×10^6 cells, 2×10^8 VP of oAd/APP, or combination of oAd/APP+DC, along with PBS group as a negative control. The tissues were homogenized and liquefied in the protease inhibitor cocktail (Sigma-Aldrich, St Louis, MO). IL-12, GM-CSF, and INF-γ level were measured by ELISA kits (R&D systems). To determine serum IL-12 and GM-CSF levels following intratumoral or intravenous oAd/APP administration *in vivo*, mice harboring B16-F10 tumors (mean tumor volume of 300 mm^3) were treated three times with 1×10^{10} VP or 2×10^9 VP of oAd/APP over 3 day-period via intratumoral or intravenous administration, respectively, along with intratumorally administered PBS as negative control group (n=3 per group). The blood samples were obtained from retro-orbital plexus at 3 days after the final treatment, which were centrifuged to obtain the serum. The serums were analyzed by conventional IL-12 and GM-CSF ELISA kit (R&D systems) according to manufacturer's instructions.

Established tumor models for *in vivo* antitumor effect

B16-F10 cells (5×10^5) were injected subcutaneously into the right abdomen of 6–7 weeks-old male C57BL/6 mice. When the average tumor volume reached of around 100 mm^3, animals were sorted into groups with similar mean tumor volumes to begin treatment (designated as day 1 of treatment). Treatment groups included DCs (1×10^6 cells/injection), oAd/APP (2×10^8 or 1×10^{10} VP for intratumoral injection, 2×10^9 VP for intravenous injection), or combination of oAd/APP and DC (oAd/APP+DC), along with PBS group as a negative control. Tumor-bearing mice were intratumorally or intravenously injected three times with oAd/APP on day 1, 3, and 5 while mature DC was intratumorally administered three times on days 2, 4, and 6. Tumor growth was monitored day after day using a caliper, and tumor volume was calculated by the following formula: volume = $0.523 \times L \times W^2$, where L is length and W is width. Animals with tumors that were > 3,000 mm^3 were euthanized for ethical reasons.

Histological and immunohistochemical analysis

Tumor tissue were harvested from mice after 9 days of the final injection, frozen in OCT compound (Sakura Finetec, Torrance, CA), and cut into 9-mm cryosections. The cryosections were stained with hematoxylin & eosin (H & E) and then observed by light microscopy. To detect lymphocytes infiltration into tumor tissues, the cryosections were immunostained with purified rat anti-mouse CD4 monoclonal antibody (Ab; BD Biosciences, San Jose, CA) or purified rat anti-mouse CD8 monoclonal Ab as a primary Ab, and then with biotin-conjugated goat anti-rat IgG Ab (BD Biosciences) as a secondary Ab for 1 hr. Subsequently, the sections were incubated with peroxidase-conjugated streptavidin (BD Biosciences). The sections were further incubated with

diaminobenzidine (DAB) (DAKO, Copenhagen, Denmark) as the chromogen substrate. All slides were counterstained with Meyer's hematoxylin (Sigma-Aldrich). To identify GFP-expressing DCs, the cryosections were immunofluorescence stained with hamster anti-mouse CD11c Ab (BD Biosciences), rat anti-mouse CD86 Ab (BD Biosciences), and rabbit anti-human GFP Ab (Millipore, Bedford, MA). Sections were incubated with primary Abs at 4°C overnight, and then incubated Alexa Flour 568-conjugated goat anti-mouse Ab and Alexa 488-conjugated goat anti-rabbit Ab as a secondary Abs for 1 hr. Nuclear staining with 4',6-diamidino-2-phenylindole (DAPI, Sigma-Aldrich) was also performed. Sections were analyzed by fluorescence microscopy using an IX81-ZDC inverted fluorescence microscope (Olympus Optics, Tokyo, Japan). To detect myeloid-derived suppressor cells (MDSC) infiltration into the tumor tissues, the B16-F10 tumor cryosections were immunostained with PE rat anti-mouse CD11b monoclonal Ab (BD Biosciences) and purified rat anti-mouse Ly-6G/6C (GR-1) Ab as a primary Ab for 2 hr, and then incubated with Alexa Flour 488-conjugated goat anti-rat Ab as a secondary Ab for 1 hr. Nuclear staining with DAPI (Sigma-Aldrich) was also performed. Sections were analyzed by fluorescence microscope (Nikon Ci-L, Japan). Double-stained (PE and 488; red and green) cell counts from four different images for each group were counted with the ImageJ Software (version 1.50b; U.S. National Institutes of Health, Bethesda, MD).

Fluorescence-activated cell sorting analysis

To investigate the ability of DCs to migrate into regional lymph nodes and spleen *in vivo*, the DCs were stained with surface molecules using immunofluorescence and analyzed by FACS analysis. Mature DCs (1×10^6 cells), oAd/APP (1×10^9 VP) alone, or oAd/APP+DCs were intratumorally injected into established B16-F10 tumors. At 4 days after final injection, the draining lymph nodes (DLNs) and spleen were harvested and stained with FITC-conjugated hamster anti-mouse CD11c Ab (BD Biosciences) or PE-conjugated rat anti-mouse CD86 Ab (BD Biosciences) at 4°C for 45 min. For the assessment of regulatory T (Treg) cell populations by flow cytometry, splenocytes, DLNs, and tumor infiltrating lymphocytes (TIL)s were harvested at 11 days after the initial treatment of B16-F10 tumor-bearing mice with intravenously administered oAd/APP (2×10^9 VP) with or without DC (1×10^6 cells). Cells were pretreated with saturating anti-CD16/CD32 Ab (Biolegend, San Diego, CA) in staining buffer (2% FBS, 0.02% sodium azide in PBS) to block cellular Fc receptors. Cells were stained extracellularly with peridinin chlorophyll protein-Cy5.5-conjugated anti-CD4 Ab (BD Biosciences) and phycoerythrin-conjugated anti-CD25 Ab (eBioscience, San Diego, CA). Cells were then permeabilized with Foxp3 fixation/permeabilization buffer (eBioscience) according to the supplier's protocol and stained with allophycocyanin-conjugated anti-Foxp3 Ab (eBioscience). To investigate the changes to the immune cell populations of thymus and bone marrow following intratumoral administration of oAd/APP, B16-F10 tumor-bearing mice were intratumorally injected three times with oAd/APP (1×10^9 VP) every other day. Single cells were obtained from thymus and bone marrow harvested at 3 days after the final injection then stained with FITC-conjugated hamster anti-mouse CD3 Ab, peridinin chlorophyll protein-Cy5.5-conjugated anti-CD8 Ab, or APC-Cy7 conjugated anti-CD45 Ab (BD Biosciences) at 4°C for 45 min. All samples were analyzed on a BD Biosciences BD-LSR II Analytic Flow Cytometer, using FACSDiva software (BD Biosciences).

Statistical analysis

Data are expressed as mean ± standard deviation (SD). Statistical significance was determined by two-tailed Student t-test (SPSS 13.0 software; SPSS, Chicago, IL, USA). *P*-values < 0.05 were considered statistically significant (*$P < 0.05$, **$P < 0.01$, ***$P < 0.001$).

Results

Characterization of Ad/APP complex-mediated therapeutic gene expression

We have previously demonstrated that Ad can be efficiently encapsulated by PTX-conjugated polymer micelle, APP, by electrostatic interaction between negatively charged Ad surface and cationic polymer, generating a cationic polyplex that could co-deliver oncolytic Ad and PTX into tumor tissues (32). A new batch of APP polymer was synthesized and different oncolytic Ad was utilized in present report, thus we assessed whether new oAd/APP complex retained similar physiochemical attributes as those generated in our previous report utilizing oAd-vp53/APP by measuring average size and zeta potential. As shown in Figure 1A, the average size and zeta potential of naked oAd were 96.9 ± 5.1 nm and -13.3 ± 2.1 mV, respectively. Complexation of oAd with APP at Ad:polymer molar ratios ranging from $1:1.75 \times 10^4$ to 3.5×10^5 led to polymer concentration-dependent increase in average size and zeta potential (at 3.5×10^5 molar ratio; 125.8 ± 3.1 nm and 5.7 ± 0.3 mV). The steep increase in complex size and charge at the molar ratio of 8.75×10^5 was due to aggregation, which is in line with our previous report where aggregation was observed at the molar ratio (32). Based on these current and past results, APP:oAd molar ratio of 3.5×10^5 was chosen as optimal molar ratio and used in all of the subsequent experiments.

To evaluate whether oAd/APP complex can effectively infect our target B16-F10 murine melanoma cells to induce expression of therapeutic genes, B16-F10 cells were infected with naked oAd or oAd/APP at an MOI of 10, 20, or 50 and the expression level of IL-12 or GM-CSF was measured by ELISA. As shown in Figures 1B, C, both naked oAd and oAd/APP showed dose-dependent increase in expression levels of IL-12 and GM-CSF. Importantly, the expression level of IL-12 and GM-CSF expression induced by oAd/APP was significantly higher than those of naked oAd (at an MOI 20 and 50; $P < 0.001$) suggesting that APP-mediated delivery of oAd can enhance the therapeutic gene expression in murine melanoma cells.

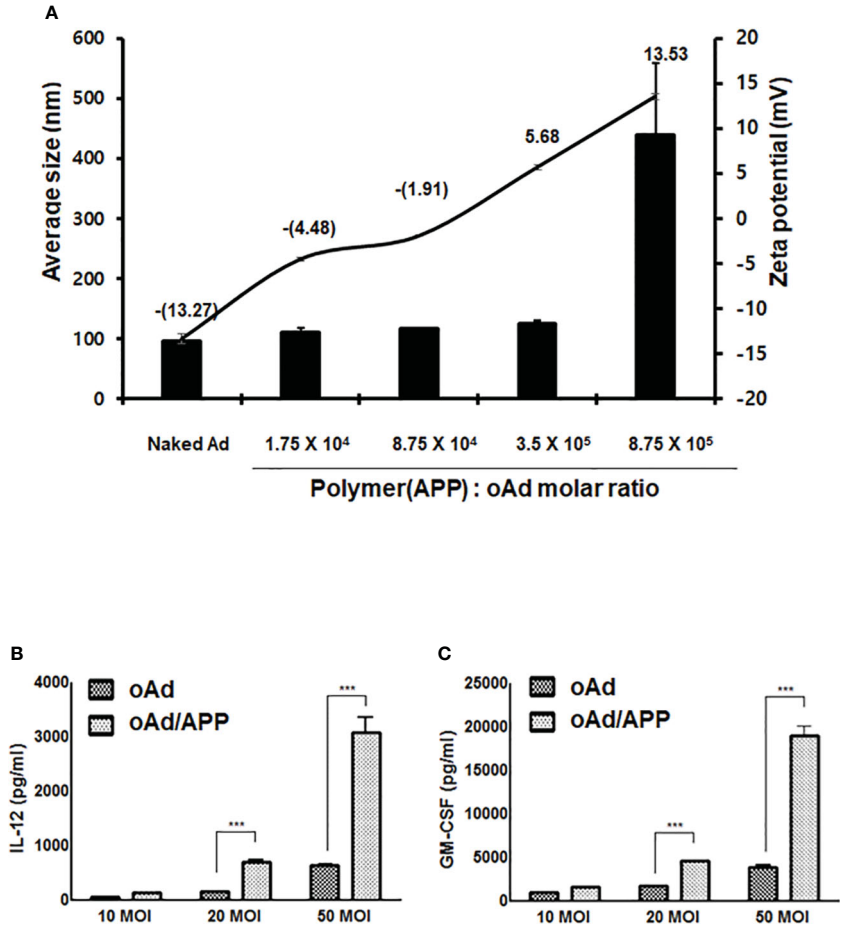

FIGURE 1
Physicochemical characterization of oAd/APP complex and complex-mediated therapeutic gene expression. The average size (nm) and zeta potential value of the oAd/APP complex were measured at various molar ratios indicated **(A)**. The size and charge determination are the mean ± SD of three independent experiments. The expression level of IL-12 **(B)** and GM-CSF **(C)** were assessed in B16-F10 cells. Cells were infected with oAd or oAd/APP and the supernatant were collected at 48 hr after infection. The level of IL-12 and GM-CSF was quantified by conventional ELISA. Data represent the mean ± SD of triplicates and similar results were obtained from at least three separate experiments. MOI, multiplicity of infection. ***$P < 0.001$.

Antitumor effect of oAd/APP in combination with dendritic cells

To evaluate the therapeutic efficacy of oAd/APP in combination with DCs *in vivo*, C57BL/6 mice were subcutaneously inoculated with B16-F10 melanoma cells. When the average tumor volume reached 100 mm^3, mice were intratumorally treated with PBS, DC, oAd/APP, or oAd/APP+DC (designated as Day 1). Based on our previous experience combining oAd with DC (5, 34), oAd/APP was administered every day in a consecutive manner (Day 1–3) followed by three consecutive dosing of DC (day 4–6). As shown in Figure 2A, mice treated with PBS control showed rapid and aggressive tumor growth and tumor volume exceeded 2,000 mm^3 at 10 days following initial treatment. In marked contrast, mice treated with either oAd/APP or oAd/APP+DC combination showed significant inhibition of tumor growth in comparison to those treated with PBS or DC alone, resulting in complete tumor regression at day 27 following initial treatment (4/6 in oAd/APP and 6/6 in oAd/APP+DC group). Furthermore, oAd/APP+DC induced complete tumor regression at earlier time points (day 14, 16, 17, and 19) than oAd/APP (day 19 and 20), suggesting that combination of oAd and DC may induce more rapid and efficient induction of antitumor immune response. At earlier time point (20 days post initial treatment), there were 4 mice without any observable tumors in oAd/APP-treated group, however, only 2 of these mice remained tumor free at 26 days post injection due to tumor regrowth. In marked contrast, 100% of oAd/APP+DC-treated mice remained free of tumor at 26 days post injection, suggesting that combination of oAd/APP with DC vaccine induced durable remission.

As it was difficult to distinguish the difference in tumor growth inhibiting effect of oAd/APP and oAd/APP+DC at the viral dose (1×10^{10} VP) utilized in Figure 2A, the therapeutic efficacy of the combination therapy utilizing lower viral doses (5×10^7 or 2×10^8 VP) under the same treatment schedule were investigated. Unexpectedly, the combination therapy of oAd/APP at 5×10^7 or 2×10^8 VP and DC did not elicit superior antitumor efficacy over respective dose of oAd/APP monotherapy (Supplementary Figure S1),

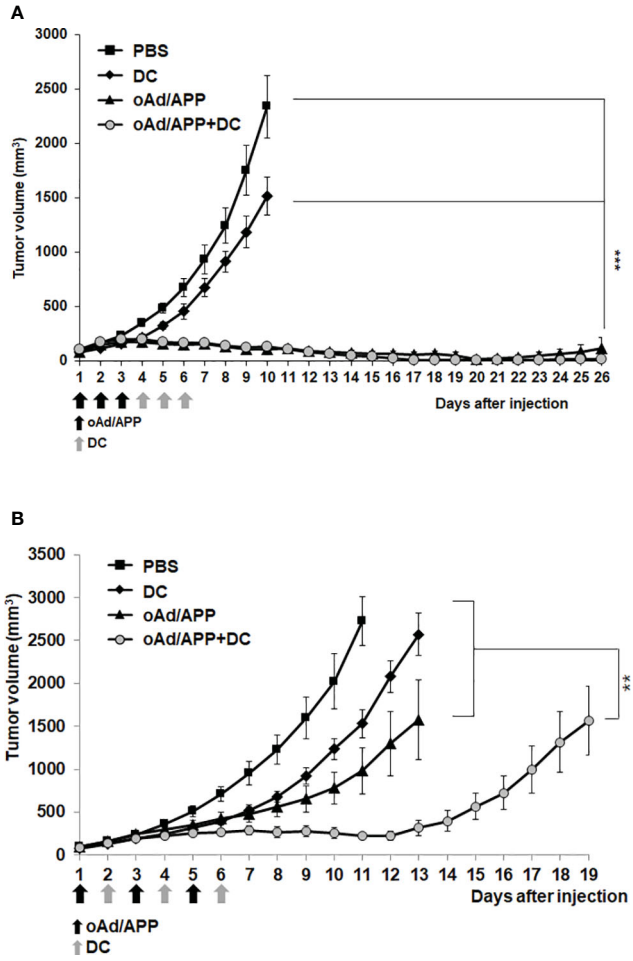

FIGURE 2
Potent antitumor effect of oAd/APP in combination with DCs. Pre-established B16-F10 tumors were injected with phosphate-buffered saline (PBS), DCs, oAd/APP complex (1×10^{10} **(A)** or 2×10^{8} **(B)** VP, respectively), or oAd/APP plus DCs (1×10^{6} cells). Tumor growth was monitored every day, data points represent the mean ± SE of the tumor size in each group (n = 6). ***$P < 0.001$ oAd/APP versus PBS or DC, ***$P < 0.001$ oAd/APP+DC versus PBS or DC, not significant (NS) for oAd/APP versus oAd/APP+DC. **(B)** **$P < 0.01$, oAd/APP+DC versus oAd/APP. (**$P < 0.01$, ***$P < 0,001$).

suggesting that the current treatment schedule based on our previous studies (5, 34) was suboptimal for present study utilizing APP as nanocarrier for oncolytic Ad. Thus, alternative dosing regimen utilizing 2×10^{8} VP of oAd/APP was investigated. As shown in Figure 2B, alternating oAd/APP (Day 1, 3, and 5) and DC (Day 2, 4, and 6) treatment led to combination therapy (oAd/APP+DC group) exerting significantly more potent antitumor efficacy than either DC or oAd/APP monotherapy ($P < 0.01$), demonstrating that combination of both therapeutics under optimal treatment schedule can induce beneficial tumor growth inhibiting effect.

Intratumoral expression of IL-12, GM-CSF and INF-γ

To further elucidate the mechanism behind the antitumor effect of each treatment, intratumoral expression level of IL-12, GM-CSF, and IFN-γ were examine by ELISA from tumor homogenate collected at 4 days post last treatment. As shown in Figure 3, all cytokines (IL-12, GM-CSF, and IFN-γ) were either not detected or detected at a low level in tumors treated with PBS or DC. In marked contrast, both oAd/APP and oAd/APP+DC treatment resulted in significantly higher expression level of cytokines. Importantly, tumor treated with oAd/APP+DC group showed significantly higher concentration of all cytokines than oAd/APP group ($P < 0.001$), demonstrating that both therapeutics can conjointly enhance expression of antitumor cytokines in immunosuppressive tumor.

Immune cell infiltration in tumor tissues treated with combination of oAd/APP and DCs

To further assess the antitumor immune response mediated by each treatment, histology and immune cell infiltration in the tumor tissues were examined by immunohistochemical staining of tumors harvested on 15 days after the initial treatment. As shown in Figure 4A, H & E staining revealed extensive accumulation of tumor cells in large areas of the PBS- or DC-treated tumor tissues. In contrast, a large portion of oAd/APP-treated tissues was necrotic,

10.3389/fimmu.2024.1355566

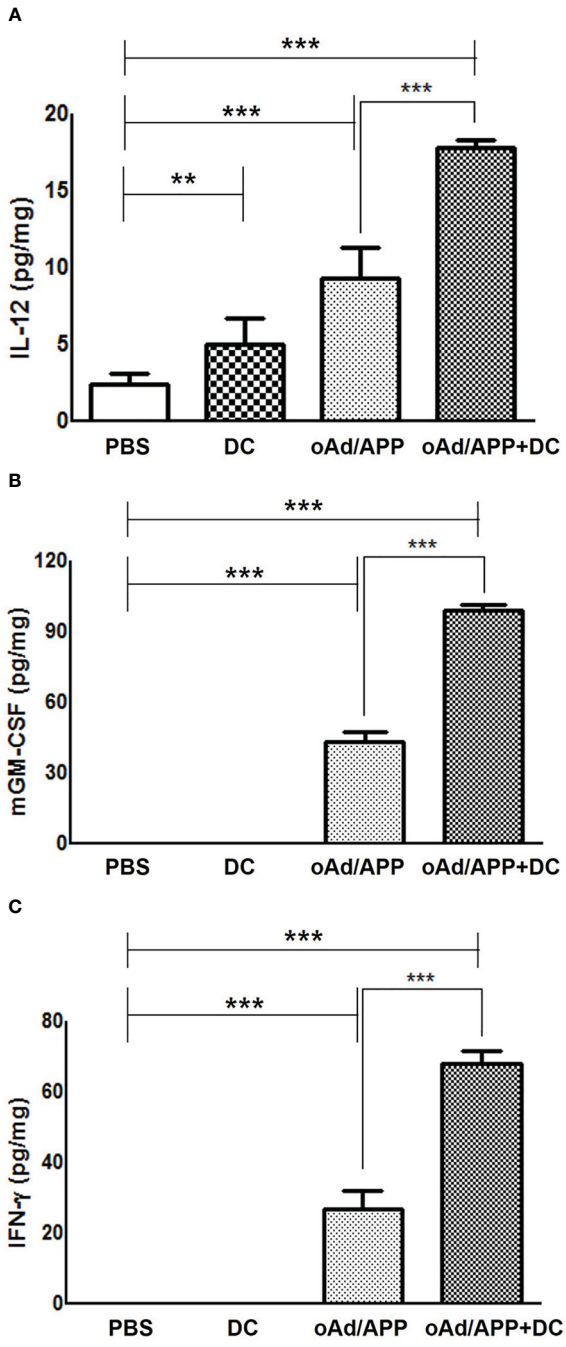

FIGURE 3
Intratumoral expression of IL-12, GM-CSF and INF-γ. Subcutaneously established B16-F10 melanoma tumor tissues were harvest at 4 days after the final intratumoral treatment with 2×10^8 VP of oAd/APP and/or 1×10^6 DCs. ELISA was performed to evaluate the expression level of **(A)** IL-12, **(B)** GM-CSF, **(C)** IFN-γ in tumor. Experiment were carried out in triplicates (n =3 mice per group). Each data point indicated mean ± SD. (**$P < 0.01$, ***$P < 0,001$).

reaffirming the potent antitumor efficacy of oAd/APP. Interestingly, oAd/APP+DC-treated tumor tissues showed markedly lower tumor cell population than any other treatment groups and extensive accumulation of normal cells were observed, suggesting that rapid induction of potent antitumor effect may contribute to proliferation of normal cells and expedite tissue recovery.

The tumor tissues were immunohistochemically stained with CD4-, CD8-, CD11c-, CD86- and GFP-specific Ab to assess immune cells infiltration. Both oAd/APP and oAd/APP+DC treatment induced higher level of CD4- or CD8-positive T cell infiltration into tumor tissues than PBS or DC treatment, with oAd/APP+DC leading to more robust infiltration than oAd/APP monotherapy. Similar results were obtained with intratumoral infiltration of DCs ($CD11c^+$) where both oAd/APP and oAd/APP +DC treatment led to markedly higher infiltration of DCs than those treated with PBS or DC (Figure 4B). Importantly, oAd/APP +DC showing markedly higher quantity of both endogenous and exogenous DCs (GFP^-CD11c^+ and GFP^+CD11c^+) than oAd/APP monotherapy. Of note, both endogenous and exogenous mature DCs (GFP^-CD86^+ and GFP^+CD86^+, respectively) were only detected in oAd/APP+DC combination therapy group (Figure 4C).

Next, we investigated the effect of each treatment on myeloid-derived suppressor cell (MDSC) population within the tumor microenvironment, as high level of MDSC can abrogate the therapeutic benefit of DC vaccine and recombinant GM-CSF therapy has been reported to promote MDSC accumulation in the tumor tissues (35–39). As shown in Supplementary Figure S2, the tumor tissues treated with PBS demonstrated highest number of $CD11b^+GR-1^+$ MDSC accumulation followed by oAd/APP monotherapy group, suggesting that GM-CSF as therapeutic transgene in our system did not increase MDSC population within the tumor. In sharp contrast, both DC and oAd/APP+DC treatment induced similarly potent reduction of MDSC population within the tumor tissues, which was in agreement with previous reports demonstrating that tumor lysate pulsed mature DC vaccine therapy can attenuate MDSC accumulation in the tumor tissues (40, 41). These findings demonstrated that high level of GM-CSF expression induced by oAd/APP did not promote recruitment of immunosuppressive MDSCs, and its combination with DCs can be an effective approach to attenuate MDSC accumulation in the tumor.

Together, these results suggest that oAd/APP can enhance retainment of exogenously administered DCs, activation of endogenous DCs, and infiltration of immune effector cells (T cells and DCs) to tumor tissues.

DC migration to draining lymph nodes following treatment with combination of oAd/APP and DCs

To assess whether each treatment can promote DC migration to DLNs to promote adaptive immune response, tumors were intratumorally injected with PBS, DC, oAd/APP, or oAd/APP+DC. Four days after the final injection, DLNs were harvested and stained with GFP, CD11c, and CD86-specific Ab. As shown in Figure 5A, both oAd/APP and oAd/APP+DC treatment led to high level of migration for endogenous mature DCs (GFP^-CD86^+) than either PBS or DC treatment, suggesting that cytokine expression mediated by oAd/APP could promote DC maturation and migration to DLNs. Importantly, oAd/APP+DC treatment led to markedly higher number of both endogenous and exogenous mature DCs migrating to DLNs than any other treatment group, demonstrating that combination therapy can promote migration of both DC vaccine

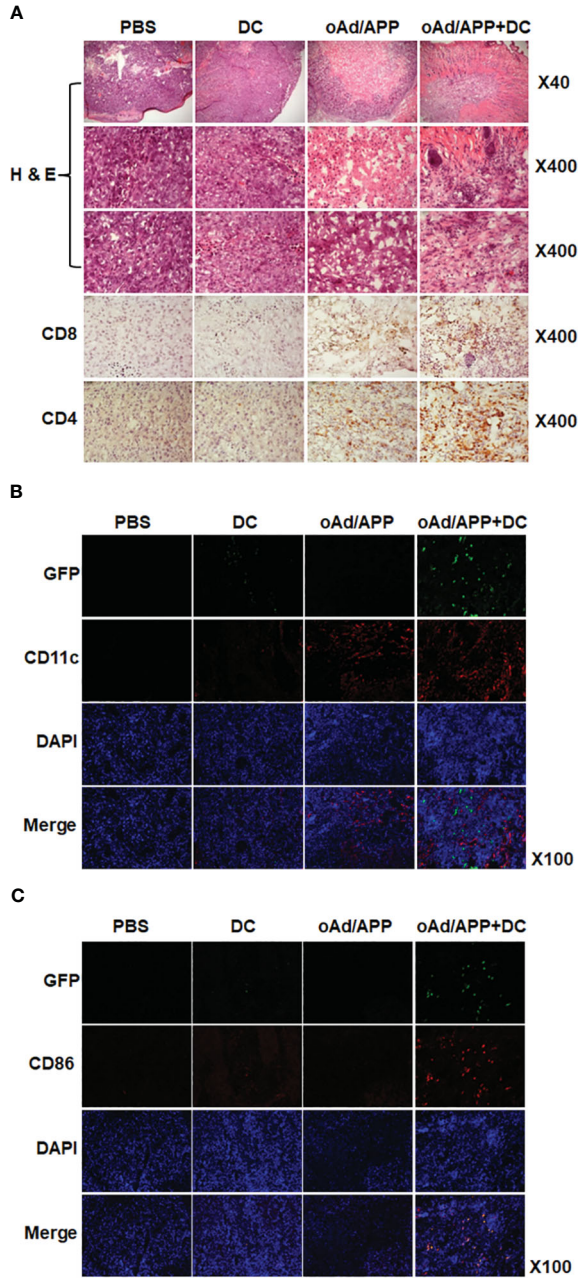

FIGURE 4
Immune cell infiltration into tumor tissues. Tumor tissues were harvested from mice at 15 days after the initial treatment for histological analysis **(A)** frozen section of the tumor was stained with hematoxylin and eosin (H & E). Frozen section of tumor tissue was stained with anti-CD4 and anti-CD8 antibodies. **(B)** Frozen sections were stained with anti-CD11c and anti-GFP antibodies. **(C)** Frozen sections were stained with anti-CD86 and anti-GFP antibodies. Original magnification: ×40, ×100, or ×400.

and endogenous DCs to DLNs and mount an effective antitumor immune response.

To further assess whether combination therapy increased the accumulation of activated DC population in secondary lymphoid organs, we examined the $CD11c^+CD86^+$ cell population in DLN and spleen by flow cytometry. Similar to our results from Figure 5A, both oAd/APP and oAd/APP+DC treatment led to markedly higher number of mature DCs ($CD11c^+CD86^+$) being detected in DLNs than either PBS or DC treatment ($P < 0.05$ or 0.001), respectively. As expected, oAd/APP+DC treatment led to significantly higher quantity of mature DCs being detected in DLNs than those treated with oAd/APP monotherapy ($P < 0.001$) (Figure 5B). Similar trends were observed in the spleen, in which oAd/APP+DC treatment led to significantly higher accumulation of mature DCs ($CD11c^+CD86^+$) than any other treatment group (Figure 5C; $P < 0.001$). These results suggest that combination therapy promoted migration of DC to secondary lymphoid organs.

Antitumor effect of systemically injected oAd/APP in combination with dendritic cells

To date, locoregional injection of the oncolytic virus remains the preferred administration route in clinical trials due to potential safety concerns, like immune-related adverse events and off-target toxicity, and inadequate therapeutic benefit by systemic administration (42, 43). Effective systemic application of oncolytic viruses remain a major goal to maximize the therapeutic potential of the virus against inaccessible tumors or distant metastases. As we had previously demonstrated that systemic administration of oAd/APP induced tumor growth inhibition in a safe manner (32), we sought to investigate whether intravenously administered oAd/APP could exert synergistic antitumor effect in combination with DCs. B16-F10 tumor-bearing mice treated with PBS control showed rapid and aggressive tumor growth, and tumor volume exceeded 3,000 mm^3 at 15 days following initial treatment (Figure 6A). oAd treatment alone also led to aggressive tumor growth and rapidly formed large tumors (over 2,500 mm^3) at day 13. In contrast, mice treated with oAd/APP or DCs alone showed significant inhibition of tumor growth. Moreover, mice treated with oAd/APP+DC showed synergistic antitumor effects that more inhibition of tumor growth than oAd/APP or DCs alone groups. On day 15, the mean tumor volumes in mice treated with oAd alone, oAd/APP, DC alone, or oAd/APP+DC groups were 3,335 ± 473, 2,121 ± 377, 1,494 ± 362, and 311 ± 29 mm^3, respectively. Tumor growth inhibition was statistically significant in mice treated with oAd/APP+DC as compared with individual treatment groups ($P < 0.05$ versus DCs, $P < 0.01$ versus oAd/APP, $P < 0.05$ versus oAd or PBS), respectively.

To assess whether effective activation and infiltration of immune cells were due to amelioration of immunosuppressive tumor microenvironment, the changes to $CD4^+CD25^+Foxp3^+$ immunosuppressive Treg cell population among splenocytes, DLN cells, and TILs were analyzed by flow cytometry. Mice treated with oAd/APP+DC showed significantly attenuated triple positive Treg populations in spleen, DLN, and TILs compared with PBS-, DC- and oAd/APP-treated mice (Figure 6B). Collectively, these results demonstrate that accumulation of immunosuppressive Treg cells in tumor microenvironments and lymphoid organs was effectively attenuated by oAd/APP+DC, leading to potent induction of antitumor immune response.

10.3389/fimmu.2024.1355566

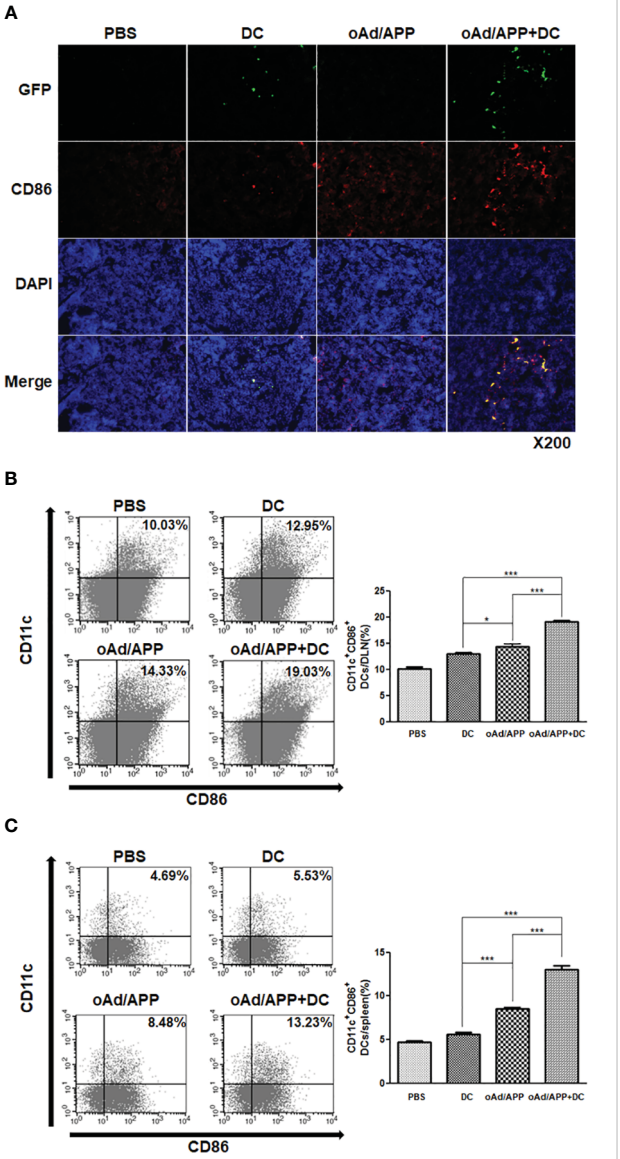

FIGURE 5
DC migration activity after treatment with combination of oAd/APP and DCs. Four days after the final treatment, single cells were collected from draining lymph nodes (DLN)s and spleen. **(A)** Frozen section of the DLN was stained anti-CD86 and anti-GFP antibodies. Original magnification: ×200. The migration DC was quantified by FACS. The population of $CD11c^{+}CD86^{+}$ cells in draining lymph nodes **(B)** and spleen **(C)** from mice treated with phosphate-buffered saline (PBS), DC, oAd/APP, or oAd/APP+DCs. *$P < 0.05$, ***$P < 0.001$.

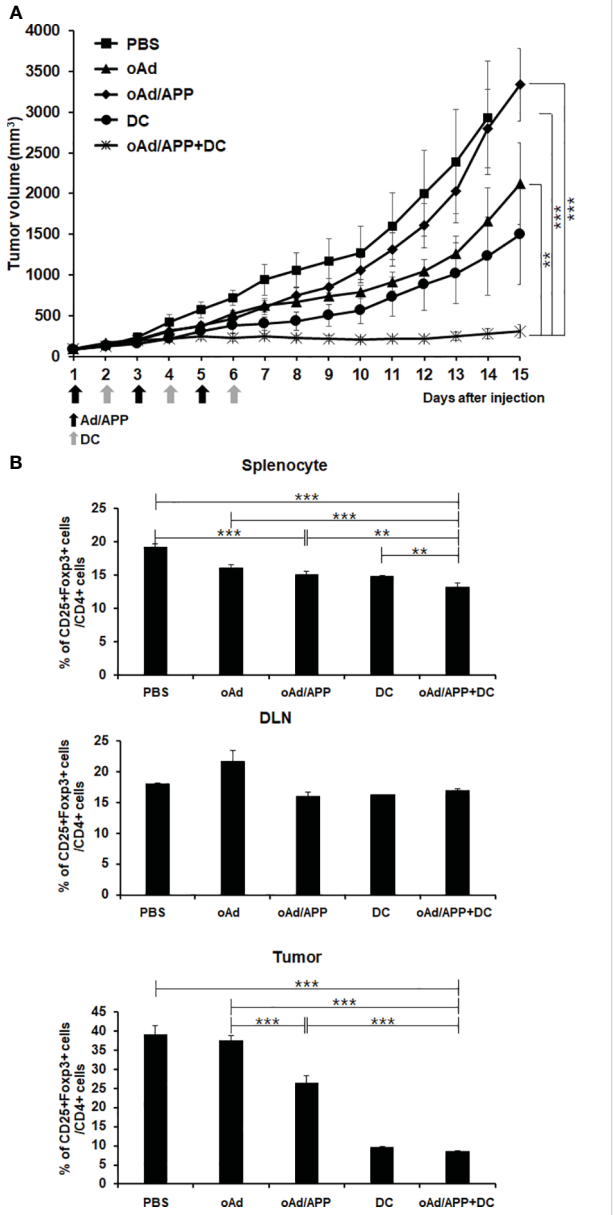

FIGURE 6
Antitumor effect and Treg population after systemic administration of Ad/APP in combination with dendritic cells. **(A)** Mice harboring established B16-F10 tumors were intravenously injected PBS, DCs (1 × 10^6 cells), oAd/APP complex (2 × 10^9 VP), or oAd/APP+DCs. Tumor growth was monitored every day, data points represent the mean ± SE of the tumor size in each group (n = 6). At Day 15, ***$P < 0.001$; oAd/APP+DC versus PBS or oAd/APP, **$P < 0.01$; oAd/APP +DC versus DC, and non-significant (NS); oAd/APP versus DC. **(B)** Treg cell population was analyzed that splenocyte, DLNs and tumor-infiltrating lymphocyte (TIL) were harvested at 11 days following final viral injection of B16-F10 tumor-bearing mice by oAd/APP (2 × 10^9 VP) intravenous injection and oAd/APP (2 × 10^9 VP)+DC (1 × 10^6 cells; intratumoral injection) by analyzing the CD25, Foxp3, and CD4 expression level with flow cytometry. Experiment were carried out triplicate (n =3 mice per group). Each data point indicated mean ± SD. (*$P < 0.01$, ***$P < 0,001$).

Discussion

We have previously demonstrated that Ad can be efficiently encapsulated by PTX-conjugated polymer micelle (APP), which showed a much higher transduction efficiency in both CAR-positive and -negative cancer cells, ultimately eliciting synergistic antitumor effect (32). oAd/APP complex retained similar physiochemical attributes (average size and surface charge) as those generated in our previous report and showed greatly enhanced expression level of cytokines compared to oAd alone (Figure 1). This is in line with several other reports demonstrating that combination of PTX and oncolytic Ad can enhance Ad-mediated transgene expression by mechanisms, such as increased expression of cellular uptake receptors-targeted by Ad (44), induction of G2/M cell cycle arrest (45), or induction of aberrant mitosis (46).

DCs, which act as professional antigen presenting cells, are crucial for activation of antitumor immune responses (47). However, DC vaccines in clinical trial as monotherapy have shown limited efficacy due to immunosuppressive tumor microenvironment preventing infiltration and activation of immune effector cells (48). In this regard, oncolytic Ad, which is not toxic to monocyte-derived immature DCs, is a particularly promising candidate for boosting DC vaccine as several reports have demonstrated antitumor immune activation by virus-mediated oncolysis and subsequent generation of tumor-associated antigens (49). This immune stimulatory attributes of oncolytic Ad can be further augmented by arming these viruses with immune stimulatory cytokines, which led to amelioration of the immunosuppressive tumor microenvironment and DC maturation (5, 9, 33). Importantly, cytokine-expressing oncolytic Ad can act as a potent immune adjuvant to promote Th1 antitumor immune response (50, 51) and overcome the obstacles of DC vaccination (52). oAd mediated expression of IL-12 enhances Th1 immunity and activate immune cells (e.g., CTLs and natural killer (NK) cells) and these cells can promote DC maturation and DC-mediated IL-12 secretion, resulting in a positive feedback loop that potentiates immune cells to elicit a potent antitumor immune response (53). In line with these findings, oAd/APP in combination with DC led to higher expression level of antitumor cytokines, such as IL-12, GM-CSF, and IFN-γ, in tumor tissues (Figure 3), suggesting that DCs stimulated with IL-12 can release IFN-γ and that both immunotherapeutics can synergistically induce cytokine expression (53, 54). Neither intratumoral nor intravenous oAd/APP administration induced upregulation of pro-inflammatory cytokines (IL-12 and GM-CSF) in the serum (Supplementary Figure S3), thus minimizing the safety concerns associated with systemic administration of recombinant IL-12. One potential Importantly, a strong positive correlation between antitumor cytokine expression levels and intratumoral infiltration of immune cells (immature and mature DCs as well as $CD4^+$ or $CD8^+$ T cells) was observed where oAd/APP+DC treatment resulted in highest level of infiltration or retainment of these immune cells (Figures 3–5), further supporting the notion that inactivation of immune cells by immunosuppressive tumor milieu could be overcome by overexpression of antitumor cytokines. Notably, treatment with oAd/APP+DC led to significantly improved retainment of intratumorally administered exogenous DCs compared to DC alone (Figures 4B, C), suggesting that combination therapy attenuates immunosuppression-mediated inactivation and clearance of DCs from tumor tissues.

One of the unexpected finding in this study was that alternating oAd/APP and DC treatments over the course of 6-day interval was necessary for the combination therapy to exert beneficial antitumor effect over respective monotherapy (Figure 2A), whereas sequential administration of oAd/APP (day 1–3; one injection/day) followed by DC (day 4–6; one injection/day) failed to exert superior antitumor efficacy over oAd/APP monotherapy). Our previous works utilizing the same oAd (oAd co-expressing IL-12 and GMCSF) in combination with DC revealed that sequential administration of oAd/APP followed by DC treatments was both experimentally and mathematically shown to be one of the optimal arrangements to exert beneficial therapeutic effect (5, 34), suggesting that APP-mediated delivery of oAd may exert profoundly different biological effect over the naked oAd. PTX moiety in APP molecule may contribute to this differential effect, since there are few studies demonstrating that PTX may inhibit pro-inflammatory cytokine (IL-12 and IFN-γ) secretion or deplete DC in tumor tissues (55, 56). Sequential dosing may promote higher level of PTX accumulation (Figure 2A; Supplementary Figure S1) in the tumor microenvironment compared to alternating dosing regimen where oAd/APP is administered every other day (Figure 2B). Still, no definitive conclusion can be made, as several publications demonstrated that PTX can promote maturation and activation DCs (57, 58) and this aspect of oAd/APP warrant further investigation in the future.

Migration of mature DCs to regional lymph nodes is an essential procedure for the induction of tumor-specific immune response by activation and maturation of T cells (59, 60). An increased retainment and infiltration of both exogenous and endogenous DCs via elevated expression of antitumor cytokines was also associated with augmented DC migration toward the DLNs and spleen following oAd/APP+DC treatment (Figures 5A-C). This is in line with previous literature demonstrating that increase in expression level of Th1 cytokines and co-stimulatory molecule promotes DC migration to lymphoid organs (61, 62). Additionally, we observed that locally administered oAd/APP elevated $CD8^+$ T cell frequency in other distant immune niche, like bone marrow and thymus, compared with PBS control group (Supplementary Figure S4), suggesting that activation and maturation of DCs in the lymphoid organs may instigate systemic $CD8^+$ T cell immune response.

Systemic administration is paramount in cancer therapy, facilitating the delivery of therapeutic agents across the entire circulatory system. This approach ensures widespread distribution, increasing the probability of reaching metastatic sites and thereby enhancing the efficacy of the treatment against disseminated cancer cells. Intravenous injection of oAd/APP+DC also led to induction of potent antitumor effect (Figure 6A) induced an immune response that reduced a number of immune-suppressive factors to circumvent the immunosuppressive microenvironment (Figure 6B). These results indicate that injection of the cytokine-expressing oAd/APP+DC can attenuate immunosuppressive Treg cells to enhance the antitumor immune response mediated by DC vaccination. This claim is supported by several other reports demonstrating that increased frequency of Treg cells occurs in patients with malignant tumors and is closely correlated to the poor survival of cancer patients (63, 64). This is due to Treg cells being dominantly responsible for the immunosuppression and impaired immune responses in the cancer-bearing hosts (65). The attenuation in Treg population from TIL, splenocytes, and DLN following oAd/APP+DC treatment was likely due to high intratumoral expression level of IL-12 (Figures 3A, 6B), as localized overexpression of IL-12 in tumor has been reported to reverse the immunosuppression by inducing apoptosis of Treg cells (66). Our findings demonstrated that diverse immune cell subsets (MDSCs, Tregs, $CD4^+$ or $CD8^+$ T cells, and DCs) across tumor tissues and lymphoid organs were

differentially regulated by oAd/APP+DC combination therapy that were suggestive of systemic antitumor immune response. Still, the complex nature (e.g., multiple anticancer modalities) of the system and potentially conflicting functions of some therapeutic components (e.g., GM-CSF transgene) necessitate more comprehensive immune profiling of the combined regimen in the future to ascertain how this system function in different tumor types.

Taken together, this study demonstrates that oAd/APP nanohybrid complex can act as a potent adjuvant for optimizing DC vaccination. The therapeutic benefit of the combination therapy is achieved via enhanced expression of antitumor cytokines, reduction of immunosuppressive cell population in tumor tissues and lymphoid organs, and augmentation of DC activity, which translated to induction of potent antitumor immune response.

Conclusion

This research aimed to maximize the strengths and overcome the shortcomings of each treatment by fusing three therapeutic platforms: oAd-mediated cancer gene therapy, nanomaterial-based drug delivery system, and dendritic cell therapy-mediated immunotherapy. oAd/APP complex induced high level of pro-inflammatory cytokine expression *in vitro*. Both intratumorally and intravenously administered oAd/APP exerted beneficial tumor growth inhibiting effect in combination with DC vaccination via induction of potent antitumor immune response. Although this study demonstrated that oAd/APP complex combined with DC therapy exhibited a strong antitumor effect under alternating dosing regimen, the beneficial effect of the combination therapy was negated when all doses of oAd/APP were administered prior to DC administration, suggesting that there may be a potentially antagonistic role of APP to DC vaccination therapy that warrants more in-depth investigation in the future. Additionally, the therapeutic efficacy of systemically administered oAd/APP was markedly lower than those achieved via intratumoral optimization, suggesting that further optimization in tumor-targeted delivery efficiency of the APP will be necessary to exert sufficient antitumor effect in a complex clinical tumor microenvironment.

Data availability statement

The original contributions presented in the study are included in the article/Supplementary Material, further inquiries can be directed to the corresponding author.

Ethics statement

Animal studies were conducted according to the institutional guidelines established by the Hanyang University Institutional Animal Care and Use Committee. The study was conducted in accordance with the local legislation and institutional requirements.

Author contributions

I-WK: Writing – original draft, Writing – review & editing, Conceptualization, Data curation, Formal analysis, Investigation, Methodology, Validation. A-RY: Writing – original draft, Writing – review & editing, Conceptualization, Data curation, Formal analysis, Funding acquisition, Investigation, Methodology, Project administration. JH: Writing – review & editing, Data curation, Methodology, Supervision, Validation. DK: Formal analysis, Investigation, Methodology, Writing – review & editing. C-OY: Conceptualization, Funding acquisition, Project administration, Resources, Supervision, Writing – original draft, Writing – review & editing.

Funding

The author(s) declare financial support was received for the research, authorship, and/or publication of this article. This work was supported by grants from the National Research Foundation of Korea (2021R1A2C301016611, 2023R1A2C1004062, C-OY.; 2022R1I1A1A01071162, 2023R1A2C1003830, A-RY).

Conflict of interest

C-OY and JH are CEO and employee of GeneMedicine Co., Ltd.

The remaining authors declare that the research was conducted in the absence of any commercial or financial relationships that could be construed as a potential conflict of interest.

Publisher's note

Supplementary material

The Supplementary Material for this article can be found online at: https://www.frontiersin.org/articles/10.3389/fimmu.2024.1355566/full#supplementary-material

SUPPLEMENTARY FIGURE 1
Potent antitumor effect of oAd/APP in combination with DCs. Pre-established B16-F10 tumors were injected with phosphate-buffered saline (PBS), 1×10^6 DCs, oAd/APP complex (5×10^7 **(A)** or 2×10^8 **(B)** VP, respectively), or oAd/APP plus DCs. Tumor growth was monitored every day, data points represent the mean ± SE of the tumor size in each group (n = 3 or 4).

SUPPLEMENTARY FIGURE 2
Myeloid-derived suppressor cells (MDSC) population in tumor tissues. B16-F10 tumor tissues were harvested from mice at 15 days after the initial

treatment for histological analysis frozen section of the tumor was stained with anti-CD11b (red) and anti-Gr1(Ly-6G/Ly-6C; green) antibodies. Original magnification: ×100. The number of $Cd11b^{+}GR\text{-}1^{+}$ cells in each group were semi-quantitatively analyzed using ImageJ software. Each data point indicated mean ± SD. [*$P < 0.05$, and non-significant (NS)].

SUPPLEMENTARY FIGURE 3
Serum level of IL-12 and GM-CSF. Serum samples were harvested from B16-F10 tumor-bearing mouse at 3 days after the third administration of oAd/APP (intratumoral injection = 1×10^{10} VP; intravenous injection = 2×10^{9} VP per injection). PBS was administered intratumorally as negative control. ELISA was performed to evaluate the serum level of (**A**) IL-12 or (**B**) GM-CSF (n = 3 mice per group). Each data point indicated mean ± SD. Non-significant (NS).

SUPPLEMENTARY FIGURE 4
Changes in immune cell population within thymus and bone marrow after intratumoral administration of oAd/APP in B16-F10 tumor bearing mice. Thymus **(A, B)** or bone marrow **(C)** was harvested at 3 days after the third administration of oAd/APP complex (1×10^{9} VP) into B16-F10 tumor-bearing mice CD3 or CD8 expression levels were analyzed by flow cytometry (n =3 mice per group). Each data point indicated mean ± SD. (**$P < 0.01$, ****$P <$ 0.0001, and non-significant (NS)).

References

1. Ratta M, Fagnoni F, Curti A, Vescovini R, Sansoni P, Oliviero B, et al. Dendritic cells are functionally defective in multiple myeloma: the role of interleukin-6. *Blood*. (2002) 100:230–7. doi: 10.1182/blood.V100.1.230

2. Sica A, Bronte V. Altered macrophage differentiation and immune dysfunction in tumor development. *J Clin Invest*. (2007) 117:1155–66. doi: 10.1172/JCI31422

3. Lim DS, Kim JH, Lee DS, Yoon CH, Bae YS. DC immunotherapy is highly effective for the inhibition of tumor metastasis or recurrence, although it is not efficient for the eradication of established solid tumors. *Cancer Immunol Immunother*. (2007) 56:1817–29. doi: 10.1007/s00262-007-0325-0

4. Podhajcer OL, Lopez MV, Mazzolini G. Cytokine gene transfer for cancer therapy. *Cytokine Growth Factor Rev*. (2007) 18:183–94. doi: 10.1016/j.cytogfr.2007.01.014

5. Zhang SN, Choi IK, Huang JH, Yoo JY, Choi KJ, Yun CO. Optimizing DC vaccination by combination with oncolytic adenovirus coexpressing IL-12 and GM-CSF. *Mol Ther*. (2011) 19:1558–68. doi: 10.1038/mt.2011.29

6. Lee YS, Kim JH, Choi KJ, Choi IK, Kim H, Cho S, et al. Enhanced antitumor effect of oncolytic adenovirus expressing interleukin-12 and B7–1 in an immunocompetent murine model. *Clin Cancer Res*. (2006) 12:5859–68. doi: 10.1158/1078-0432.CCR-06-0935

7. Choi IK, Li Y, Oh E, Kim J, Yun CO. Oncolytic adenovirus expressing IL-23 and p35 elicits IFN-gamma- and TNF-alpha-co-producing T cell-mediated antitumor immunity. *PloS One*. (2013) 8:e67512. doi: 10.1371/journal.pone.0067512

8. Choi KJ, Kim JH, Lee YS, Kim J, Suh BS, Kim H, et al. Concurrent delivery of GM-CSF and B7–1 using an oncolytic adenovirus elicits potent antitumor effect. *Gene Ther*. (2006) 13:1010–20. doi: 10.1038/sj.gt.3302759

9. Huang JH, Zhang SN, Choi KJ, Choi IK, Kim JH, Lee MG, et al. Therapeutic and tumor-specific immunity induced by combination of dendritic cells and oncolytic adenovirus expressing IL-12 and 4–1BBL. *Mol Ther*. (2010) 18:264–74. doi: 10.1038/mt.2009.205

10. Hwang JK, Hong J, Yun CO. Oncolytic viruses and immune checkpoint inhibitors: preclinical developments to clinical trials. *Int J Mol Sci*. (2020) 21:8627. doi: 10.3390/ijms21228627

11. Yun CO, Hong J, Yoon AR. Current clinical landscape of oncolytic viruses as novel cancer immunotherapeutic and recent preclinical advancements. *Front Immunol*. (2022) 13:953410. doi: 10.3389/fimmu.2022.953410

12. Bernstock JD, Blitz SE, Hoffman SE, Gerstl JVE, Chiocca EA, Friedman GK. Recent oncolytic virotherapy clinical trials outline a roadmap for the treatment of high-grade glioma. *Neurooncol Adv*. (2023) 5:vdad081. doi: 10.1093/noajnl/vdad081

13. Biegert GWG, Rosewell Shaw A, Suzuki M. Current development in adenoviral vectors for cancer immunotherapy. *Mol Ther Oncol*. (2021) 23:571–81. doi: 10.1016/j.omto.2021.11.014

14. Muscolini M, Tassone E, Hiscott J. Oncolytic immunotherapy: can't start a fire without a spark. *Cytokine Growth Factor Rev*. (2020) 56:94–101. doi: 10.1016/j.cytogfr.2020.07.014

15. Trinchieri G. Interleukin-12 and the regulation of innate resistance and adaptive immunity. *Nat Rev Immunol*. (2003) 3:133–46. doi: 10.1038/nri1001

16. Steinman RM. The dendritic cell system and its role in immunogenicity. *Annu Rev Immunol*. (1991) 9:271–96. doi: 10.1146/annurev.iy.09.040191.001415

17. Bhatt DK, Wekema L, Carvalho Barros LR, Chammas R, Daemen T. A systematic analysis on the clinical safety and efficacy of onco-virotherapy. *Mol Ther - Oncol*. (2021) 23:239–53. doi: 10.1016/j.omto.2021.09.008

18. Lin D, Shen Y, Liang T. Oncolytic virotherapy: basic principles, recent advances and future directions. *Signal Transduct Target Ther*. (2023) 8:156. doi: 10.1038/s41392-023-01407-6

19. Yoon AR, Hong J, Jung BK, Ahn HM, Zhang S, Yun CO. Oncolytic adenovirus as pancreatic cancer-targeted therapy: Where do we go from here? *Cancer Lett*. (2023) 579:216456. doi: 10.1016/j.canlet.2023.216456

20. Packiam VT, Lamm DL, Barocas DA, Trainer A, Fand B, Davis RL 3rd, et al. An open label, single-arm, phase II multicenter study of the safety and efficacy of CG0070 oncolytic vector regimen in patients with BCG-unresponsive non-muscle-invasive bladder cancer: Interim results. *Urol Oncol*. (2018) 36:440–7. doi: 10.1016/j.urolonc.2017.07.005

21. Breitbach CJ, Moon A, Burke J, Hwang TH, Kirn DH. A phase 2, open-label, randomized study of pexa-vec (JX-594) administered by intratumoral injection in patients with unresectable primary hepatocellular carcinoma. *Methods Mol Biol*. (2015) 1317:343–57. doi: 10.1007/978-1-4939-2727-2_19

22. Toulmonde M, Cousin S, Kind M, Guegan JP, Bessede A, Le Loarer F, et al. Randomized phase 2 trial of intravenous oncolytic virus JX-594 combined with low-dose cyclophosphamide in patients with advanced soft-tissue sarcoma. *J Hematol Oncol*. (2022) 15:149. doi: 10.1186/s13045-022-01370-9

23. Choi KJ, Zhang SN, Choi IK, Kim JS, Yun CO. Strengthening of antitumor immune memory and prevention of thymic atrophy mediated by adenovirus expressing IL-12 and GM-CSF. *Gene Ther*. (2012) 19:711–23. doi: 10.1038/gt.2011.125

24. Ma B, Wang Y, Zhou X, Huang P, Zhang R, Liu T, et al. Synergistic suppression effect on tumor growth of hepatocellular carcinoma by combining oncolytic adenovirus carrying XAF1 with cisplatin. *J Cancer Res Clin Oncol*. (2015) 141:419–29. doi: 10.1007/s00432-014-1835-8

25. Siurala M, Bramante S, Vassilev L, Hirvinen M, Parviainen S, Tahtinen S, et al. Oncolytic adenovirus and doxorubicin-based chemotherapy results in synergistic antitumor activity against soft-tissue sarcoma. *Int J Cancer*. (2015) 136:945–54. doi: 10.1002/ijc.29048

26. Long M, Yin G, Liu L, Lin F, Wang X, Ren J, et al. Adenovirus-mediated Aurora A shRNA driven by stathmin promoter suppressed tumor growth and enhanced paclitaxel chemotherapy sensitivity in human breast carcinoma cells. *Cancer Gene Ther*. (2012) 19:271–81. doi: 10.1038/cgt.2011.89

27. Torchilin VP. Micellar nanocarriers: pharmaceutical perspectives. *Pharm Res*. (2007) 24:1–16. doi: 10.1007/s11095-006-9132-0

28. Zhu L, Wang T, Perche F, Taigind A, Torchilin VP. Enhanced anticancer activity of nanopreparation containing an MMP2-sensitive PEG-drug conjugate and cell-penetrating moiety. *Proc Natl Acad Sci U.S.A*. (2013) 110:17047–52. doi: 10.1073/pnas.1304987110

29. Sugahara KN, Teesalu T, Karmali PP, Kotamraju VR, Agemy L, Greenwald DR, et al. Coadministration of a tumor-penetrating peptide enhances the efficacy of cancer drugs. *Science*. (2010) 328:1031–5. doi: 10.1126/science.1183057

30. Yang HW, Hua MY, Liu HL, Tsai RY, Chuang CK, Chu PC, et al. Cooperative dual-activity targeted nanomedicine for specific and effective prostate cancer therapy. *ACS Nano*. (2012) 6:1795–805. doi: 10.1021/nn2048526

31. Nam K, Nam HY, Kim PH, Kim SW. Paclitaxel-conjugated PEG and arginine-grafted bioreducible poly (disulfide amine) micelles for co-delivery of drug and gene. *Biomaterials*. (2012) 33:8122–30. doi: 10.1016/j.biomaterials.2012.07.031

32. Kasala D, Lee SH, Hong JW, Choi JW, Nam K, Chung YH, et al. Synergistic antitumor effect mediated by a paclitaxel-conjugated polymeric micelle-coated oncolytic adenovirus. *Biomaterials*. (2017) 145:207–22. doi: 10.1016/j.biomaterials.2017.08.035

33. Oh E, Choi IK, Hong J, Yun CO. Oncolytic adenovirus coexpressing interleukin-12 and decorin overcomes Treg-mediated immunosuppression inducing potent antitumor effects in a weakly immunogenic tumor model. *Oncotarget*. (2017) 8:4730–46. doi: 10.18632/oncotarget.v8i3

34. Wares JR, Crivelli JJ, Yun CO, Choi IK, Gevertz JL, Kim PS. Treatment strategies for combining immunostimulatory oncolytic virus therapeutics with dendritic cell injections. *Math Biosci Eng*. (2015) 12:1237–56. doi: 10.3934/mbe

35. Sánchez-León ML, Jiménez-Cortegana C, Cabrera G, Vermeulen EM, de la Cruz-Merino L, Sánchez-Margalet V. The effects of dendritic cell-based vaccines in the tumor microenvironment: Impact on myeloid-derived suppressor cells. *Front Immunol*. (2022) 13:1050484. doi: 10.3389/fimmu.2022.1050484

36. Ugolini A, Tyurin VA, Tyurina YY, Tcyganov EN, Donthireddy L, Kagan VE, et al. Polymorphonuclear myeloid-derived suppressor cells limit antigen cross-presentation by dendritic cells in cancer. *JCI Insight*. (2020) 5:e138581. doi: 10.1172/jci.insight.138581

37. Triozzi PL, Achberger S, Aldrich W, Elson P, Garcia J, Dreicer R. Differential immunologic and microRNA effects of 2 dosing regimens of recombinant human granulocyte/macrophage colony stimulating factor. *J Immunother*. (2012) 35:587–94. doi: 10.1097/CJI.0b013e31826b20b6

38. Thorn M, Guha P, Cunetta M, Espat NJ, Miller G, Junghans RP, et al. Tumor-associated GM-CSF overexpression induces immunoinhibitory molecules via STAT3 in myeloid-suppressor cells infiltrating liver metastases. *Cancer Gene Ther*. (2016) 23:188–98. doi: 10.1038/cgt.2016.19

39. Kumar A, Taghi Khani A, Sanchez Ortiz A, Swaminathan S. GM-CSF: A double-edged sword in cancer immunotherapy. *Front Immunol*. (2022) 13. doi: 10.3389/fimmu.2022.901277

40. Jadidi-Niaragh F, Atyabi F, Rastegari A, Kheshtchin N, Arab S, Hassannia H, et al. CD73 specific siRNA loaded chitosan lactate nanoparticles potentiate the antitumor effect of a dendritic cell vaccine in 4T1 breast cancer bearing mice. *J Control Release*. (2017) 246:46–59. doi: 10.1016/j.jconrel.2016.12.012

41. Vandenberk L, Garg AD, Verschuere T, Koks C, Belmans J, Beullens M, et al. Irradiation of necrotic cancer cells, employed for pulsing dendritic cells (DCs), potentiates DC vaccine-induced antitumor immunity against high-grade glioma. *Oncoimmunology*. (2016) 5:e1083669. doi: 10.1080/2162402X.2015.1083669

42. Thambi T, Hong J, Yoon AR, Yun CO. Challenges and progress toward tumor-targeted therapy by systemic delivery of polymer-complexed oncolytic adenoviruses. *Cancer Gene Ther*. (2022) 29:1321–31. doi: 10.1038/s41417-022-00469-y

43. Kasala D, Hong J, Yun CO. Overcoming the barriers to optimization of adenovirus delivery using biomaterials: Current status and future perspective. *J Control Release*. (2021) 332:285–300. doi: 10.1016/j.jconrel.2021.02.018

44. Seidman MA, Hogan SM, Wendland RL, Worgall S, Crystal RG, Leopold PL. Variation in adenovirus receptor expression and adenovirus vector-mediated transgene expression at defined stages of the cell cycle. *Mol Ther*. (2001) 4:13–21. doi: 10.1006/mthe.2001.0414

45. AbouEl Hassan MA, Braam SR, Kruyt FA. Paclitaxel and vincristine potentiate adenoviral oncolysis that is associated with cell cycle and apoptosis modulation, whereas they differentially affect the viral life cycle in non-small-cell lung cancer cells. *Cancer Gene Ther*. (2006) 13:1105–14. doi: 10.1038/sj.cgt.7700984

46. Ingemarsdotter CK, Baird SK, Connell CM, Oberg D, Hallden G, McNeish IA. Low-dose paclitaxel synergizes with oncolytic adenoviruses via mitotic slippage and apoptosis in ovarian cancer. *Oncogene*. (2010) 29:6051–63. doi: 10.1038/onc.2010.335

47. Tagawa M, Kawamura K, Ueyama T, Nakamura M, Tada Y, Ma G, et al. Cancer therapy with local oncolysis and topical cytokine secretion. *Front Biosci*. (2008) 13:2578–87. doi: 10.2741/2867

48. Belderbos RA, Aerts J, Vroman H. Enhancing dendritic cell therapy in solid tumors with immunomodulating conventional treatment. *Mol Ther Oncol*. (2019) 13:67–81. doi: 10.1016/j.omto.2019.03.007

49. Schierer S, Hesse A, Muller I, Kampgen E, Curiel DT, Schuler G, et al. Modulation of viability and maturation of human monocyte-derived dendritic cells by oncolytic adenoviruses. *Int J Cancer*. (2008) 122:219–29. doi: 10.1002/ijc.23074

50. Yan Y, Xu Y, Zhao Y, Li L, Sun P, Liu H, et al. Combination of E2F-1 promoter-regulated oncolytic adenovirus and cytokine-induced killer cells enhances the antitumor effects in an orthotopic rectal cancer model. *Tumour Biol*. (2014) 35:1113–22. doi: 10.1007/s13277-013-1149-5

51. Yang Z, Zhang Q, Xu K, Shan J, Shen J, Liu L, et al. Combined therapy with cytokine-induced killer cells and oncolytic adenovirus expressing IL-12 induce enhanced antitumor activity in liver tumor model. *PloS One*. (2012) 7:e44802. doi: 10.1371/journal.pone.0044802

52. Banchereau J, Palucka AK. Dendritic cells as therapeutic vaccines against cancer. *Nat Rev Immunol*. (2005) 5:296–306. doi: 10.1038/nri1592

53. Gerosa F, Baldani-Guerra B, Nisii C, Marchesini V, Carra G, Trinchieri G. Reciprocal activating interaction between natural killer cells and dendritic cells. *J Exp Med*. (2002) 195:327–33. doi: 10.1084/jem.20010938

54. Ohteki T, Fukao T, Suzue K, Maki C, Ito M, Nakamura M, et al. Interleukin 12-dependent interferon gamma production by CD8alpha+ lymphoid dendritic cells. *J Exp Med*. (1999) 189:1981–6. doi: 10.1084/jem.189.12.1981

55. Maulhardt HA, Marin AM, diZerega GS. Intratumoral treatment of melanoma tumors with large surface area microparticle paclitaxel and synergy with immune checkpoint inhibition. *Int J Nanomed*. (2024) 19:689–97. doi: 10.2147/IJN.S449975

56. John J, Ismail M, Riley C, Askham J, Morgan R, Melcher A, et al. Differential effects of Paclitaxel on dendritic cell function. *BMC Immunol*. (2010) 11:14. doi: 10.1186/1471-2172-11-14

57. Pfannenstiel LW, Lam SSK, Emens LA, Jaffee EM, Armstrong TD. Paclitaxel enhances early dendritic cell maturation and function through TLR4 signaling in mice. *Cell Immunol*. (2010) 263:79–87. doi: 10.1016/j.cellimm.2010.03.001

58. Zhong H, Han B, Tourkova IL, Lokshin A, Rosenbloom A, Shurin MR, et al. Low-dose paclitaxel prior to intratumoral dendritic cell vaccine modulates intratumoral cytokine network and lung cancer growth. *Clin Cancer Res*. (2007) 13:5455–62. doi: 10.1158/1078-0432.CCR-07-0517

59. Lu L, Hsieh M, Oriss TB, Morel PA, Starzl TE, Rao AS, et al. Generation of DC from mouse spleen cell cultures in response to GM-CSF: immunophenotypic and functional analyses. *Immunology*. (1995) 84:127–34.

60. Jin JO, Park H, Zhang W, de Vries JW, Gruszka A, Lee MW, et al. Modular delivery of CpG-incorporated lipid-DNA nanoparticles for spleen DC activation. *Biomaterials*. (2017) 115:81–9. doi: 10.1016/j.biomaterials.2016.11.020

61. de Winde CM, Munday C, Acton SE. Molecular mechanisms of dendritic cell migration in immunity and cancer. *Med Microbiol Immunol*. (2020) 209:515–29. doi: 10.1007/s00430-020-00680-4

62. Feng M, Zhou S, Yu Y, Su Q, Li X, Lin W. Regulation of the migration of distinct dendritic cell subsets. *Front Cell Dev Biol*. (2021) 9:635221. doi: 10.3389/fcell.2021.635221

63. Xu L, Xu W, Qiu S, Xiong S. Enrichment of CCR6+Foxp3+ regulatory T cells in the tumor mass correlates with impaired CD8+ T cell function and poor prognosis of breast cancer. *Clin Immunol*. (2010) 135:466–75. doi: 10.1016/j.clim.2010.01.014

64. Wang HY, Wang RF. Regulatory T cells and cancer. *Curr Opin Immunol*. (2007) 19:217–23. doi: 10.1016/j.coi.2007.02.004

65. Zou W. Regulatory T cells, tumour immunity and immunotherapy. *Nat Rev Immunol*. (2006) 6:295–307. doi: 10.1038/nri1806

66. Kilinc MO, Aulakh KS, Nair RE, Jones SA, Alard P, Kosiewicz MM, et al. Reversing tumor immune suppression with intratumoral IL-12: activation of tumor-associated T effector/memory cells, induction of T suppressor apoptosis, and infiltration of CD8+ T effectors. *J Immunol*. (2006) 177:6962–73. doi: 10.4049/jimmunol.177.10.6962

Frontiers in Immunology

Explores novel approaches and diagnoses to treat immune disorders.

The official journal of the International Union of Immunological Societies (IUIS) and the most cited in its field, leading the way for research across basic, translational and clinical immunology.

Discover the latest Research Topics

See more →

Frontiers

Avenue du Tribunal-Fédéral 34
1005 Lausanne, Switzerland
frontiersin.org

Contact us

+41 (0)21 510 17 00
frontiersin.org/about/contact